




Universitat Autònoma de Barcelona

**ADVERTIMENT.** L'accés als continguts d'aquesta tesi queda condicionat a l'acceptació de les condicions d'ús establertes per la següent llicència Creative Commons:  [http://cat.creativecommons.org/?page\\_id=184](http://cat.creativecommons.org/?page_id=184)

**ADVERTENCIA.** El acceso a los contenidos de esta tesis queda condicionado a la aceptación de las condiciones de uso establecidas por la siguiente licencia Creative Commons:  <http://es.creativecommons.org/blog/licencias/>

**WARNING.** The access to the contents of this doctoral thesis it is limited to the acceptance of the use conditions set by the following Creative Commons license:  <https://creativecommons.org/licenses/?lang=en>



Universitat Autònoma  
de Barcelona

Escola de Enginyeria

Departament d'Enginyeria Química, Biològica y Ambiental

Environmental Science and Technology Studies

**PROTEASES FROM PROTEIN-RICH WASTE: PRODUCTION BY SSF,  
DOWNSTREAM, IMMOBILISATION ONTO NANOPARTICLES AND  
APPLICATION ON PROTEIN HYDROLYSIS**

**PhD Thesis**

**Noraziah Abu Yazid**

Supervised by

Dr. Antoni Sánchez Ferrer and Dra. Raquel Barrena Gomez

Bellaterra, Cerdanyola del Valles, Barcelona

May 2017



**Antoni Sánchez Ferrer** profesor titular del Departamento de Ingeniería Química, Biológica y Ambiental de la Universitat Autònoma de Barcelona y **Raquel Barrena Gomez** investigadora Postdoctoral del mismo departamento,

Certifican:

Que, la bioquímica **Noraziah Abu Yazid** ha realizado, bajo nuestra dirección, el trabajo con título **“Proteases from protein-rich waste: production by SSF, downstream, immobilisation onto nanoparticles and application on protein hydrolysis”**, que se presenta en esta memoria, la cual constituye su Tesis para optar al Grado de Doctor en Filosofía en Ciencia y Tecnología Ambiental por la Universitat Autònoma de Barcelona.

Y para que se tenga conocimiento y conste a los efectos oportunos, presentamos en la Escola d'Enginyeria de la Universitat Autònoma de Barcelona la citada Tesis, firmando el presente certificado.

Bellaterra, Mayo de 2017.

Dr. Antoni Sánchez Ferrer

Dra. Raquel Barrena Gomez



## **Acknowledgements**

In the name of Allah, the most beneficent and the most merciful. All praises to Allah the Almighty for giving me the strength, guidance, and patience in completing this thesis.

My great appreciation goes to my supervisors, Dr. Antoni Sanchez and Dra. Raquel Barrena Gomez for their intellectual support, encouragement, patience, and enthusiasm throughout my study.

My special acknowledgement goes to the Government of Malaysia, University Malaysia Pahang and the Spanish Ministerio de Economia y Competitividad (Project CTM2012-33663-TECNO) for their financial support. Further gratitude goes to the local industries in Barcelona, Spain particularly Pere de Carme tannery at Igualada, Natursoy, Castelltercol, and local sewage treatment plant at Sabadell for supplying the organic residues as substrates for my work.

I would like to express my thanks to the administrative and technical staff especially Pili Marti and Manuel Plaza for their valuable help. Also, I would like to thanks, LA research group especially Goyo, Gerard and Daniela for letting me use the “roller” for my immobilisation work.

The deepest gratitude goes to GICOM research group that considered as my small family here, which made me contented being miles away from my dear family. The warmest welcome that I received made me enjoyed the “Spanish culture” that embraced the warmth bonding towards each other. Thanks to Dr. Xavier Font, Dr. Teresa Gea, Dr. Adriana Artola, and Dr. Amanda Alonso. Not to mention, my dearest groupmates Pedro Jimenez, Maria Marin, Cindy, Ahmad, Oscar, Beatriz, Lucia, Alejandra and others for their kindness and moral support during my research work. Thank you for all the friendship, fun, and memories that we have had in the last three years. I am so grateful being in “compostatge” as the spirit

never goes down. By the same token, I would like to thank, many great people that I made friend with, in DEQBA throughout my study.

I feel indebted to my best friend a.k.a my housemate, Tijah for her help in many ways and bittersweet memories during my study in UAB. I also wish to thank my love one, who is always by my side, for his warm support and understanding.

Special thanks go to my family for their love and support. Without their love and thought, I would not be able to deal with ups and downs during my study. Finally, my heartfelt gratitude goes to my beloved parents, Abu Yazid Mohd Jani and Rokiah Mohd Daud for their loves and inspirations. My graduation could not have been possible without their warm support and understanding.

Thanks to all...

## Overview of the thesis

In line with the main research lines of Composting research group (GICOM), this thesis focuses on the valorisation of solid organic residues and the utilisation of nanomaterials. Thus the thesis mutually linked the studies by transforming the solid waste using solid state fermentation (SSF) into value-added products and the use of nanoparticles to enhance the use of products obtained from SSF.

The first major part covers the valorisation of solid waste and transforms it into valuable product namely protease. The protease was produced through the fermentation of hair waste and anaerobically digested sludge (ADS) acting as co-substrate and inoculum. For industrial application, the protease produced from this work has shown a good result on dehairing of cowhides. This chapter not only demonstrated from the production of protease until application on industrial activity but also exhibited the downstream processing in SSF and reutilisation of the remaining residues after SSF which was a crucial thing to establish a zero discharge.

The second major part consisted of a preliminary screening work intending to determine the most suitable support for immobilisation of proteases. Proteases produced from two different protein-rich solid wastes: hair waste and soy fibre residue. The work aimed to find the feasible, reusable, reproducible, and cost-effective supports or carrier to be exploited for protease immobilisation. There were 10 materials were assessed for their biocompatibility with the protein: gold nanoparticles (AuNps), chitosan beads (wet and dry), chitosan beads coupled with gold nanoparticles (chitosan/Au), functionalised zeolite particles, the anionic resin (A520), anionic resin coupled with gold nanoparticles (A520/Au), magnetic iron oxide ( $\text{Fe}_3\text{O}_4$ ) nanoparticles (MNPs), titanium oxide nanoparticles ( $\text{TiO}_2\text{-A}$  and  $\text{TiO}_2\text{-B}$ ). The immobilisation efficiency was monitored based on immobilisation yield (% IY) and enzyme



loading per carrier (U/mg). Iron oxide nanoparticles were shown as a promising support thanks to its low-cost and easy separation by a magnetic force, thus increasing their possibilities of reuse.

In the last part of the thesis, both of the proteases from hair waste and soy fibre residue were immobilised on the support and were tested for application in protein hydrolysis. The efficiency of immobilised enzymes was compared with the free enzymes during the protein hydrolysis. Not to mention, the use of the different type of proteases (animal and plant origin) also was assessed during the protein hydrolysis of different type of protein (casein, egg white albumin, and oat bran protein isolate), since different protease produce different effect towards certain substrates. The amino acids released after hydrolysis reaction were well balanced with the degree of hydrolysis according to each protein substrates.

Overall, the study represented a multidisciplinary research field spanning waste management using solid state fermentation including the downstream processing and its application. In addition, the immobilisation of proteases on low-cost nanoparticles has been shown to be effective in the hydrolysis of proteins, being a low-cost alternative (both production and support) to actual techniques.

## Resumen

El trabajo realizado en esta tesis se enmarca dentro de las principales líneas de investigación del grupo de compostaje (GICOM), por una parte, en la valorización de residuos sólidos por medio de la fermentación en estado sólido (FES) para la obtención de productos de valor añadido en consonancia con el nuevo paradigma de considerar los residuos como materias primas y, en segundo lugar, en la utilización de nanomateriales para potenciar el uso de los productos obtenidos mediante FES.

La primera parte se centra en el aprovechamiento de residuos sólidos para la producción de enzimas de interés, concretamente proteasas. Las enzimas se produjeron a partir de la FES de la mezcla de residuo de pelo vacuno procedente de la industria de curtidos y lodos procedentes del proceso de digestión anaerobia utilizado como cosustrato e inóculo. Por una parte se ha demostrado la capacidad de producir proteasas y sus posibles aplicaciones en la propia industria, ya que se han obtenido buenos resultados en el proceso del depilado del cuero. Además, se ha establecido un esquema para el tratamiento posterior a la fermentación, incluida la reutilización de los residuos generados a lo largo del proceso de modo que se aproxime a un sistema de residuo cero.

La segunda parte del trabajo consistió en una exploración preliminar para determinar cuáles son los soportes más eficientes para inmovilizar las proteasas producidas por FES de cara a su uso continuado y su mejor preservación. Se utilizaron proteasas obtenidas a partir de la FES de residuos ricos en nitrógeno, pelo vacuno utilizado en la primera parte del trabajo y residuo de soja de una industrial alimentaria. Se evaluó la aplicabilidad, reutilización, reproducibilidad y coste de los soportes para su uso en la inmovilización de dichas proteasas. La evaluación se efectuó con 10

materiales considerando su bio-compatibilidad con las proteasas: nanopartículas de oro (NpAu), perlas de quitosano (húmedas y secas), perlas de quitosano con nanopartículas de oro (Quitosan/Au), zeolitas funcionalizadas, resina aniónica A520, resina aniónica con nanopartículas de oro (A520/Au), nanopartículas de óxido de hierro ( $\text{Fe}_3\text{O}_4$ ) y nanopartículas de óxido de titanio ( $\text{TiO}_2$ ). La eficiencia de la inmovilización se determinó a partir del rendimiento de inmovilización y la carga enzimática de cada soporte (U/mg). Las nanopartículas de óxido de hierro resultaron ser un soporte prometedor gracias a su bajo coste y a su fácil separación de forma magnética, aumentando así sus posibilidades de reutilización.

En último lugar, tanto las proteasas obtenidas a partir de los residuos de pelo como las de residuo de soja se inmovilizaron para ser evaluadas en la hidrólisis de proteínas, cuya eficiencia se comparó con la de las enzimas libres en el medio. Se utilizaron sustratos de diferente origen (animales y vegetales): caseína, albúmina de huevo y proteína de salvado de avena, observando un efecto diferente según el origen de la proteasa utilizada. Estos resultados se corroboraron con los aminoácidos liberados tras la hidrólisis de las proteínas.

En términos globales, este estudio representa una investigación multidisciplinaria que abarca, por una parte, la gestión y valorización de residuos orgánicos mediante el proceso de fermentación en estado sólido, con la producción y recuperación del producto de interés, incluyendo la etapa de postratamiento y así como la aplicabilidad del producto. Además, la inmovilización de las proteasas sobre nanopartículas de bajo coste se ha demostrado efectiva en la hidrólisis de proteínas tipo, consistiendo en una alternativa de bajo coste (tanto su producción como el soporte) a las técnicas actuales.

## Table of Contents

### Chapter 1

Introduction.....	1
1.1 Solid state fermentation as a paradigm for organic solid waste valorisation.....	3
1.2 Organic waste and its potential.....	4
1.2.1 Agricultural organic waste.....	5
1.2.2 Industrial organic waste.....	8
1.2.3 Municipal/domestic food waste.....	9
1.3 Solid state fermentation (SSF).....	11
1.3.1 General aspects of solid state fermentation.....	11
1.3.2 Advantages and challenges of solid state fermentation.....	14
1.3.3 Production and application of enzymes from solid state fermentation.....	16
1.3.4 Downstream processing in SSF and residues reutilisation.....	22
1.3.5 Economic viewpoint.....	26
1.3.6 Future perspectives.....	27
1.4 Industrial enzyme – Protease.....	28
1.4.1 Application of proteases in environmentally friendly processes.....	31
1.5 Enzyme (proteases) preservation via immobilisation.....	33
1.5.1 Adsorption.....	35
1.5.2 Covalent binding.....	36
1.5.3 Encapsulation / entrapment.....	37
1.5.4 Cross-linking.....	38

### Chapter 2

<i>Research Objectives</i> .....	39
----------------------------------	----

## Chapter 3

<i>Materials and Methods</i> .....	43
Summary.....	45
3.1 Materials: Organic solid wastes, bulking agents and reactors used in solid state fermentation (SSF).....	45
3.1.1 Organic solid wastes and bulking agents.....	45
3.1.2 General reactors set-up for protease production in SSF.....	46
3.2 Methods for determination of biological stability of organic mixtures.....	49
3.2.1 Dynamic respiration index (DRI).....	49
3.2.2 Oxygen uptake rate (OUR).....	51
3.3 Standard Analytical Methods.....	52
3.3.1 Total solid content (TS) and moisture content (MC).....	52
3.3.2 Volatile solid content (VS).....	53
3.3.3 Bulk density.....	53
3.3.4 pH and electric conductivity (EC).....	53
3.3.5 Total Organic Carbon (TOC).....	54
3.3.6 Total Kjeldahl Nitrogen (TKN).....	54
3.3.7 Ammonia soluble content.....	55
3.4 Methods for enzymes and protein determination and characterisation.....	55
3.4.1 Enzyme extraction.....	55
3.4.2 Lyophilisation and enzyme concentration by ultrafiltration.....	56
3.4.2 Protease activity assay.....	57
3.4.3 Total soluble protein – Bradford assay, Lowry assay.....	60
3.4.4 Amino acid determination using Ninhydrin method.....	61
3.4.5 Degree of hydrolysis.....	62
3.4.6 Characterisation of the hydrolysate using liquid chromatography-mass spectroscopy (LC-MS).....	62
3.4.7 Polyacrylamide electrophoresis gel (PAGE).....	64

3.4.8 Effect of pH and temperature (T) on protease stability.....	67
3.4.9 Inhibition study.....	67
3.5 Methods for supports/carrier synthesis for enzyme immobilisation.....	68
3.5.1 Magnetic nanoparticles (MNPs).....	68
3.5.2 Titanium oxide nanoparticles (TiO <sub>2</sub> ).....	69
3.5.3 Gold nanoparticles (AuNP).....	69
3.5.4 Chitosan beads.....	70
3.5.5 Chitosan and gold nanocomposite (Cs/Au).....	71
3.5.6 Anionic resin (A520) and gold nanocomposite (A520/Au).....	71
3.6 Methods for surface modification of carrier/support by amino silanes.....	72
3.6.1 Preparation of amino-functionalised magnetic nanoparticles (MNPs).....	72
3.6.2 Preparation of amino-functionalised zeolite.....	72
3.7 Methods for enzyme immobilisation.....	72
3.8 Characterisation of immobilised enzyme.....	74
3.9 Biochemical stability of immobilised enzyme.....	74
3.9.1 Operational stability.....	74
3.9.2 Storage stability.....	75
3.9.3 Reusability.....	75
3.10 Methods for protease application.....	76
3.10.1 Preparation of hides for enzymatic dehairing.....	76
3.10.2 Protease application in enzymatic dehairing.....	77
3.10.3 Preparation of protein isolates from oat bran.....	77
3.10.4 Application of immobilised protease in protein hydrolysis.....	78

## **Chapter 4**

<i>Production and biochemical characterisation of protease from hair waste in SSF and its application.....</i>	79
Graphical abstract.....	80

Summary.....	81
4.1 The reproducibility of protease production in solid state fermentation (SSF).....	82
4.1.1 Solid state fermentation (SSF).....	82
4.2 Downstream processing in SSF.....	87
4.2.1 Extraction methods.....	87
4.2.2 Partial purification and recovery of crude protease.....	89
4.3 Remaining residues reutilisation.....	90
4.3.1 Organic matter stability.....	91
4.4 Biochemical characterisation of protease.....	95
4.4.1 Operational stability and statistically analysis.....	95
4.4.2 Inhibition study.....	100
4.4.3 Polyacrylamide electrophoresis gel (PAGE).....	102
4.5 Application of protease in dehairing process.....	104
Conclusion.....	106
 <b>Chapter 5</b>	
<i>Screening and optimisation of protease immobilisation on different type of support/carrier .....</i>	<i>109</i>
Graphical abstract.....	110
Summary.....	111
5.1 Assessment of the suitable support/carrier for protease immobilisation.....	111
5.2 Gold nanoparticles (AuNps) as a carrier.....	111
5.2.1 Protein/enzyme loading on AuNps.....	113
5.2.2 Box-Hunter experimental design.....	115
5.2.3 Operational stability of immobilised protease on AuNps.....	119
5.2.4 Reusability of immobilised enzyme.....	121
5.3 Immobilisation of proteases on different support/carrier.....	123
5.4 Magnetite (Fe <sub>3</sub> O <sub>4</sub> ) nanoparticles as a carrier.....	132

5.4.1 Effect of stabiliser in MNPs suspension towards immobilisation yield.....	132
5.4.2 Enzyme loading per carrier – Box Hunter experimental design.....	138
Conclusion.....	140

## **Chapter 6**

<i>Immobilisation of protease produced from SSF on magnetic nanoparticles and its application.....</i>	141
Graphical abstract.....	142
Summary.....	143
6.1 Production of proteases from hair waste and soy residue in SSF.....	144
6.2 Immobilisation of protease onto functionalised magnetic nanoparticles (MNPs).....	147
6.3 Characterisation of the functionalised magnetic nanoparticles (MNPs).....	150
6.3.1 Characterisation of MNPs using TEM, electron diffraction, and SEM.....	150
6.3.2 Characterisation of MNPs using FT-IR.....	155
6.4 Biochemical characterisation of immobilised proteases (Phw, Psr).....	157
6.4.1 Operational stability of immobilised Phw and Psr.....	157
6.4.2 Storage stability of immobilised Phw and Psr.....	160
6.4.3 Reusability of immobilised Phw and Psr.....	162
6.5 Application of immobilised proteases (Phw, Psr) in the hydrolysis of proteins.....	163
6.5.1 Degree of hydrolysis.....	163
6.5.2 Peptide and amino acid analysis after treated with immobilised proteases.....	165
Conclusion.....	169

## **Chapter 7**

<i>Conclusions and future research.....</i>	171
---	-----

<b>References.....</b>	177
------------------------	-----

## **Annexes**

Annexe 1 Calibration curves.....	197
Annexe 2 Publications.....	221





## List of abbreviations

<i>Abbreviation</i>	<i>Definition</i>	<i>Units</i>
A520/Au	anionic resin and gold nanocomposite	
ADS	anaerobically digested sludge	
ANOVA	analysis of variance	
APCI	atmospheric pressure chemical ionisation	
APTES	3-aminopropyltriethoxysilane	
ATPE	aqueous two-phase extraction	
AuNps	gold nanoparticles	
BD	bulk density	kg L <sup>-1</sup>
BSA	bovine serum albumin	
CCD	central composite design	
CGA	colloidal gas aphon	
Chitosan/Au	chitosan and gold nanocomposite	
CLEAs	cross-linked enzyme aggregates	
CLECs	cross-linked enzyme crystals	
CO <sub>2</sub>	carbon dioxide	
CTAB	cetyl trimethylammonium bromide	
CV	coefficient variance	
DCM	dichloromethane	
DFP	diisopropyl-fluoro-phosphate	
DH	degree of hydrolysis	% w/w, wet basis
DM	dry matter	% w/w, wet basis
DRI	dynamic respiration index	g O <sub>2</sub> kg <sup>-1</sup> DM h <sup>-1</sup>
E64	L-3-carboxytrans 2,3-epoxypropyl-leucylamido(4-guanidine)butane	
EDC	1-ethyl-3-(3-dimethylaminopropyl) carbodiimide hydrochloride	
EDTA	ethylenediaminetetracetic acid	
ESI	electrospray ionisation	
Fe <sub>3</sub> O <sub>4</sub>	magnetite	
FT-IR	Fourier transform infrared spectroscopy	
GA	glutaraldehyde	
h	hour	
H <sub>2</sub> SO <sub>4</sub>	sulphuric acid	
HCl	hydrochloric acid	
HRTEM	high resolution transmission electron microscopy	
IY	immobilisation yield	
kDa	kilodalton	
LC-MS	liquid chromatography mass spectroscopy	
MC	moisture content	% w/w, wet basis

MNPs	magnetic nanoparticles	
MW	molecular weight	
MWCO	molecular weight cut-off	
NaCO <sub>3</sub>	sodium carbonate	
NaOH	sodium hydroxide	
NH <sub>4</sub> <sup>+</sup>	ammonium	% dry basis
Np	nanoparticles	
O <sub>2</sub>	oxygen	
OBPI	oat bran protein isolate	
OFAT	one factor at a time	
OM	organic matter	% w/w, dry basis
PA	protease activity	U ml <sup>-1</sup> , U g <sup>-1</sup> DM
PAGE	polyacrylamide electrophoresis gel	
pCMB	p-chloromercuribenzoate	
PEG	polyethylene glycol	
Phw	protease from SSF of hair waste and ADS	
PLC	programmable logic controller	
PMSF	phenylmethylsulfonyl fluoride	
PSr	protease from SSF of soy fibre residue and ADS	
PTMS	propyletrimethoxysilane	
RP-HPLC	reverse phase high pressure liquid chromatography	
SEM	scanning electron microscopy	
SIM	selected ion monitoring	
SISF	slurry state fermentation	
SmF	submerged fermentation	
sOUR	specific oxygen uptake rate	g O <sub>2</sub> kg <sup>-1</sup> DM h <sup>-1</sup>
sPA	specific protease activity	U mg <sup>-1</sup> protein
SSF	solid state fermentation	
TCA	trichloroacetic acid	
TFA	trifluoroacetic acid	
TIC	total ion current	
TiO <sub>2</sub>	titanium oxide nanoparticles	
TKN	total Kjeldahl nitrogen	% w/w, dry basis
TLCK	Tosyl-L-lysine chloromethyl ketone	
TMAOH	Tetramethylammonium hydroxide	
TMOS	tetramethoxysilane	
TOC	total organic carbon	% w/w, dry basis
TS	total solids	% w/w, wet basis
TSS	total suspended solid	
U	unit activity of enzyme	
VS	volatile solids	% w/w, dry basis

---

# Chapter 1

## *Introduction*

*Part of this chapter has been published in Sustainability 9:224, 1 – 28, 2017.*

*Solid state fermentation as a novel paradigm for organic waste valorisation: A review.*

*Noraziah Abu Yazid, Raquel Barrena, Dimitrios Komilis, Antoni Sánchez*



## **1.1 Introduction**

The generation of organic solid waste is dramatically increasing each year. The problems related to organic solid waste disposal become more pronounced in recent years due to the rapid pace of development towards modernisation throughout the world. Most of the organic waste is composed of household food waste, agricultural waste, human and animal wastes, which typically are used as animals feed, are incinerated or go to landfill (Mussatto et al., 2012). However, incineration is an expensive disposal method and causes air pollution, while in landfills the organic waste is broken down by microorganisms and forms leachate that can contaminate the groundwater (Reckinger and Seim, 2016). Also, the degradation of organics in these conditions produces methane, which is 25 times more harmful greenhouse gas compared to carbon dioxide (Sánchez et al., 2015). Incorrect waste management practices can result in public health and environmental problems, regarding issues such as odours and diseases (Giuntini et al., 2006). Nevertheless, organic wastes are comprised of materials rich in sugars, minerals, and proteins that could be used for other processes as substrates or raw materials. Since the cultivation of microorganism requires carbon, nutrient, and moisture, organic wastes could be a good candidate to provide an appropriate condition for the development of microorganisms.

In this view, solid state fermentation (SSF) is presented as a promising technology for waste valorisation through the bioconversion of organic wastes used as either substrate or inert support (Thomas et al., 2013). Microorganisms in SSF will play a role in the degradation of organic wastes into its constituents to convert them into high value-added products. SSF shows sustainable characteristics in the bioconversion of solid wastes that have been proved to be able to give high efficiency regarding product yields and productivities,

low energy consumption and solving disposal problems (Chen and He, 2012; Mussatto et al., 2012).

SSF is a process carried out with microorganisms growing on solid and moist substrates that act as nutrient sources and support the microbial growth in the absence or near absence of water (Hölker and Lenz, 2005; Pandey, 2003). Although SSF is not a new technology in bioprocessing, and it has been mainly applied in the Asian region. Nowadays it is gaining much attention due to the increasing use of different types of organic wastes and the larger production of add-value products (Pandey et al., 2000; Thomas et al., 2013). The search for sustainable and green processes to transform traditional chemical processes also highlights the potential of SSF. Thus, the bioconversion of organic wastes into valuable bioproducts could substitute non-renewable materials and replace the chemical processes into cleaner practices in the industrial sector. The particular interest of SSF is due to its relative simplicity as a process that uses abundant low-cost biomaterials with minimal or no pre-treatment for bioconversion, less waste water generation and the capacity of simulating similar microenvironments favourable to microorganisms growth (Wang and Yang, 2007). Similarly, SSF simulates the natural microbiological processes like composting and ensiling (Singhania et al., 2009).

## **1.2 Organic waste and its potential**

Organic waste can be practically defined as any material or unused by-product from a process that is biodegradable and comes from either plant or animal. The main forms of organic waste are household food waste, agricultural waste, industrial waste and human and animal waste. Organic waste tends to be degraded over time by other organisms depending on its composition and moisture content. The composition of organic waste varied from the nature of the original material. Based on the type of organic waste, SSF can be applied with

the aim of producing different valuable bio-products (Dave et al., 2012; El-Bakry et al., 2015; Motta and Santana, 2014; Pandey et al., 2000). In this sense, Table 1.1 summarises the use of different organic wastes with their potential to produce bioproducts.

### **1.2.1 Agricultural organic waste**

Agricultural and agro-industrial activities generate a lot of lignocellulosic by-products such as bagasse, straw, stem, stalk, cobs, fruits peel and husk, among others. These wastes are mainly composed of cellulose (35-50%), hemicellulose (25-30%), and lignin (25-30%) (Behera and Ray, 2016). Typically, in lignocellulosic materials, the main cellulose constituent is glucose; hemicellulose is a heterogeneous polymer that is mainly comprised of five different sugars (L-arabinose, D-galactose, D-glucose, D-mannose and D-xylose) and some organic acids; whereas lignin is formed by a complex three-dimensional structure of phenylpropane units (Mussatto et al., 2012).

Despite the complex structure and composition of agricultural organic wastes, SSF has been successfully applied to the production of hydrolytic and ligninolytic enzymes (De Castro et al., 2015; Do-Myoung et al., 2014; Mtui, 2009). Lignin peroxidase has been produced using corn cobs as a substrate in SSF (Mehboob et al., 2011). Furthermore, considering the rising price and shortage grains as a custom animal feed, the lignocellulosic materials have a high potential to produce edible animal feedstuff (Graminha et al., 2008). However, the direct application for animal feedstuff is limited because of the present of lignin that reduces its digestibility. Several pre-treatments of straw have been made using SSF for cellulose and lignin degradation to increase the digestibility of the feed (Chang et al., 2012). In this sense, SSF can have a great potential in producing enzymes to improve the digestibility of rich fibre materials such as soybean cotyledon (Lio and Wang, 2012). *Jatropha* seed cake has been reported for the production of cellulases through SSF without any pre-treatment (Dave et al., 2012).



**Table 1.1** List of organic wastes and their potential in bioprocessing and production of value-added bioproducts

Category of organic waste	Type of products /processes	Waste materials/Residues	Potential use	References
Municipal/domestic food waste	Kitchen waste	Preparation waste, leftover food, sludge, cocoyam peels	Biopesticide, animal feedstuff, organic acids, antibiotics	(Ohkouchi and Inoue, 2007; Zhang et al., 2015)
	Commercial/market /hotel	Used coffee grounds, used tea bags, waste bread, leftover, expired foods, sludge, organic fraction	Enzymes, animal feedstuff, biopesticide, bioethanol, bioplastic	(Jooste et al., 2013; Rocha et al., 2014)
Industrial organic waste	Animal products /tannery /slaughterhouse	Skin, hides, fleshings wastes, fats, horns, shaving wastes, bones, liver, intestines	Enzymes, animal feedstuff, glue, surfactant, lubricant, filler	(Abraham et al., 2014; Kanagaraj et al., 2006; Wiradimadja et al., 2014; Yazid et al., 2016)
	Paper/wood industry	Pulp, sawdust	Enzymes, bioethanol, fuel	(Rathna et al., 2014)
	Sugar industry	Molasses	Enzymes, fructooligosaccharides	(Ghazi et al., 2006)
	Poultry processing	Skin, blood, fats, hairs, feathers, bones, liver, intestines, wings, trimmed organs	Enzymes, animal feedstuff, fertiliser	(Jayathilakan et al., 2012)
	Marine products processing	Shells, roes, pincers, trimmed parts	Enzymes, bioactive compound	(Kandra et al., 2012; Kim and

				Mendis, 2006)
	Cereals and spices processing	Husk, hull, chaff, stalks, residues	Biorefinery, enzymes, activated carbon	(Elmekawy et al., 2013)
	Fruits and vegetable processing	Skin, peels, pomace, fibre, kernel, stones, seeds	Pectinolytic enzymes, bioenergy, animal feed, organic acid	(Embaby et al., 2014; Panda et al., 2016)
	Nuts processing	Shells, coir, pith	Biopulping, biochar, activated carbon	(Mtui, 2009)
Agricultural organic waste	Corn, wheat, rice, soya, coffee, sugarcane, barley	Fibre, meal, straw, bran, husk, pulp, bagasse	Enzymes, animal feedstuff, fuel, bioethanol, furfural, compost, chemical feedstock, biopolymer, organic acid	(Govumoni et al., 2015; Mussatto et al., 2012)
	Cattle, broiler	Fleshing waste, dung, litter	Animal glue, animal feed supplement, methane production, biochar, activated carbon, biofertiliser, biopesticide	(Adams et al., 2002; Sebola et al., 2015; Ukpai and Nnabuchi, 2012)
	Fruits and vegetables	Seeds, peels, pomace, husks	Enzymes, animal feed, fuel, compost	(Botella et al., 2007; Mtui, 2009)
	Oils and oilseeds	Shells, husks, fibres, sludge, press cake	Bioethanol, enzymes, fuel, fertiliser, activated carbon	(Jørgensen et al., 2010)
	Coconuts	Fibres, shell, kernel	Resins, pigments, fillers, mats, activated carbon, tanning materials	(Gratuito et al., 2008; S et al., 2015; Sapuan et al., 2003)

Several authors present other uses for similar materials such as the reinforcement of composite materials for application in building materials, furniture, fishnet (Sapuan et al., 2003) or as activated carbons (Gratuito et al., 2008). Agricultural organic wastes also include livestock manure. Cow dung has been reported to have a high nitrogen content that made it suitable for methane production (Sebola et al., 2015; Ukpai and Nnabuchi, 2012). The production of biochar and activated carbon were favoured by utilisation of chicken manure and cow dung (Demiral and Demiral, 2008; Nguyen and Lee, 2015). Furthermore, high-quality bio fertiliser was produced employing liquid amino acid hydrolysed from animal carcasses as an additive to mature compost of chicken or pig manure by SSF (Liu et al., 2016).

### **1.2.2 Industrial organic waste**

Industrial organic wastes include any organic by-product in a large variety of industries such as slaughterhouses, fruit and vegetable processing plants, poultry processing, paper and pulp manufacturing, marine processing, sugar industry and dairy industry, among others. Most of these wastes have the potential to be used as a substrate or support in SSF processes to produce high-value products. For instance, sawdust, which is an easily available by-product of the wood industry has been used as a support substrate in SSF to obtain high laccase production by white rot fungi *Coriolopsis gallica* (Daâssi et al., 2016). Leather industry and slaughterhouses generate many organic wastes containing protein such as animal fleshing, hair wastes, skin trimming, keratin wastes, chrome shaving, and buffing wastes that being underutilised. Several authors have reported the utilisation of animal fleshing as a substrate in SSF for protease production (Ravindran et al., 2011). The mixture of hair wastes with activated sludge or anaerobically digested sludge showed a high yield of protease production (Abraham et al., 2014; Yazid et al., 2016). By-products of sugar industry such as molasses and sugarcane bagasse have been reported in the production of invertase by SSF

(Veana et al., 2014). Molasses also was chosen as a low-cost substrate to replace an expensive feedstock (cane sugar) in ethanol production (Kanwar et al., 2012). Additionally, tapioca industry waste which contains much organic matter with a strong odour that could cause environmental pollution has been successfully converted into poly(3-hydroxybutyrate) (PHB) via SSF, thus possibly become an alternative process and reduce the total production cost (Sathiyarayanan et al., 2013). Food processing industries generate many by-products able to be used in SSF for producing valuable bio-products (Elmekawy et al., 2013; Mandalari et al., 2008). The use of fruits and vegetables waste for production of organic acid and vital enzymes has been widely reported (Panda et al., 2016). Due to its high and easily degradable organic content, vegetable wastes show a significant potential for energy bioconversion, particularly in biofuel production (Singh et al., 2012). Crustaceans by-products, generated in industrial seafood processing, has been reported in the production of chitinase and chitosanase with a broad range of applications in biomedical, food and agrochemical sectors (Nidheesh et al., 2015; Suresh and Anil Kumar, 2012). Fish processing wastes in SSF are favourable since the waste is easy to obtain at low-cost and provides appropriate conditions for microorganism cultivation. Fish processing wastes, rich in lipids and proteins, have been suitable to produce esterase, a product with a varied industrial application in organic chemical processing, detergent formulations, surfactant and oleo-chemical industry (Esakkiraj et al., 2012).

### **1.2.3 Municipal/domestic food waste**

Most countries around the world are facing a great challenge to manage domestic food waste as it is wet, putrescible and sometimes mixed with inorganic waste (impurities). The composition of domestic food waste is complex and includes oil, water, spoiled and leftover foods from kitchen wastes and markets. These substances are chemically comprised of starch, cellulose, protein, fats, lipids, and other organic matter. High moisture and salt

contents lead to rapid decomposition of the organic wastes and produce unpleasant odours that can attract flies and bugs, which are vectors for various diseases. Apart from being perishable, municipal solid waste including household kitchen waste and domestic food waste from restaurants and markets contained high lignocellulosic materials that could be exploited to produce valuable bio-products. Domestic food wastes such as waste bread, savoury, waste cakes, cafeteria waste, fruits, vegetables and potato peels wastes have been reported as a suitable substrate for glucoamylase enzymes production by *Aspergillus awamori* via SSF technology (Melikoglu et al., 2015; Uçkun Kiran et al., 2014). Bread waste has been used to produce amylase (Cerda et al., 2016), whereas municipal solid waste and kitchen waste residues principally composed of potato peels, orange peels, onion peels, carrot peels, cauliflower leaves, banana stalks and pea pods has been used to produce cellulase by SSF (Abdullah et al., 2016; Janveja et al., 2014). The cultivation of selected industrial yeast strains using orange peel as a substrate resulted in a high yield of aroma esters (Mantzouridou et al., 2015). The utilisation of household food wastes with high dry content to produce high yields of ethanol by SSF has also been reported in several studies (Matsakas and Christakopoulos, 2015; Matsakas et al., 2014). Likewise, mixed food wastes collected from restaurants and inoculated with fungal inoculum can produce glucoamylase-rich media and protease-rich media by SSF, suitable to be used as a feedstock to produce succinic acid which has wide range application in laundry detergents, plastics, and medicines production (Sun et al., 2014). Cocoyam peels are common household kitchen wastes in Nigeria presenting a capability to become a very useful substrate for oxytetracyclines, which are an important antibiotic to treat many infections (Ezejiofor et al., 2012). The complex composition of food wastes also makes them suitable for microbial growth, having the potential to produce *Bacillus thuringiensis* (Bt) biopesticide through SSF (Zhang et al., 2015).

### 1.3 Solid state fermentation (SSF)

#### 1.3.1 General aspects of solid-state fermentation

Solid state fermentation (SSF) has received considerable attention in the past years. The successful development of bioprocesses in SSF is regarded to several general aspects including the suitability of different types of microorganisms, substrates and process parameters. There are different kinds of microorganisms used in SSF process including fungi, yeasts, and bacteria. However, fungi and yeast are the most commonly reported for the fact that SSF can provide similar natural habitat, which has low water activity in the fermentation media. The most common yeast genera reported in SSF are *Candida*, *Saccharomyces*, and *Aureobasidium* (López-Pérez and Viniegra-González, 2016). While common fungal genera are *Aspergillus*, *Penicillium*, and *Rhizopus*, which have a broad range of species for the production of a wide number of valuable bioproducts through SSF (El-Bakry et al., 2015). Although SSF seems to be more favourable for fungi and yeast growth, there is also increasing evidence of bacteria positive used in producing bioproducts in SSF. The most common bacteria genera used are *Bacillus* and *Streptomyces* (Martins et al., 2011; Singhanian et al., 2009). Many studies are reporting the use of filamentous fungi, mainly chosen in SSF because of their ability to produce thermostable enzymes of high commercial value (Ávila-Cisneros et al., 2014; Liu et al., 2011; Martins et al., 2011; Saqib et al., 2012). However, there are also several studies reporting that bacteria strains can produce thermostable enzymes especially from *Bacillus* species (Afrisham et al., 2016; Özdemir et al., 2012; Prajapati et al., 2015; Tsegaye and Gessesse, 2014).

Selection of suitable substrates also plays a key role in an efficient and economical production of the desired product. In selecting proper substrates for SSF process, it is important to ensure the availability and cost of the substrates. They can supply appropriate

nutrients and physical support for the development of microorganisms in SSF. Organic wastes from agricultural, industrial processing and domestic food waste are the most suitable substrates to be used due to their abundance at low or no cost and their chemical composition. Additionally, by using these organic wastes as substrates, their environmental pollution problems can be minimised. However, in some cases, an additional supplement has to be added to the organic wastes. In other situations, a chemically or mechanically pretreatment (especially for lignocellulosic materials) is necessary due to the inaccessibility of certain nutrients for microorganisms. For example, a chemical pre-treatment of municipal solid waste was performed to prepare the solid fraction for an easier microbial uptake in the production of cellulase (Abdullah et al., 2016). Pulp and paper solid waste were pre-treated with acid hydrolysis in a microwave prior SSF as a substrate to produce fumaric acid (Das et al., 2016). In the production of an anti-cancer prodrug, camptothecin (CPT) by SSF, complex protein sources (whey concentrate powder) were added to soybean waste to enhance the productivity of *Fusarium oxysporum* producing a secondary metabolite (Bhalkar et al., 2016).

Other important aspects to improve the efficiency of SSF are the selection and optimisation of the process variables including initial moisture, particle size, pH, temperature, media composition, sterilisation, water activity, inoculum density, agitation, aeration, extraction of product and its downstream process (Pandey, 2003). Among these aspects, particle size and moisture content have been mainly studied, reported and reviewed by others (de Castro and Sato, 2015; Martins et al., 2011; Pandey et al., 2000; Singhania et al., 2009). Ideally, it is apparent that small substrate particles could provide large surface area for microbial attachment. However, too small particles would result in substrate agglomeration that could affect the oxygen transfer, thus retarding the microorganism development. However, although a large particle size of the substrate provides better aeration efficiency, it

can limit the surface area for microbial attachment (Chen and He, 2012; de Castro and Sato, 2015; Pandey, 2003). Hence, the conditions that are favourable in a particular process are an aspect that needs to be thoroughly assessed. Moisture content also has a significant role in SSF as bacteria and fungi have different moisture content requirements. Fungi needs lower moisture content around 40-60% (Singhania et al., 2009), whereas bacteria can need high moisture content (60-85%) (Martins et al., 2011). The optimum moisture content in a solid substrate is closely related to the correct nutrient and oxygen/carbon dioxide diffusion during fermentation (Orzua et al., 2009). High moisture content would decrease porosity, thus loss the structure of the particles and interfere in the oxygen diffusion. On the contrary, low moisture content can limit the nutrient solubility hindering the microorganism development. An increase of temperature during the fermentation will indicate the growth of the microorganism. In aerobic fermentation, oxygen is supplied and exchanged with carbon dioxide, and heat is generated by microorganisms, leading to a temperature increase. In some cases, high temperatures will negatively affect the growth of microorganisms and product formation (Pandey, 2003). However, in other cases, high temperatures increase the yield of the enzyme produced (Abraham et al., 2014, 2013; Yazid et al., 2016).

These general aspects are relevant to point out a general idea to design an efficient strategy using organic wastes in SSF according to the product required and considering the cost and waste availability. Fig. 1.1 summarises the whole general processes involve in the valorisation of organic waste via SSF.



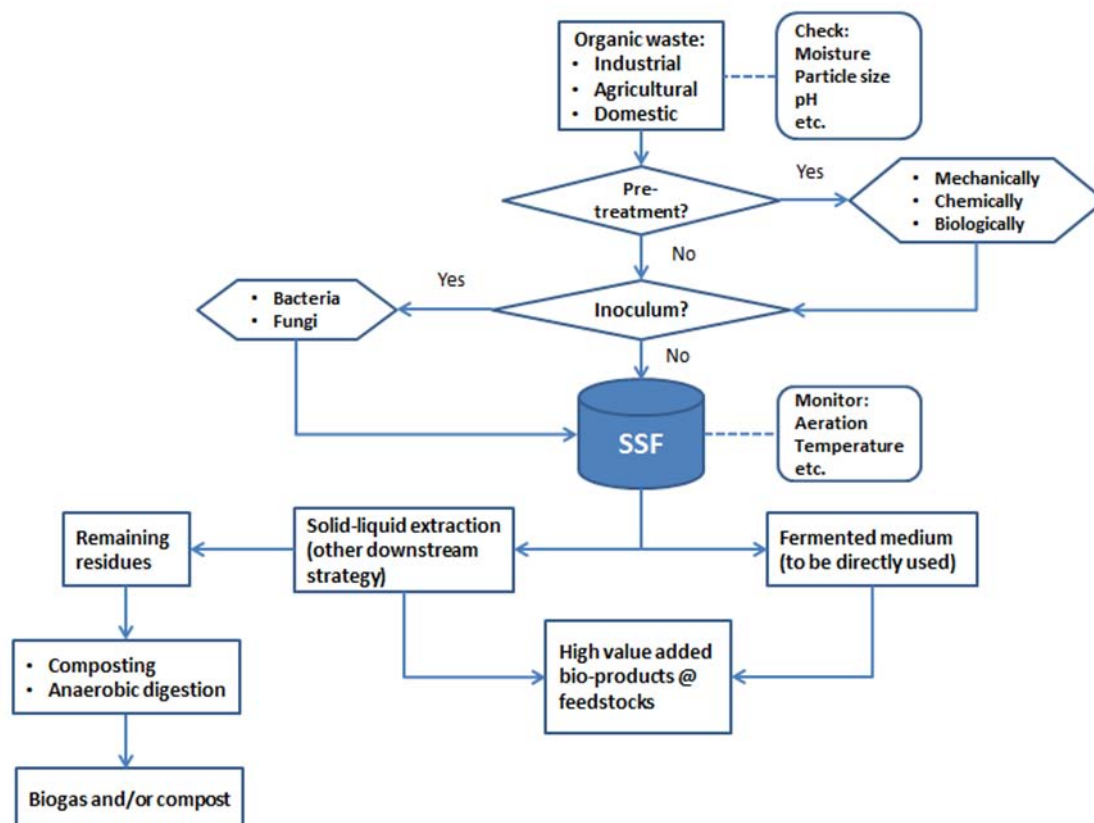


**Fig. 1.1** Flowchart of valorisation of organic waste to produce valuable bio-products using solid state fermentation (SSF)

### 1.3.2 Advantages and challenges of solid-state fermentation

In recent years, there is an increasing trend in using SSF in the biotechnology field due to its simplicity and ability to perform the bioconversion of low-cost solid substrates, in some cases achieving higher productivity than that of submerged fermentation (SmF) (Vinięra-González et al., 2003). With the prominent characteristic of SSF employing low requirement of water mimic a natural atmosphere for microbial growth. This condition favour filamentous fungi growth, enhanced sporulation, and cultivation of mixed culture which is hard to implement in SmF (Hölker et al., 2004) due to broth rheology problems that affect the transport phenomena and mass transfer in a SmF reactor (Gabelle et al., 2012). Also, the lack of liquid phase in SSF reduces waste water and lower down the risk of bacterial contamination. In this sense, SSF offers an advantage by using unsterilized substrates and

creates non-strict sterile conditions for the process (De la Cruz Quiroz et al., 2015). Also, SSF provides a simple media preparation with the reduction of reagents use, since the media normally contain the appropriate nutrient for the process and present negligible foaming problems during the process. As a matter of fact, the process requires low consumption of energy since agitation and sterilisation are not always necessary. Similarly, this process reduces purification costs due to higher end product concentration or by using the product in a crude form (López-Pérez and Viniestra-González, 2016).

Despite these advantages, SSF also faces several challenges such as mass and heat transfer, scale-up, biomass estimation and recovery and operational control. Also, the utilisation of natural substrates is often limited by their poor reproducibility and heterogeneity (Hongzhang et al., 2011). Also, the heterogeneity of the substrate related to porosity can lead to mass and heat transfer problems in SSF. The substrate bed inside SSF is a complex medium comprised of a combination of solid, liquid and gas phases that requires an optimal porosity for mass and heat transfer process. Too much water content compact a substrate result in reducing the porosity that leads to poor oxygen transfer and may prone to contamination, while in adverse condition inhibits microbial growth and limits the transfer of nutrients (Raghavarao et al., 2003). Moreover, the diffusion of mass and heat in SSF depends on aeration which may differ according to the substrate types. In small scale, an appropriate aeration allows heat dissipation and a regulation of the mass moisture level. However, the removal of heat generated during metabolic growth can be a problem at large scale. The high solid concentration requires a large quantity of air (Mansour et al., 2016). Furthermore, biomass determination is quite a challenge in SSF, especially involving fungi that usually develop a strong interaction between mycelia and solid substrate making difficult the complete recovery of biomass (Rahardjo et al., 2004). Due to this difficulty in biomass quantification, a lack of important basic scientific engineering and fermentation operational

control is often found in publications and only a qualitatively or empirically characterisation is done (Sindhu et al., 2015). The same happens when establishing kinetics of reactions in SSF.

### **1.3.3 Production and application of enzymes from solid state fermentation**

SSF has opened a new paradigm of bioconversion of organic solid wastes using SSF with uprising application of SSF in the production of biologically active secondary metabolites both in lab scale and industrial scale. There are abundant of studies regarding the application of SSF in the production of various bio-products have been published including enzymes, organic acids, biofertiliser, biopesticide, biosurfactant, bioethanol, aroma compounds, animal feeds, pigments, vitamins, antibiotics, and so forth.

In search of green technology, enzyme production has received much attention in industrial biotechnology processes with the objective of the substitution of chemical processes, with potentially adverse effects on humans and environment. Various enzymes are emerging from biotechnology processes, mostly from submerged fermentation, are playing a key role in a significant number of industrial processes. In recent years, the production of enzymes from SSF has gained attention due to its simplicity, high productivity, and stability that make them suitable for industrial processes. Several reviews on the production of enzymes from SSF have been published in recent years (El-Bakry et al., 2015; Pandey et al., 2000; Singhania et al., 2009; Thomas et al., 2013). The setup for enzyme production in SSF is quite straightforward and economical since the abundance of organic wastes can be used as substrates for the production plus reduces chemicals, energy, and water consumption. Fungi, yeasts, and bacteria are capable of producing various enzymes through SSF, as the environment in SSF is favourable for most of the microorganisms. Table 1.2 shows a

compilation of several organic solid wastes used as substrates for enzyme production with or without inoculation of specific strains.

**Table 1.2** List of several enzymes produced and organic waste used as substrate in solid state fermentation

ENZYME	MICROORGANISM	SUBSTRATE	Reference
cellulase	<i>T.reesei</i>	Municipal solid waste	(Abdullah et al., 2016)
	<i>Thermoascus aurantiacus</i>	jatropha deoiled seed cake	(Dave et al., 2012)
	<i>A.niger</i>	kitchen waste	(Janveja et al., 2014)
	<i>Penicillium</i> sp	empty fruit bunch	(Do-Myoung et al., 2014)
	<i>T.reesei</i>	wheat bran	(Ortiz et al., 2015)
	<i>A.niger</i>	groundnut husk	(Salihu et al., 2014)
	<i>Trichoderma viridae</i>	banana peel	(Hai-Yan Sun et al., 2011)
	<i>Candida tropicalis</i> , <i>A. oryzae</i>	Ginkgo biloba residues	(Zhou et al., 2015)
	<i>A. niger</i>	wheat bran	(Bansal et al., 2014)
	<i>Trametes hirsuta</i>	wheat bran	(Dave et al., 2015)
	<i>T. reesei</i>	soybean bran	(Gasparotto et al., 2015)
	<i>A. fumigatus</i>	lignocellulosic materials	(Liu et al., 2011)
	<i>T. harzianum</i>	wheat bran	(Pathak et al., 2014)
	<i>T. asperellum</i>	lignocellulosic materials	(Raghuwanshi et al., 2014)
	glucoamylase	<i>A.niger</i>	rice straw and wheat bran
<i>Phanerochaete chrysosporium</i>		grass powder	(Saratale et al., 2014)
<i>A.nidulans</i>		black gram residues	(Kumar et al., 2016)
<i>Aspergillus</i> sp		banana peels, pineapple peels	(Anto et al., 2006)
<i>A.awamori</i>		domestic food waste	(Uçkun Kiran et al., 2014)
amylase	<i>A.awamori</i>	bread waste	(Melikoglu et al., 2015, 2013)
	<i>Bacillus</i> sp.	Mustard Oilseed cake	(Saxena and Singh, 2011)
	<i>Thermomyces</i> sp.	soy and bread waste	(Cerda et al., 2016)

	<i>Bacillus subtilis</i>	wheat bran and wheat rava	(Pandi et al., 2016)
	<i>A.fumigatus</i>	wheat bran	(Singh et al., 2014)
protease	<i>A.niger</i>	wheat bran, soybean meal, cottonseed meal, orange peel	(De Castro and Sato, 2014)
	<i>Pseudomonas aeruginosa</i>	Jatropha curcas seed cake	(Mahanta et al., 2008)
	<i>A.awamori</i>	bread waste	(Melikoglu et al., 2015, 2013)
	<i>A. oryzae</i>	wheat bran, soya bran	(Novelli et al., 2016)
	<i>Bacillus sp.</i>	green gram husk	(Prakasham et al., 2006)
	<i>A. fumigatus</i>	wheat bran	(da Silva et al., 2013)
	<i>B. cereus</i>	cow dung	(Vijayaraghavan et al., 2014)
	<i>Candida tropicalis,</i> <i>A. oryzae</i>	Ginkgo biloba residues	(Zhou et al., 2015)
	<i>Thermus sp.</i>	soy fibre	(El-Bakry et al., 2016)
	N.S.	hair waste, activated wastewater sludge	(Abraham et al., 2014)
	<i>Thermoactinomyces sp.</i>	agricultural and household waste	(Verma et al., 2014)
	N.S.	hair waste, anaerobic digested wastewater sludge	(Yazid et al., 2016)
keratinase	<i>Paenibacillus woosongensis</i>	dry feathers	(Paul et al., 2014)
lipase	<i>Pseudomonas aeruginosa</i>	Jatropha curcas seed cake	(Mahanta et al., 2008)
	N.S.	vegetable oil refining waste	(Santis-Navarro et al., 2011)
	<i>A.niger</i>	oil palm waste residues	(Silveira et al., 2016)
xylanase	<i>A.japonicus</i>	castor bean waste	(Herculano et al., 2016)
	<i>A. tubingensis</i>	wheat straw	(Pandya and Gupte, 2012)
	<i>B. pumilus</i>	wheat bran	(Asha Poorna and Prema, 2007)
	<i>T. harzianum</i>	wheat bran	(Pathak et al., 2014)
	<i>Colletotrichum graminicola</i>	wheat bran	(Zimbardi et al., 2013)
	<i>A.nidulans</i>	black gram residues	(Kumar et al., 2016)
inulinase	<i>A. ficuum</i>	wheat bran	(Chen et al., 2011)

	<i>Kluyveromyces marxianus</i>	Sugarcane bagasse	(Mazutti et al., 2006)
laccase	<i>Coriolopsis gallica</i>	sawdust waste	(Daâssi et al., 2016)
	<i>Trametes versicolor</i>	oak sawdust	(Martínez-Morales et al., 2015)
esterase	<i>B. altitudinis</i>	fish processing waste	(Esakkiraj et al., 2012)
lignin peroxidase	<i>Ganoderma leucidum</i>	waste corn cob	(Mehboob et al., 2011)
invertase	<i>A.niger</i>	Molasses and sugarcane bagasse	(Veana et al., 2014)
$\beta$ -xylosidase	<i>A. tamaritii</i>	ground oats	(El-Gindy et al., 2015)
	<i>Colletotrichum graminicola</i>	wheat bran	(Zimbardi et al., 2013)
$\beta$ -glucosidase	<i>Colletotrichum graminicola</i>	wheat bran	(Zimbardi et al., 2013)
multienzyme protease, xylanase, cellulase, endomylase	<i>A. awamori</i>	babassu cake	(López et al., 2013)

N.S.: non-specified

In SSF, non-sterilized and non-inoculated media are often suitable. This aspect can positively affect the economic feasibility for the production of enzymes at industrial scale. For example, protease production from hair waste and sewage sludge in 4.5 L reactor (469 U g DM<sup>-1</sup>) has been successfully scaled up to a 10 L reactor resulting in a stable proteolytic activity of 435 U g DM<sup>-1</sup> (Yazid et al., 2016). Also, the production of lipase from the mixture of winterization residue and waste water sludge in a 4.5 L SSF reactor under non-sterilized conditions resulted in a high lipolytic activity (120000 U g DM<sup>-1</sup>) (Santis-Navarro et al., 2011). It has been proved that non-sterilized conditions are applicable in the production of enzymes by SSF even without specific inoculation (El-Bakry et al., 2016).

Kriaa and Kammoun (Kriaa and Kammoun, 2016) compared the production of glucose oxidase by *Aspergillus tubingensis* in SSF and SmF. Preliminarily, both conditions

were compared using glucose and gluconic acid as substrates which led to higher activity of glucose oxidase in SSF (170.59 U ml<sup>-1</sup>) compared to SmF (43.73 U ml<sup>-1</sup>). Then, the production of glucose oxidase was carried using the mixture of agro-residues such as wheat bran, molasses and fish meal. Enhance of yield was observed, in a 74% higher than preliminary SSF and SmF. Similarly, peptidase production by *Aspergillus fumigatus* in SSF using wheat bran and SmF using casein as a substrate was compared. An improved yield of peptidase production, approximately 30 times higher, was obtained through SSF compared with SmF (da Silva et al., 2013).

In another comparative study among SSF, slurry state fermentation (SISF) and SmF, revealed that maximum  $\beta$ -xylosidase was obtained in SSF (33.7 U ml<sup>-1</sup>) followed by SISF (24.9 U ml<sup>-1</sup>) and SmF (5.5 U ml<sup>-1</sup>) (El-Gindy et al., 2015). The enzymes produced by SSF maintain a similar or enhanced capability for chemical processes or commercial enzymes normally produced by SmF. Several studies have been successfully applied the crude enzymes produced from SSF to industrial processes such as dehairing of hides, hydrolysis of lignocellulosic materials, detergent formulation, de-inking and biobleaching paper waste, bioethanol production, xylitol production, silver recovery from X-ray films, and so forth.

Tanning and leather industries release a lot of hazardous chemicals. In this sense, some authors have explored the use of crude enzymes such as protease, keratinase, and amylase from SSF in the leather processing as an alternative to chemical processes. Crude protease produced from hair waste and sewage sludge in SSF showed a high potential to substitute chemical dehairing (Abraham et al., 2014; Yazid et al., 2016). The results in cowhide dehairing were as efficient as using chemical and commercial powder enzymes, indicating the economic viability of the process. Likewise, the crude protease produced by *Bacillus cereus* from agro-industrial residues and cow dung as substrates in SSF were

effectively using for the dehairing of goat hides for 18 h at 30 °C (Vijayaraghavan et al., 2014). In other studies, the use of crude keratinase in dehairing of goat skins has also been reported (Paul et al., 2014). The keratinase produced by *Paenibacillus woosongensis* by SSF employing chicken feather and rice straw as substrates, showed similar or improved characteristics than using chemical treatments, without causing damage to the collagen layers after the dehairing process. Integrated bioprocessing in leather processing including detaining and fibre opening normally needs a commercial enzyme. This enzyme is expensive for common processes of tanning and contains some added stabilisers that could contribute to the pollution of the effluent. Correspondingly, amylase produced by *Bacillus subtilis* on wheat bran through SSF showed a good performance in fibre opening process developed on goat skins in comparison to chemicals and commercial enzymes. Besides, the employment of crude amylase during the process showed a lower pollution load (COD, TS) (Pandi et al., 2016).

Crude cellulase produced from agricultural residues under SSF has been used in the saccharification of lignocellulosic materials such as rice straw, sugarcane bagasse, corn cob, fruits peel, and wheat bran enhanced the sugar yield for bioethanol production (Bansal et al., 2014; Dave et al., 2015; Gasparotto et al., 2015; Raghuwanshi et al., 2014; Sandhu et al., 2013). The utilisation of grass powder as a carbon source in the production of cellulase and hemicellulase by *Phanerochaete chrysosporium* by SSF has yielded an efficient enzyme complex to be employed for hydrolysis of rice husk. Then, the hydrolysate was used by *Clostridium beijerinckii* and resulted in higher biohydrogen production, which was better than other values reported (Saratale et al., 2014). Production of cellulase and xylanase by SSF inoculating *Trichoderma harzianum* showed a better activity and stability at optimum pH and temperature. The crude enzyme complex produced by SSF enhanced the toner removal of photocopier waste papers with superior strength properties (fibre and microfibrils) compared



to chemical treatment, and the enzyme complex improves the brightness and drainage as well (Pathak et al., 2014). Similarly, the crude enzyme complex (cellulase, xylanase,  $\beta$ -glucosidase) by *Aspergillus nidulans* cultivated on low-cost crop residues as a substrate under SSF was efficiently used in the saccharification of pearl millet stover and bio-deinking of mixed office waste paper with enhanced physical properties (Kumar et al., 2016). There was reported the use of crude protease produced from low cost agricultural and household waste by *Thermoactinomyces* sp. via SSF (Verma et al., 2014). The enzyme was used as an additive to commercial detergents as an alternative to caustic soda. Interestingly, the crude enzyme also showed gelatinase activity capable of hydrolysing the gelatine layer locking the silver salt on used X-ray film for silver recovery.

#### **1.3.4 Downstream processing in SSF and residues reutilisation**

Downstream processing is the processes involved in fermentation process mainly bioseparation such as extraction, purification, and recovery. There are very few studies reporting about downstream processing in SSF which hampers the process development in up-scaling. Not to mention the downstream processing that typically engages with complicated processes and additional facilities that cost up to 70% of production cost (Zidehsaraei et al., 2009). Since SSF is a process occurs in a limited or absence of liquid; therefore, extraction with an appropriate solvent is necessary to recover secreted products that bind to the solid substrates. For this reason, extraction efficiency is crucial to obtain complete recovery of products from SSF.

Dhillon et al. (2013a) achieved higher citric acid extraction from the SSF process using response surface methodology involving process parameters such as extraction time, agitation rate, and solvent volume. Solid-liquid ratio, solvent or buffer type, pH, temperature, stirring rate, repeated extraction, and extraction time are process parameters that also have

been studied to optimise the extraction of products from SSF (Ahmed and Mostafa, 2013; Aikat and Bhattacharyya, 2000; Arantes et al., 2011; Chandra et al., 2010; Pirota et al., 2013; Rodríguez-Fernández et al., 2010). However, in these studies usually, a small amount of solid substrate from SSF range from 1 g – 20 g in a shake flask was used for the extraction. Only some of them reported the extraction using the whole substrate fermented (in kg) with the aim of knowing the total recovery of the product (Yazid et al., 2016). This assessment is considerably important since it affects the extraction efficiency and product recovery from SSF. In fact, it was reported that on a scale up system, there was a reduction of product activity per gramme of dry substrate of about 60% compared to the activity obtained at the lab scale, yet the total product activity obtained was high (Salariato et al., 2010).

Szabo et al. (2015) found that sonication has a significant effect on enzyme extraction. They observed that multiple extractions with sonication improved the recovery of enzymes from SSF with an increment of enzyme yield more than twice that of conventional single stage extraction. Furthermore, to improve the enzyme recovery from SSF, it has been observed that extraction followed by diafiltration can enhance the activity recovery by removing inhibitory phenolic compounds from the extracts (Rezaei et al., 2011). Since the recovery and concentration steps are significant in enzyme production employing ultrafiltration with 10kDa cut off after solid-liquid extraction can improve the rate of enzyme recovery about 74% (Poletto et al., 2015; Yazid et al., 2016).

Moreover, the recovery of biosurfactant such as sophorolipid from SSF can be improved by employing solid-liquid extraction using methanol followed by multiple re-extractions of the fermented material with ethyl acetate with continuous mixing for 1h, subsequently filtered using 0.2 µm membrane filtration (Rashad et al., 2014). The resulting crude extracts were further purified using a rotary evaporator at 40 °C to remove any solvent. Then, hexane was used to wash the remaining hydrophobic residue after vacuum drying, and

the partially purified sophorolipid was obtained after vaporising the residual hexane at 40 °C under vacuum (Hu and Ju, 2001).

An innovation of downstream processing in SSF has been proposed with using simultaneous extraction and recovery of products scheme (Zidehsaraei et al., 2009). In this method, the enzyme has been produced through SSF followed by combined separation method (simultaneous extraction and recovery) based on aphron flotation. Briefly, the colloidal gas aphron (CGA) was generated by mixing solid biomass from SSF with distilled water and aluminium sulphate as a flocculating agent. Then the purified enzyme was recovered by filtration (Fig. 1.2b). This method was considered straightforward by eliminating the extraction step in conventional SSF (Fig. 1.2a) and producing a relatively pure enzyme. Furthermore, an efficient employment of single step aqueous two-phase extraction (ATPE) for downstream processing of enzyme produced from SSF (Fig. 1.2c) has been reported, avoiding the conventional multi-step procedures involving salt precipitation, dialysis, and chromatography processes (Bhavsar et al., 2012). In addition, the high recovery of the enzyme within a short time (3 h) shows the potential for the commercial interest of this technique.

A novel simplified configuration for conversion of biomass to ethanol using the whole SSF cultivation medium for the hydrolysis of steam-exploded sugarcane bagasse has been reported (Pirota et al., 2014). This configuration would allow a single reactor system thus avoiding additional separation steps. The industrial production of biopolymers such as PHA (polyhydroxyalkanoate) is usually hampered by the high production cost which involves capital investment in fermentation media and downstream processing. In this sense, SSF has been proposed as an alternative to SmF for more feasible PHA production using agro-industrial waste instead of using expensive defined media (Sindhu et al., 2015).

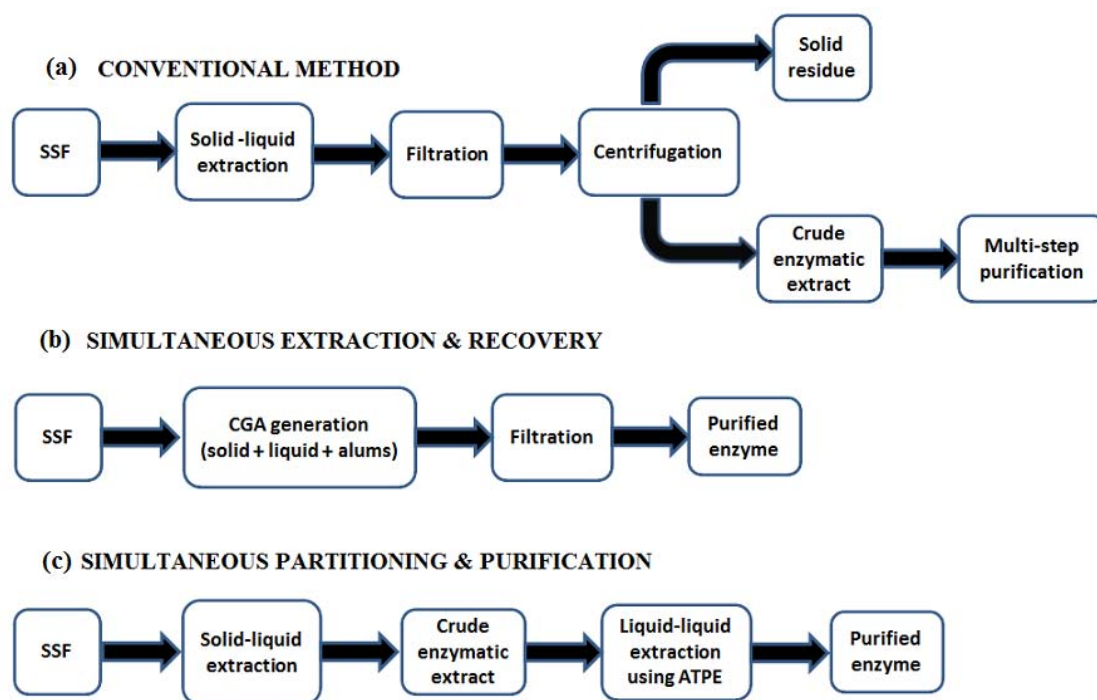


**Fig. 1.2** Schematic diagram of conventional and innovation of downstream processing in SSF (a) conventional method; (b) simultaneous extraction and recovery based on aphyron flotation; (c) simultaneous partitioning and purification using ATPE system.

While in downstream processing an enzymatic method is more favourable compared to a chemical method due to the high recovery rate, the implementation has been limited by the high cost of the enzyme. A novel downstream separation processing using crude enzyme produced via SSF using sunflower meal as the main substrate has been proposed to reduce the high cost of PHA recovery (Kachrimanidou et al., 2016). The enzymatic lysis of bacterial cells facilitated a high recovery (98%) and purity (96.7%) of poly(3-hydroxybutyrate-co-3-hydroxyvalerate) showing that enzymatic digestion can be used as an alternative process to PHA recovery.

After the recovery of products, a solid waste with different level of biodegradability remains once SSF processing is finished. Late work by our research group (data not published yet) indicates the possibility to reutilising the remaining solid by composting and anaerobic digestion. The stabilisation of the remaining organic matter was done by

composting in the same reactors, and continuing the process until no increment in temperature was observed; the stability measured by means of the dynamic respiration index (DRI) was lower than  $1 \text{ g O}_2 \text{ kg}^{-1} \text{ OM h}^{-1}$  (Yazid et al., 2016). Solid and liquid wastes generated after enzyme extraction of SSF during the ethanol fermentation process were reutilised as a substrate for anaerobic digestion to produce biogas in a zero waste approach (Narra and Balasubramanian, 2015). Moreover, it has been observed that solid residues remained after production of citric acid in SSF can be reutilised in a sequential extraction process to produce fungal chitosan as an eco-friendly alternative to the chitosan derived from marine shells (Dhillon et al., 2013b).

### 1.3.5 Economic viewpoint

Solid state fermentation has proved to yield high biomolecules concentrations making further additional downstream processes easier than in SmF. Consequently, SSF minimised the requirements for additional equipment as well as energy and water consumption. Since the cost of substrates represents 30-40% of total production costs (Zhang et al., 2007), the valorisation of organic solid waste as a substrate in SSF effectively reduces the operational costs. The superiority of SSF over SmF in several biotechnological processes poses an attractive economic feasibility. For instance, Zhuang et al. (Zhuang et al., 2007) compared an economic analysis of cellulase for bioethanol production in SSF and SmF. The analysis reported on the unit costs of the cellulase production in SSF ( $\$15.67 \text{ kg cellulase}^{-1}$ ) and SmF ( $\$40.36 \text{ kg cellulase}^{-1}$ ), while the market price for cellulase was approximate  $\$90 \text{ kg cellulase}^{-1}$ . Comparatively, a sensitivity analysis was performed indicating that the production cost using SSF was lower than SmF with an efficiency of 99.6%. Furthermore, another report studied the economic analysis of hydrolases enzyme cocktails (amylase, cellulase, xylanase, protease) by *A. awamori* on babassu cake in SSF. They suggested that solid residues or

fermented cake generated after enzyme extraction can be sold as animal feed, which in turn compensates the enzyme production costs (Castro et al., 2010). By the same token, SSF expedites development of formulations of biopesticide from solid organic wastes and utilisation of low aeration rate and water consumption as well as simple unit operation decreases the production costs.

However, it seems evident that there is a significant lack of systematic economic studies on SSF economics, especially those related to the comparison between SSF and SmF.

### **1.3.6 Future perspectives**

The use of SSF in various biotechnological processes and production of value-added bioproducts seems very appealing and promising as reported in this review. As SSF valorises organic solid waste, it leads to the reduction of operational and production costs, concurrently contributes to solid waste management and decreases environmental pollution. Various types of organic solid waste can be easily used and converted into valuable bioproducts such as enzymes, organic acids, bioethanol, biopesticides, biosurfactants, and so forth using SSF. Apart from these apparent advantages, SSF presents a limited application at industrial level due to several technical aspects that need to be improved and well established, such as scientific engineering and fermentation operational control. However, with the uprising of studies related to SSF that are being currently explored, it is believed that there are numerous aspects of bioreactors technology suitable to enhance the processes to compensate the lack of application at the industrial level. With the understanding of SSF theory and the development of current SSF technology for the production of biomolecules, SSF can be considered a novel paradigm for organic solid waste valorisation.

#### **1.4 Industrial enzyme – Protease**

Industrial enzymes can be divided into three groups which are technical enzymes, food enzymes, and feed enzymes (Kumar et al., 2014). In a broad sense, technical enzymes are denoted as products for environments and industries such as leather, detergent, textile, fuel ethanol, pharmaceutical, and various smaller industries. Food enzymes included products for food and beverage such as the brewing, alcohol industry, baking industry, dairy industry, oil and fats industry, aroma and flavour industry. Feed enzymes included the production of swine, ruminant, poultry, and aqua feedstuff for growth and production efficiency. According to a market survey, global industrial enzyme demand is forecast to grow at a rate 6.9% for 2010-2020 (Kumar et al., 2014). Among industrial enzymes available in a market, proteases are exhibited as one of the most versatile enzymes, since they involve a broad range of applications including as technical enzymes, food enzymes and feed enzymes (Kumar et al., 2014). Proteases represent one of the major industrial enzymes groups which accounted for 60% of the total enzyme market worldwide (Rao et al., 1998).

Proteases or peptidases are proteolytic enzymes that catalyse the peptide bonds cleavage in proteins. They are responsible for complete hydrolysis of proteins and associated with essential biological pathways. Due to their diversity of action and structure, characterisation of proteases is quite challenging. Previously, proteases were categorised according to their molecular size, charge or substrate specificity. With the emergence of molecular biology, the protease can be categorised based on chemical nature of the catalytic or active sites, mechanism of action, and the evolutionary relationship of their three-dimensional structure (Beynon and Bond, 2001). Also, due to their variety of specificity of their action and application, they have captured worldwide attention to exploit their physiological as well as biotechnological applications (Sawant and Saraswathy, 2014).

Commonly, proteases produced commercially are non-toxic and non-pathogenic that can be considered as eco-friendly and safe for every biotechnological sector.

Typically, proteases are divided into exopeptidase or endopeptidase based on their action site. In particular, proteases are classified as exopeptidases if the enzymes cleave the peptide bond at the amino (N) or carboxyl (C) terminus of the protein which known as aminopeptidases and carboxypeptidase respectively, whereas if the enzymes cleave at internal peptide bonds termed as endopeptidases or proteinases (Fig. 1.3). Conventionally, endopeptidases are further classified into four prominent groups according to their functional group present at the active site namely serine proteases, cysteine proteases, metalloproteases, and aspartic proteases (Rao et al., 1998). Usually, they are referred to acidic, neutral or alkaline proteases based on their optimal pH (Rao et al., 1998; Sawant and Saraswathy, 2014).

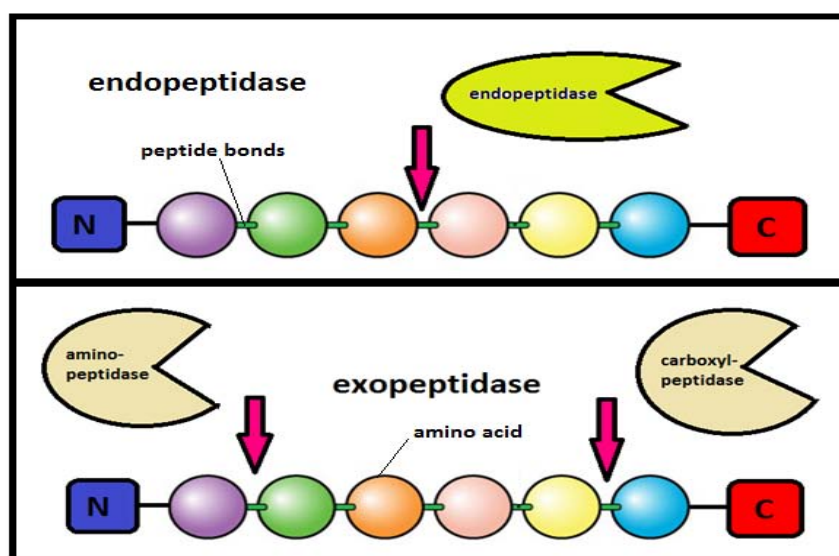


**Fig. 1.3** Class of proteases according to their cleavage of action site on protein molecule

Serine proteases are known to have a reactive serine residue in the active site. They are extensively distributed among microbial and animal as they play a vital role in organisms (Rao et al., 1998). This type of proteases are inhibited by L-3-carboxytrans 2,3-epoxypropyl-leucylamido(4-guanidine)butane (E64), diisopropyl-fluoro-phosphate (DFP),



phenylmethylsulfonyl fluoride (PMSF), and tosyl-L-lysine chloromethyl ketone (TLCK). Also, some of the serine proteases are inhibited by thiol reagents such as p-chloromercuribenzoate (pCMB) due to the presence of cysteine residue near the active site which is possibly not involved in the catalytic mechanism of the enzymes. Normally, serine proteases are active at neutral and alkaline pH, plus optimum at pH range from 7 to 11. The isoelectric points of this type of proteases are between pH 4 and 6. They have broad substrate specificities comprising amidase and esterolytic activity. Among serine proteases, serine alkaline proteases constitute the largest subgroup, which are active at highly alkaline pH. They hydrolyse a peptide bond which has tyrosine, phenylalanine, or leucine at the carboxyl side of the splitting bond with optimal pH at 10 and their isoelectric point at approximately pH 9 (Rao et al., 1998).

Cysteine proteases are active in the presence of reducing agents such as hydrogen cyanide (HCN), ethylenediaminetetraacetic acid (EDTA) or cysteine, while susceptible to sulphhydryl reagents such as pCMB, iodoacetic acid, iodoacetamide or heavy metals (Ellaiah et al., 2002). Cysteine proteases work better in neutral pH, and most of them are active within the range of 5 to 8. The cysteine proteases occur in both prokaryotes and eukaryotes, predominantly in the plant.

Metalloproteases are the vastly varied catalytic type of proteases with optimum pH at 5 to 9. These enzymes are prone to metal-chelating reagents such as EDTA, but not affected by sulphhydryl agents of DFP. However, many of the EDTA-inhibited enzymes can be reactivated by ions such zinc, cobalt, and calcium as they are characterised by the requirement of divalent metal ion for their activity (Rao et al., 1998). Most of the bacterial and fungal metalloproteases are zinc-containing enzymes, where the zinc atom is significant

for enzyme activity, and calcium has the function to stabilise the protein structure (Ellaiah et al., 2002).

Aspartic proteases are also known as acidic proteases due to their optimal activity at low pH 3 to 4 and depend on the aspartic acid residues for their catalytic activity. Aspartic proteases are inhibited by pepstatin and can be affected by the presence of diazoketone compounds and copper ions. Moreover, microbial acid proteases exhibit specificity against aromatic or bulky amino acid residues on both sides of the peptide bond, similar to pepsin although their action is less stringent than pepsin (Rao et al., 1998). Most of the fungal aspartic proteases are unstable above neutral pH (Ellaiah et al., 2002).

#### **1.4.1 Application of proteases in environmentally friendly processes**

Nowadays people are seeking for greener technology to achieve a cleaner environment. Many chemical processes have been substituted by microbial or enzymatic processes, which are environmentally friendly. In that sense, alkaline proteases have been positively used in several industrial processes such as the production of detergents, leather, meat tenderizers, pharmaceuticals and medical, protein hydrolysates, food products, and waste processing.

Additionally, the excess of the sludge produced in waste water treatment plant is a worldwide problem. That is no clear destination for this sludge that can end up in landfills which imply a significant number of environmental problems. Occasionally, to cope with this problem, physical and chemical approaches are utilised in the existing treatment plant. However, this may increase in additional handling costs in term of energy consumption and emission of secondary pollution. Since protein and carbohydrate are the main content in activated sludge with 71% and 8%, respectively, but the proportions due to change depending on sample sludge (Song and Feng, 2011). The use of the sludge to produce proteases together

with other wastes is a promising alternative for the excess sludge. The proteases catalyse the hydrolysis of peptide bonds in proteins and responsible for reducing solids content and flocculation in sludge.

In other scenario, proteases have been recently considered in leather processing substitute to the conventional methods using hydrogen sulphide and other chemicals, which have an adverse effect towards safety hazards and environments. Unlike in chemical processing, proteases have been a preference due to several advantages such as being easy to control, reliable and rapid reaction, undamaged the grain structure of skin layers, waste reduction, and eco-friendly technologies. Alkaline proteases speed up the dehairing process by facilitating the swelling of hair roots that enable an easy removal of the hair from the hides without damaging the grain structure which is critical for high quality of leather (Khandelwal et al., 2014). Additionally, the use of proteases in the leather processing can help in solubilizing the proteinaceous waste, which consequently decreases the biological oxygen demand in the resulting wastewater. By the same token, alkaline proteases namely keratinase were used for the treatment of waste feathers from the poultry industry. Insoluble keratins were hydrolysed and transformed into a high protein source for animal feedstuff and bio-fertilizers (Kumar et al., 2012; Vigneshwaran et al., 2010).

Hair is composed of protein filament notably keratin which has many disulphide bonds (S-S) that contribute to the toughness of keratin. Correspondingly, a formulation in a detergent and household cleaning solvent containing proteases expedite hair degradation and assist in cleaning drain clogged with deposits containing hair (Jacobson et al., 1987; Takami et al., 1992). Moreover, a detergent formulation containing proteases as an alternative to chemical washes assist in bioprocess cleaning operations especially when involving protein-based residues such as dairy products and meat processing (Sawant and Saraswathy, 2014).

The employment of proteases has a significant advantage in reducing potential hazard towards workforces, equipment, and the environment.

Used X-ray offers a great advantage as a source of silver recovery since it can be found abundance in many public and private hospitals every year. It was estimated approximately 69 tonnes of silver could be recovered from used X-ray films obtained from healthcare centres (Bas et al., 2012). A single X-ray film may contain nearly 1.5-2.0% (w/w) of silver in a gelatin layer. There are several ways to recover silver from X-ray film such as burning the films, oxidation of metallic silver following electrolysis, stripping the gelatin layer using different chemicals, and enzymatic hydrolysis of gelatin (Nakiboğlu et al., 2001). Traditionally, the films are burned directly for silver recovery producing the emission of detrimental unpleasant smell. Whereas stripping the gelatin layer chemically (e.g. using ammonium thiosulphate, sodium thiosulphate, nitric acid, sodium cyanide, NaOH) may cause environmental and safety hazards plus incur an additional cost in term of resources and time (Shankar et al., 2010). In view to this, hydrolysis of gelatin by the proteolytic enzyme is considered the best alternatives to recover silver from used X-ray films. It is an eco-friendly process, cheap and efficient with 99.9% purity of silver recovered (Amira and Eida, 2016; Radha and Arun, 2010; Shankar et al., 2010).

The use of proteases that have broad substrate specificity in industrial processes poses a practical and eco-friendly value. Besides, at the end of the processes, there will be no accumulation of biomass or chemicals in the effluent due to autolysis nature of proteases that can degrade among themselves. Thus, no further treatment of the effluent will be required.

### **1.5 Enzyme (proteases) preservation via immobilisation**

In many biotechnology processes, employment of enzymes may offer an advantage in the manipulation of stability factors such as pH and temperatures. These factors can be

changed in a wider range, unlike when using microorganisms. However, there are also many enzymatic hydrolytic processes that can be hampered by the instability of the enzyme chain or by low reaction rate. The instability of the enzymes leads to the irreversible thermal denaturation of protein which normally involves with unfolding step followed by an irreversible process namely protein aggregation or proteolysis (Eijsink et al., 2004). Particularly in proteases which known as a proteolytic enzyme, there is a prominent problem regarding autolysis since proteases can use neighbouring proteases chains as substrates that lead to auto-digestion (Tavano, 2013). Therefore, it is necessary to find a way to preserve the proteases and also to enhance the stability of the enzymes throughout the processes. For this reason, enzyme immobilisation could provide an enhancement towards the stability of the enzymes by preventing a dissociation of the subunit, unfolding rate of protein chains, and also forms inflexibility and rigidity of three-dimensional enzyme structures which lead to resistance of conformational changes induced by heat or pH (Talbert and Goddard, 2012). Moreover, employment of immobilised enzyme simplifies the end process with easily removed the catalyst from the reaction medium without the requirement of inactivation of the enzyme. In a nutshell, utilisation of immobilised enzymes, chiefly proteases would provide better process control and feasibility, economical production for various biotechnological applications.

Few significant factors need to be considered to achieve an efficient and economic enzyme immobilisation such as the type of support, the method of immobilisation, and the purpose of immobilised enzymes (Mohamad et al., 2015). The support or matrix for biocatalyst should be inert and biocompatible to the environment; it will not interfere with the reaction of the substrate and the enzyme, plus do not cause any harm to the environment (Cipolatti et al., 2014). Various type of supports has been reported in the literature such as nanomaterials (e.g. nanometals, gold nanoparticles, nanotubes, nanofibrous), natural

polymers (e.g. alginate, chitosan, collagen, carragenan, gelatin, cellulose), inorganic materials (e.g. ceramic, silica, zeolites, activated carbon, celite) (Cipolatti et al., 2014; Datta et al., 2012). Furthermore, the mode of immobilisation also can influence the enzyme stability and efficiency of enzyme loading. The binding protein/enzyme on solid supports can be achieved by several modes such as adsorption, covalent binding, encapsulation, entrapment, and cross-linking as shown in Fig. 1.4 (Asgher et al., 2014).

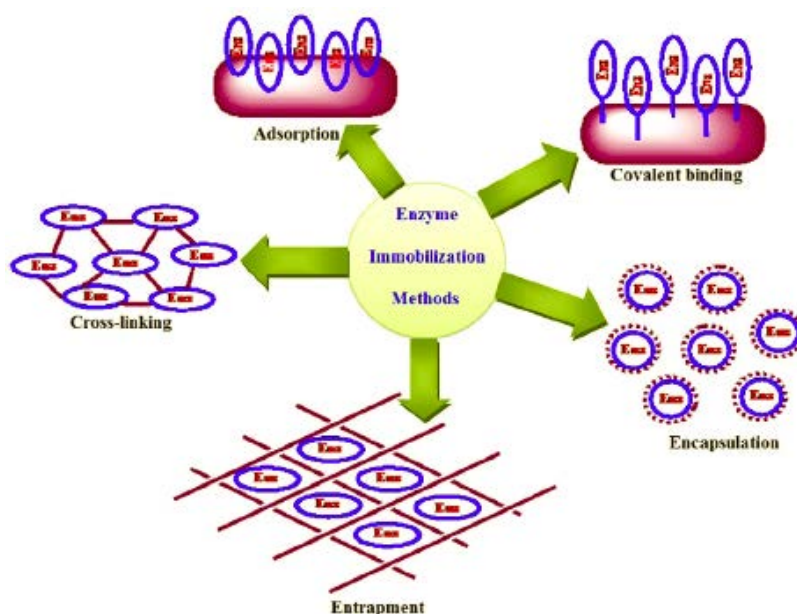


**Fig. 1.4** Basic methods of enzyme immobilisation (Asgher et al., 2014)

### 1.5.1 Adsorption

This method of immobilisation can be considered as the simplest method for enzyme immobilisation since it involves the attachment of enzymes on a solid surface by dipping the material into enzyme solution without additional coupling reagents and surface modification required. Though, this method is the slowest among the available methods of immobilisation. Adsorption method engages with comparatively weak interactions such as electrostatic interactions, hydrogen bonds, van der Waals forces, hydrophobic interactions. Also, the

binding stability is influenced by environmental conditions such as pH, temperature, ionic strength, and biomolecule concentration. Therefore, the proteins immobilised by this method easily stripped off from the support. This fact implies a loss of activity and the contamination of reaction media and thus affects the robustness and recyclability of the immobilised enzymes. In another point, adsorption method normally faces the denaturation of proteins and activity loss caused by steric interaction, which results in conformational changes (Xu et al., 2014).

### 1.5.2 Covalent binding

This method involves covalent binding of the enzyme to the solid support by chemical reaction with covalent linkages or cross-linking reagent. This method is considered effective as the enzyme can be immobilised by multipoint covalent attachment leading to enhancement of activity, stability, and reusability of the enzymes (Asgher et al., 2014). Fig. 1.5 (a,b) shows an ideal covalent binding of enzyme and their support. However, most of the cases, the enzyme tends to encounter the situation in Fig. 1.5 (c, d) which can be overcome by the addition of spacer molecule/arm or coupling agent such as polyethylene glycol (PEG), glutaraldehyde (GA), genipin, 1-ethyl-3-(3-dimethylaminopropyl)carbodiimide hydrochloride (EDC). The addition of spacer arm or coupling agent helps to reduce the steric hindrance by the surface and the substrate, which enhancing the rigidity of the enzyme on the surface that can prevent enzyme denaturation (Talbert and Goddard, 2012). Moreover, the coupling agents are useful as their functional groups (e.g. aldehyde group) can interact with both functional groups of modified support and proteins (Xu et al., 2014). The drawbacks of this method are non-specific immobilisation and the fact that once the activity of the enzyme decays, the support must be discarded as well (Xu et al., 2014).

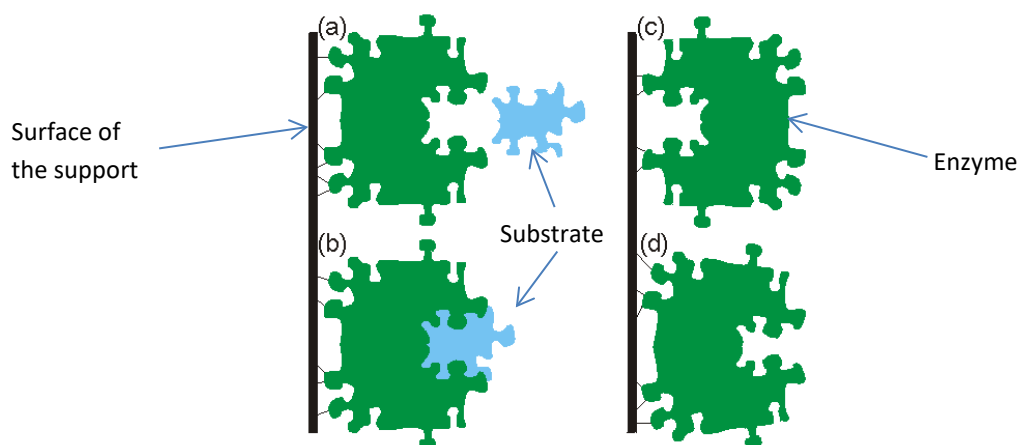


**Fig. 1.5** Effect of covalent binding of enzyme to support; (a) (b) immobilised enzyme with its active site facing outward and ready to accept substrate molecule, (c) non-productive mode due to the attachment of active site to the surface of the support, (d) distortion of active site leads to an inactive immobilised enzyme. (<http://www1.lsbu.ac.uk/water/enztech/immmethod.html>)

### 1.5.3 Encapsulation / entrapment

Encapsulation or entrapment is one of the immobilisation methods that confined or trapped enzymes in the semipermeable membrane, insoluble beads, microspheres, or hydrophobic sol-gels such as calcium alginate beads or gels consist of propyletrimethoxysilane (PTMS) and tetramethoxysilane (TMOS) as shown in Fig. 1.2. This method associates with simple adsorption method which involves ionic interactions, van der Waals forces, and hydrogen bonds. As a matter of fact, this method is preferable rather than other methods due to its straightforward and economical preparation, as well as the high stability of the immobilised enzyme (Asgher et al., 2014). Two types of supports are often implemented, which are hydrophobic and hydrophilic biomaterials. Typically, hydrophobic materials are favourable as they are capable of containing a large number of enzymes and retaining higher activity. The most interesting evidence is the use of sol-gels for enzyme immobilisation. This permit the biotechnology application as their ability to immobilise enzymes in defined thin films that are robust and stable with the structure of entrapped enzymes remains (Asgher et al., 2014).



#### 1.5.4 Cross-linking

This method is known as cross-linked enzyme aggregates (CLEAs) and crosslinked enzymes crystals (CLECs). Cross-linking of enzyme aggregates is reported to be easier in recovery, stable and recyclable (Asgher et al., 2014). CLEAs are economically and environmentally advantageous as they are easily prepared from crude enzyme extracts and can improve operational and storage stability which prevents denaturation by temperature, organic solvents, autoprolysis and leaching in aqueous media (Sheldon, 2011). This method allows co-immobilising of two or more enzymes which make CLEAs able to catalyse various biotransformation reactions, independently or in sequence as catalytic cascade processes (Sheldon, 2011). CLEAs are prepared by using a precipitating agent to precipitate the enzymes, and subsequently, the enzyme aggregates are crosslinking chemically to avoid enzyme re-dissolution after the precipitating agent is removed (Asgher et al., 2014). CLEAs could be used only in organic media if there is a lack of proper crosslinking, on the contrary, the particle could remain insoluble under any reaction conditions (Garcia-Galan et al., 2011). However, there are some setbacks in this method such as low mechanical resistance and severe diffusional limitations (Sheldon, 2011). Since some enzymes with poor superficial Lys residues hinder a proper crosslinking, thus the addition of polymer rich in amino residues (e.g. poly-ethylenimine) may improve the process (López-Gallego et al., 2005).

In a nutshell, to achieve an efficient immobilisation, several aspects has to be considered including the amount of enzyme loading, type of supports, the technique of immobilisation and type of biotechnology process involves.

## Chapter 2

### *Research Objectives*



As a continuation of previous research done in solid state fermentation, the main objective of this thesis is to valorise protein-rich solid wastes using solid state fermentation (SSF) as a medium to produce proteolytic enzymes and utilise them for biotechnological processing.

To cater the main objective, several specific objectives have been established for this research study as follows:

- To produce protease from the protein-rich solid waste of different nature through solid state fermentation (SSF) using a pilot-batch mode operation.
- To investigate the suitable extraction method for protease production in 10 L reactor as it is the most critical downstream processing in solid-state fermentation.
- To evaluate the viability to continue the process until to obtain stable compost-like material.
- To characterise protease obtained regarding pH and temperatures stability and to classify the type of protease by respective inhibitors.
- To examine the ability of protease produced in biotechnological processes such as enzymatic dehairing and also compare it with commercial enzyme and chemical methods used in dehairing.
- To choose suitable support for protease immobilisation by screening several materials including nanoparticles and nanocomposite taking into account the immobilisation efficiency, reusability, and cost effective for the immobilisation process.
- To optimise the enzyme loading per support to avoid the excessive enzyme loading.

- To characterise the most suitable support involving nanomaterials for protease immobilisation.
- To explore different techniques of immobilisation (adsorption and covalent attachment) that suitable to produce an efficient immobilisation in terms of immobilisation yield (% IY), enzyme loading (U/mg), immobilisation efficiency (%), and activity recovery (%).
- To study operational and storage stability of immobilised proteases.
- To determine reusability of immobilised protease by repeating the reaction for several consecutive cycles until the residual activity exhausted.
- To apply immobilised protease in proteins hydrolysis (vegetal and animal sources) to investigate the effectiveness of immobilisation and to check the effect of different protease towards different protein substrate as well.

# Chapter 3

*Materials and Methods*



## **Summary**

This chapter describes all the experimental set-up and the analytical methods used in this research comprised of solid state fermentation, immobilisation, and application of the proteases produced in this study. The materials and methods are explained in details in this chapter, but the process methodology in term of graphical abstract will be specified in each Chapter of Results and Discussion for better illustration.

### **3.1 Materials: Organic solid wastes, bulking agents and reactors used in solid state fermentation (SSF)**

#### **3.1.1 Organic solid wastes and bulking agents**

The main organic solid wastes used throughout this research are hair wastes, soy fibre residues, and anaerobically digested sludge (Fig. 3.1). All of them were acquired from local industries in Barcelona, Spain. The hair waste used in this research was hydrolysed hair produced during the dehairing of bovine hide and obtained from a local tanning industry Pere de Carme tannery located in Igualada (Barcelona, Spain). While the soy fibre residues were obtained after pressing the soya grains during the production of soy milk and derivatives which received from Natursoy, Castelltercol (Barcelona, Spain). Anaerobically digested sludge was used as a co-substrate and inoculum to the SSF process was obtained from a local wastewater treatment plant (Sabadell, Barcelona, Spain). Apart from that, wood chips (Fig. 3.1) were used as a bulking agent to provide an adequate porosity to the mixture during the SSF, was procured from a composting treatment plant (Manresa and Torrelles, Barcelona, Spain).



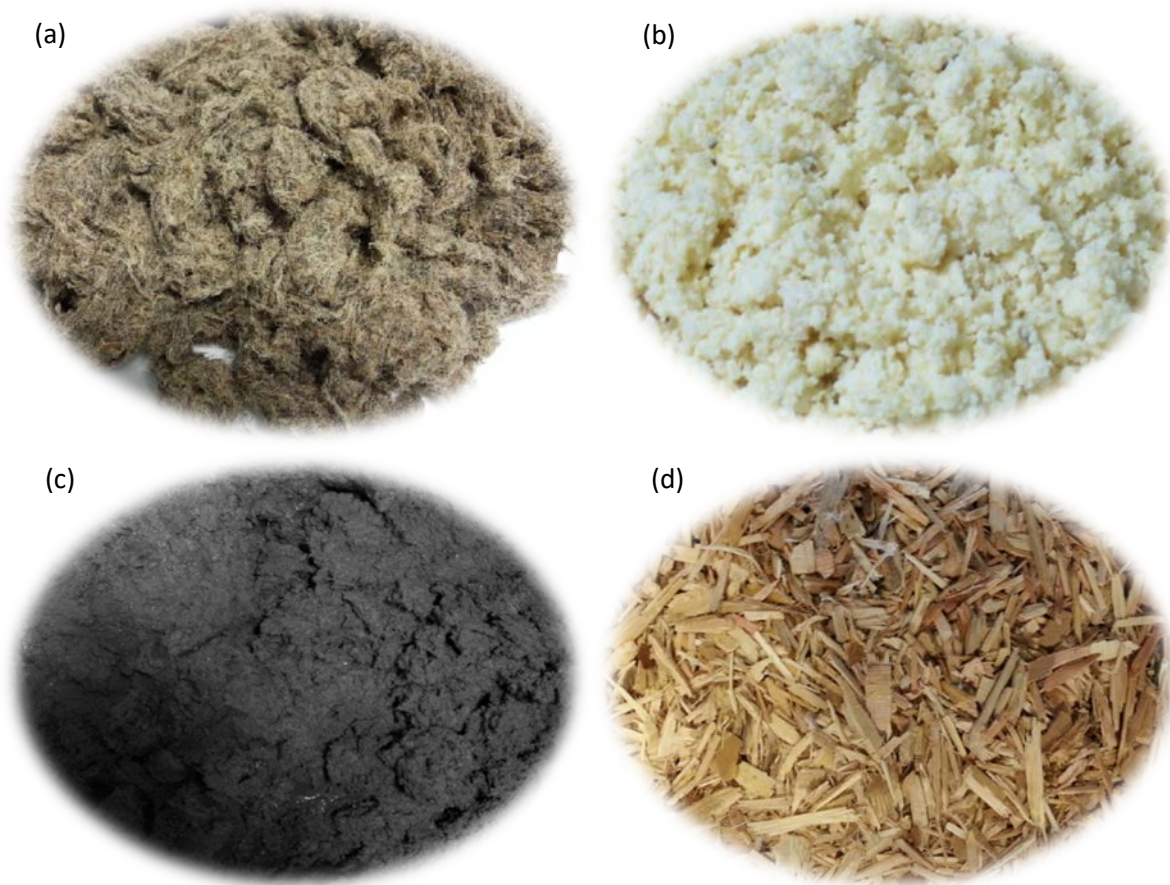


**Fig. 3.1** Organic solid wastes and the bulking agent used for the research (a) hair wastes; (b) soy fibre residue; (c) anaerobically digested sludge; (d) wood chips.

### **3.1.2 General reactors set-up for protease production in SSF**

Before setting up a reactor, the mixture consists of hair waste or soy fibre residues, anaerobically digested sludge (ADS), and bulking agents were prepared with specific quantities. Firstly, hair waste or soy fibre residues and ADS were mixed in a weight ratio of 1:2 as describes in previous studies (Abraham et al., 2014; Barrena et al., 2007a), the mixture was defined as M1. Afterwards, wood chips were used as a bulking agent and mixed to the M1 in a 1:1 volumetric ratio to create the proper porosity in mixtures (Barrena et al., 2007b) and the mixture was denoted as M2 as shown in Fig. 3.2.

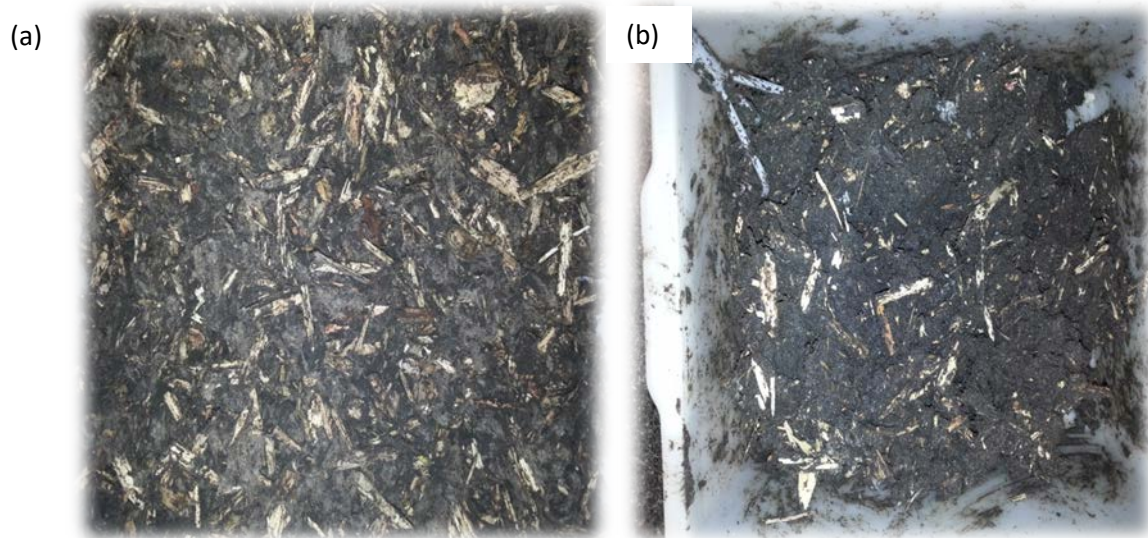


**Fig. 3.2** Initial mixture (M2) of substrates (a) hair waste and ADS; (b) soy fibre residue and ADS; and bulking agents prepared before fermentation process

Several fermentations were carried out under – aerobic environment to ensure the reproducibility of the process. The reactor set-up consists of 10 L airtight reactors that equipped with a temperature probe, oxygen sensors, and water trap (Fig. 3.3). A preliminary fermentation was done to establish a reference profile for protease production in SSF to identify the highest protease production. The mixtures (M2) which approximately 3.7 kg per reactors were prepared in duplicate (C1 and C2) in 10 L air tight reactors and fermented for specified duration according to the type of mixtures content, which was considered as the control experiments. Samples of 100 g were collected at a time interval (e.g. 0, 3, 6, 14, 20, and 23 days) after a manual homogenisation of the entire mass in all reactors.

While the production experiments were prepared with the same composition of the mixture (M2) in triplicate (R1, R2, R3) and fermented in 10 L reactors. These reactors are used to both produce and extract the proteases in the same reactor in the moment of higher protease activity detected in the control experiments.

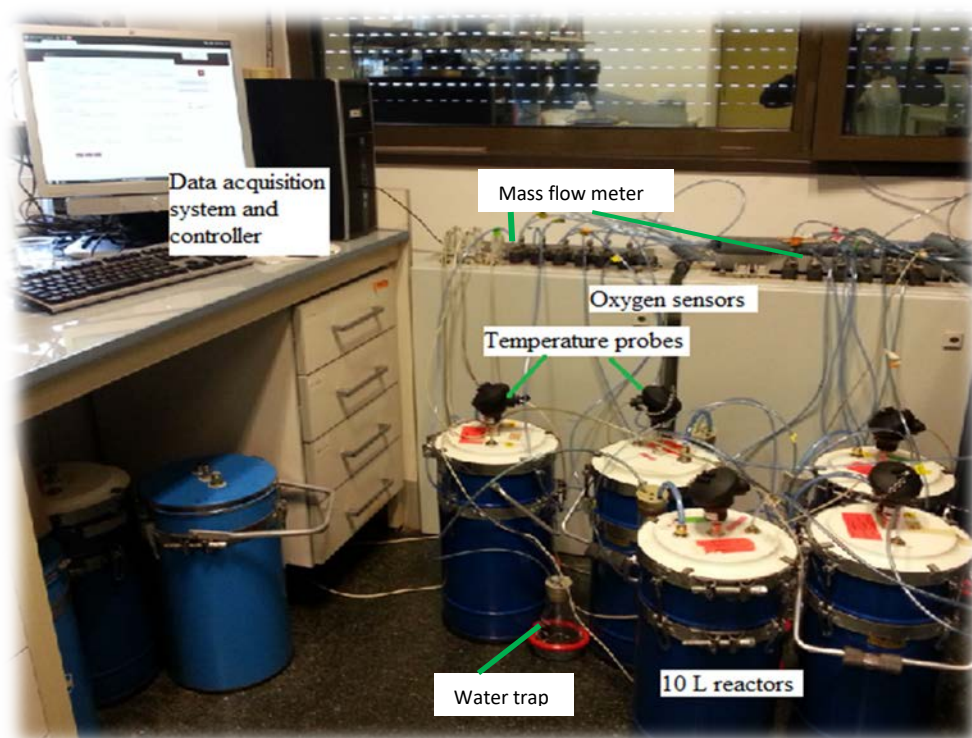


**Fig. 3.3** Solid state fermentation (SSF) experimental set-up using 10 L airtight reactors equipped with data acquisition and sensors for control and monitoring.

The experiments were performed under near-adiabatic conditions with continuous aeration at a minimum rate of 0.1 L/min. The experimental set-up included a data acquisition system with programmable logic controllers (PLC), data reader, and user interfaces for visualisation and experimental controls (Fig. 3.3). Particularly, PLC system consists of a microcontroller that interprets the changes in the difference of voltage potential of the sensors connected to its entries in numerical values, thereby allowing an automatic control and monitoring. It reads the values of oxygen, temperature, and air flow (allows 0-100 ml/min of flow rate).

The controller performs roughly 25 readings per second that are sending a temporal data every second and a real data every minute through serial port interfaces to the reader to build a continuous database from the acquired results. Each PLC controls three sensors of oxygen, three flow meters, and three temperature sensors, which resulting in three dynamic

respiration index (DRI) calculations. The oxygen was regulated using air flow manipulation in the exhaust gas to maintain the system in favourable aerobic conditions (calibrating the oxygen sensor to 20.9% of oxygen in air) as previously described (Puyuelo et al., 2010). The air flow was not supplied excessively to maintain a significant difference between the values of oxygen concentration at the entrance and exit of the material.

### **3.2 Methods for determination of biological stability of organic mixtures**

#### **3.2.1 Dynamic respiration index (DRI)**

The methodology for dynamic respiration index (DRI) determination was as established by previous studies (Adani et al., 2006, 2004; Barrena et al., 2009; Ponsá et al., 2010). The dynamic respirometer set-up as shown in Fig. 3.4 is capable of measuring DRI and cumulative respiration index ( $AT_n$ ) simultaneously. DRI denotes the average oxygen uptake rate for 24 h of maximum biological activity observed during the respirometric assay which indicates the degree of stability of the sample. While,  $AT_n$  is the cumulative oxygen consumption observed for  $n$  days of maximum respiration activity. Both of the indexes are significant to evaluate and characterise the biodegradable organic matters as well as for estimation of process requirements (Ponsá et al., 2010).

Fig. 3.4 shows the experimental set-up consists of three glass reactors of 500 mL and three glass humidifiers placed in a water bath at 37°C coupled with three air mass flow meters independently, three oxygen sensors, and data acquisition system that has been mentioned in Section 3.1.2. The reactor is constructed using an Erlenmeyer flask containing a plastic mesh placed on the floor of the flask that acts as a support to the organic mixture and to create an air distribution chamber as shown in detail of the reactor (Fig. 3.4).

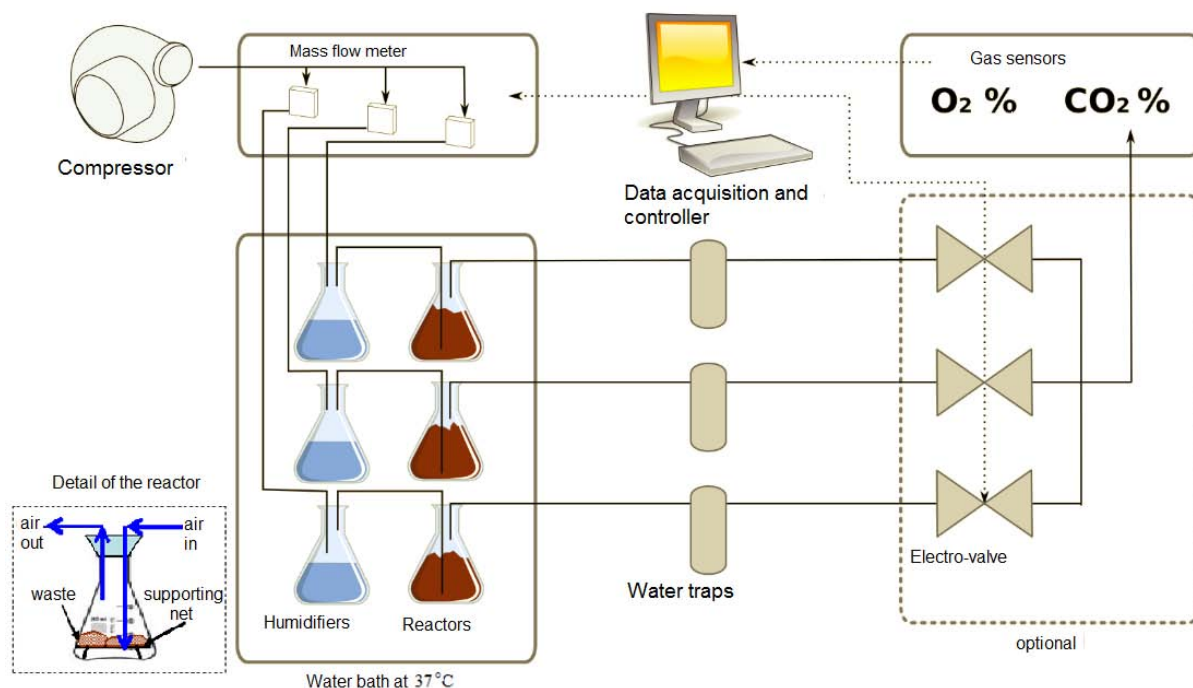


**Fig. 3.4** Experimental set-up of dynamic respirometer for DRI determination

About 100 g of sample was placed in each reactor and incubated at 37°C. The sample was continuously aerated and controlled by airflow controller to provide constant airflow. Exhaust air from the reactors was sent to an oxygen sensor. To build a database for dynamic respiration index, data acquisition system continuously recording values from mass airflow meters and oxygen sensors. By using the recorded database the DRI and  $AT_n$  can be calculated using Eq. 3.1 and Eq. 3.2, respectively (Ponsá et al., 2010).

$$DRI_t = \frac{(O_{2,i} - O_{2,o}) \times F \times 31.98 \times 60 \times 1000^a}{1000^b \times 22.4 \times DM} \quad (\text{Eq. 3.1})$$

Where  $DRI_t$  is dynamic respiration index for a given time  $t$ ,  $\text{mg O}_2 \text{ g}^{-1} \text{ DM h}^{-1}$ ;  $(O_{2,i} - O_{2,o})$  is difference in oxygen content between airflow in and out the reactor at that given time;  $F$  is volumetric airflow measured under standard conditions (1 atm and 273 K),  $\text{mL min}^{-1}$ ; 31.98 is oxygen molecular weight,  $\text{g mol}^{-1}$ ; 60 is conversion factor,  $\text{min h}^{-1}$ ;  $1000^a$  is conversion factor,  $\text{mg g}^{-1}$ ;  $1000^b$  is conversion factor,  $\text{mL L}^{-1}$ ; 22.4 is volume occupied by one mole of ideal gas under normal conditions, L;  $DM$  is dry mass of sample loaded in the reactor, g.

$$AT_n = \int_{t_l}^{t_l+n} DRI_t \cdot dt \quad (\text{Eq. 3.2})$$

Where  $AT_n$  is cumulative oxygen consumption in  $n$  days,  $\text{mg O}_2 \text{ g}^{-1} \text{ DM}$ ;  $t_l$  is a time when lag phase finishes. Lag phase ends when oxygen uptake rate reaches 25% of the maximum uptake rate calculated as the average of 3 h (Federal Government of Germany, 2001).

A DRI curve can be constructed, and  $AT_n$  can be calculated based on data collected on-line as shown in Fig. 3.5.

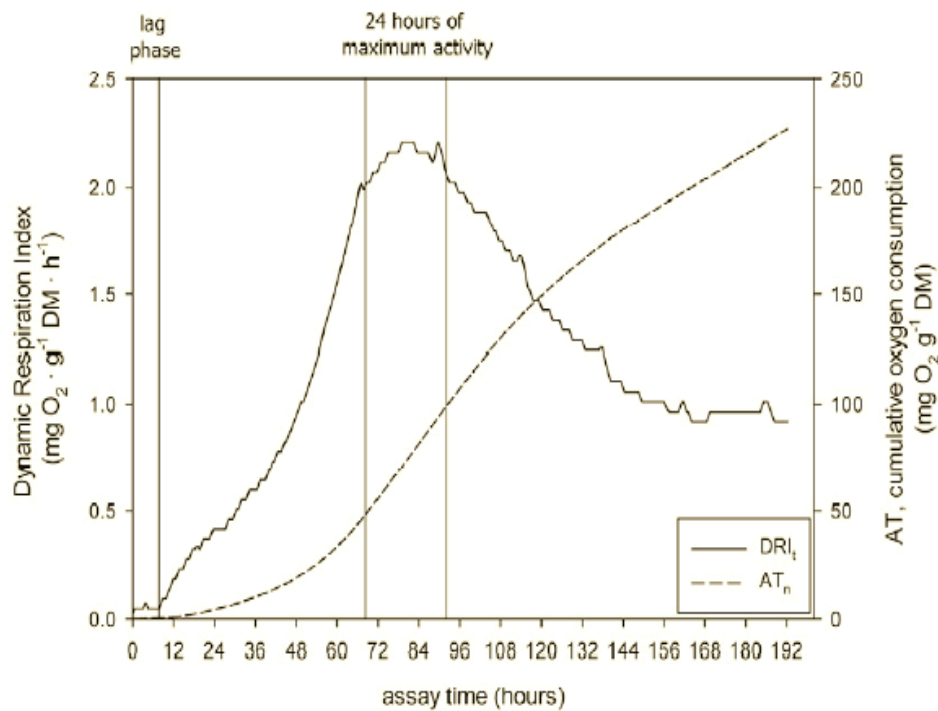


**Fig. 3.5** Typical curve for dynamic respiration index evolution and calculation (Ponsá et al., 2010)

### 3.2.2 Oxygen uptake rate (OUR)

In the biological system, the oxygen uptake rate (OUR) can be used as an indirect measure of biological activity during the fermentation process. During SSF process, DRI is an analytical procedure used to assess the stability of organic sample, and OUR is used as a process parameter that can be monitored on-line (Gea et al., 2004). For monitoring in this

work, we are calculating the average specific oxygen uptake rate for 1h and 24 h ( $sOUR_1$  and  $sOUR_{24}$ ) using following equation (Eq. 3.3):

$$sOUR (gO_2kg^{-1}DMh^{-1}) = \frac{(O_{2,i} - O_{2,0}) \times F \times 31.98 \times 60}{22.4 \times DM} \quad (\text{Eq. 3.3})$$

Where,  $sOUR$ : specific oxygen uptake rate;  $(O_{2,i} - O_{2,0})$ : the difference in the oxygen content (volumetric fraction) between airflow in (0.209) and out of the reactor at the given time;  $F$  volumetric airflow measured under standard conditions (1 atm and 273 K)( $L \text{ min}^{-1}$ ); 31.98: the molecular mass of oxygen, ( $g \text{ mol}^{-1}$ ); 60: the conversion factor for minutes to hours; 22.4: the volume occupied by 1 mol of gas under the normal conditions;  $DM$ : dry matter of sample loaded in the reactor (kg).

### 3.3 Standard Analytical Methods

Standard analytical methods were determined according to the standard procedures (The USDA and the US Composting Council, 2001) with triplicates of each sample.

#### 3.3.1 Total solid content (TS) and moisture content (MC)

Total solid content (TS) which is corresponding to dry matter (DM) was determined by drying the sample in an oven at  $105^\circ\text{C}$  for 24 h. The weights of the samples were taken before and after drying. The TS and moisture content (%) were calculated using Eq. 3.5 and Eq. 3.6:

$$TS(\%) = 100 - \frac{M_w - M_d}{M_w - M_0} \times 100 \quad (\text{Eq. 3.5})$$

$$MC(\%) = 100 - TS(\%) \quad (\text{Eq. 3.6})$$

Where,  $M_w$ : a wet mass of samples, (g);  $M_d$ : a dry mass of samples, (g);  $M_0$ : a mass of empty container, (g).

### 3.3.2 Volatile solid content (VS)

Volatile solid content (VS) which is corresponding to organic matter (OM) was obtained by sample ignition in a furnace at 550°C for 4h. The VS (%) was expressed as follows (Eq. 3.7):

$$VS(\%) = \frac{M_d - M_a}{M_d - M_0} \quad (\text{Eq. 3.7})$$

Where,  $M_d$ : a dry mass of samples, (g);  $M_a$ : a mass of ashes of the samples, (g);  $M_0$ : a mass of empty container, (g).

### 3.3.3 Bulk density

Bulk density (BD) was determined on a wet basis dividing the sample weight by the sample volume and expressed as follows (Eq. 3.4):

$$BD_w(kg \cdot L^{-1}) = \frac{M_s}{V_s} \quad (\text{Eq. 3.4})$$

Where,  $M_s$ : a mass of the sample, (kg);  $V_s$ : volume of sample, (L).

### 3.3.4 pH and electric conductivity (EC)

The slurry of tested material and deionised water was mixed at a ratio of 1:5 (v/v). The sample mixture was agitated for 30 min at 25°C to obtain a homogeneous mixture. The pH was measured using an electrometric pH meter (Crison, microPH200), the pH probe was dipped directly in the slurry or the extracted solution. Electrical conductivity (EC) was measured by an electrical conductometer (Crison, microCM2100) using the sample aforementioned.



### 3.3.5 Total Organic Carbon (TOC)

Total organic carbon (TOC) content was determined using a Solid TOC Analyzer O.I. Analytical Instrument. About 0.5 g of dried and granulated sample was placed in a quartz cup that has been pre-heated at 950°C. Carbonates were eliminated by adding one drop of HCl into the quartz cup containing the sample. Then the sample was put into the instrument and burned at 950°C. A CO<sub>2</sub> infrared detector quantified the CO<sub>2</sub> produced by the ignition of the sample carbon content. The results were expressed as mg of C.

### 3.3.6 Total Kjeldahl Nitrogen (TKN)

The organic nitrogen content as Kjeldahl nitrogen (TKN) was determined using 0.5 g of dried and milled sample. The sample was digested at 400°C for 1.5 h using 20 mL of H<sub>2</sub>SO<sub>4</sub> (96%) in 300 mL glass Kjeldahl tubes using a block digester with six posts (J.P. Select S.A., Barcelona, Spain). Before the acid digestion, a catalyst (Kjeltab<sup>®</sup>) was added. After the acid digestion, a Büchi Distillation Unit K-355 (Flawil, Swiss) was used for sample distillation with an excess of NaOH solution (35%). The condensate was collected in a glass flask containing 100 mL of boric acid (4%) with indicator 4,4, mixed (methyl red – methylene blue) RV. The solution was titrated with HCl to determine nitrogen content. The TKN was expressed using following equation (Eq. 3.8).

$$TKN(\%) = \frac{(V_s - V_c) \times N \times 1.4}{M_{db}} \quad (\text{Eq. 3.8})$$

Where, V<sub>s</sub>: volume of consumed HCl in sample titration, (mL); V<sub>c</sub>: volume of consumed HCl in control titration, (mL); N: normality of the HCl; M<sub>db</sub>: a mass of the sample, dry basis (g).

### 3.3.7 Ammonia soluble content

The inorganic nitrogen content denoted as  $N-NH_4^+$  was determined on a fresh sample. A fresh solid sample was placed in a flask with an extraction solution of KCl 1M at ratio 1:5 (v/v) and hermetically sealed. The solution was agitated for 30 min at room temperature. Then, an aliquot of 10 mL was poured in a Kjeldahl glass tube. A Büchi Distillation Unit K-355 (Flawil, Swiss) was used for sample distillation with an excess of NaOH solution (10%). The condensate was collected in a glass flask containing 100 mL of boric acid (4%) with indicator 4,4, mixed (methyl red – methylene blue) RV. The solution was titrated with HCl to determine the nitrogen content. The  $N-NH_4^+$  was expressed using following equation (Eq. 3.9).

$$N - NH_4^+ (mg \cdot kgW_w^{-1}) = \frac{(V_s - V_c) \cdot 1000 \cdot N \cdot 14 \cdot D}{M_w} \quad (\text{Eq. 3.9})$$

Where,  $V_s$ : volume of consumed HCl in sample titration, (mL);  $V_c$ : volume of consumed HCl in control titration, (mL); N: normality of the HCl; D: dilution factor (volume of extraction solution/volume of sample distilled);  $M_w$ : mass of sample, wet basis (g).

## 3.4 Methods for enzymes and protein determination and characterisation

### 3.4.1 Enzyme extraction

Typically, about 10 g of homogenised solid samples were taken from the reactors at different days of SSF, as explained in the previous section. Unless specified otherwise, for extraction, the samples were mixed with 50 mM HCl – Tris buffer (pH 8.10) at 1:5 (w/v) ratios for 45 min at room temperature and then centrifuged at 10 000 rpm for 10 min. The supernatant was collected and filtered through a 0.45  $\mu\text{m}$  filter to be used as crude enzyme extract for further used. All the extractions were done in triplicates.

For protease production experiments, the extraction was done directly in the reactors. The reproducibility of proteases was determined by an extraction of the whole fermented mass in triplicate of 10 L reactors at day 14 of SSF for experiments with hair waste and ADS as substrates, while for experiments with soy residue and ADS the extraction time was after day 3 of SSF. Those times were selected as the highest production of protease according to the protease profile showed in control experiments. In this mode of extraction, the entire batch was submerged in each reactor with 50 mM HCl – Tris buffer (pH 8.10) at 1:1 (v/v) ratio for 1h (Fig. 3.6 (a)). Then the extracts were sieved with 2.0 mm stainless steel sieve and centrifuged as aforementioned (Fig. 3.6 (b)). The supernatant was taken as the crude enzyme extract (Fig. 3.6 (c)), whereas the remaining solid residues continued the SSF process until 42 days (for SSF with hair waste) and 12 days (for SSF with soy fibre residue) for final matter stabilisation.



**Fig. 3.6** Extraction of whole fermented materials in a single reactor, (a) air bubble supplied to extract the bioproduct from the solid substrate; (b) stainless steel mesh used to separate the solid and liquid extract; (c) image of crude protease extract.

### 3.4.2 Lyophilisation and enzyme concentration by ultrafiltration

The crude enzyme extract obtained after the extraction was frozen at  $-80^{\circ}\text{C}$  before lyophilisation using a vacuum with a bench top VirTis Sentry 5L freeze dryer (Fig. 3.7). The

frozen samples were attached to quick seal valves on stainless steel drum manifolds. The lyophilisation process lasts approximately 24 h. The lyophilised extracts were collected and preserved at 4°C for further use.



**Fig. 3.7** Lyophilisation using a vacuum bench top VirTis Sentry 5 L freezes dryer.

The crude extracts were concentrated using Amicon<sup>®</sup> Ultra-15 centrifugal filter devices (Millipore, Ireland) with 10k molecular weight cut-off (MWCO) Ultracel<sup>®</sup> low-binding regenerated cellulose membrane. The concentrated ultrafiltered liquid was recovered and stored for further experiments of protease characterisation. In these processes, recovery yield is defined as the percentage of residual activity on the initial activity of crude extract, whereas purification fold is the quotient between specific enzymatic activities after purification on the specific activity of the initial crude extract.

### **3.4.2 Protease activity assay**

The proteolytic activity of the protease was determined using casein as a substrate according to the method described by Alef and Nannipieri (Alef and Nannipieri, 1995) with slight modifications. There were several reaction solutions need to be prepared beforehand as follows:

- *Tris buffer (50 mM, pH 8.1)*

About 6.05 g Tris-(hydroxyl methyl) aminomethane was dissolved in 700 mL Milli-Q water. Subsequently, the pH was adjusted to 8.1 with HCl, and then Milli-Q water was added to make up the volume to 1000 mL and stored at 4°C until further use.

- *Sodium caseinate (2%)*

10 g of sodium caseinate was dissolved in 500 mL warm Milli-Q water at 50°C. The slurry was mixed homogeneously. The solution needs to be freshly prepared.

- *Trichloroacetic acid (TCA, 15%)*

75 g of crystalline TCA was dissolved in 300 mL Milli-Q water. Then the volume was made up to 500 mL and stored at 4°C until further use.

- *Alkaline reagent*

There were three reaction solutions need to be prepared individually and mixed freshly during the assay as an alkaline reagent. Firstly, 60 mL of NaOH (1M) was diluted with Milli-Q water before adding 50 g of NaCO<sub>3</sub> anhydrous. Milli-Q water was added to make up the volume to 1000 mL (Sol1). The second reagent was prepared by dissolving 0.5 g CuSO<sub>4</sub>·5H<sub>2</sub>O in 100 mL of Milli-Q water (Sol2). The third reagent was prepared by dissolving 1 g potassium sodium tartrate (C<sub>4</sub>H<sub>4</sub>KNaO<sub>6</sub>·4H<sub>2</sub>O) in 100 mL Milli-Q water (Sol3).

The alkaline reagent was prepared by mixing 1000 mL of Sol1 with 20 mL of Sol2 and 20 mL of Sol3.

- *Folin – Ciocalteu reagent (25%)*

One part of the reagent was diluted with three parts of Milli-Q water. The dilution needs to be prepared for 5 min before use.

- Tyrosine standard solution ( $500 \text{ ug mL}^{-1}$ )

The standard solution was prepared by dissolving 50 mg of tyrosine in 100 mL of Tris buffer

Briefly, 1 ml of the enzyme extract was added into 4 mL Tris buffer (pH 8.1). Then, 5 ml of a 2% (w/v) casein solution was added to the mixture and incubated at 50°C with 100 rpm for 1 hour. The reaction was terminated by adding 5 ml of 15% (w/v) TCA. The samples were centrifuged at 10,000 rpm for 10 min at 4°C. An aliquot of 0.5 ml of the supernatant was added to the alkaline reagent and incubated for 15 min at room temperature before the addition of 0.5 ml of 25% (v/v) Folin-Ciocalteu phenol reagent. The resulting solution was incubated at room temperature in the dark for 1h. The absorbance was measured at 700 nm using a tyrosine standard. One unit of alkaline protease activity was defined as the liberation of 1 µg of tyrosine per minute under the assay conditions. All activity tests were performed in triplicate. The calibration curve was established by using standard tyrosine solution and following all the assay procedure excluding only the incubation part. The standard calibration curve was presented in the annexe (A.1). The protease activity in this work was calculated using Eq. 3.10 and Eq. 3.11.

$$PA (UmL^{-1}) = \frac{C \times 15}{1 \times t \times v} \quad (\text{Eq. 3.10})$$

$$PA(Ug^{-1}DM) = \frac{C \times 15 \times f}{t \times DM} \quad (\text{Eq. 3.11})$$

$$sPA(U \text{ mg}^{-1} \text{ protein}) = \frac{\text{total activity (U)}}{\text{total soluble protein (mg)}} \quad (\text{Eq. 3.12})$$

Where, PA: protease activity; sPA: specific protease activity; U: activity unit; C:  $\mu\text{g}$  tyrosine; 15: total volume of assay, (mL); 1: volume of enzyme used, (mL); t: time of incubation, (min); v: volume in colorimetric determination, (mL); f: factor conversion considering the extraction from the solid sample; DM: the dry weight of the sample, (g); total soluble protein was determined from Bradford or Lowry assay.

### 3.4.3 Total soluble protein – Bradford assay, Lowry assay

In standard Bradford assay, the protein determination was done by mixing 1 part of protein sample with 30 parts of the Bradford Reagent (Sigma-Aldrich, 2012). The sample was a blank, a protein standard, or a protein sample. The blank consisted of a buffer with no protein. The protein standard consists of a known concentration protein. Bradford reagent is stored at  $2 - 8^{\circ}\text{C}$  and the assay was performed at room temperature to begin the colour development. The absorbance was measured at 595 nm, and the protein concentration was determined by comparing to the standard curve. In this work, we were used Standard 3.1 ml assay protocol, which enables to do an assay directly in a cuvette by adding just 1.5 mL of Bradford Reagent to 0.05 mL of sample (Sigma-Aldrich, 2012). The Bradford Reagent was brought to room temperature and gently shaken prior the assay.

In Lowry assay, protein was determined by the modified method of Lowry (Lowry et al., 1951) using bovine serum albumin (BSA) as a standard protein. In this assay, three reactions solution were prepared as a Lowry solution (SolA + SolB + SolC) with a ratio of 100:1:1 volume basis, respectively. For SolA about 2.86 g of NaOH and 14.31 g of  $\text{Na}_2\text{CO}_3$  were dissolved in 500 mL of deionized water. SolB was prepared by dissolving 1.42 g of  $\text{CuSO}_4 \cdot 5(\text{H}_2\text{O})$  in 100 mL of deionized water. SolC was prepared by dissolving 2.86 g in 100 mL of  $\text{Na}_2\text{Tartrate} \cdot 2(\text{H}_2\text{O})$  in 100 mL of deionized water. Folin Reagent was freshly prepared every assay by mixing 5 mL of 2N Folin and Ciocalteu's Phenol Reagent with 6 mL of

deionized water. The assay was initiated by mixing 0.5 mL sample with 0.7 mL of Lowry solution. Then the sample mixture was incubated for 20 min at room temperature in dark condition. After 20 min of incubation, the sample mixture was immediately added to 0.1 mL of Folin Reagent and mixed vigorously. Subsequently, the mixture was incubated for 30 min at room temperature in dark condition again. After the incubation, the mixture was vortex briefly, and the absorbance was measured shortly. The protein content was estimated by measuring the absorbance at 750 nm using Varian Cary® 50 UV-visible spectrometers.

The protein standard curve was established by serially diluted 2 mg ml<sup>-1</sup> BSA protein standard as shown in Annex 1 (A.2 for Bradford assay and A.3 for Lowry assay).

#### **3.4.4 Amino acid determination using Ninhydrin method**

Ninhydrin method is used to detect amino acid by colour development. Originally, the colour of ninhydrin solution is yellow and will turn to deep purple. It reacts with a free alpha – amino group, NH<sub>2</sub>-C-COOH which present in amino acids, peptides, or proteins. However, the decarboxylation reaction will only carry on in free amino acid which neither occurs in proteins nor peptides (Gohel et al., 2006). The ninhydrin reagent was freshly prepared by dissolving 8 g of ninhydrin in 100 mL of acetone. 1 mL of sample was put into a capped test tube and diluted with deionized water up to 4 mL. The blank was prepared with protein solution in the absence of protease. Then, 1 mL of ninhydrin reagent was added to each tube, and the contents were mixed well. Subsequently, the capped test tubes were placed in boiling water for 15 min. Later, the test tubes were placed in cold water, and 1 mL of ethanol was added to each tube and mixed well. The absorbance was read at 570 nm using a spectrophotometer. The measurement was compared with the calibrating curve of amino acid standard (Gohel et al., 2006).



### 3.4.5 Degree of hydrolysis

The degree of hydrolysis was determined by quantifying the soluble protein content after precipitation with TCA (Silvestre et al., 2013; Sinha and Khare, 2015). 1ml of protein hydrolysate was mixed with 1 ml of 10% (w/v) TCA and incubated at 37°C for 30 min to allow for precipitation followed by centrifugation (10,000 x g, 10 min). Then, the soluble protein content in the supernatant was determined by the Lowry method (Lowry et al., 1951), and the soluble protein content was expressed in milligrammes (mg). The degree of hydrolysis (DH) was determined using the following equation (Eq.3.13):

$$DH(\%) = \frac{\text{soluble protein content in 10\% TCA}}{\text{total protein content}} \times 100 \quad (\text{Eq. 3.13})$$

Where, DH: degree of hydrolysis; TCA; Trichloroacetic acid.

### 3.4.6 Characterisation of the hydrolysate using liquid chromatography-mass spectroscopy (LC-MS)

The liquid chromatography-mass spectroscopy (Shimadzu LCMS-2010) (Fig. 3.8) was used for hydrolysate characterisation of amino acids using Atmospheric Pressure Chemical Ionisation (APCI) coupled with electrospray ionisation (ESI). Sample molecules are ionised at atmospheric pressure from a highly charged aerosol, and then the ions are electrostatically extracted to the mass analyser. The sample ions are separated according to the mass-to-charge ratio (m/z) and amplified by the signal detector, then analysed by processing software, LCMS solution. The analysis time for all 20 amino acids was 30 minutes and correlated with an amino acids standard solution from Sigma-Aldrich. The amino acids fragments were full scan using TIC (total ion current) and characterised using ions in SIM (selected ion monitoring) mode that can scan over a small mass range,

specifically one mass unit. The characteristic fragment of amino acids in SIM mode used for quantification was tabulated in Table 3.1.

The hydrolysate was analysed by injecting 2  $\mu\text{L}$  of sample into Aeris Peptide 5U XB-C18 column (Micron-Phenomenex, USA) with core-shell of 3.6  $\mu\text{m}$  (100  $\text{\AA}$ , 250 x 4.6 mm). The separations were performed using the mixture of 0.01 mM acetic acid in 0.2% aqueous solution of a formic acid at a flow rate of 0.2  $\text{mL min}^{-1}$ . The critical MS conditions were as follows: positive APCI ionisation mode, 300°C drying gas temperature, 1.5  $\text{L min}^{-1}$  drying gas flow rate, 21 bar nebuliser gas pressure, 1.5 kV capillary voltage, 20 V skimmer voltage, and 55 V fragment voltage.



**Fig. 3.8** Image of the liquid chromatography-mass spectrometry (Shimadzu LCMS-2010)

**Table 3.1** Amino acids quantification during LC-MS analysis using positive APCI ionisation mode in SIM mode

Constituent	mol wt.	ion m/z
Glycine (gly)	75.1	76
Alanine (ala)	89.1	90
Serine (ser)	105.1	106
Proline (pro)	115.1	116
Valine (val)	117.2	118
Threonine (thr)	119.1	120
Cysteine (cys)	121.2	122
Cystine (cys-cys)	240.3	241
Hydroxyproline (hyp)	131.1	132
Leucine-isoleucine (leu-ile)	131.1	132
Asparagine (asn)	132.1	133
Aspartic acid (asp)	133.1	134
Glutamine (gln)	146.2	147
Glutamic acid (glu)	147.1	148
Lysine (lys)	146.2	147
Methionine (met)	149.2	150
Histidine (his)	155.2	156
Phenylalanine (phe)	165.2	166
Arginine (arg)	174.2	175
Tyrosine (tyr)	181.2	182

### 3.4.7 Polyacrylamide electrophoresis gel (PAGE)

Theoretically, protein electrophoresis is the movement of proteins within an electric field, and it is widely used to separate proteins for analysis and purification purposes. Protein separation electrophoresis was performed in a polyacrylamide gel (PAGE) which serves as a size-selective sieve, covering a protein size range of 5 – 250 kD. The proteins move through a gel due to the electric field, where the pore structure of the gel allows smaller proteins to travel faster than the larger proteins as shown in Fig. 3.9.

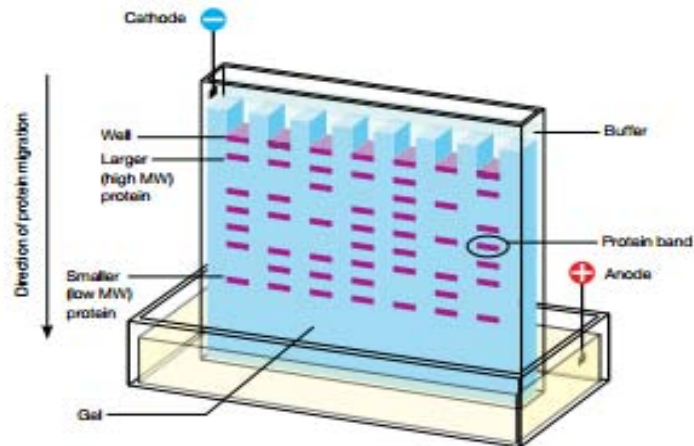


**Fig. 3.9** Schematic of electrophoretic protein separation in a polyacrylamide gel-based on molecular weight, MW. (Source: Bio-rad.com)

- *Native PAGE*

In this system, proteins are prepared in nonreducing, nondenaturing sample buffer, and the PAGE is performed in the absence of denaturing and reducing agents. The native charge-to-mass ratio and the interaction of proteins are preserved during separation; make proteins move in random manners as they can move according to their charge. Thus, this system is not suitable for molecular determination. However, it allows the separation of proteins in their active state that can determine proteins of the same molecular weight (Bio-Rad, 2012).

Typically, the 12% (w/v) Mini-PROTEAN polyacrylamide gel was used using running buffer Tris/Glycine 1X (dilute 100 mL of buffer 10X with 900 mL of Milli-Q water). The sample was prepared by adding 1 part of the sample to 2 parts of sample buffer. Then 15  $\mu$ L of the samples were load into each well (Fig. 3.5) and one well was set for the standard molecular marker as a reference (Precision Plus Protein<sup>TM</sup> Dual Color standard). The voltage was set to 150 V and let it running until the samples reach the bottom of the gel. After that, the gel was removed from the plastic covers and washed three times with Milli-Q water before staining the gel with Bio-Safe Coomassie G-250.

- *SDS-PAGE*

In this system, the electrophoresis was performed in the presence of sodium dodecyl sulphate (SDS) and reducing agents such as 2- $\beta$ -mercaptoethanol. The addition of the detergent is to disrupt hydrophobic interactions between and within proteins, while the reducing agent disrupts intramolecular and intermolecular disulphide bonds. These characteristics enable the protein to be separated by its size and suitable to estimate molecular weight (Laemmli, 1970).

The basic procedure is the same with the Native PAGE except that the running buffer used was Tris/Glycine/SDS 1X. The sample was prepared by adding 15  $\mu$ L of the sample to 5  $\mu$ L of sample buffer 4X which consists of Tris-HCl 125 mM (pH 6.8), 4% w/v SDS, 10% w/v bromophenol, and 10% v/v 2- $\beta$ -mercaptoethanol. Prior to sample loading into the well, the samples were heated at 90°C for 5 min, followed by vortexing and centrifugation at 14000 x g for 1 min. Until here, the procedure then follows the Native PAGE.

Tricine-SDS PAGE was used to observe the pattern of smaller proteins generated after the hydrolysis reaction. Electrophoresis was performed using 10-20% Mini-PROTEAN Tris-Tricine gels under denaturing and reducing conditions. The reduction was achieved by heating the sample at 90°C for 5 min in the presence of  $\beta$ -mercaptoethanol (2% v/v). The gel was fixed with methanol (40% v/v) and acetic acid (10% v/v) and subsequently stained with Coomassie Brilliant Blue R-250. Then, the gel was destained with a solution containing methanol, acetic acid, and water (20: 4: 26 v/v).

- *Zymogram PAGE*

Zymogram PAGE is used to detect and characterise collagenases and proteases. The electrophoresis was performed using gelatin or casein as a substrate for the enzymes that are separated in the gel under nonreducing conditions. The procedure is following the same as Native PAGE procedure. The gel was incubated with the casein 2% for 1 h at 50°C before stain using Coomassie Brilliant Blue R-250 stain, which then leaving clear areas around active proteases.

### **3.4.8 Effect of pH and temperature (T) on protease stability**

The stability of the enzyme was determined by incubating the protease for 1 h at different temperatures range from 30°C – 70°C and pH range at 5 – 11. The pH values were prepared using the following buffers: Acetic acid-sodium acetate 1 M (pH 5), Tris-HCl 1 M (pH 8), Tris-NaOH 1 M (pH 11). The stability was analysed using the Design – Expert software (version 6.0.6) using a full central composite design (CCD) that consisted of 13 experimental points, including five replications at the central point and four star points ( $\alpha = 1$ ). Residual activity was selected as objective function (in %) for each pH and temperature tested assuming that the initial activity of the enzyme is 100%.

### **3.4.9 Inhibition study**

The effect of various protease inhibitors such as phenylmethylsulfonyl fluoride (PMSF), trans-epoxysuccinyl-L-leucylamido-(4-guanidino)butane (e64), pepstatin A, and ethylene diamine tetraacetic acid (EDTA) was determined by the addition of the corresponding inhibitors at 1 mM and 10 mM (final concentration) to the aliquot of the protease. The reaction mixtures were preincubated at 37°C for 1 h without the substrate

fraction and assay under the standard conditions. The recorded residual activities were compared with that of the control (without inhibitors).

### 3.5 Methods for support/carrier synthesis for enzyme immobilisation

The proteases produced using SSF were immobilised on different supports/carrier to study their biocompatibility and to enhance the stability of the enzyme by using a different type of immobilisation.

#### 3.5.1 Magnetic nanoparticles (MNPs)

Magnetic nanoparticles (MNPs) were synthesised by co-precipitation in the water phase as described previously (Abo Markeb et al., 2016; Hu et al., 2015) with slight modifications. A mixture of 25 mM ferrous sulphate ( $\text{FeSO}_4 \cdot 7\text{H}_2\text{O}$ ) and 50 mM of ferric chloride ( $\text{FeCl}_3 \cdot 6\text{H}_2\text{O}$ ) were dissolved in 100 ml of Milli-Q water with the addition of 0.1% of CTAB as a stabiliser. The mixture was stirred at 40°C for 1 hour under the nitrogen atmosphere. Then, 125 ml of deoxygenated NaOH (0.5 M) was added dropwise to the mixture. The mixture was stirred for 1 hour at 40°C to let the solution chemically precipitate. The resultant MNPs were separated magnetically and washed five times with Milli-Q water (Fig. 3.10). The recovered MNPs were dried overnight at 60°C.



**Fig. 3.10** Magnetic nanoparticles separated using a magnetic drive and final product after dried

### 3.5.2 Titanium oxide nanoparticles (TiO<sub>2</sub>)

Titanium oxide nanoparticles (TiO<sub>2</sub>) was synthesised following previous procedure (Pottier et al., 2003) with slight modifications. Two stocks solution of different Ti<sup>4+</sup> ion concentration (TiO<sub>2</sub>\_A and TiO<sub>2</sub>\_B) were prepared by dissolving TiCl<sub>4</sub> in 10 mL of 3 M HCl that resulted to 0.7 M (5g of Ti) and 0.35 M (2.5g of Ti) of Ti<sup>4+</sup>, respectively. Then, each stock solution was diluted with pre-heated 60 mL Milli-Q water at 60°C resulting in Ti<sup>4+</sup> ion concentration of 0.1 M and 0.05 M correspondingly. Subsequently, the pH was adjusted to pH 5 using 0.5 M NaOH. The suspensions were aged at 60°C without stirring for 1 h. The solid formed after precipitation was separated by centrifugation at 6000 rpm and washed three times with Milli-Q water (pH 5). Titanium nanoparticles (white solid precipitate) (Fig. 3.11), were dried at 80°C for 24 h.

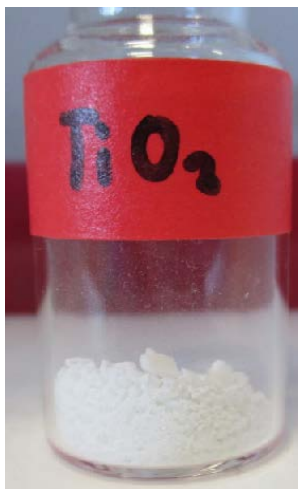


**Fig. 3.11** Titanium oxide nanoparticles after dried at 80°C for 24 h

### 3.5.3 Gold nanoparticles (AuNP)

Gold nanoparticles (AuNP) was synthesised according to a previous study (Bastus et al., 2011). Prior to the AuNP synthesis, 10 mM stock solution of chloroauric acid (HAuCl<sub>4</sub>) was prepared by dissolving 1.0 g HAuCl<sub>4</sub>·3H<sub>2</sub>O in 250 mL Milli-Q water and kept in an



amber bottle at 4°C. Firstly, 150 mL of 2.2 mM sodium citrate solution was heated at 70°C for 15 min. Then, 100 mL of 1.0 mM HAuCl<sub>4</sub> from the stock solution was added into preheated sodium citrate solution under continuous mixing. Colour development from yellow to bluish grey and later to ruby-red was observed (Fig 3.12).

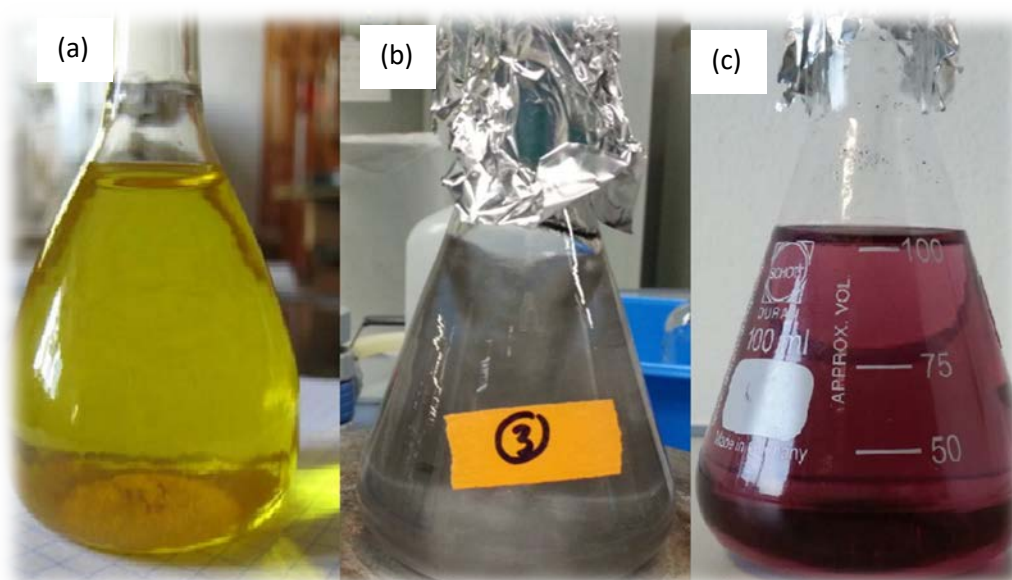


**Fig. 3.12** Colour development during gold nanoparticles synthesis, (a) stock solution of HAuCl<sub>4</sub>; (b) reduced form of a gold solution; (c) stabilised form of gold nanoparticles (AuNP).

### 3.5.4 Chitosan beads

The chitosan beads were prepared by modifying the procedure from a previous study (Barreiro-Iglesias et al., 2005). About 2 g of chitosan was mixed with 100 mL of 2% (v/v) acetic acid solution and agitated for 2 h. Subsequently, into the chitosan solution, 250 mL of 0.5 M NaOH solution containing 12.5% glutaraldehyde was added dropwise using peristaltic pump equipped with 3 mm needle to form the beads. The beads remained in NaOH solution for 12 h. Then, the beads were washed with Milli-Q water until the pH become neutral. The beads were stored at 4°C for further application.

### 3.5.5 Chitosan and gold nanocomposite (Chitosan/Au)

Preparation of chitosan beads coated with gold nanoparticles was carried out using a combination of previous procedure (Barreiro-Iglesias et al., 2005; Bastus et al., 2011). Briefly, 4% (w/v) of chitosan beads were put into 50 mL of trisodium citrate, then heated at 70°C and stirred for 15 min. Subsequently, an aqueous solution of H<sub>Au</sub>Cl<sub>4</sub> was poured into the mixture with constant stirring until pink colour developed on the beads (Chitosan/Au). The Chitosan/Au nanocomposite was washed with Milli-Q water and air-dried.

### 3.5.6 Anionic resin (A520) and gold nanocomposite (A520/Au)

The preparation of anionic resin (A520) coated with gold nanoparticles was done using previous method (Alonso et al., 2012; Bastus et al., 2011). Firstly, A520 was treated with 1 M of trisodium citrate at 70°C for 1 h to allow the ion chloride exchange. Then, 0.5 g of the polymer was incubated in 50 mL of 2.2 mM trisodium citrate at 70°C for 15 min. Subsequently, the solution of H<sub>Au</sub>Cl<sub>4</sub> was added to the mixture and stirred until pink colour formed. Later A520/Au nanocomposite was washed three times with Milli-Q water and let it dried (Fig. 3.13).

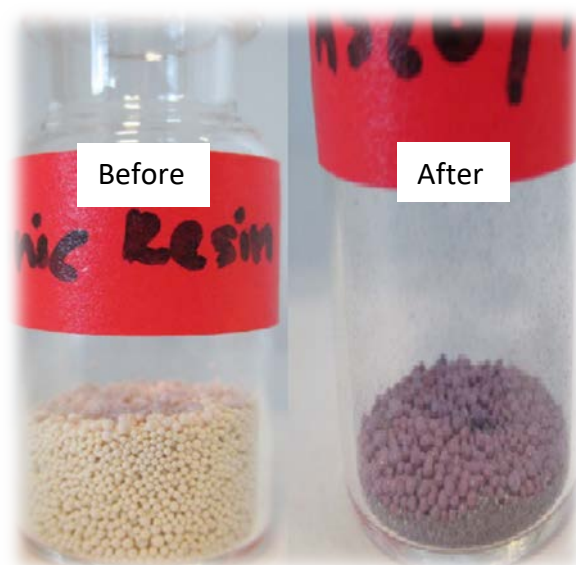


**Fig. 3.13** Illustration of anionic resin before and after coated with gold nanoparticles

### **3.6 Methods for surface modification of supports/carrier by amino silanes**

#### **3.6.1 Preparation of amino-functionalised magnetic nanoparticles (MNPs)**

The surface of the MNPs was modified using a silanisation reaction. Approximately 0.61 g of MNPs was dispersed in a solution containing 3.05 ml of 3-aminopropyltriethoxysilane (APTES), 0.763 ml of Milli-Q water, and 45.75 ml of methanol. The mixture was ultrasonically agitated for 30 min. Then, 10 ml of glycerol was added and heated at 90°C for 6 h, and the mixture was stirred until separation (Hu et al., 2015). The surface-modified MNPs were recovered by applying a magnet, and they were washed three times with Milli-Q water.

#### **3.6.2 Preparation of amino-functionalised zeolite**

The protocol to prepare amino-functionalised zeolite was followed as described elsewhere (Phadtare et al., 2004). About 1.0 g of zeolite powder was added to a mixture consists of 1 mL of APTES in 30 mL of dichloromethane (DCM). The mixture slurry was stirred for 16 h at room temperature. The resulted white amino-functionalised zeolite powder was repeatedly washed with DCM and vacuum dried. The obtained powder was stored at room temperature.

### **3.7 Methods for enzyme immobilisation**

For immobilisation of protease onto surface-modified MNPs, 1 ml of alkaline protease from hair waste (Phw) with an initial activity 466 U/ml and alkaline protease from soy residue (Psr) with an initial activity 330 U/ml, respectively, was dissolved in 9 ml of Tris-HCl buffer (pH 8.1). Then, 100 mg of amino-functionalized MNPs was dispersed into the mixture. Afterwards, the activation of the NH<sub>2</sub> groups in the nanoparticles was carried out by adding glutaraldehyde as a crosslinking agent at various concentrations (1%, 2.5%, and 5%

(v/v)) in the mixtures, followed by gentle agitation at 4 °C for 8 h (Fig. 3.14). Subsequently, the MNPs that had immobilised proteases (MNPs-protease) were separated by a magnetic field and washed five times with Tris buffer (50 mM, pH 8.1) to remove any unbound glutaraldehyde and enzyme. Finally, the MNPs-protease were resuspended in 1 ml of Tris buffer (50 mM, pH 8.1) and stored at 4 °C for further application.

For immobilisation via adsorption, approximately 100 mg of supports were dispersed in 9 ml of the Tris buffer solution (50 mM, pH 8.1). Then, 1 ml of free alkaline protease from hair waste (466 U/ml) or soy residue (330 U/ml) was added. The mixture was gently agitated at 4°C for 8 to 24 h according to specified experiments. Later, the immobilised proteases were separated physically either by magnetic force or centrifugation and treated as previously described.

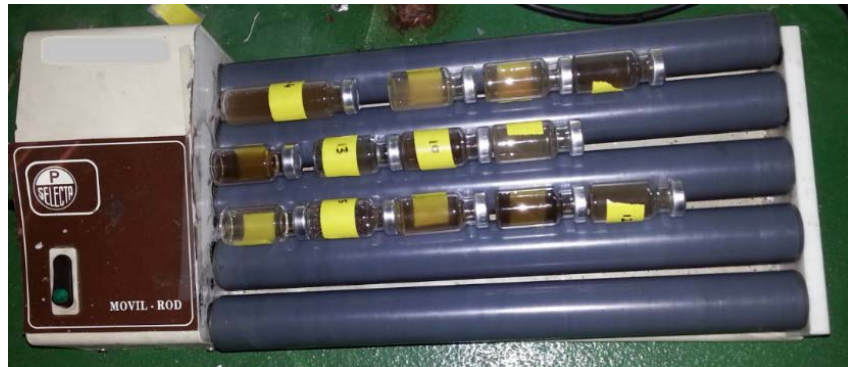


**Fig. 3.14** Immobilisation of protease by gentle agitation by using JP Selecta roller placed in 4°C.

The immobilisation yield (%) and the amount of immobilised protease ( $P_{hw}$ ,  $P_{sr}$ ) loading on nanoparticles (U/mg) were calculated using following equations (Eqs. 3.14,3.15) (Sheldon and Van Pelt, 2013):

$$\text{Enzyme loading (U/mg)} = (U_i - U_{sp})/W \quad (\text{Eq. 3.14})$$

$$\text{Immobilisation yield (\%)} = (U_i - U_{sp})/U_i \times 100 \quad (\text{Eq. 3.15})$$

Where  $U_i$  is the initial enzyme activity (U),  $U_{sp}$  is the enzyme activity in the supernatant after immobilisation (U), and  $W$  is the weight of nanoparticles used for immobilisation (mg). Furthermore, the immobilisation efficiency (%) and activity recovery (%) were calculated as follows (Eqs. 3.16, 3.17) (Sheldon and Van Pelt, 2013):

$$\text{Efficiency (\%)} = (U_e/U_{imm}) \times 100 \quad (\text{Eq. 3.16})$$

$$\text{Activity recovery (\%)} = (U_e/U_i) \times 100 \quad (\text{Eq. 3.17})$$

Where  $U_e$  is the activity of a bound enzyme that is measured in the immobilisation (U),  $U_{imm}$  is the immobilised enzyme activity determined by subtracting the remaining enzyme activity in the supernatant from the initial activity (U).

### 3.8 Characterisation of immobilised enzyme

Functionalized magnetic nanoparticles before and after immobilisation were characterised using high-resolution transmission electron microscopy (HRTEM, JEM-2011/JEOL) and scanning electron microscopy (SEM, Zeiss Merlin). The samples were prepared by placing a drop of the sonicated solutions on a copper grid, and then, the samples were allowed to dry. Samples with the immobilised enzyme were stained with uranyl acetate (2%) prior to analysis. Functionalized nanoparticle immobilisation was then confirmed using Fourier Transform Infrared spectroscopy (FT-IR, Bruker Tenser 27) within a range of 500-4,000  $\text{cm}^{-1}$

### 3.9 Biochemical stability of immobilised enzyme

#### 3.9.1 Operational stability

To study the operational stability, both immobilised and free enzymes were incubated for 1 h at various pH and temperature values according to the response surface of the central

composite design (CCD) performed using the Design-Expert software (version 6.0.6). The CCD consisted of 13 experimental points, including five replications at the central point and four star points ( $\alpha = 1$ ). The pH was adjusted using the following buffers: acetic acid-sodium acetate 1 M (pH 5), Tris-HCl 1 M (pH 8), and Na<sub>2</sub>HPO<sub>4</sub>-NaOH 0.05 M (pH 11). Analysis of variance (ANOVA) was conducted to determine the significance of the main effects.

The residual activity of each factor was calculated by assuming that the initial activity of the immobilised or free enzyme is 100%.

### **3.9.2 Storage stability**

The storage stability was determined by maintaining the immobilised enzymes via crosslinking and simple adsorption at 4°C for 60 days. The activity of the enzymes was measured at day 0<sup>th</sup> as the initial activity, while the activity for the 60<sup>th</sup> and 7<sup>th</sup> days were used as the final activity of the immobilised enzymes and free enzymes, respectively.

### **3.9.3 Reusability**

The reusability of immobilised proteases from hair waste (Phw) and soy fibre residue (Psr) was tested on casein as a model protein. The initial activities of the immobilised enzymes were measured and compared with seven consecutive repeated uses of immobilised enzymes under the assay conditions. After each cycle, immobilised enzymes were magnetically separated and washed with Tris-HCl buffer (50 mM, pH 8.1). Then, they were resuspended in fresh medium and incubated at 50°C for 120 min. The activity of immobilised enzymes from the first batch was considered to be 100%.

### 3.10 Methods for protease application

#### 3.10.1 Preparation of hides for enzymatic dehairing

The wet salted hides were obtained from the same tannery that supplying the hair waste for this research (Pere de Carme tannery, Igualada, Barcelona). The hides were cut into small pieces with the same area ( $10.68 \text{ cm}^2$ ) for the dehairing process (Fig. 3.15a, 3.15b). The small pieces of hides were desalted by washing them several times and soaked in tap water for 24 h (Fig. 3.15c).

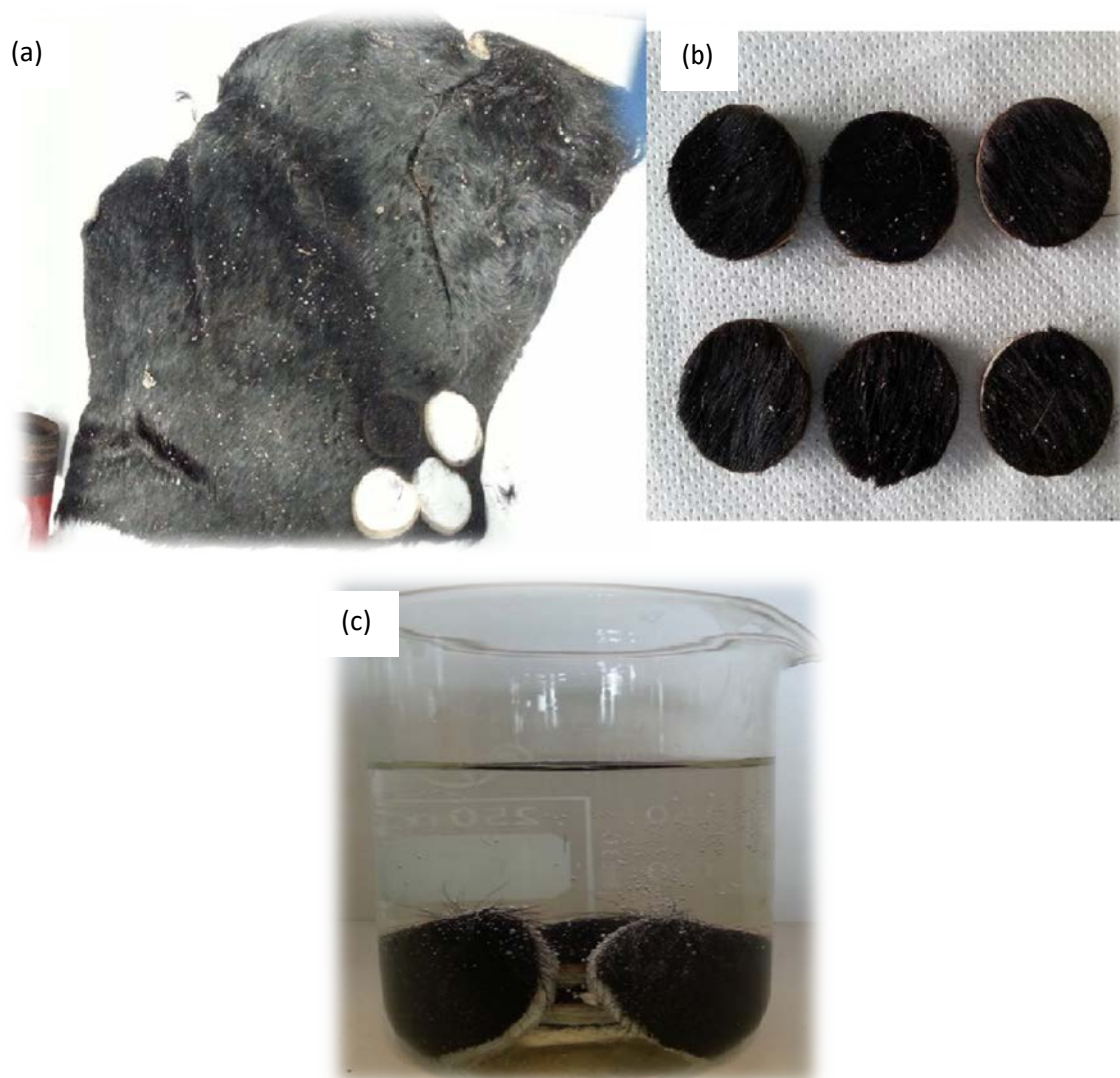


**Fig. 3.15** Preparation of hides for the dehairing experiment.(a) wet-salted hide; (b) small pieces of hides with the same surface area; (c) desalted process by washing and soaking the small pieces of hides with tap water

### **3.10.2 Protease application in enzymatic dehairing**

About 0.4 g of protease extracts was dissolved in 15 mL of Tris-HCl buffer to incubate the hides. The dehairing efficiency of the enzyme was assessed in comparison with the chemical dehairing process, where the initial amount of hair was assumed to be the same for each piece. Additionally, a commercial powder provided for tanning industry was tested as a control. The dehairing process was performed by scraping the hair using tweezers in a plate fill with water after 24 h incubated with protease or chemicals. The hair was harvested and measured as total suspended solids (TSS). Dehairing was expressed as percentage removal where the hair being removed by the chemical treatment was considered as 100%.

Briefly, the chemical treatment consists of a sequential treatment of the cowhides with the following reagents: sodium carbonate (15 mL, 0.3% w/v) with a non-ionic surfactant (0.3% w/v) (soaking for 22 h), calcium hydroxide (50 mL, 1% w/v, 1 h) and sodium hydrosulfide (50 mL, 1% w/v, 30 min in orbital agitation) to simulate the chemical dehairing process used in tannery industries.

### **3.10.3 Preparation of protein isolates from oat bran**

The preparation of oat bran protein isolate (OBPI) was performed as described elsewhere (Jodayree, 2014) with slight modifications. Briefly, oat bran was added to 1.0 M NaCl at a ratio of 1:8 (w/v), and the pH was adjusted to 9.5 using 1.0 M NaOH. The mixture was agitated for 30 min at room temperature. Then, the supernatant was collected after centrifuged at 5,000 x g for 25 min at 4°C. The pH was adjusted to 4 with 1.0 M HCl before centrifugation at 5,000 x g for 40 min at 4°C. The supernatant was then discarded, and the protein isolate was dissolved in Milli-Q water and adjusted to pH 7 with 0.1 M NaOH. The protein isolate was lyophilised and stored at -20°C for future use (Fig. 3.16).





**Fig. 3.16** Protein isolate (right) prepared from oat bran (left) for protein hydrolysis experiment

#### **3.10.4 Application of immobilised protease in protein hydrolysis**

Before hydrolysis, 4% (w/v) suspension of selected proteins (casein from bovine milk, egg white albumin, and OBPI) in Tris-HCl buffer (50 mM, pH 8.1) were incubated at 50°C for 15 min. Then, the reaction was initiated by adding 1 ml of free enzymes (330-460 U/ml) or 1 ml immobilised enzymes suspension (31.9-45.9 U/mg NP) into 9 ml of substrate. The mixture was incubated in a water bath at 50°C with mechanical agitation at 100 rpm. An aliquot of 6 ml was withdrawn at 0.5, 2, 4, 6, and 24 h. The free enzyme activity was deactivated by heating the samples in boiling water for 15 min. Then, the samples were cooled by placing the samples in a cold water bath for 15 min. Subsequently, the samples were centrifuged at 5,000 x g for 15 min to separate any impurities or enzyme from the hydrolysate. The immobilised enzyme was separated from the hydrolysate by a magnetic drive. The hydrolysate was kept frozen at -80 °C before lyophilisation. The residual activity of each protein hydrolysis was calculated by assuming the initial activity of the immobilised or free enzyme as 100%.

## Chapter 4

*Production, downstream processing, biochemical characterisation,  
and application of protease from hair waste in SSF*

*Part of this chapter has been published at Waste Management 49,420 – 426, 2016.  
Assessment of protease activity in hydrolysed extracts from SSF of hair waste by an  
indigenous consortium of microorganisms.*

*Noraziah Abu Yazid, Raquel Barrena, Antoni Sánchez.*

Graphical abstract

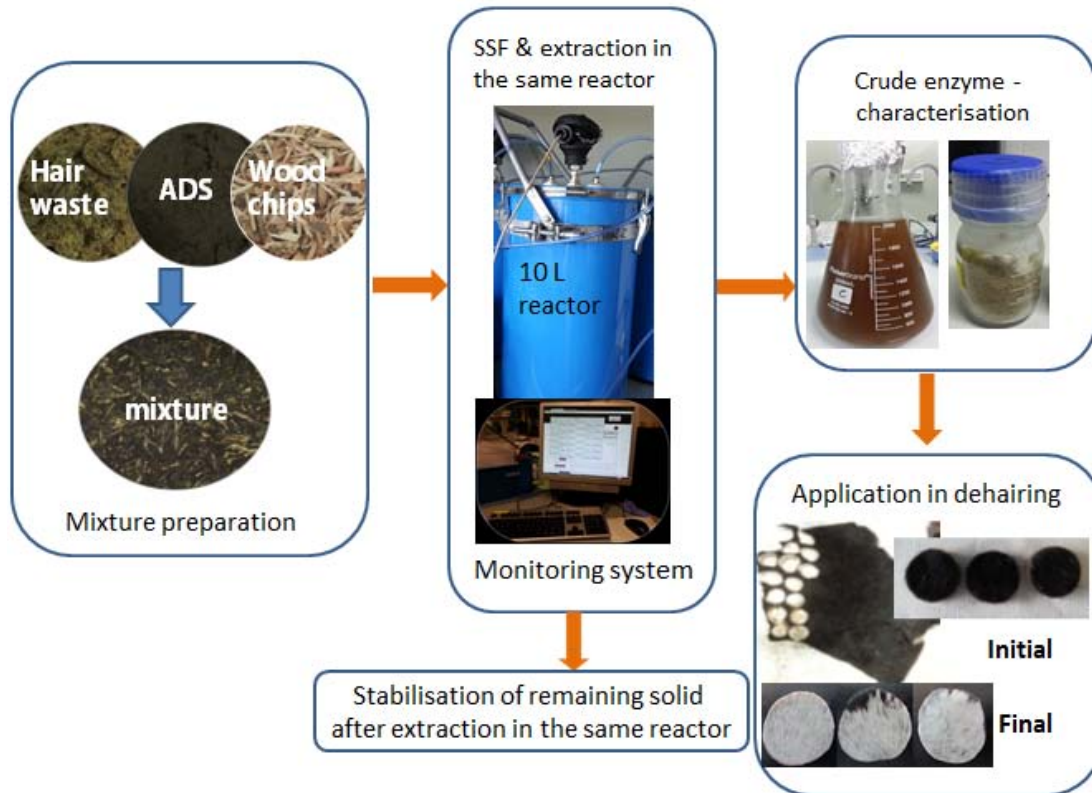


**Fig. 4.1** Graphical abstract from protease production in SSF until application of the produced protease in dehairing

## **Summary**

This chapter comprised of production of protease from hair waste using solid state fermentation (SSF) process in 10 L airtight reactors. It is known that SSF can produce concentrated product such as enzyme due to the less water consumption during the process compare to submerged fermentation. Therefore, the extraction is crucial in its downstream processing. Thus, this chapter has investigated the effect of agitation and extraction ratio during the enzyme extraction. Subsequently, the remaining solid after the extraction was proceeded to stabilised the end material to produce a stable compost-like material. This chapter covers the process from fermentation to downstream, characterisation, application, and residues reutilisation as a platform to assist at the industrial level. Fig. 4.1 illustrated the whole processes involve in this experimental work for better conception.

Briefly, hair waste from the tannery industry was assessed for its suitability as substrates for protease production by SSF using a pilot-batch mode operation and anaerobically digested sludge (ADS) as co-substrate. Maximum protease activity ( $435.3 \pm 13.3$  U g<sup>-1</sup> DM) was observed at the 14<sup>th</sup> day of SSF. Single step purification resulted in 2 fold purification with 74% of recovery by ultrafiltration with 10 kDa cut-off. The recovered enzyme was stable at a temperature of 30 °C and pH 11; optimal conditions that were determined by a central composite full factorial experimental design. The enzyme activity was inhibited by phenylmethylsulfonyl fluoride (PMSF), which indicates that it belongs to serine protease group. The remaining solid material after protease extraction could be easily stabilised to obtain a final good quality compost-like material as the final dynamic respiration index was lower than 1 g O<sub>2</sub> kg<sup>-1</sup> OM h<sup>-1</sup>. The lyophilised recovered enzymes were a good alternative in the process of cowhides dehairing with respect to the current chemical treatment, avoiding the production of solid wastes and highly polluted wastewaters. In a

nutshell, the entire process can be considered a low-cost, sustainable technology for the dehairing process, closing the organic matter cycle in the form of value-added product and a compost-like material from waste.

#### **4.1 The reproducibility of protease production in solid state fermentation (SSF)**

In this work, protease was produced from solid state fermentation (SSF) of hair waste and anaerobically digested sludge (ADS) in 10 L air tight reactors. The process was conducted in aerobic condition with continuous aeration. Before the fermentation, the mixture was prepared as mentioned in Section 3.1.2. Briefly, the mixture was prepared by mixing hair waste and ADS at 1:2 weight ratios with manually homogenised. Then, the mixture was added with wood chips as a bulking agent at 1:1 volumetric ratio. Unless mentioned otherwise, these fermentation conditions were maintained throughout the studies. There are several SSF processes with the same condition were carried out to investigate the reproducibility of protease production in 10 L reactors. Each fermentation process was undergone for 23 – 42 days of SSF with sampling at interval time.

##### **4.1.1 Solid state fermentation (SSF)**

In typical experiments, primarily, the initial dynamic respiration index (DRI) of the mixture was determined in respirometric experimental setup (Section 3.2.1). The obtained DRI was considered high ( $4.7 \pm 0.7 \text{ g O}_2 \text{ kg}^{-1} \text{ DM h}^{-1}$ ) and appropriate to initiate degradation aerobically during SSF process. This material can be classified as moderately biodegradable waste as suggested elsewhere (Ponsá et al., 2010). The moisture content (>60%), alkaline pH and C/N ratio (11) of the mixture were maintained to favour degradation process to produce alkaline protease enzyme during thermophilic and mesophilic condition. The characterisation of substrates utilised in SSF was tabulated in Table 4.1. In all experiments, unless specified otherwise, these fermentation conditions were maintained throughout the study.

**Table 4.1** Characterisation of anaerobically digested sludge, hair waste and initial mixture for SSF process.

Characteristics	Hair waste	Anaerobically digested sludge (ADS)	Mixture <sup>a</sup>
<u><i>Physical characteristics</i></u>			
Organic matter (% db)	85.5 ± 0.7	71.3 ± 0.6	84.6 ± 0.4
Water content (% db)	61.9 ± 3.0	85.6 ± 3.6	72.3 ± 4.4
Dynamic respiration index (DRI) (g O <sub>2</sub> kg <sup>-1</sup> DM h <sup>-1</sup> )	N.D	2.4 ± 0.3	4.7 ± 0.7
Electrical conductivity (mS cm <sup>-1</sup> )	4.07 ± 0.9	1.2 ± 0.7	1.6 ± 0.8
pH	10.7 ± 0.1	8.32 ± 0.04	8.52 ± 0.01
<u><i>Chemical characteristics</i></u>			
Total carbon (% db)	57.2 ± 0.9	42.0 ± 0.1	68.3 ± 0.4
Total nitrogen (% db)	12.1 ± 0.1	7.2 ± 0.6	6.9 ± 0.1
C/N ratio	4.7	5.9	11

db: dry basis; DM: dry matter; N.D.: not determined.

<sup>a</sup>Ratio 1:2 (sludge: hair waste)

The results presented in Fig. 4.2 showed the protease production and fermentation profiles (temperature and oxygen exhaust content) of SSF. With the aim to demonstrate the reproducibility of the protease production, only one replicate of fermentation profiles was shown since the profiles were similar for all experiments with the same substrate condition, though the proteases profiles were obtained from several experiments. No lag phase was observed because of the previous hydrolysis of hair waste, as pointed in other studies (Du et al., 2008). The fermentation showed a normal operating condition where the thermophilic temperature (60°C – 61°C) occurred at the beginning of the SSF (day 2) and decreases towards the end of the fermentation. In Fig. 4.2, oxygen contents were low during the thermophilic stage as an evidence of high aerobic respiration activity during that period in the profile (Gea et al., 2004). The oxygen profiles showed a similar trend to that of co-composting hair waste and raw activated sludge profiles (Abraham et al., 2014; Barrena et al., 2007). Based on several replicates of SSF with the same conditions, maximum protease activity was obtained at day 14<sup>th</sup> of fermentation (Fig. 4.2).

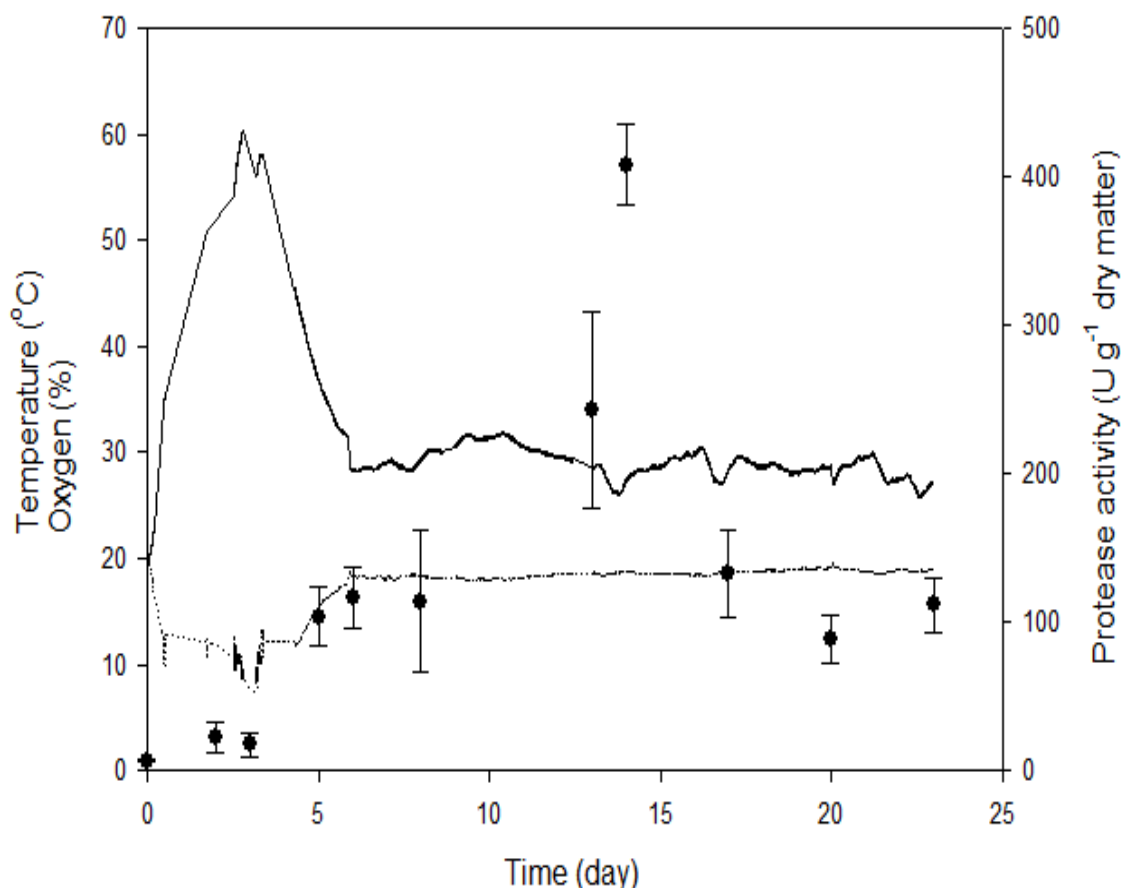


**Fig. 4.2** Typical solid state fermentation profiles (one replicate is shown) for 23 days of SSF. Temperature (—, solid line), the oxygen content in exhausts gas (····, dotted line), protease activity profile (●) obtained from several SSF processes.

To validate the processes performances of the replicates, they were assessed through the statistical comparison of temperature and oxygen profiles that have been summarised in Table 4.2. Thus, to evaluate the performance of mixtures of hair waste and ADS the area below the temperature curve, the area below sOUR (specific oxygen uptake rate), the maximum protease activity, the specific activity and dry mass reduction were calculated until 14 days of SSF. The dry mass reduction of all fermentations was in the range from 7% – 17% indicated that biomass degradation occurred resulting in the production of protease. Apparently, there was no considerable difference between replicates for the temperature curve, where the average was  $499 \pm 15^\circ\text{C day}^{-1}$ . The coefficients of variation (CV) for all the fermentations were lower than 5%, thus validating the process statistically and confirming

non-statistically differences between replicates (de Guardia et al., 2010). Additionally, the maximum specific oxygen uptake rate (sOUR max) and accumulated oxygen content throughout the SSF process were correlated well with a correlation coefficient of 0.951. Overall, the correlation between the area under the temperature curve and the maximum protease activity reached, the sOUR max and the maximum protease activity were significant at  $p < 0.001$ . As sOUR max value also correlated to the increasing value of the area below sOUR (Table 4.2) ( $p = 0.017$ ), it can be stated that the SSF for the production of proteases from hair and ADS under this pilot conditions is highly reproducible and the results are consistent.



**Table 4.2** Summary of the replicates of solid state fermentation (SSF) using 10-L air tight reactors with hair waste and anaerobically digested sludge as substrates

Initial water content of mixture (%)	Bulk density (kg L <sup>-1</sup> )	Process parameters during SSF					Max PA <sup>a</sup> (U g <sup>-1</sup> DM)	sPA <sup>a</sup> (U mg <sup>-1</sup> soluble protein)	Dry mass reduction <sup>a</sup> (%)	Stability after SSF
		Area T <sup>a</sup> (°C day <sup>-1</sup> )	sOUR max (g O <sub>2</sub> kg <sup>-1</sup> DM h <sup>-1</sup> )	Area sOUR <sup>a</sup> (g O <sub>2</sub> kg <sup>-1</sup> DM)	Time sOUR max (h)	DRI (gO <sub>2</sub> kg <sup>-1</sup> OMh <sup>-1</sup> )				
Experiment performed with in-situ enzyme extraction										
R1		513.4	3.9	387	11.7	435.3 ± 13.3	105.1 ± 9.3	10		
R2	76.1	0.5	475.8	3.1	337	11.3	314.4 ± 13.4	128.4 ± 75.8	7	0.39±0.04
R3			500.3	5.3	538	10.9	314.9 ± 12.6	112.9 ± 52.2	10	
Control experiment										
C1	73.3	0.67	497.0	2.8	220	48.4	403.1 ± 6.5	28.8 ± 3.5	11	0.87±0.01
C2			507.9	2.3	165	71.8	413.2 ± 27.1	34.6 ± 14.3	17	

R1, R2 and R3: replicates SSF experiments; C1 and C2: control SSF experiments.

PA: protease activity; sPA: specific protease activity; OUR: oxygen uptake rate; DRI: dynamic respiration index; DM: dry matter; OM: organic matter; values are the average of three replicates of experiments ± standard deviation of triplicates.

<sup>a</sup>The parameters were calculated after 14 days of SSF (maximum protease production).

## 4.2 Downstream processing in SSF

In general, the downstream processing involved with bioseparation processes such as extraction, purification, and recovery. In SSF, extraction is crucial since SSF is performed in limited or absence of liquid unlike in submerged fermentation. As a matter of fact, the moisture available after the fermentation process is insufficient for complete extraction, as if squeezing the fermented solid substrates barely yields any extract (Aikat and Bhattacharyya, 2000). An extraction with an appropriate solvent and condition is necessary to recover the secreted products that bind to the solid substrates (Yazid et al., 2017). This work was an attempt to cater all the processes from fermentation to downstream processing in a single reactor.

### 4.2.1 Extraction methods

Preliminarily, to investigate the extraction efficiency, we introduced one-factor-at-a-time (OFAT) method which involved process parameters such as the type of solvent, solid-liquid ratio, and mechanical assistance. OFAT was chosen to analyse the effect of one factor towards protease activity and subsequently evaluate another factor with the effect of the previous factor. These extractions were done after 5 days of SSF. Firstly, we extracted the fermented material with water or Tris buffer (pH 8.1) using normal solid-liquid ratio (1:5) to investigate the effect of solvent type towards protease activity. In Fig. 4.3, there was no much different between water (protease activity:  $62.9 \pm 46.8 \text{ U g}^{-1} \text{ DM}$ ) or Tris buffer (protease activity:  $73.7 \pm 29.4 \text{ U g}^{-1} \text{ DM}$ ) as a solvent for the extraction which can favour an economical means in the downstream process. However, based on the stability study that was done during this whole study, the protease produced in the SSF process was alkaline protease; it was more stable with an alkaline solution such as Tris buffer (pH 8.1). Also, the isoelectric point test determined by the protein precipitation validated that the protease

produced from the SSF has a negative charge which can be considered as basic. Therefore, the subsequent extraction was done using Tris buffer (pH 8.1) as a solvent.

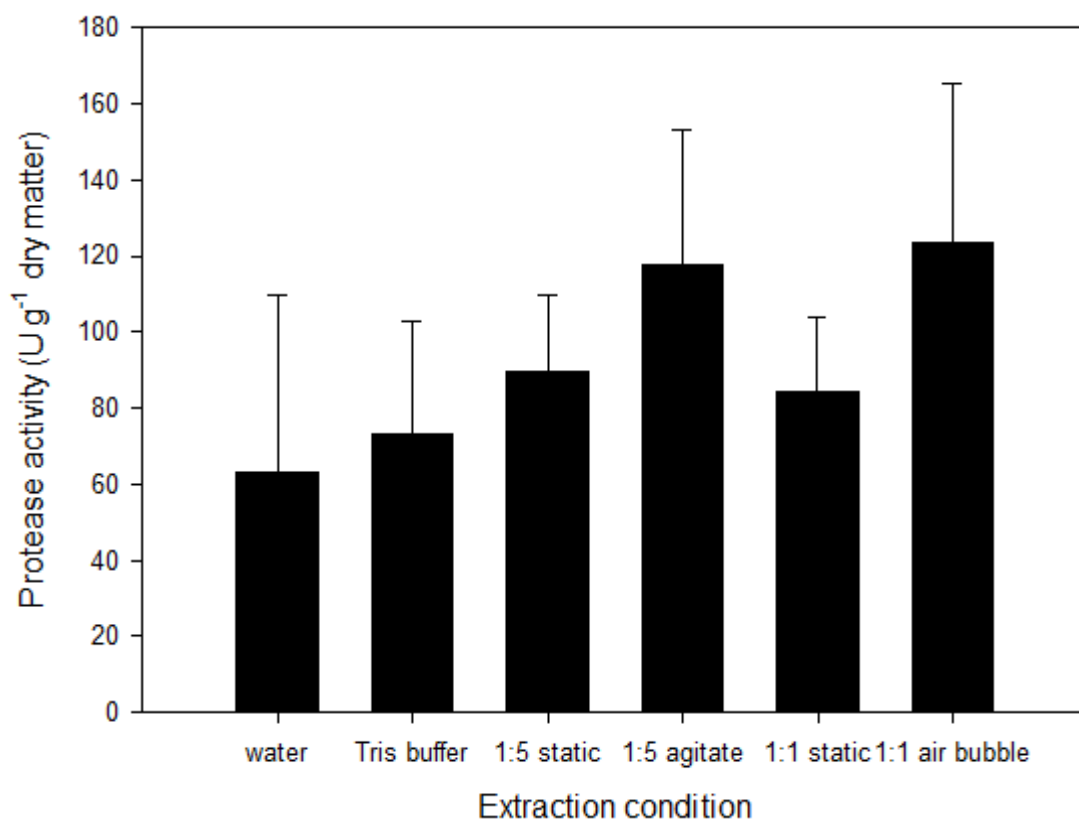


**Fig. 4.3** Protease activity obtained with the different condition of extraction after 5 days of SSF.

The extraction was carried out with the different solid-liquid ratio (1:5 and 1:1) and with mechanical assistance (static, agitation, and air-bubble). As mentioned in Section 3.4.1 the extraction at a solid-liquid ratio (1:5) with agitation and static condition for 45 min was designated as the control. In like manner, in the 10 L reactor, the extraction of the solid-liquid ratio at 1:1 was conducted in static and air-bubble (as an alternative of agitation), provided that the extraction time was extended to 1 h. In Fig. 4.3, the protease activity for both solid-liquid ratio (1:5 and 1:1) gave relatively similar result for both in static ( $89.4 \pm 20.1$  U g<sup>-1</sup> DM and  $84.2 \pm 19.8$  U g<sup>-1</sup> DM, respectively) and agitation/air-bubble ( $117.9 \pm 35.5$  U g<sup>-1</sup> DM and  $123.5 \pm 41.7$  U g<sup>-1</sup> DM, respectively).

As a result, in the following experiments for the realisation of downstream processing in a single reactor, the whole fermented material was used for the extraction solid-liquid ratio (1:1) provided with air-bubble to assist the extraction of bio-product for 1 h. In this manner, the whole fermented materials were utilised which enable to yield maximum recovery of the protease from SSF. To point out in Fig. 4.2, the protease extracted at day 14th, showed the highest protease activity production, which resulted in an average value of  $408.1 \pm 72.7 \text{ U g}^{-1} \text{ DM}$  with a CV equal to 1.8%. These results are in agreement with previous studies using 4.5 L reactors where the highest activity of protease was observed at 14 days of SSF with hair waste and different co-substrate (Abraham et al., 2014, 2013).

#### **4.2.2 Partial purification and recovery of crude protease**

Table 4.3 shows the summary of the partial purification steps tested for the alkaline protease in the three replicates (R1, R2, and R3). In all cases, the partial purification of protease resulted in a 2 fold purification factor with 74% of recovery by ultrafiltration using Amicon Ultra-15 centrifugal filter device with 10 kDa MWCO. Additionally, protease activity was not detected in permeate as the size of alkaline proteases produced were in the range between 26 and 100 kDa. Some studies reported that there was no protease activity detectable in all permeates due to the lost as a deposit in the membrane of the tube (Bezawada et al., 2011). However, during lyophilisation the loss of activity resulted in 21%, being this step the most critical for the recovery of protease.

**Table 4.3** Partial purification of protease enzyme from extraction

Sample	Purification step	Total activity (U)	Total protein (mg)	Specific activity (U mg <sup>-1</sup> )	Recovery (%)	Purification fold
R1	Crude extract	1037	9.91 ± 0.04	104.7 ± 18.5	100	1
	Lyophilisation	787	9.86 ± 0.03	79.8 ± 40.1	76	0.76
	Ultrafiltration	710	4.10 ± 0.72	173.3 ± 52.6	68	1.66
R2	Crude extract	715	5.83 ± 0.01	122.6 ± 75.8	100	1
	Lyophilisation	518	5.34 ± 0.20	97.1 ± 20.3	72	0.79
	Ultrafiltration	502	3.39 ± 0.16	148.2 ± 27.2	70	1.21
R3	Crude extract	855	6.43 ± 0.01	133.1 ± 52.2	100	1
	Lyophilisation	752	6.37 ± 0.28	117.9 ± 31.3	88	0.89
	Ultrafiltration	720	3.34 ± 0.38	215.4 ± 24.8	84	1.62

### 4.3 Remaining residues reutilisation

This work deals with the remaining residues after the downstream process in SSF namely extraction. Normally, in SSF the remaining residues after downstream process will be discarded or incinerated (Dhillon et al., 2013). There were very few studies reporting the reutilisation of remaining residues from downstream processing in SSF. In this attempt, the remaining residues were reutilised in the composting course to produce a compost-like organic material that is stable and easier to handle and can be applied for agricultural purpose. The stabilisation of the remaining organic residues after extraction process has been done by composting in the same 10 L reactors (where the SSF and extraction took place). The stability of the organic materials from the composting course was compared with the organic materials from typical SSF. The biological stability is an important measure to control and optimise the process of biodegradable organic matter. Not to mention, the stability may influence the odour generation, biomass reheating, residual biogas production, phytotoxicity, process parameters such as airflow rate and retention time (Iannotti et al., 1993).

### **4.3.1 Organic matter stability**

Unless specified otherwise, in the typical SSF with hair waste and ADS, the fermentation was ended after 23 days which was when the fermentation profile showed a stagnant mesophilic and after the protease activity showed no longer increment in the activity. Normally only some part of the fermented materials were undergone the extraction process, and another part was used to measure the stability of the organic materials. This end material will be compared with the organic materials obtained after the downstream and composting processes.

In the reutilisation scheme, the composting process was carried out and continued in the same reactors until 42 days with the organic materials after extraction process, to complete the entire process that implies the stabilisation of the remaining material. The water content of the material was increased about 40% to 43% (wet basis) of the total remaining material after extraction process, where it was the main concerned in this work. However, after continuing with the experiment until 42 days, the result turned out to favour the stabilisation process. The stabilisation of the materials was continued in the respirometers to analyse the biodegradability and the stability of the remaining materials.

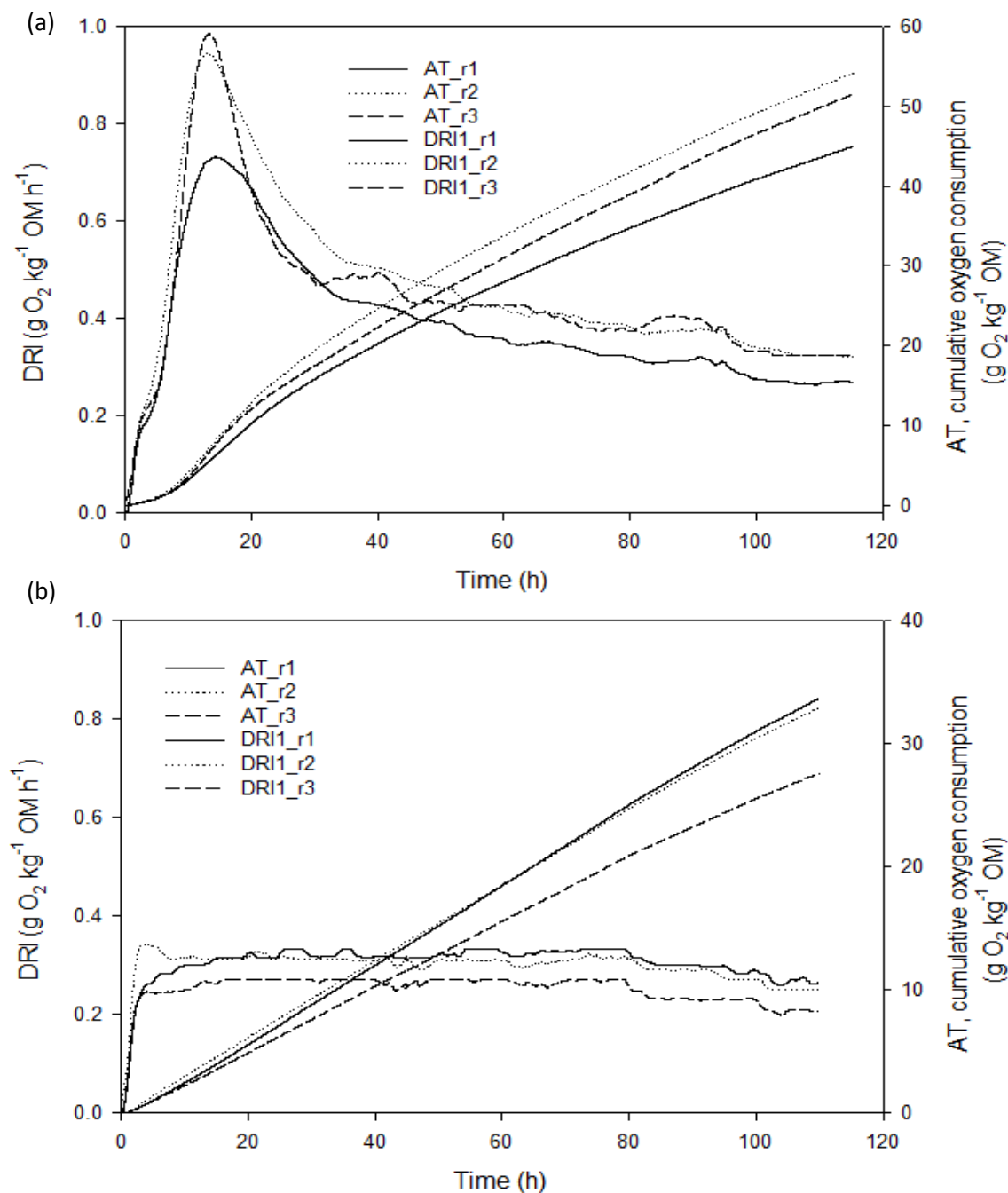


**Fig 4.4** Dynamic respiration index (DRI) and cumulative oxygen consumption (AT) measured in 96 h for remaining material from three reactors after stabilisation from (a) typical SSF, (b) SSF + extraction + composting for 42 days.

For stabilisation measurement, dynamic respiration index (DRI) was used as an indicator of the biodegradability and biological stability of organic materials as suggested elsewhere (Adani et al., 2006, 2004; Barrena et al., 2009; Ponsá et al., 2010). Fig. 4.4 shows the profiles of DRI in the 1 h of maximum activity and cumulative oxygen consumption is

taken for 4 days (AT<sub>4</sub>) for typical SSF stabilisation and single reactor of composting stabilisation (SSF + extraction + composting). Fig. 4.4 (a) shows a typical trend of stabilisation of organic matter after finished the fermentation by a short lag phase, DRI peak at 1 g O<sub>2</sub> kg OM h<sup>-1</sup>, and a successive decreasing phase. While in Fig. 4.4 (b), there were less pronounced DRI profiles were displayed with low respirometric activity indicated the high biological stability as been suggested by others (Adani et al., 2004). Thus, shows that the remaining materials after extraction process can be further stabilised by composting process disregard of the additional water content after the extraction process. Both of the profiles from different remaining materials stabilisation treatments were characterised by short lag phase meaning that the respirometric activity was sufficiently completed within 96 h. As observed in Fig 4.4 (a), AT<sub>4</sub> of end SSF material stabilisation were 45-55 g O<sub>2</sub> kg<sup>-1</sup> OM with 10 h of lag phase which corresponds to 88% of the final cumulative oxygen consumption. While AT<sub>4</sub> of material stabilisation by composting process were 30-35 g O<sub>2</sub> kg<sup>-1</sup> OM with no lag phase was noticed and corresponds to 62% of the final cumulative oxygen consumption.

The activity of protease at the end of SSF process (42 days) was  $27.3 \pm 11.2$  U g<sup>-1</sup> DM, showing a significant decrease of activity at the end of the fermentation. The dry mass reduction was 21% – 32% and the pH was approaching neutral pH after stabilisation process (Table 4.4) indicated that the biomass still can be degraded and stabilised after the extraction of the whole fermented substrates to produce stable compost-like organic materials. Additionally, the dynamic respiration index (DRI<sub>24max</sub>) and cumulative oxygen consumption (AT<sub>4</sub>) obtained in the materials that had undergone composting process after the downstream process (indicated as Cp1, Cp2, Cp3) were relatively lower and stable (<0.5 g O<sub>2</sub> kg OM h<sup>-1</sup>), compared to the materials that taken directly from the end SSF process (indicated as N1, N2, N3) (<1.0 g O<sub>2</sub> kg OM h<sup>-1</sup>) as shown in Table 4.4. As been reported by Adani et al., (2004) the DRI<sub>24</sub> of 1 g O<sub>2</sub> kg OM h<sup>-1</sup> can be used to indicate medium biological stability like fresh



compost and  $0.5 \text{ g O}_2 \text{ kg OM h}^{-1}$  can be used to indicate high biological stability like mature compost. The results obtained from both experimental works indicate the degradation of biodegradable matter and shows that a further stabilisation is useful to get a very stable compost-like material. Thus, it can be concluded that, even after extraction, DRI showed a high biological stability, as reported in previous studies (Gupta et al., 2002; Ponsá et al., 2010).

**Table 4.4** Characteristics of remaining material after stabilisation by composting process and typical SSF

Replicates	DRI <sub>24</sub> <sub>max</sub> ( $\text{gO}_2\text{kg}^{-1}\text{OMh}^{-1}$ )	AT <sub>4</sub> ( $\text{gO}_2\text{kg}^{-1}\text{OM}$ )	Dry mass reduction (%)	pH	conductivity (mS/cm)
Cp1	0.29±0.04	26.5±12.9	21	7.77	2.53
Cp2	0.35±0.05	29.9±14.1	23	7.11	1.22
Cp2	0.27±0.03	24.6±11.7	32	6.92	1.02
N1	0.61±0.12	39.7±13.3	11	8.84	3.60
N2	0.75±0.15	47.8±15.9	9	8.85	3.95
N3	0.69±0.12	45.2±15.2	12	8.74	4.30

Cp1, Cp2, Cp3: Replicates of remaining materials that undergone composting process for stabilisation

N1, N2, N3: Replicates of end materials after typical SSF process

AT<sub>4</sub> : cumulative oxygen consumption after 4 days of stabilisation

DRI<sub>24</sub><sub>max</sub> : average of dynamic respiration index (DRI1) in the 24 h of maximum biological activity

The growth of white fungi after the stabilisation process indicated the stable compost-like material approaching maturity compost (Fig. 4.5). Additionally, by physical observation, we can notice that the hair waste has been degraded during the process with the colour of the material turned from dark colour to brownish colour material with a mushroom-like odour or earthy odour contradicted to the initial unpleasant smell of the mixture. Thus, confirmed the stability of the remaining material.



**Fig. 4.5** Remaining materials after composting and stabilisation process

#### **4.4 Biochemical characterisation of protease**

##### **4.4.1 Operational stability and statistically analysis**

In this study, the effects of pH ( $x_1$ ) and temperature ( $x_2$ ) were investigated on the stability of the protease produced from SSF using response surface methodology (RSM). Table 4.5 presents the coded and actual values with  $\alpha=1$ . The pH was studied based on the pH buffer used for a normal assay which is pH 8 at the centre point, and  $\pm 3$  gave the effect at acidic (pH 5) and basic (pH 11). While for the temperature, 50°C was chosen as the centre point followed the normal assay of the protease and  $\pm 20$  gave the effect at mesophilic temperature (30°C) and thermophilic temperature (70°C).

**Table 4.5** Coded and actual value of independent variables in the experimental design

Independent variables	Coded factor		Range and level		
			$-\alpha$	0	$+\alpha$
pH	$x_1$	Coded	-1	0	+1
		Actual	5	8	11
Temperature (°C)	$x_2$	Coded	-1	0	1
		Actual	30	50	70

The full factorial centre composite design (CCD) consisted of 13 experimental points which included five replications at the centre points as shown in Table 4.6. There were duplicates at the central coding condition with the experimental condition; pH 8 and 50°C. These were used to evaluate the reproducibility of the experiment and experimental error. The observed responses in term of residual activity of 13 combination experiments for studying the enzyme stability on the effect of two independent variables are presented in Table 4.6. The experiment was done with three replicates of protease obtained from R1, R2, and R3.

**Table 4.6** Central composite experimental design matrix of independent variables in coded values and three replicates of residual activity as the response

RUN	Coded factor level		Residual activity (%)	Residual activity (%)	Residual activity (%)
	$x_1$	$x_2$	R1	R2	R3
1	-1	-1	55.4	65.3	60.3
2	1	-1	70.2	70.5	73.3
3	-1	1	4.4	10.9	7.6
4	1	1	26.9	5.8	16.3
5	-1	0	45.8	37.4	41.6
6	1	0	57.3	50.7	54.0
7	0	-1	65.2	74.1	69.6
8	0	1	34.3	6.2	20.3
9	0	0	53.2	50.3	51.8
10	0	0	54.6	45.7	50.2
11	0	0	54.8	53.7	54.3
12	0	0	49.4	49.8	49.6
13	0	0	54.4	50.0	52.2

The response surface of protease in front of several conditions of pH and temperature was determined to assess the stability of the protease. For this, it was analysed using the regression equation obtained from the analysis of variances (ANOVA) by the Design Expert software to determine the suitability of the model. Using the multiple regression analysis on the experimental data, the second order model fitted the residual activity for all replicates indicating the homogeneity of proteases obtained from the SSF (Eq. 4.1-4.3). In the models,  $pHT$  indicates the interaction term between temperature and pH, however only with R2 the interaction between pH and temperature not significant. The negative coefficient of  $T$  (Eq. 4.1-4.3) suggested that high temperature has a pronounced effect on activity and, as shown in Fig. 4.6, pH effect becomes insignificant at higher temperatures for all replicates (R1, R2, and R3). Correspondingly, it can be concluded that the protease produced in the SSF using hair waste and ADS showed similar stability towards pH and temperature indicating a high reproducibility.

$$Res. activity (\%)_{R1} = 52.79 + 4.17pH - 29T - 2.78pH^2 - 7.8T^2 - 3.25pHT \quad (Eq. 4.1)$$

$$Res. activity (\%)_{R2} = 49.37 + 2.23pH - 31.2T - 4pH^2 - 7.9T^2 \quad (Eq. 4.2)$$

$$Res. activity (\%)_{R3} = 51.86 + 5.68pH - 26.5T - 4.7pH^2 - 7.5T^2 - 1.07pHT \quad (Eq. 4.3)$$

Table 4.7 shows that the regression for residual activity yield model was significant (242.97, 82.18, 247.82) and the lack of fit was not significant (0.58, 3.67, 1.29) at  $p < 0.0001$  relative to pure error. The lacks of fit of the F-value for the residual yield for all replicates were less than the  $F_{critical}$  value ( $\alpha = 0.05$  at the degree of freedom 4, 3) of 9.12 for R1 and R3, while for R2 the  $F_{critical}$  value was 6.39, respectively which indicates that the treatment differences were highly significant.

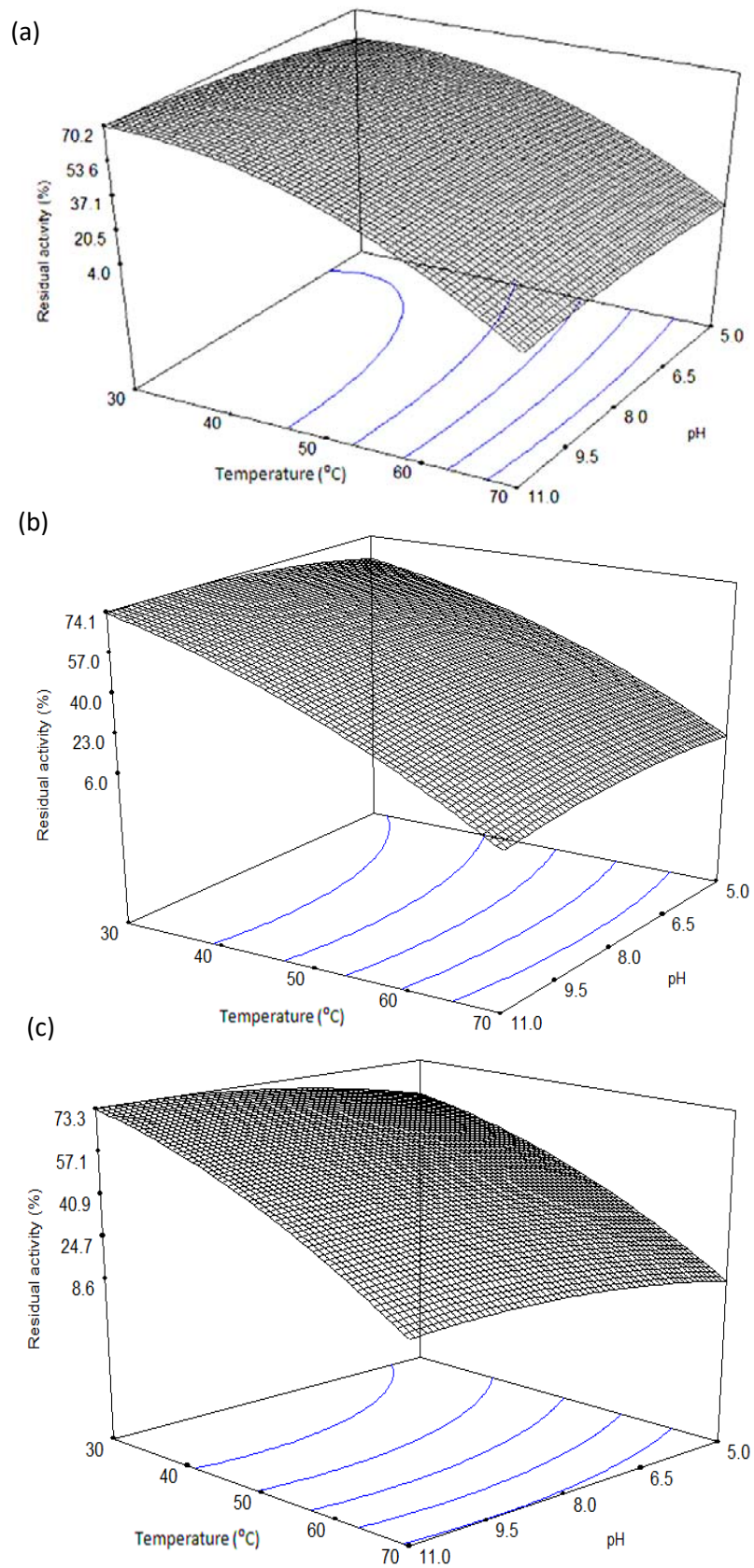


**Fig. 4.6** Response surface of residual protease activity (%) on the stability of enzymes on pH and temperature; (a) R1, (b) R2, (c) R3.

The fit of the models was checked by the determination of correlation coefficient,  $R^2$ . In this case, for all replicates, the value of the coefficient for residual activity were  $R^2 = 0.9943$ ,  $R^2 = 0.9762$ , and  $R^2 = 0.9944$ . The values showed that only 0.57%, 2.38%, and 0.56% of the variables behaviour is not explained by the models. The closer the  $R^2$  is to 1, the firmer the model and the better in predicting the response (Amini et al., 2008). The values of the predicted  $R^2$  for all models were also high to support for a high significance of the model. To point out, for all replicates (R1, R2, R3), the predicted  $R^2$  (0.9797, 0.9129, 0.9692) for the models were in reasonable agreement with the adjusted  $R^2$  of 0.9902, 0.9644, 0.9904, respectively. Therefore, it can be concluded that the proposed models adequately approximated the response surface and it could be used to predict the values of the variables within the experimental domain (Gilmour, 2006; Myers et al., 2004).

**Table 4.7** Analysis of variance (ANOVA) for the response surface quadratic model

Source of variations	Sums of squares	Degrees of freedom	Mean square	F-value	(P value)
<i>R1</i>					
Regression	6184.36	5	1236.87	242.97	< 0.0001
Residual	35.64	7	5.09		
Pure error	24.8	4	6.2		
Lack of fit	10.84	3	3.61	0.58	
Total	6220	12			
<i>R2</i>					
Regression	6189.57	4	1547.39	82.18	< 0.0001
Residual	150.63	7	18.83		
Pure error	32.26	4	8.06		
Lack of fit	118.37	4	29.59	3.67	
Total	6340	12			
<i>R3</i>					
Regression	4751.23	5	950.25	247.82	< 0.0001
Residual	26.84	7	3.83		
Pure error	13.65	4	4.4		
Lack of fit	13.19	3	3.41	1.29	
Total	4778.07	12			

R1:  $R^2$  0.9943; adjusted  $R^2$  0.9902; predicted  $R^2$  0.9797

R2:  $R^2$  0.9762; adjusted  $R^2$  0.9644; predicted  $R^2$  0.9129

R3:  $R^2$  0.9944; adjusted  $R^2$  0.9904; predicted  $R^2$  0.9692

The partially purified protease was found to be an alkaline protease displaying the residual activity more than 70% when approaching alkaline pH up to 11 (Fig. 4.6). As it was stable in alkaline pH up to 11, it can be used for industrial purposes where commercially proteases have highest activity in alkaline pH ranges of 8–12 (Gupta et al., 2002; Kumar et al., 1999). For thermal stability, the enzymes exhibited good activities over a temperature range 30–50°C in a wide range of alkaline pH from pH 7 to 11. The optimum enzyme activity ( $411.2 \pm 45.7 \text{ U g}^{-1} \text{ DM}$ ) was obtained at 30°C and pH 11. However, the enzymes were rapidly inactivated and retained approximately 4–8% of residual activity after incubation at 70°C at any tested pH (Fig. 4.6). These results were in accordance with previous studies (Abraham et al., 2014, 2013) reported that the protease produced from hair waste was highly stable in alkaline and mesophilic temperatures, which coincides with the conditions of the SSF when it is mainly produced (Fig. 4.2).

#### **4.4.2 Inhibition study**

The study and selection of distinct properties of protease may improve operations whether in food processing or waste management industries. It is important to know the catalytic mechanisms of protease produced during the fermentation since protease can be divided into four classes which are serine, cysteine, metalloprotease, and aspartic protease as been mentioned in Chapter 1 (Section 1.4) that can serve different reaction in certain processes. Briefly, serine protease is active at pH 7-11 and has broad substrate specificities; cysteine protease is active at pH 5-8 and sensitive to heavy metal; metalloprotease is active at pH 5-9 which containing zinc, and the protein structure can be stabilised by addition of calcium; aspartic or acid protease is active at pH 3-4 which is specifically against aromatic or bulky amino acids.

To evaluate the class of the protease, the reduction of protease activity in a response of inhibitors was used, as the mechanisms of inhibition are relatively different. Some proteases form covalent complexes between the enzyme and the substrate site such as serine and cysteine proteases, whereas, there are proteases that do not form covalent enzyme – substrate complexes which are aspartic and metalloproteases (Garcia-Carreno, 1992). The inhibitors with highly electrophilic groups including double bond are required to cope with proteases that form covalent complexes at their catalytic site, whereas the proteases that form non – covalent complexes are reacted on acid or base catalysis (Garcia-Carreno, 1992). In order to instigate the inhibition study, there are recommended several inhibitors and their appropriate enzyme control as listed in Table 4.7.

**Table 4.7** List of inhibitors and enzyme control to identify the class of protease

Class	Inhibitor	Enzyme control
Serine	Phenylmethylsulfonyl fluoride (PMSF)	Trypsin (bovine or porcine) Chymotrypsin (bovine or porcine)
	Soybean trypsin inhibitor (SBTI)	
	Tosyl-lysine chloromethyl ketone (TLCK)	
	Trypsin-inhibitor	
	Tosyl-phenylalanine chloromethyl ketone (TPCK)	
Cysteine	Chymotrypsin-inhibitor	Papain
	Iodoacetamide (IA)	
	p-Hydroxy-mercuribenzoic acid (PHMB)	
	N-Ethyl-maleimide (NEM)	
Aspartic	trans-Epoxy succinyl-L-leucylamido-(4-guanidino)butane (e64)	Cathepsin D Pepsin
Metallo	Pepstatin A	Thermolysin Carboxypeptidase A
	Ethylendiaminetetraacetic acid (EDTA)	
	Ethylene glycol-bis(β-aminoethyl ether)-N,N,N',N'-tetraacetic acid (EGTA)	

To classify the protease produced from hair waste and anaerobically sludge in SSF the protease was tested with several inhibitors. PMSF was used as an inhibitor of a serine protease, and trypsin was used as the enzyme control. For cysteine, protease e64 was used as an inhibitor and papain was used as the control. Pepstatin A is the specific inhibitor of aspartic proteases, and the appropriate enzyme control was pepsin. For metalloproteases



classification, the inhibitor used was EDTA with thermolysin as the enzyme control. The inhibitory assay was followed a normal protease assay with casein as a substrate.

In the present study, pepstatin A, e64, and EDTA which were inhibitors for aspartic, cysteine, and metalloproteases respectively, had a minimal effect on the protease activity as shown in Table 4.8. On the contrary, PMSF as an inhibitor of serine protease demonstrated the reduction in proteolytic activity with 36% – 49% inhibition for all replicates (R1, R2, and R3) at very low concentration (1mM). Therefore, the protease produced in this study can be considered as a serine protease. Since serine proteases are active at pH 7-11 and have broad substrate specificities it may be used in the dehairing process or other industrial processes as reported in other studies (Huang et al., 2003; Ito et al., 2010; Wang et al., 2007).

**Table 4.8** Effect of protease inhibitors on protease activity from different replicates.

Inhibitor	Concentration (mM)	Residual activity (%)		
		R1	R2	R3
Control	-	100	100	100
Pepstatin A	1	98	94	99
	10	97	91	96
PMSF	1	36	47	49
	10	3.8	5.1	6
e64	1	99	98	98
	10	93	87	89
EDTA	1	98.7	94	99.4
	10	81	78	86

The residual activity was assayed under the standard assay conditions in the presence of various inhibitors. 1 mM is the initial concentration of the inhibitors, and 10 mM is the final concentration of the inhibitors. Enzyme activities measured in the absence of any inhibitor were taken as 100%.

#### 4.4.3 Polyacrylamide electrophoresis gel (PAGE)

In the SDS-PAGE the bands for several proteins were observed and calculated using the standard curve (A.4). The observed molecular weights (MW) in SDS-PAGE were 41.7 kDa, 51 kDa, and 65.9 kDa. The validation of the molecular weight of protease produced in this work was conducted using zymogram. The proteolytic activity of concentrated alkaline

protease (R1, R2, and R3) subjected to a zymogram revealed five clear hydrolytic zones around the blue background with a molecular weight from 14.2 kDa, 20.5 kDa, 32.2 kDa, 65.9 kDa, and 103.4 kDa (Fig. 4.7). The molecular weights of the proteases coincided with a previous study (Abraham et al., 2014) that were obtained after 14 days of SSF in 4.5 L reactors when the best results in dehairing were observed. Also, it had been reported that in enzymatic dehairing studies *Bacillus* sp. had dominated to produce the protease with MW for *B. cereus* BGI was 34 kDa (Gupta et al., 2002), *B. cereus* MCM B-326 was 45 kDa (Zambare et al., 2007), *B. cereus* was 66 kDa (Ravindran et al., 2011), *B. cereus* VITSN04 was 32 kDa (Sundararajan et al., 2011), and *B. pumilus* was 32 kDa (Huang et al., 2003). In these regards, probably, the proteases that had been produced in this study were produced by the same consortia of microorganisms mainly from *Bacillus* sp. that may coexist in the mixture of hair waste and ADS for protease production. However, further analysis such as 16S rDNA gene sequencing can be done to validate the consortia involved in this work.

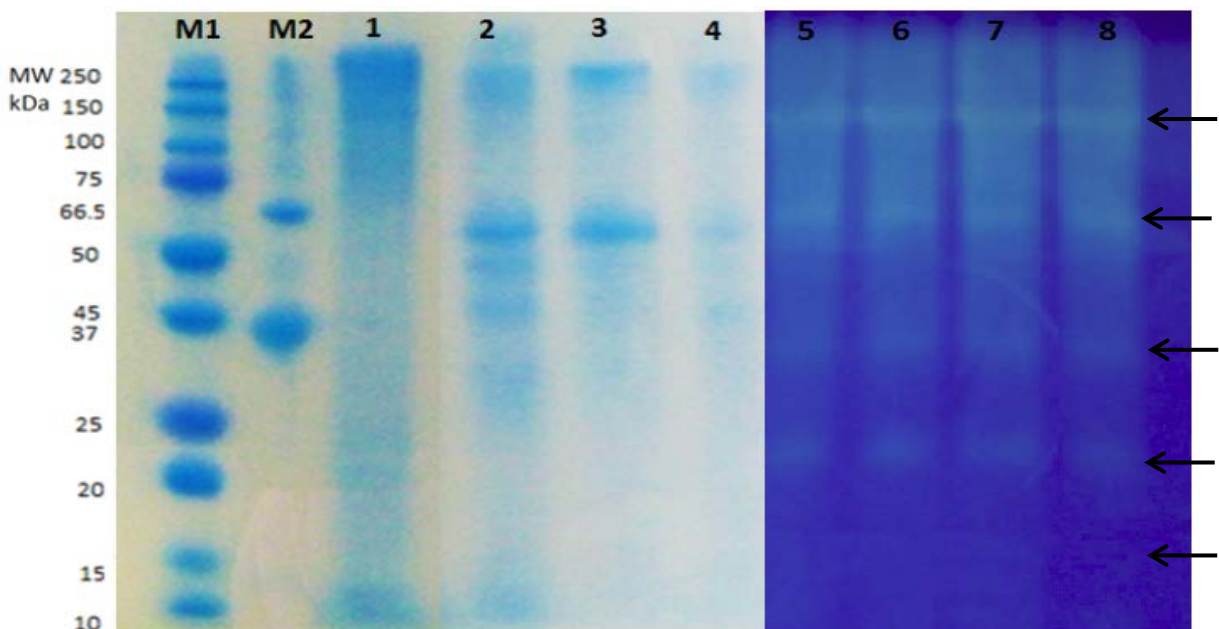


**Fig. 4.7** SDS-PAGE and zymogram of partially purified enzyme on 12% polyacrylamide gel under non-reducing condition (Lane M1: Standard molecular mass marker proteins in kDa; Lane M2: egg albumin (45 kDa); bovine serum albumin (66 kDa); Lane 1: crude extracts; Lane 2, 3, 4: partially purified enzymes from R1, R2, and R3 in SDS-PAGE; Lane 5, 6, 7, 8: partially purified enzymes from R1, R2, and R3 in zymogram)

#### 4.5 Application of protease in dehairing process

In order to evaluate the feasibility of the proposed process at industrial scale, the protease produced was tested on dehairing of high pigmentation cowhides as an alternative to conventional chemical dehairing. Since chemicals dehairing often cause health and environmental hazards due to the toxic chemicals employment for dehairing which consists of lime and sodium sulphide that is highly toxic and has an obnoxious odour (Madhavi et al., 2011). Normally, in tanning industries, the solubilisation of black and brown hair is slower compared to the white and calfskin due to melanin and colour pigmentation (Onyuka, 2010). To validate the possibility of using proteases from SSF in the dehairing process, the lyophilized enzyme (R1, R2, and R3) with similar initial enzymatic activities of  $63.1 \pm 21.6$  U cm<sup>-2</sup>,  $71.3 \pm 12.0$  U cm<sup>-2</sup> and  $78.1 \pm 48.6$  U cm<sup>-2</sup> respectively, were used for dehairing of black cowhides. Fig. 4.8 indicates the percentage of hair removal of the rawhide that was processed for dehairing using Tris–HCl buffer as control, enzymatic and chemical treatments for comparison.

The promising application of protease produced in this study can be observed in Fig. 4.9. Additionally, the dehairing activity of the obtained enzyme was compared with a commercial powder used for dehairing that was being used in the tanning industry with a similar activity ( $624.4 \pm 56.1$  U mL<sup>-1</sup> and  $729.9 \pm 28.5$  U mL<sup>-1</sup> for lyophilised extract and commercial powder respectively). Approximately, between 90% and 95% of hair removal with respect to chemical treatment was observed in treatment with proteolytic enzymes from R2 and R3 after 24 h of incubation. The commercial powder was very close to the chemical treatment. These results suggest that using appropriate enzymatic conditions results in good dehairing performance as pointed out in other studies (Asker et al., 2013; Dayanandan et al., 2003; Sundararajan et al., 2011). In the case of R1, protease showed a weaker activity with only 50% of hair removal probably due to the lower specific protease activity already

detected in SSF (Table 4.3). Sivasubramanian et al., (2008) suggested that dehairing of hides is substantially difficult as the structural features and thickness of skin and hide vary greatly; therefore the dehairing efficiency of the enzyme may vary accordingly. Furthermore, it can be stated that the protease produced in this work presents the possibility to be an alternative to chemical dehairing as reported in other studies carried out at lower scales (Dayanandan et al., 2003; Saravanan et al., 2014; Sivasubramanian et al., 2008; Sundararajan et al., 2011).

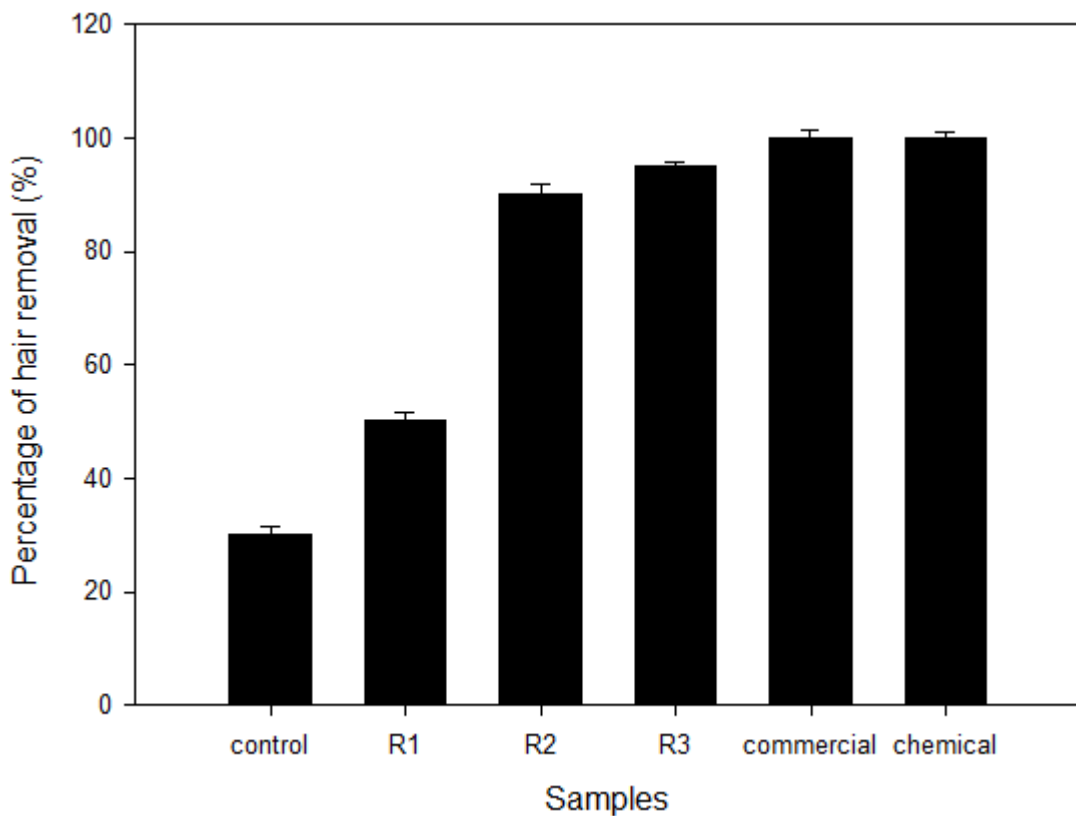


**Fig. 4.8** Percentage of enzymatic dehairing with respect to chemical treatment; hair removal of cowhide using the chemical treatment was considered as 100% of dehairing. Percentage of hair removal for each treatment was calculated as the hair removed using enzymatic dehairing with respect to chemical dehairing on a dry matter basis.



**Fig. 4.9** Dehairing of cow hides treated with (a) Tris buffer as control; (b) chemical dehairing; (c) commercial enzyme; (d) protease from R1; (e) protease from R2; (f) protease from R3.

## Conclusion

The use of hair waste in SSF was found to be a practical approach to produce alkaline proteases that can be utilised in the dehairing process as an alternative to chemical dehairing that is not environmental friendly. Moreover, in-situ protease extraction could make SSF process easier to scale up, due to the employment of single reactor for the process from fermentation to downstream processing. Additionally, after extraction, SSF can be continued with the remaining residues to reach final stabilisation, similar to the composting process. With regards to the enzyme properties, protease activity produced in this study was only inhibited by PMSF, suggesting that it belongs to the serine protease group. The enzyme produced has highly and stable alkaline properties with moderate heat stability (30 – 50°C), which is of relevance during industrial dehairing application. In conclusion, the process presented can be considered a complete alternative to chemical dehairing. By all means, solid

waste valorisation of hair waste and ADS via SSF could potentially produce high yield alkaline serine protease which has broad substrate specificities that may be used in industrial processes. In future works, to improve the efficiency of wastes utilisation, the use of hair waste should be investigated with a particular focus on biorefinery concepts (possibility of obtaining other valuable products). At the same time, subsequent studies should be concentrated on a deep economic and environmental study of the entire process.



## Chapter 5

*Screening and optimisation of protease immobilisation on different  
type of support/carrier*



Graphical abstract

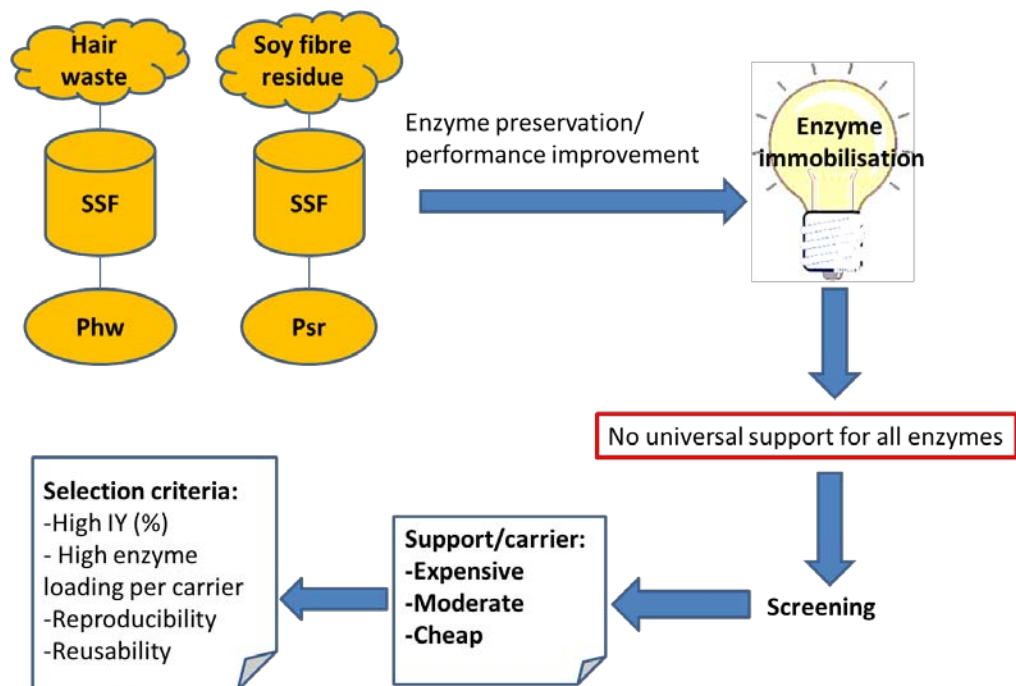


**Fig. 5.1** Graphical abstract of preservation and improvement of proteases produced from SSF by selection of promising support/carrier.

## **Summary**

This chapter comprised of a preliminary study of immobilisation, screening various materials that appropriate for protease immobilisation including the optimisation of enzyme loading and characterisation of the support/carrier (Fig. 5.1) in order to preserve and improve the performance of enzymes produced by solid state fermentation (SSF). The initial criterion for the selection of the most suitable support/carrier was depended on the retention of the catalytic activity of immobilised enzyme, thus the immobilisation efficiency was monitored using immobilisation yield (%) and enzyme loading (U/mg) for each support/carrier. Later the optimum condition obtained from these studies will be carried forward in Chapter 6.

### **5.1 Assessment of an appropriate support/carrier for protease immobilisation**

To achieve an efficient and economical enzyme immobilisation, few significant factors need to be considered such as the type of support, a method of immobilisation, and purpose of immobilised enzymes (Mohamad et al., 2015). The support or matrix for biocatalyst should be inert and biocompatible to the environment so that it will not interfere with the reaction of the substrate and the enzyme, plus do not cause any harm to the environment (Cipolatti et al., 2014).

As we concerned, finding a suitable support or carrier is the most crucial step for protein immobilisation. Nanoparticles have captured our attention as a carrier due to the high enzyme loadings. Since the nanoparticles maximized surface per unit mass, internal diffusion limitations are avoided, and external agitation seems unnecessary as nanoparticles undergo Brownian dispersion efficiently (Jia et al., 2003). The most compelling evidence is in the enhancement of the enzymatic activity and stability (Gole et al., 2001).

## 5.2 Gold nanoparticles (AuNp) as a model carrier

Gold nanoparticles (AuNp) has demonstrated to be an excellent biocompatible surfaces for the immobilisation of enzymes (Ardao et al., 2012; Phadtare et al., 2004). After the protein has been immobilised, the protein shell may promote the colloidal stability of AuNps, which in turn AuNps deliberately render an extra stability to the proteins (Koller et al., 2010; Pandey et al., 2007). Therefore, gold nanoparticles (AuNp) were chosen as a model carrier for the protease that we produced by SSF from protein-rich waste.

As the first attempt, proteases produced by SSF from hair waste and ADS were used. A stock solution of  $10^{12}$  AuNp/ml with an estimated size of 10 nm was provided by Catalan Institute of Nanotechnology (ICN). To check the biocompatibility of AuNp, about 100  $\mu$ l of the protease with  $115 \pm 39$  U/ml (approx. 100 mg/ml of lyophilised enzyme) was added to 1 ml of AuNp solution and then were left to conjugate in 4°C for 1 h provided with mild agitation. The immobilisation process was done in 4°C to reduce the denaturation rate of the protease enzyme. Fig. 5.2 shows the UV-Vis spectra of the colloidal AuNp solution and the colloidal AuNp after conjugation with protease.

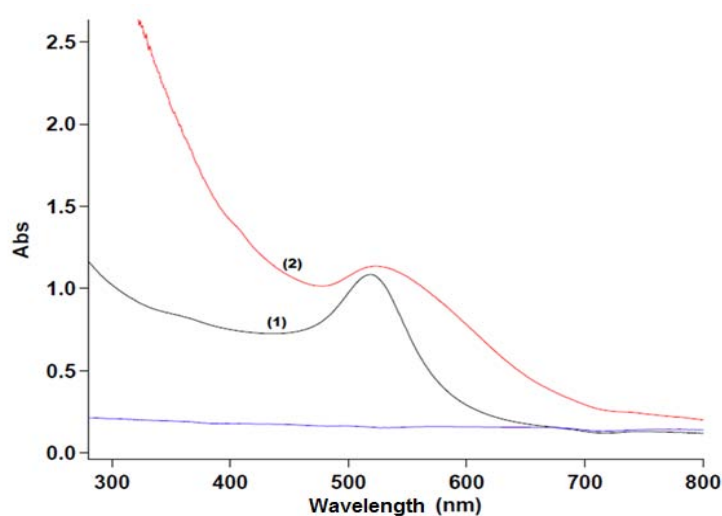


**Fig. 5.2** UV-Vis spectra of the colloidal AuNps solution (curve 1; —) and the colloidal AuNps solution after conjugation with protease (curve 2; →) for 1 h

The surface plasmon resonance in UV-Vis spectra for colloidal AuNps solution ( as shown in Fig. 5.2 curve 1) shows that the absorbance was 1.084 at 520 nm, which is similar to other studies with AuNps solution (Ardao et al., 2012; Phadtare et al., 2004). After conjugation of protease to AuNps the peak was enhanced (abs 1.270) and slightly modified (wavelength 524) in the UV-Vis spectra as can be seen in Fig. 5.2 (curve 2). This fact showed the successful immobilisation of protease to AuNps surfaces as indicated in previous studies regarding with the attachment of the protein to AuNps (Kobayashi et al., 2012).

### **5.2.1 Protein/enzyme loading on AuNps**

An excessive protein or enzymatic loading can reduce the activity and stability of the enzyme where it can develop a steric hindrance against the substrate (Zhang et al., 2009). Therefore, to avoid the denaturation and oversaturation of protein loading, the determination of an appropriate concentration of enzyme to form a bioconjugate with AuNps were explored. In this experiment different concentration of enzyme (approx. lyophilised extracts: 5.5 mg/ml – 55 mg/ml) were tested with a constant concentration AuNps ( $4.5 \times 10^{11}$  Np/ml). The enzyme and nanoparticles were left to form a bioconjugate at 4°C with mild agitation for 1 h.

The loading of protease on AuNps surface was calculated according to Equation 3.14 (Section 3.5.3) and analysed by UV-Vis spectroscopy (Fig. 5.3). A peak shift of absorbance was observed from 517 nm AuNps with 5.5 mg/ml of lyophilised extracts up to saturation at 522 nm for the concentration higher than 40 mg/ml, whereas the surface plasmon resonance intensity was kept increasing along with increasing lyophilized enzyme extracts concentration from 2.31 to 2.38. Similarly, in the case of an immobilised enzyme, the protease loading was increasing as the amount of lyophilised extracts increased. Since the concentration of AuNps was kept constant in these experiments, the activity per nanoparticle was increasing due to the more available free surface of AuNps to attach to proteases. This means that higher

amount of protease activity can be added to the AuNps solution. Since the enzyme loading on the AuNps surface was not well known, thus it is necessary to examine the optimum condition using experimental design which will be discussed afterwards.

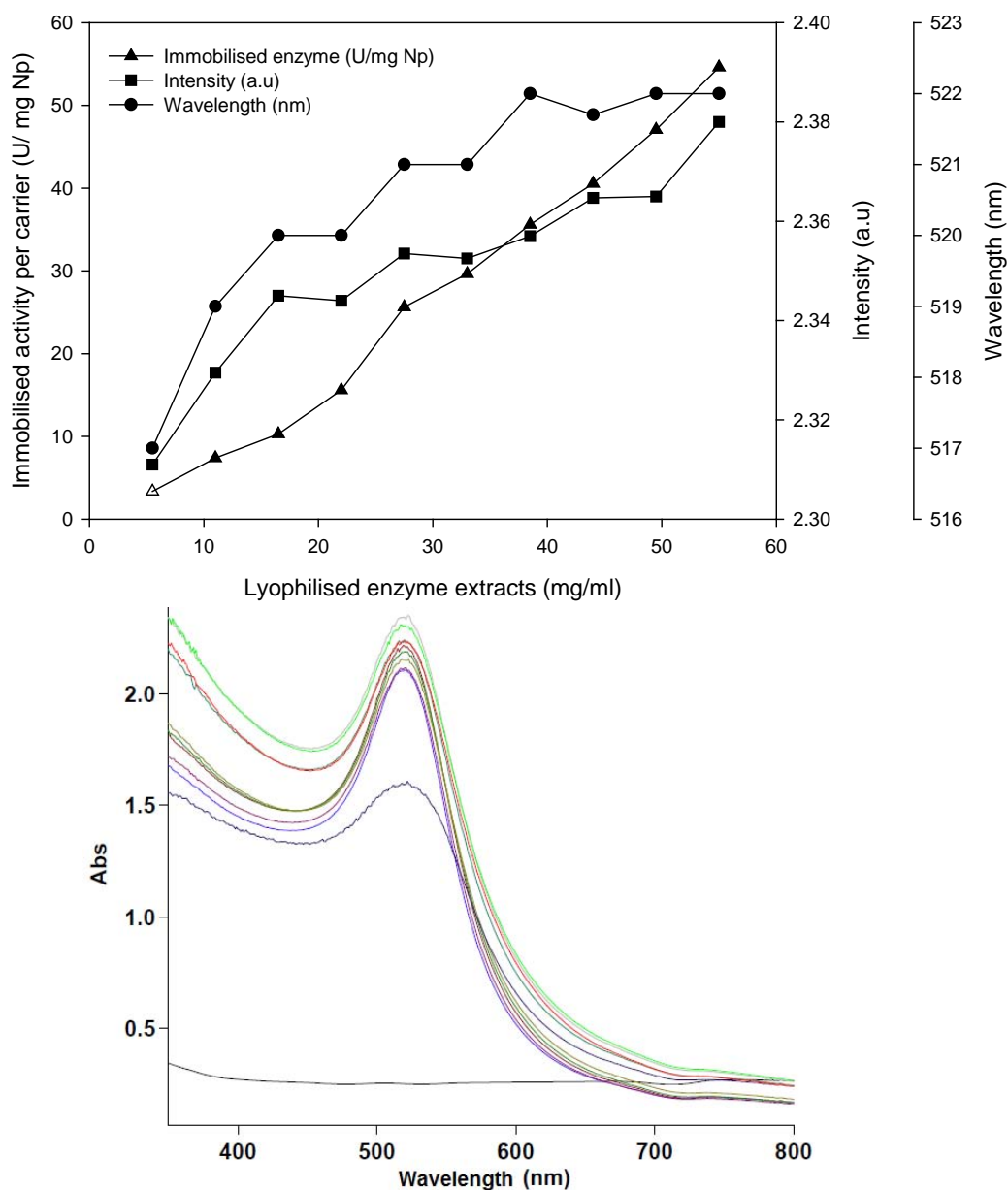


**Fig. 5.3** Evaluation of protein loading on AuNps surface with different concentration of lyophilised enzyme extracts (above). UV-Vis spectra recorded with various concentration of protein loading (below).

Furthermore, the immobilisation process was investigated with varying time (0 h – 48 h) and the agitation or static condition. The immobilisation yield was calculated using Equation 3.15 (Section 3.5.3). In all cases, the protease reaches the AuNps surface almost instantaneously after mixing and readily conjugates (Fig. 5.4). The immobilisation yield reached the maximum rate after 1 hour of mixing. The effect of agitation after 1 h was 85% and the effect of static loading was 82% which not give much different to the loading rate of protease on AuNps surfaces. It was in agreement with another study (Jia et al., 2003) which suggested unnecessary of external agitation. Therefore, further experiments were carried out with mild agitation just to obtain a homogeneous solution for 1 h of immobilisation time.

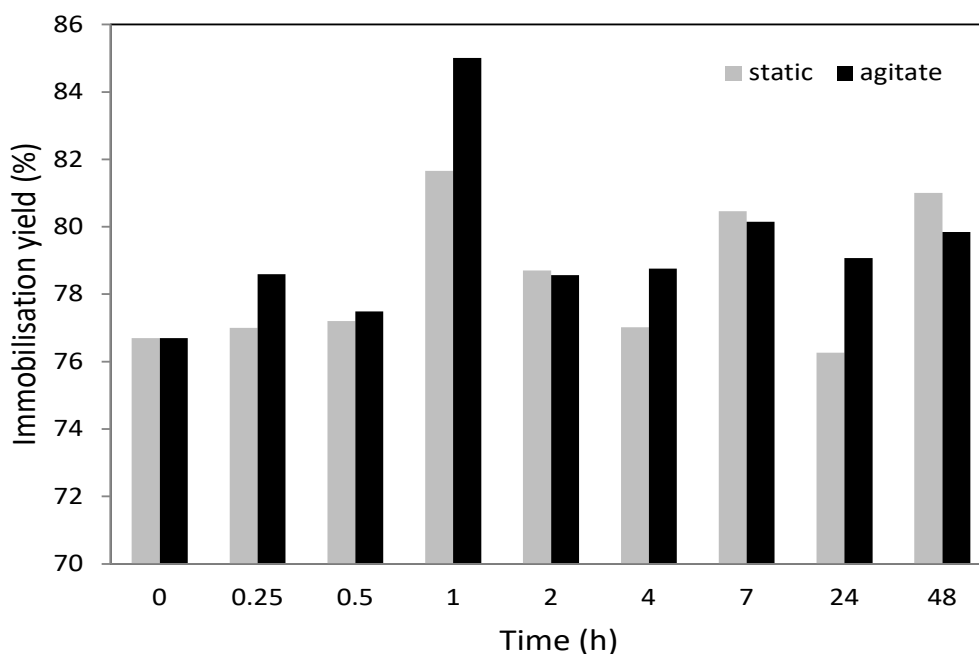


**Fig. 5.4** Immobilisation yields (%) of the enzyme on AuNps surfaces during conjugation for 48 h under static and agitate condition at 4°C.

### 5.2.2 Box-Hunter experimental design

In order to determine the optimum condition for enzyme loading per nanoparticles, an experimental design was constructed according to the Box-Hunter technique as shown in Fig. 5.5. Accordingly, the experimental points were distributed in the extreme values (bullet

points) and in a circumference of radius which are marked as star points in Fig. 5.5. The distribution used was to confirm that the information obtained from each experiment to be the same since all the points were equidistant from the centre point (Sánchez et al., 2000).

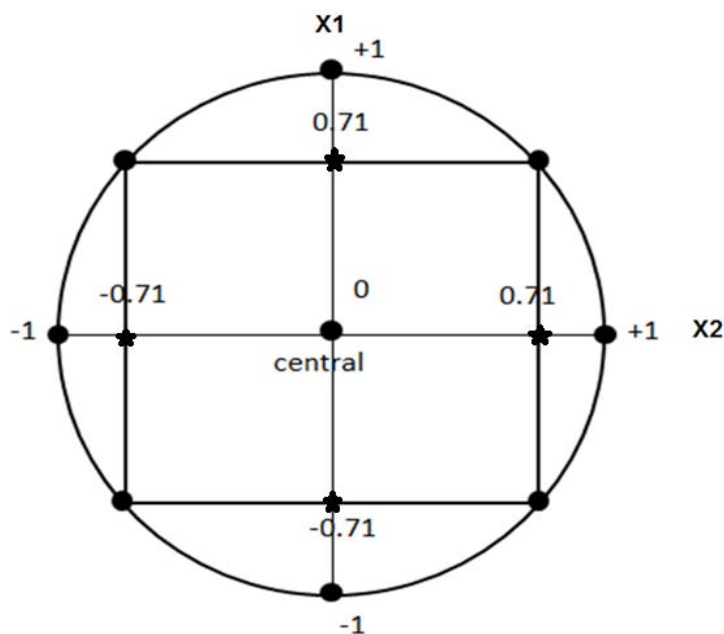


**Fig. 5.5** Experimental design with two factors (X1 and X2) according to Box-Hunter experimental design. The dot points represent the condition tested.

The design of experiment by Box-Hunter for determining the appropriate amount of protease and AuNps to establish a decent bioconjugate was tabulated in Table 5.1 consists of 16 experiments with 4 replicates at the centre. Two factors were used to set up the design, which were the concentration of nanoparticle (Np/ml) as X1, and the lyophilised enzyme extracts concentration (mg/ml) as X2. Correspondingly, it resulting in three responses as the objective function, where F1 was protease activity per weight of AuNps (U/mg Np), F2 was the percentage of immobilized enzyme (%), and  $\alpha$  was a specific objective function with the combination of 75% of F1 and 25% of F2. The results suggested that F1 and F2 gave different responses towards the optimisation of the immobilisation condition. Therefore, the specific objective function ( $\alpha$ ) was employed because of its influence on the optimum

immobilisation condition that comprises both enzyme loading (U/mg Np) and immobilisation yield (%). This response was illustrated in Fig. 5.6.

**Table 5.1** Experimental design of protein loading on AuNps surfaces and its responses

Run	X1 (coded)	X2 (coded)	X1 (actual) (Np/ml)	X2 (actual) (mg/ml)	A	B	Uo	F1 A/B (U/mg)	F2 A/Uo (%)	$\alpha=(0.40*F1)$ $+(0.25*F2)$
1	0	0	$4.5 \times 10^{11}$	45	84	2.27	105	37	80	34
2	0	0	$4.5 \times 10^{11}$	45	87	2.27	105	38	82	35
3	0	0	$4.5 \times 10^{11}$	45	85	2.27	105	38	81	34
4	0	0	$4.5 \times 10^{11}$	45	88	2.27	105	39	84	36
5	1	1	$1.0 \times 10^{12}$	100	162	5.06	229	32	70	30
6	1	-1	$1.0 \times 10^{12}$	10	18	5.06	26	4	69	19
7	-1	1	$1.0 \times 10^{11}$	100	80	0.51	229	157	35	68
8	-1	-1	$1.0 \times 10^{11}$	10	19	0.51	26	38	73	32
9	0.71	0.71	$7.7 \times 10^{11}$	77	131	3.89	177	34	74	31
10	0.71	-0.71	$7.7 \times 10^{11}$	13	29	3.89	33	7	87	25
11	-0.71	0.71	$1.3 \times 10^{11}$	77	131	0.66	177	199	74	94
12	-0.71	-0.71	$1.3 \times 10^{11}$	13	30	0.66	33	45	90	39
13	1	0	$1.0 \times 10^{12}$	45	97	5.06	105	19	92	30
14	-1	0	$1.0 \times 10^{11}$	45	97	0.51	105	192	92	96
15	0	1	$4.5 \times 10^{11}$	100	213	2.27	229	94	93	58
16	0	-1	$4.5 \times 10^{11}$	10	16	2.27	26	7	62	18

X1: AuNps concentration; X2: lyophilised enzyme extracts concentration; A: activity of immobilised enzyme (U); B: weight of AuNps (mg); Uo: initial activity of enzyme (U); F1: objective function of activity per weight of AuNps; F2: objective function of percentage of immobilised enzyme;  $\alpha$ : objective function of F1 and F2.

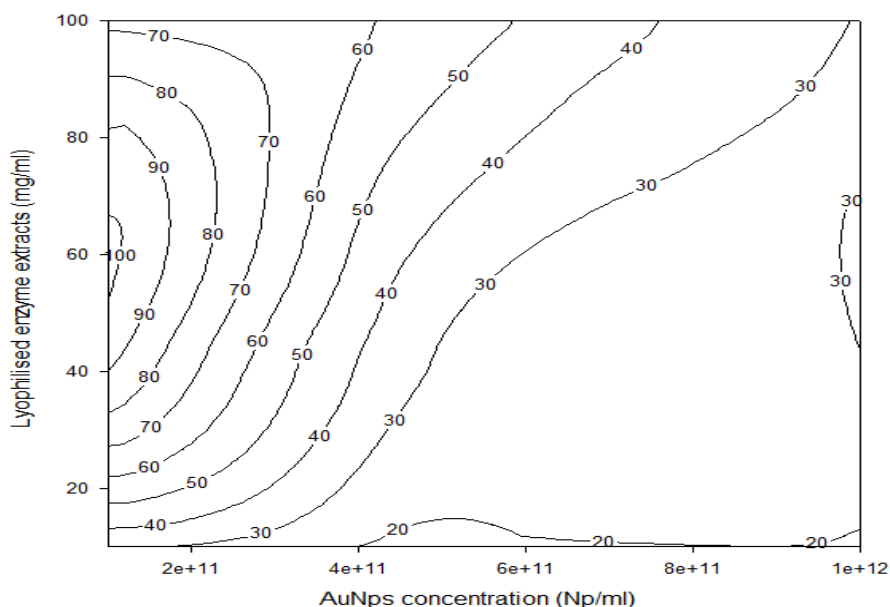


**Fig. 5.6** Contour plot of specific objective function ( $\alpha$ ) towards protein loading and immobilisation yield



By applying  $\alpha$ , the appropriate and optimised concentration of lyophilised enzyme extracts was around 60 mg/ml (approx. initial activity 138 U) using a lower concentration of AuNps ( $1.15 \times 10^{11}$  NP/ml; approx. 0.581 mg), which resulted in the maximum immobilisation yield.

In order to verify the immobilisation of the enzyme on the nanoparticles, transmission electron microscopy (TEM) was used. Fig. 5.7 (a) shows the AuNp before the immobilisation process, a particle with a clear surrounding can be observed. While after the immobilisation one can notice a layer covering the surface of the nanoparticle (Fig. 5.7 b). This result was in accordance with other studies where a layer as halo covering the AuNps after enzyme immobilisation was observed (Ardao et al., 2012). Thus we can conclude that the immobilisation of the produced proteases was successful using AuNps as a carrier.

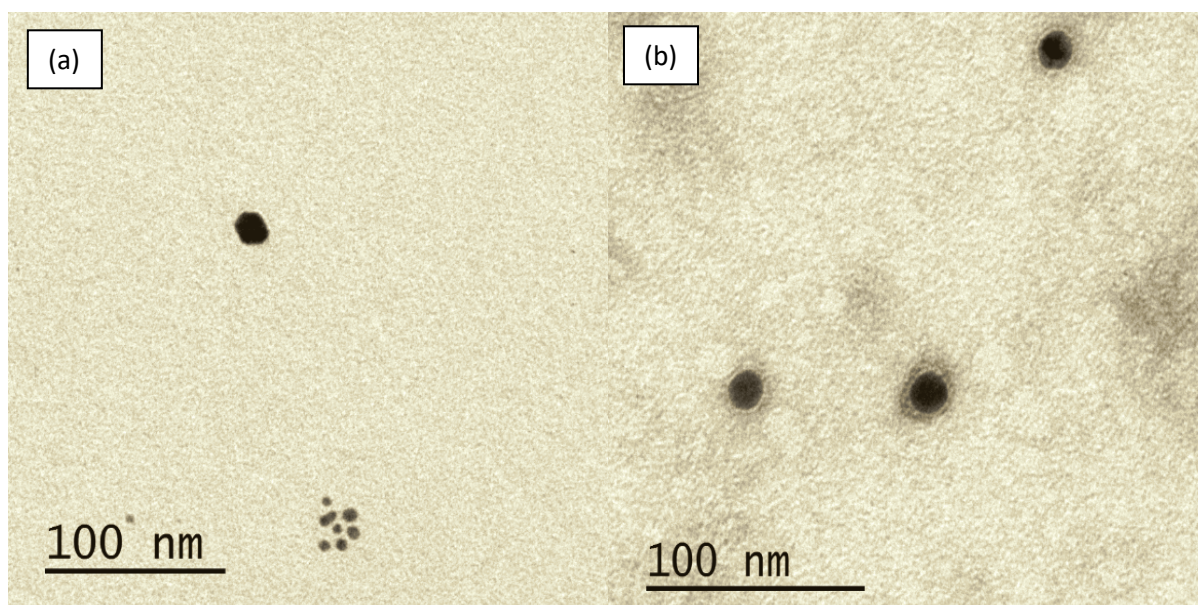


**Fig. 5.7** TEM image of AuNps: 100 nm before (a) and after (b) enzyme immobilisation

### **5.2.3 Operational stability of immobilised protease on AuNps**

The investigation on immobilisation efficiency was carried forward by comparing free and immobilised enzyme operational stability in terms of the pH and temperature using optimum enzyme loading condition. The pH was varied within a range of 5-11 and temperature was varied between 30°C-70°C, where the residual activity was determined by comparing the initial activity of the enzyme before each treatment, denoted as 100%. The immobilised enzyme showed a significantly enhanced pH and temperature stability and a shift in the optimum temperature operation. At 30°C both of the enzymes were stable at pH 11, but immobilised enzyme had 20% more activity at pH 11 than free enzyme (Fig. 5.8 a). Furthermore, at 50°C, the immobilisation enzyme maintained more activity at pH 11 unlike to free enzyme, that only had 54% of residual activity at pH 11 (Fig. 5.8 c). While at 70°C, the immobilised enzyme depicted improvement of residual activity at pH 11 where the residual activity was more than 80% at the end of the incubation reaction. However, the free enzyme showed its optimum at pH 8, whereas the activity was drop at pH 11 (Fig. 5.8 b).

Uniquely, during the experiments, the nanoparticles showed no aggregation in the colloidal solution whenever treated with each condition. It is known that nanoparticles tend to aggregate in high pH condition (Koller et al., 2010). However, in this experiment, this phenomenon was not observed. This could be due to the formation of AuNps-enzyme complex, which formed a protein shell that provides a colloidal stability to the nanoparticles as reported previously by others (Koller et al., 2010; Pandey et al., 2007). These observations suggested that the immobilised enzyme on AuNps could enhance the enzyme activity and stability of the enzyme as proposed previously (Gole et al., 2001).

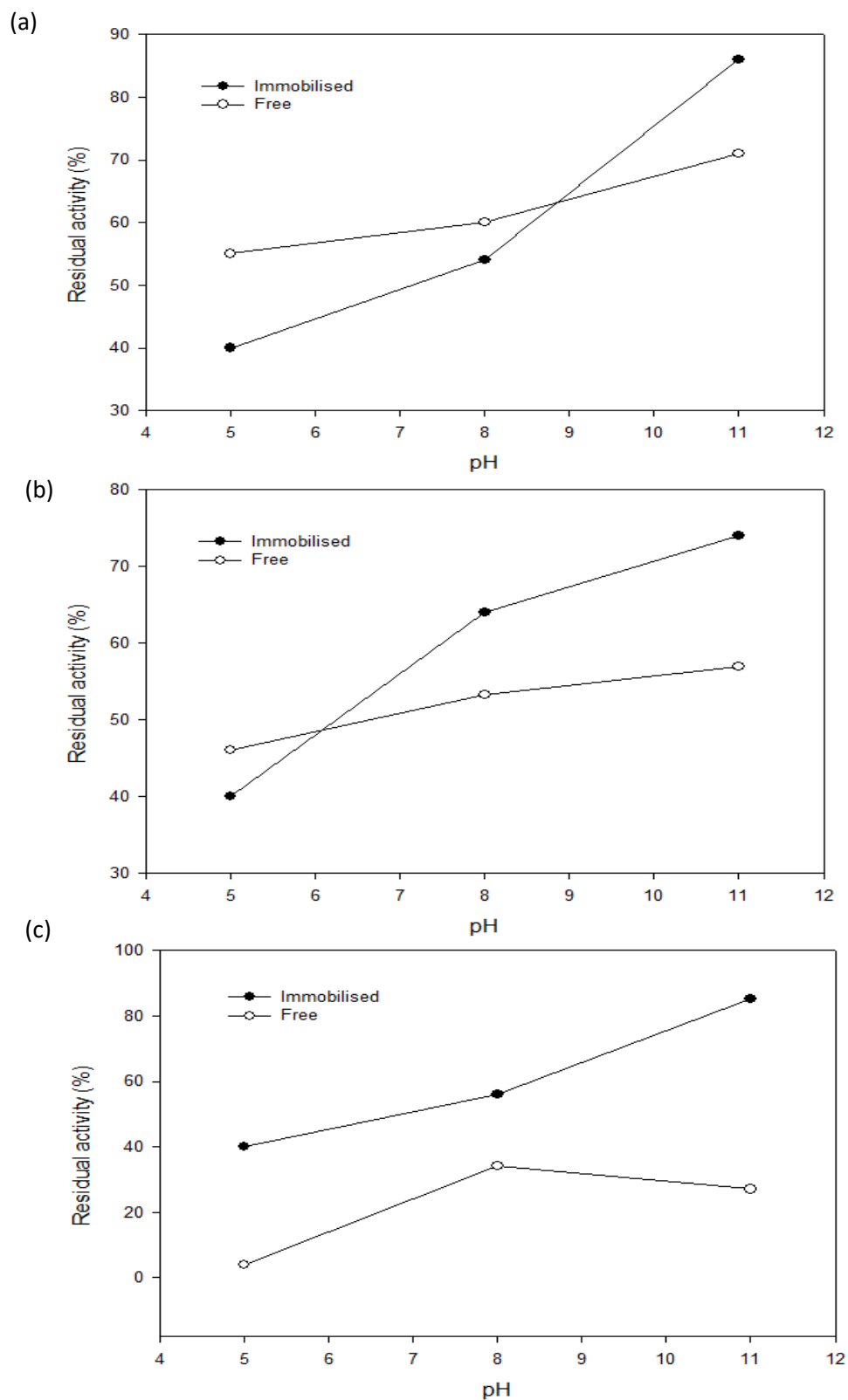


**Fig. 5.8** Comparison of free and immobilised enzyme in various pH at temperature (a) 30°C, (b) 50°C, and (c) 70°C

#### 5.2.4 Reusability of immobilised enzyme

The reusability was performed using the optimum enzyme loading condition obtained from the Box-Hunter experimental design. To study the reusability of immobilised enzyme, the activity of protease was calculated from the reaction of bioconjugate materials over 4 consecutive reuse cycles. The separation process was done using centrifugation at 5000 rpm for 30 min. The supernatant was taken to analyse the activity, and the pellet with AuNps-enzyme and casein residues was washed thoroughly using Tris buffer. Then the casein hydrolysis reaction was reinitiated using the resuspended pellet in 1 mL of Tris buffer. The first batch was considered as 100% of reaction. In the next cycle was observed less than 80% of reusability. After that, the activity was drop abruptly, completely losing activity by the fourth cycle of the reaction. The reusability of the enzyme immobilised on AuNps was lasting until fourth cycles (Table 5.2).

**Table 5.2** Biocatalytic activity of protease immobilised on AuNps during successive reuses.

No of cycle	Immobilised activity on AuNps (U/mg Np)	% Reusability
1	214	100
2	168	79
3	42	20
4	17	8

The main reason to establish immobilised enzyme was to enable the reusability of the enzyme to reduce the operating cost. Moreover, it is important to consider that enzyme immobilisation is not only for enzyme stabilisation but also to avoid the enzyme inactivation at the end of the reaction process as the catalyst can easily be removed from the reaction medium (Tavano, 2013). In this work, the immobilisation on AuNps surfaces was successful. However, the problem came whenever to recover the nanoparticles from the reaction

medium. As observed in Fig. 5.9, the casein was interspersed with AuNps-enzyme complex and required a washing process to remove the casein from the pellet. The inefficiency of reusability of the immobilised enzyme was due to AuNps-enzyme loss during the washing process. As a matter of fact, the loss of biocatalytic activity of immobilised enzyme also corresponds to the weakly bound of an enzyme that leaches out during the reaction cycle.

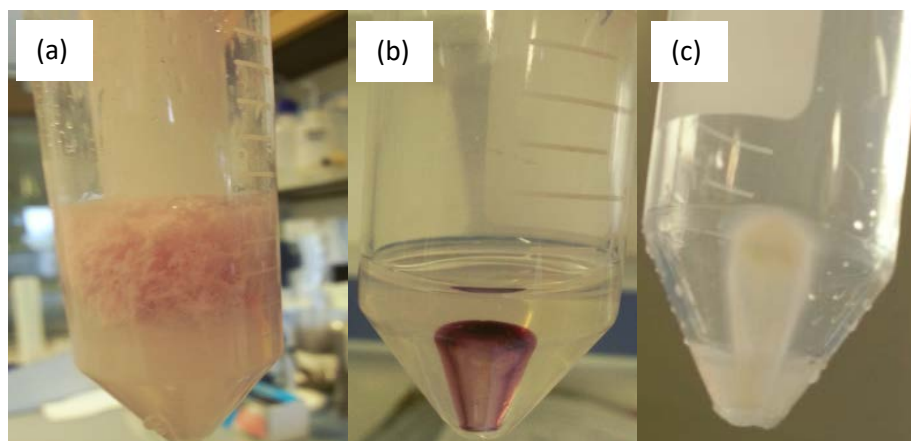


**Fig. 5.9** Observation of reusability of immobilised protease on AuNps (a) after incubation with substrate in hydrolysis reaction, (b) after separation by centrifugation for 1-3 cycles where casein residue bound with the nanoparticles, (c) after separation by centrifugation for 4<sup>th</sup> cycle

Even though AuNps demonstrated an efficient immobilisation yield and enzyme loading that prove the biocompatibility as a carrier, but the reusability of the immobilised enzyme on AuNps was insignificant. Not to mention, the price for AuNps also is considered as expensive comparing to other available materials used for immobilisation. Likely, the problem of reusability may be overcome if the AuNps could be tethered at high density to a more large surface, such as that provided by micron-sized particles as suggested by others (Phadtare et al., 2004). They had demonstrated AuNps loaded on amine-functionalized Na-Y zeolite particles (pore diameter 12 Å, particle size 0.8 μm) provided a biocompatible surface for the immobilisation of the fungal protease enzyme. Moreover, the use of other nanoparticles can be explored for the proteases immobilisation such as zeolite particles,

chitosan, magnetic nanoparticles, titanium oxide nanoparticles, and others that are considered as cheap materials in comparison to gold nanoparticles.

### **5.3 Immobilisation of proteases on different support/carrier**

To find a better and feasible support/carrier for the proteases immobilisation, different supports were tested. The ideal supports/carrier for enzyme immobilisation should include high affinity to proteins, availability for chemical modifications, mechanical stability and rigidity, reusability, ease of preparation, biodegradable, and affordable (Datta et al., 2012; Mohamad et al., 2015).

The work done here was considered as a screening process using simple adsorption technique to see the biocompatibility of the support/carrier towards the protease. As AuNps resulted an excellent biocompatibility with the proteases from SSF using hair waste and ADS (Phw), it has been chosen as a model support/carrier for the other materials in the screening for immobilisation support/carrier. Also, protease from SSF of soy fibre residue and ADS (Psr) was assessed for the biocompatibility with the support/carrier along with Phw. The adsorption and desorption activity of proteases (both Phw and Psr) were tested on different supports that were classified in term of price (cheap, moderate, and expensive) relative to the gold nanoparticles. All the supports/carriers were synthesised according to the method in the Section 3.5.1. The supports/carriers had been synthesised by direct supervision of PhD student in UAB (Gicom). In details, the list of supports used in this work is as follows:

#### **A) Cheap support**

- 1) Chitosan beads (wet and dry)
- 2) Functionalised zeolite particles
- 3) Anionic resin (A520)
- 4) Fe<sub>3</sub>O<sub>4</sub> nanoparticle (MNPs)

#### **B) Moderate support**

- 1) Titanium oxide (TiO<sub>2</sub>\_A nanoparticles)

- 2) Titanium oxide (TiO<sub>2</sub>\_B nanoparticles)
- 3) Chitosan/Au
- 4) A520/Au

**C) Expensive support**

- 1) AuNps

For conjugation process, 3 ml of proteases enzyme with an initial activity of 519 U/ml for Phw and 336 U/ml of Psr respectively were added to each tube containing 27 ml of Tris buffer and supports. The tubes were agitated gently for 24 hours at 4°C. Sampling was done in every 2 hours after conjugation to check the performance of the immobilisation process. Since the weights of the supports were varied (approx. 0.1 g), the results were expressed as immobilisation yield (% IY) according to Equation 3.15 (Section 3.5.3). All experiments were run simultaneously.

Naturally, chitosan dissolves readily in acidic solution and forms viscous solution upon an increase in pH. In the first assessment, chitosan beads were used after preparation using neutralisation method and subjected to crosslinking with glutaraldehyde as mentioned in Section 3.5.1.4. Chitosan is considered as a cheap material as it is derived from low-cost crustacean shell wastes and readily available in powder and flakes forms commercially (Krajewska, 2004). Chitosan was made into beads to facilitate the separation after conjugation that increases the enzyme reusability of the immobilised enzyme later on. By the same token, to overcome the separation and reusability problems, AuNps were tethered to the large surface with more density (Phadtare et al., 2004); chitosan beads were coated with AuNps to enhance the biocompatibility for protease immobilisation.

During 24 h of immobilisation process, immobilisation of Phw on nanocomposite of chitosan and AuNps (Chitosan/Au) exhibited an enhanced (60% of immobilisation yield after 5 h) and consistent conjugation with immobilisation of Phw on AuNps alone with 58% of

immobilisation yield after 5 h (Fig. 5.10 a). However, the immobilisation of Psr on Chitosan/Au showed an insignificant effect towards immobilisation yield where the maximum immobilisation yields was only 13% after 7 h (Fig. 5.10 b). With Psr, dry chitosan beads rather demonstrated a better immobilisation yield compared to wet chitosan beads achieving a maximum immobilisation yield of 23% after 7 h, while an opposite effect was observed when using Phw. After all, AuNps still showed as an excellent carrier for both of the proteases (Phw and Psr).

Since a good yield was achieved using Chitosan/Au with Phw comparable with using AuNps as a carrier, further TEM analysis was taken to compare the image before and after immobilisation process as shown in Fig. 5.11.

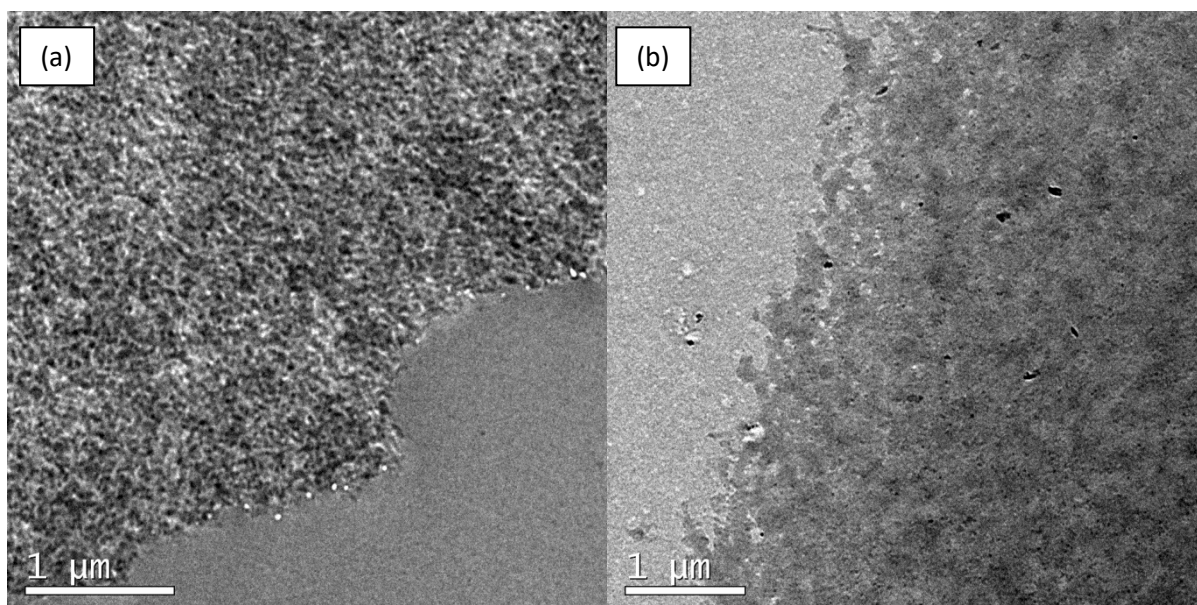


**Fig. 5.11** (a) TEM image of cross-sectioned chitosan coated with gold nanoparticle (Chitosan/Au) before immobilisation, (b) TEM image of cross-sectioned chitosan coated with gold nanoparticle (Chitosan/Au) after enzyme immobilisation.



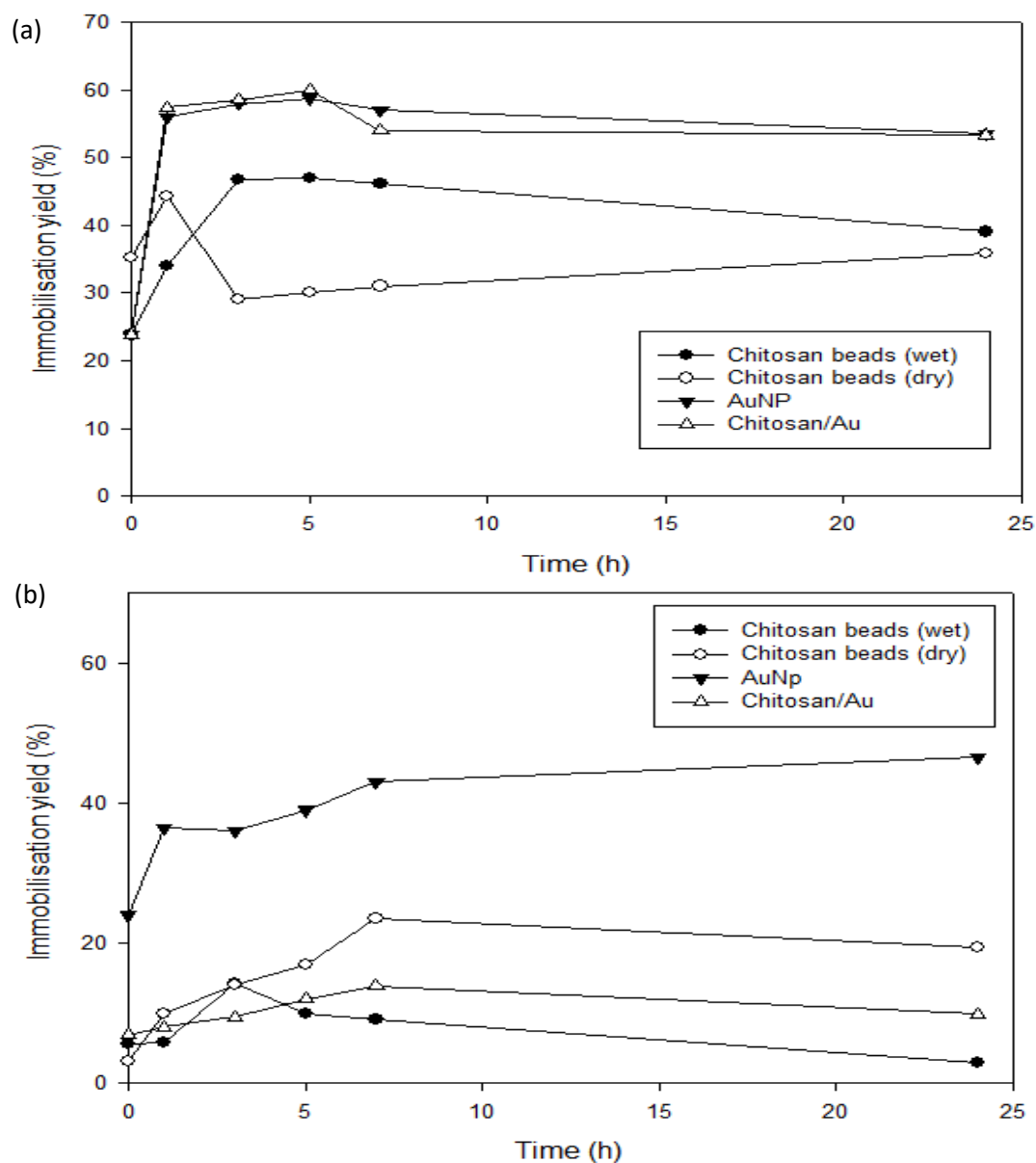


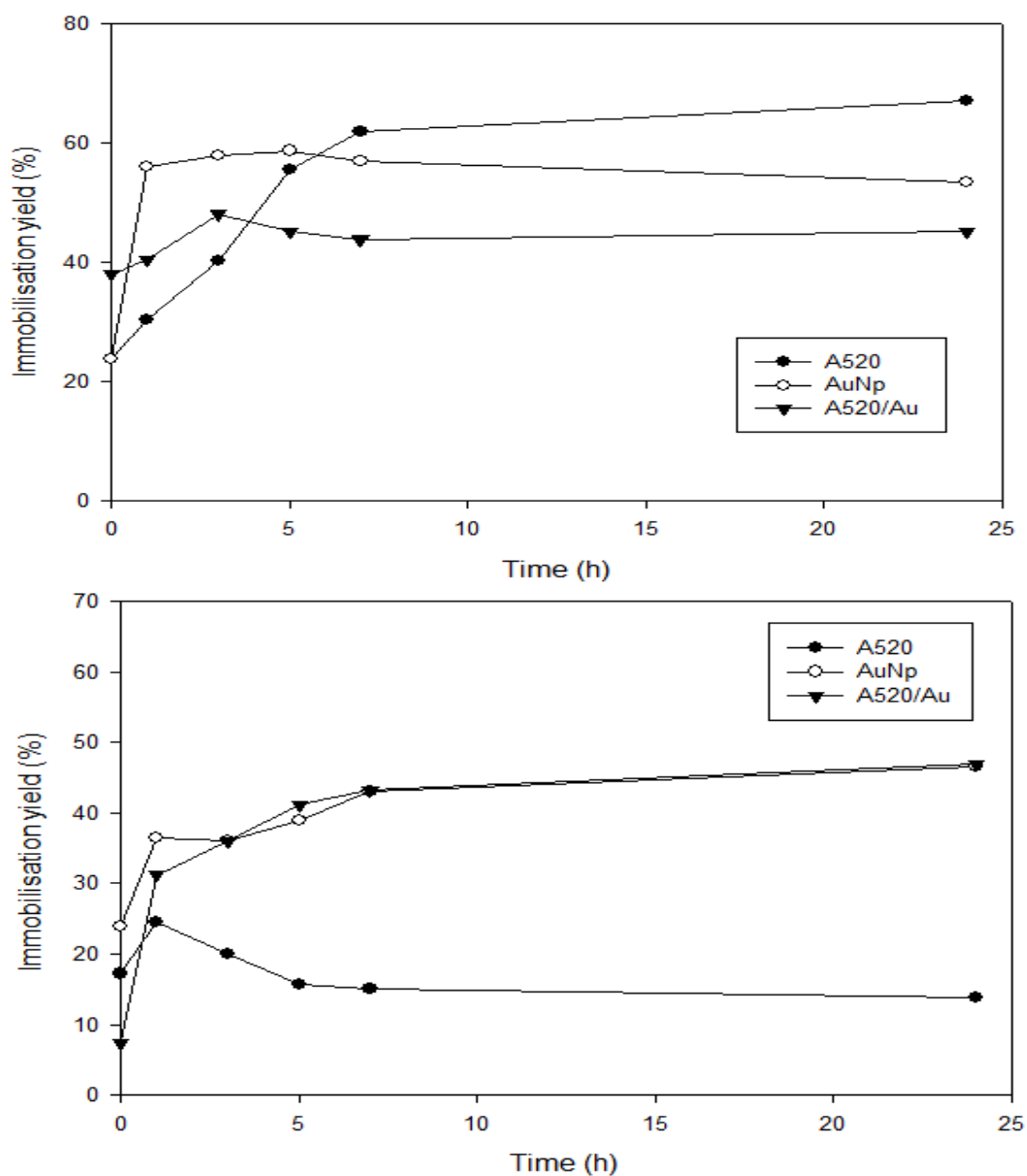
**Fig. 5.10** Enzyme immobilisation yield of (a) Phw and (b) Psr on chitosan beads, chitosan-AuNPs nanocomposite and compared with AuNPs as a model carrier.

As shown in Fig. 5.11 (a), the AuNPs coated chitosan were well dispersed as suggested by the dark area due to denser particles. They presented a crystalline form with approximately 10-25 nm in size. The chitosan/Au particles were cross-sectioned, fixed, and embedded before the analysis. The white contrast on the surface is supposed to be the pores of chitosan. Due to the small channel of the pores, the resin used to prepare the sample before analysis is not able to go into them resulting in a brighter contrast in the image. In Fig. 5.11

(b) the surface seems covered with particles in a smoother way than that of Fig. 5.11 (a). It was probably due to the enzyme attachment and covering the surface of the chitosan/Au, thus confirming the immobilisation of the enzyme.

Furthermore, the immobilisation assessment was carried on adsorption of Phw and Psr on anionic resin (A520). The anionic resin is considered as cheap, mechanically resistant, chemically stable, nontoxic, non-polluting and ease of renewability (Ribeiro and Vitolo, 2005). Also in this work, the surface of A520 was coated with AuNps to investigate the effect of immobilisation efficiency. A520 alone showed a maximum immobilisation yield with Phw (67%) after 24 h of conjugation (Fig. 5.12 a), while with Psr the maximum immobilisation yield was 27% at the beginning of the conjugation process. Then desorption occurred until 24 h (Fig. 5.12 b). At the end of the conjugation period, the colour of the resin changes from white to a brownish colour. It was due to the enzyme adsorption since the enzyme solution was brown in colour.

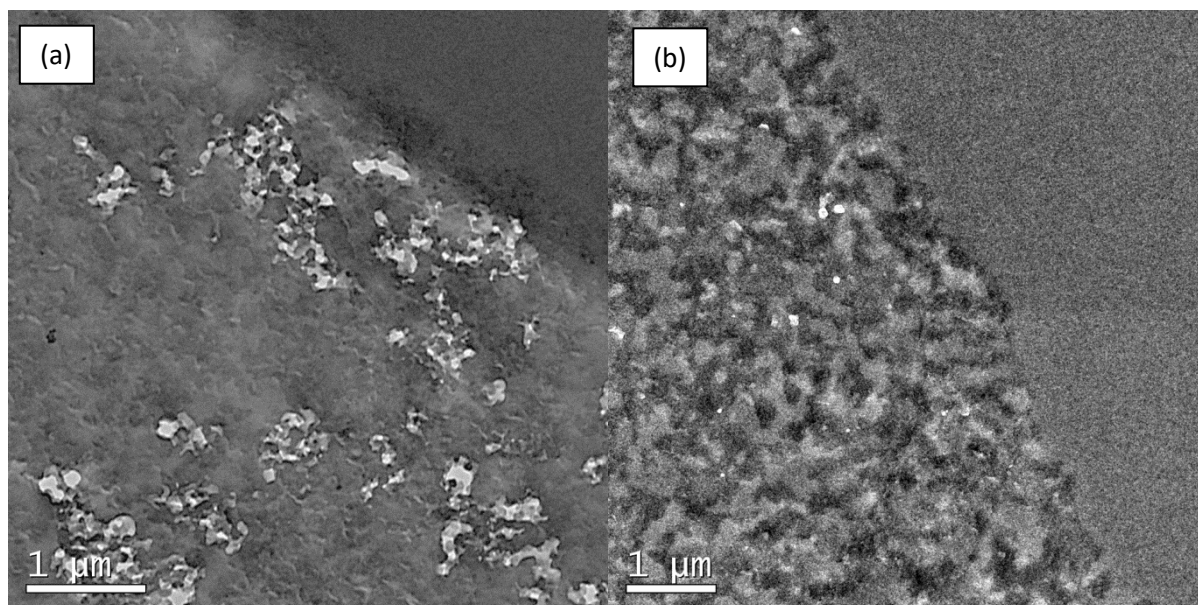
Moreover, the effect of coating the anionic resin with AuNps (A520/Au) gave a similar yield with AuNps alone for Psr after 24 h of conjugation period. However, for the Phw in the similar conditions, there was no improvement was observed in the immobilisation yield in comparison with the immobilisation on AuNps alone (Fig. 5.12). However, immobilisation yield with Phw was similar to that of Psr after 24 h which was 48% achieved only after 3 h of conjugation period with A520/Au. Different proteases (Phw and Psr) presented a different immobilisation profile and the preference for the conjugation seem unclear. Though, immobilisation on the anionic resin surface displays no further desorption occurred during 24 h and reached plateau, which indicated the stability of the support for immobilisation process (Ribeiro and Vitolo, 2005).



**Fig. 5.12** Enzyme immobilisation yield of (a) Phw and (b) Psr on anionic resin, anionic resin-AuNps nanocomposite and compared with AuNps as a model carrier.

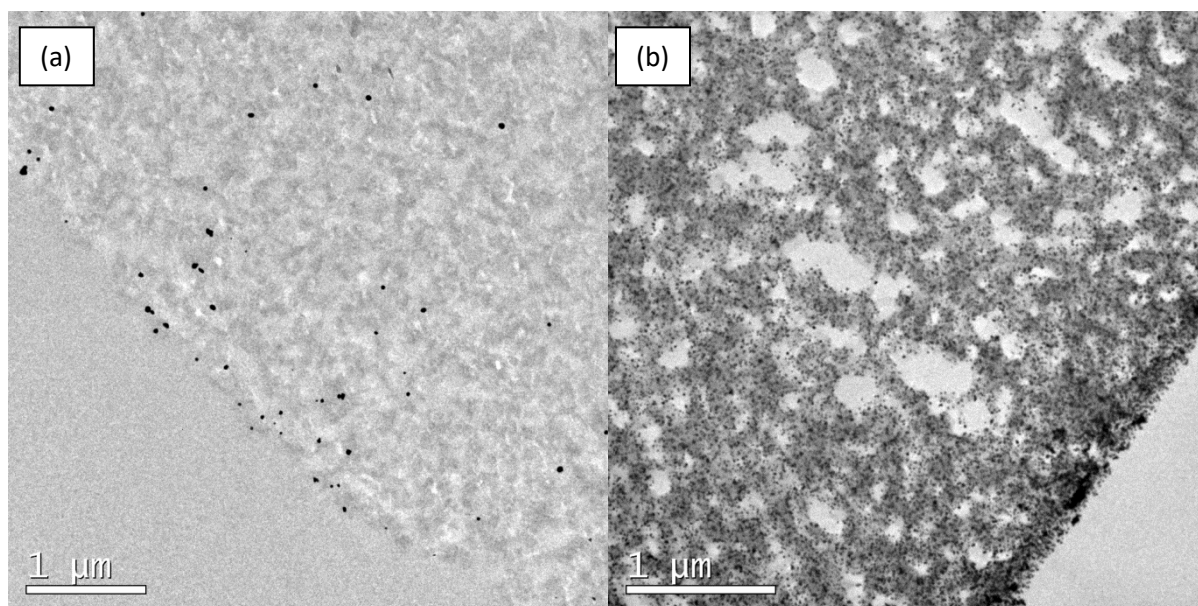
Fig. 5.13 shows a TEM image of cross-sectioned anionic resin. Image before enzyme immobilisation (Fig. 5.13 a) presented a grey surface of anionic resin that is similar to the image of the resin used for fixation and embedding of the sample before the analysis. It only distinguished by some of the bright colours in a certain area due to the surface that was not being covered by the resin as the resin cannot penetrate in such small channels. After

immobilisation Fig. 5.13(b), the pores with bright colour were filled with enzyme making the image look different from Fig. 5.13(a), where the pores look denser than before.



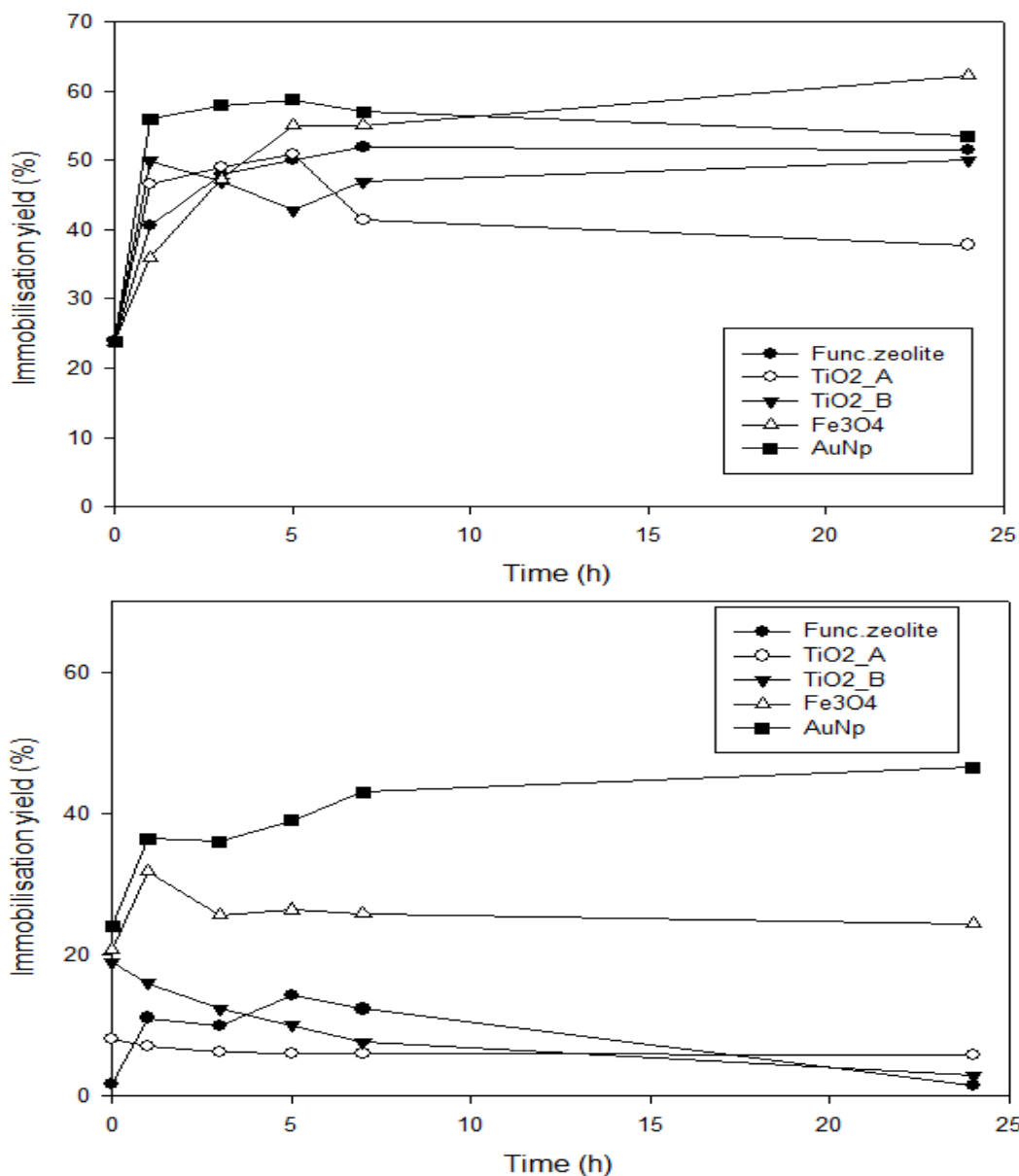
**Fig. 5.13** (a) TEM image of cross-sectioned anionic resin (A520) before immobilisation, (b) TEM image of anionic resin (A520) after enzyme immobilisation

Fig. 5.14 shows a cross-sectioned TEM image of A520/Au before and after immobilisation of proteases. The AuNps were noticeable as scattered dark spot on the surface of the resin, the resin was in grey colour due to less dense than metal (Fig. 5.14 a). The size of gold nanoparticle was estimated to be approximately 25 nm. After immobilisation in Fig. 5.14(b) the concentration of gold nanoparticle became denser due to the attachment of enzyme via weak bonding and also the enzyme was attached to the pores of the resin surface when comparing with the material without enzyme in Fig. 5.14(a). The image of the particles appeared darker than the previous image because of gold nanoparticles can crosslink to the protein and act as a marker for a protein making them more visible in TEM (Iborra et al., 2004).



**Fig. 5.14** TEM image of cross-sectioned anionic resin coated with gold nanoparticle (A520/Au) (a) before enzyme immobilisation, (b) after enzyme immobilisation.

The search of an appropriate support/carrier was continued with cheap materials with the aim to find a substitute of AuNps as a support/carrier. Immobilisation of Phw on different cheap materials with large surface area and pore sizes such as zeolite,  $\text{TiO}_2$ , and  $\text{Fe}_3\text{O}_4$  nanoparticles showed a considerable effect on the immobilisation yield achieved similarly with AuNps (maximum yield in the range 50% – 62%) during 24 h of conjugation period (Fig. 5.15 a). Besides, the immobilisation on  $\text{Fe}_3\text{O}_4$  nanoparticles (MNPs) presented an enhanced yield after 24 h showing a high potential to be used as a support for proteases immobilisation. Likewise, the percentage of immobilisation of Psr on MNPs (32%) showed an immobilisation yield comparable to those obtained with AuNps (47%) at the beginning of conjugation period (Fig. 5.15 b). However, there is no significant effect on immobilisation yield using functionalised zeolite and  $\text{TiO}_2$  nanoparticles even when increasing the concentration of titanium (Section 3.5.2) during the synthesis.



**Fig. 5.15** Enzyme immobilisation yield of (a) Phw and (b) Psr on cheap materials (zeolite, TiO<sub>2</sub> nanoparticles, Fe<sub>3</sub>O<sub>4</sub> nanoparticles; MNPs) and compared with AuNps as a model carrier.

In the quest to find a suitable support/carrier for enzyme immobilisation, 10 materials had been tested. The immobilisation yield (%) after 24 h has been considered taking into account the adsorption and desorption reaction occurred during the period of conjugation. The immobilisation yield (%) of each material was compared with immobilisation yield (%) of AuNps in Fig. 5.16. AuNps was chosen as a model carrier as explained previously, this support showed an excellent biocompatibility for Phw and Psr.

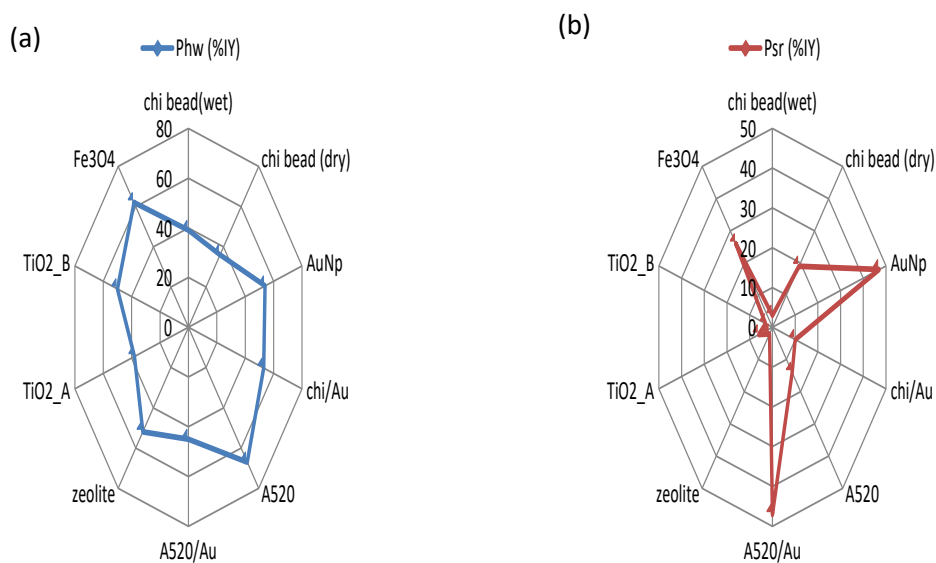


**Fig. 5.16** Analysis of immobilisation yield (% IY) of 10 materials used as a support/carrier for proteases (Phw and Psr) immobilisation via adsorption for 24 h at 4°C in relative to AuNp as a model carrier for both of the proteases. (a) Phw; (b) Psr.

For Phw, the potential supports for immobilisation relative to AuNps were anionic resin (A520) followed by  $\text{Fe}_3\text{O}_4$  nanoparticles (MNPs) with the radar localised similarly to AuNps radius (Fig. 5.16 a). While for Psr, the significant supports were A520/Au and MNPs relative to AuNps radius (Fig. 5.16 b). Although both of the proteases showed different potential supports, MNPs as a suitable common support for both proteases immobilisation. Therefore MNPs was chosen as a suitable support for Phw and Psr immobilisation.

## 5.4 Magnetite ( $\text{Fe}_3\text{O}_4$ ) nanoparticles as a carrier

### 5.4.1 Effect of stabiliser in MNPs suspension towards immobilisation yield

The use of magnetic nanoparticles (MNPs) as a support for immobilisation of the proteases produced by SSF was supposed to be practical and feasible as they are easy to prepare at low cost and present a limited toxicity. However, MNPs in suspension are usually unstable and tend to spontaneously form agglomeration to minimise their high surface energies (Andrade et al., 2012). In order to improve colloidal, chemical stability and allow

further functionalisation of the MNPs, coating with stabilisers by metals (e.g gold), inorganic materials (e.g silica), organic polymer (e.g polyacrylamides, esters, polyethylene amine, polyethylene glycol, polydopamine), or monomers (e.g. fatty acids, citric acid, phosphoric acids, phosphates) has been proposed (Cîrcu et al., 2016). Coating nanoparticles with stabiliser can affect the size, shape, and magnetism of the MNPs. On the other hand, pH, temperature, ionic strength, can prevent agglomeration phenomena as previously reported in other studies (Cîrcu et al., 2016; Lu et al., 2007).

In order to study the effect of stabiliser in MNPs suspension towards immobilisation yield, three stabilisers were considered. Tetramethylammonium hydroxide (TMAOH), cetyltrimethylammonium(CTAB), and citrate were chosen as stabilisers because they were effective to control the surface charge in previous studies (Andrade et al., 2012; Nigam et al., 2011; Ramos Guivar et al., 2015). Prior the immobilisation of protease on MNPs suspension, the enzyme was tested with the stabilisers to check the inhibition effect of them towards enzymatic activity. The initial activity was taken as 100% of activity. Interestingly, the stabiliser turned out to enhance the enzyme activity instead of inhibits the activity as shown in Table 5.3.

**Table 5.3** Inhibition effect of proteases (Phw and Psr) activity towards different stabiliser

	Residual activity (%)	
	Psr	Phw
initial	100	100
enzyme + 10 mM TMAOH	110	113
enzyme + 2.2 mM CTAB	108	111
enzyme + 2.2 mM citrate	100	107



Subsequently, the immobilisation was carried out using a magnetite suspension with the addition of the different stabilisers (TMAOH, CTAB, citrate). The concentration of stabiliser was the same used in the inhibition test, as mentioned in Table 5.3. Before adding the stabilisers, two protocols of MNPs synthesis involving different base for precipitation were used. Briefly, in protocol A, the MNPs was synthesised with ammonium hydroxide ( $\text{NH}_4\text{OH}$ ) and protocol B was synthesised using sodium hydroxide ( $\text{NaOH}$ ). Each stabiliser was added to the both prepared MNPs (MNPs synthesised with protocol A and B). Fig. 5.17 shows a TEM image of MNPs synthesised with the different protocol using base  $\text{NH}_4\text{OH}$  or  $\text{NaOH}$ .

As observed in Fig. 5.17, the TEM image shows that MNPs synthesised using precipitating agent  $\text{NH}_4\text{OH}$  (Fig. 5.17 a) were more uniform and monodisperse compared to those obtained with  $\text{NaOH}$  (Fig. 5.17 c). The electron diffraction image confirmed the uniform and crystalline form of MNPs obtained with  $\text{NH}_4\text{OH}$ . The size of MNPs was estimated by Software ImageJ to be 16 nm (Fig. 5.17 b). In contrast, when synthesised with  $\text{NaOH}$ , the image of the particles confirmed the crystalline structure of the materials with several larger particles observed around the crystalline rings with the estimated size of MNPs of 13 nm (Fig. 5.17 d).

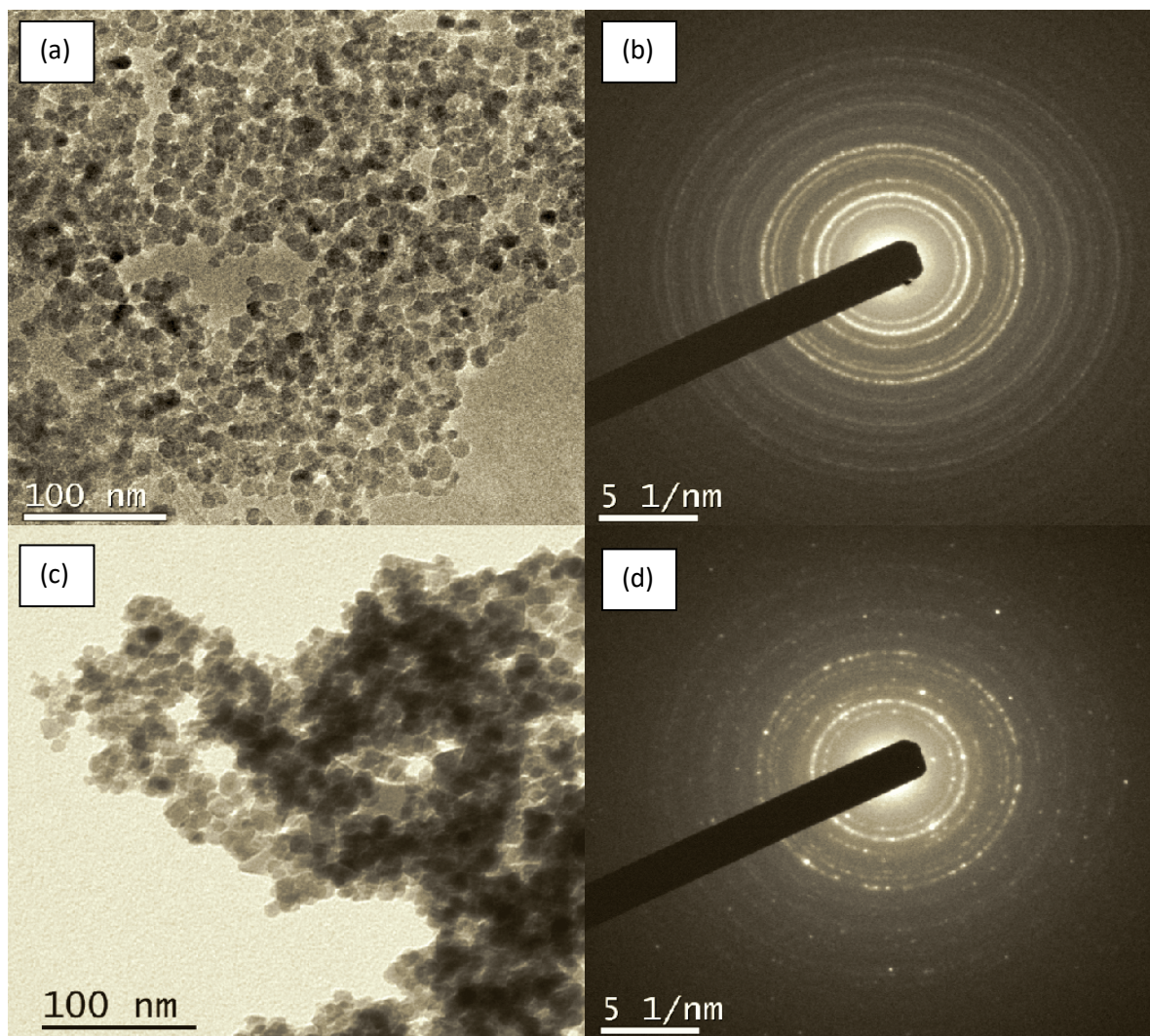


**Fig. 5.17** TEM and electron diffraction images of MNPs with CTAB as stabiliser (a) TEM image of MNPs synthesised following protocol A ( $\text{NH}_4\text{OH}$ ), (b) electron diffraction image of MNPs synthesised using protocol A ( $\text{NH}_4\text{OH}$ ), (c) TEM image of MNPs synthesised following protocol B ( $\text{NaOH}$ ), (d) electron diffraction image of MNPs synthesised using protocol B ( $\text{NaOH}$ ).

This might be due to small size of MNPs that are possibly embedded into larger particles as observed in the TEM image (Fig. 5.17 c). This was in accordance with previous studies where the effect of different precipitating agent ( $\text{NH}_4\text{OH}$  and  $\text{NaOH}$ ) in magnetite synthesis were studied (Peternele et al., 2014). They suggested that the differences in the MNPs size obtained with  $\text{NH}_4\text{OH}$  and  $\text{NaOH}$  were due to differences in the nucleation process and grain growth during synthesis. Since  $\text{NH}_4\text{OH}$  is a weak base that produces a smaller number of magnetite cores which favouring crystal growth that resulted in particles

of larger sizes, contrary to NaOH that considered as a strong base (Gnanaprakash et al., 2007; Peternele et al., 2014).

Table 5.4 shows the different pH of the MNPs suspension synthesised from different precipitating agent NH<sub>4</sub>OH (A) and NaOH (B) after addition of enzymes. In all cases the pH was approaching alkaline condition that favours the proteases activity.

**Table 5.4** pH of MNPs suspension with different stabiliser before and after addition of proteases

MNPs in different solvent/stabiliser	pH before enzyme addition	pH after enzyme addition
MNPs_CTA	3.75	8.11
MNPs_CTB	8.93	7.79
MNPs_TA	11.79	8.15
MNPs_TB	11.77	8.18
MNPs_CA	7.08	7.45
MNPs_CB	9.32	7.43

MNPs: magnetic nanoparticles; CTA: MNPs synthesised with NH<sub>4</sub>OH and CTAB; CTB: MNPs synthesised with NaOH and CTAB; TA: MNPs synthesised with NH<sub>4</sub>OH and TMAOH; TB: MNPs synthesised with NaOH and TMAOH; CA: MNPs synthesised with NH<sub>4</sub>OH and citrate; CB: MNPs synthesised with NaOH and citrate.

Effect of immobilisation yield (%) using MNPs suspension with stabiliser and naked MNPs without the stabiliser was used as a control for comparison as shown in Fig. 5.18. As we can see, the addition of CTAB as a stabiliser gave a significant yield of immobilisation of Phw before 24 h that was 70-75% (Fig. 5.18 a) compared to those treated with TMAOH and citrate. The result was satisfactory in terms of cost and time. Likewise, the immobilisation yield of Psr also improved (53%-61%) after addition of CTAB compared to the naked MNPs (Fig. 5.18 b). The addition of CTAB on the nanoparticles surface often gives stabilisation to quantum dots in an aqueous medium as observed previously using metal nanoparticles (Ramos Guivar et al., 2015). Even though MNPs synthesised with NH<sub>4</sub>OH presented uniform particles compared to those obtained with NaOH, the immobilisation of SSF proteases were

more efficient using MNPs synthesised using NaOH based on the immobilisation yield observed in both proteases (Phw and Psr) using CTAB as a stabiliser (Fig. 5.18). Therefore, for further experiments, NaOH was chosen as a precipitating agent as it favoured the immobilisation.

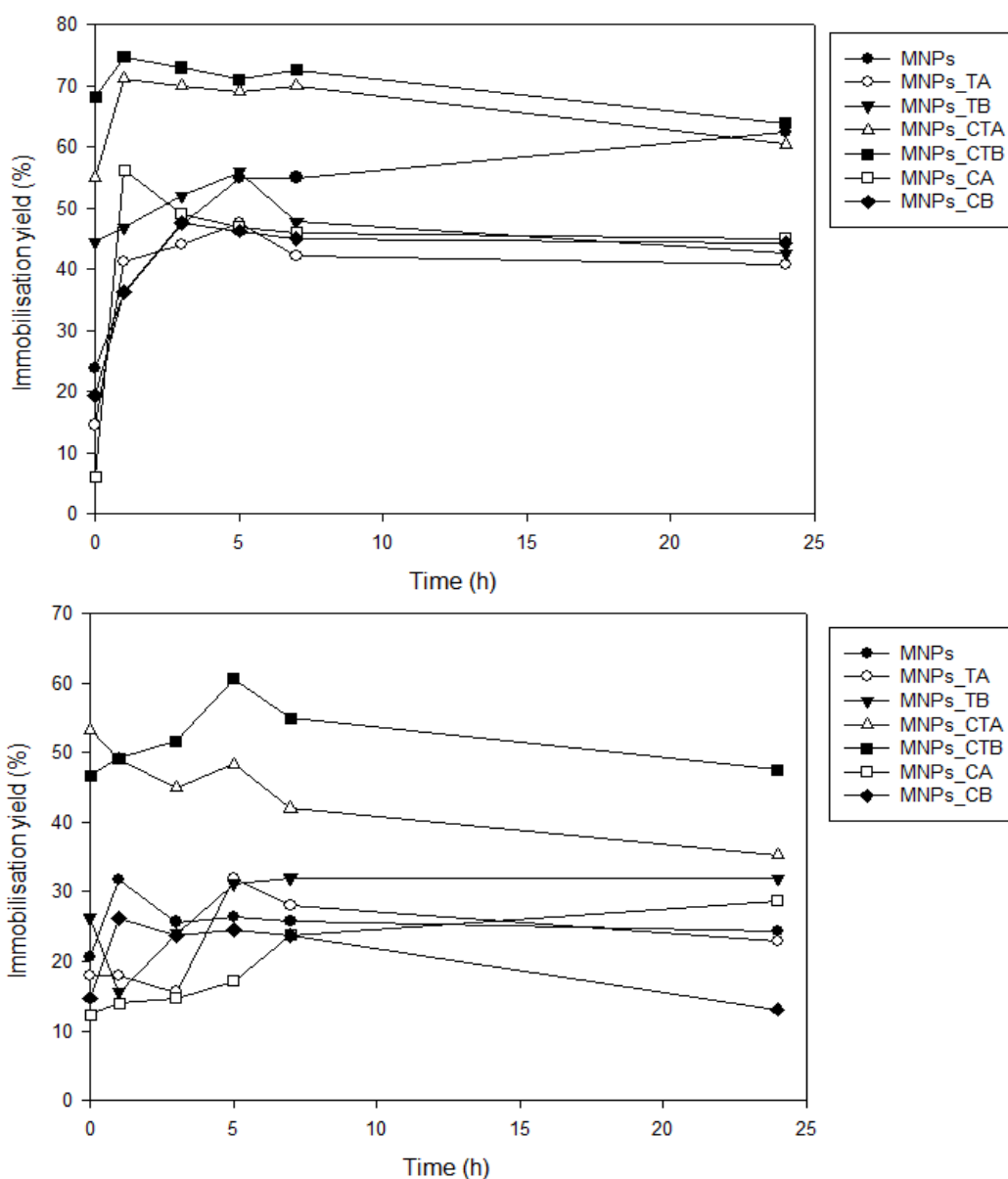


**Fig. 5.18** Immobilisation yield of magnetic nanoparticles suspension using different stabilisers (TMAOH, CTAB, and citrate) and naked magnetic nanoparticles for 24 h. Note that MNPs\_TA: magnetic nanoparticles (protocol A) with TMAOH; MNPs\_TB: magnetic nanoparticles (protocol B) with TMAOH; MNPs\_CTA: magnetic nanoparticles (protocol A) with CTAB; MNPs\_CTB: magnetic nanoparticles (protocol B) with CTAB; MNPs\_CA: magnetic nanoparticles (protocol A) with citrate; MNPs\_CB: magnetic nanoparticles (protocol B) with citrate.

### 5.4.2 Enzyme loading per carrier – Box Hunter experimental design

To optimise the immobilisation yield, enzyme loading per carrier was carried out using Box-Hunter experimental design as mentioned in previous section (Section 5.2.2). Sixteen experimental runs were conducted with four replicates at the centre point with both of the proteases (Phw and Psr) individually. The experimental design was tabulated in Table 5.5. In this work, the immobilisation yield and enzyme loading were chosen to reflect the efficiency of the immobilisation, thus we taking  $\alpha_2$  as the objective function which was 25% of immobilisation yield and 75% of enzymatic loading. Both proteases favour the condition with a higher amount of MNPs and initial activity of the enzyme as shown in Fig. 5.19. In addition, we also calculated another objective function to standardise condition for both proteases which was  $\alpha_3$  that comprised of 50% of  $\alpha_1$  and 50% of  $\alpha_2$ .

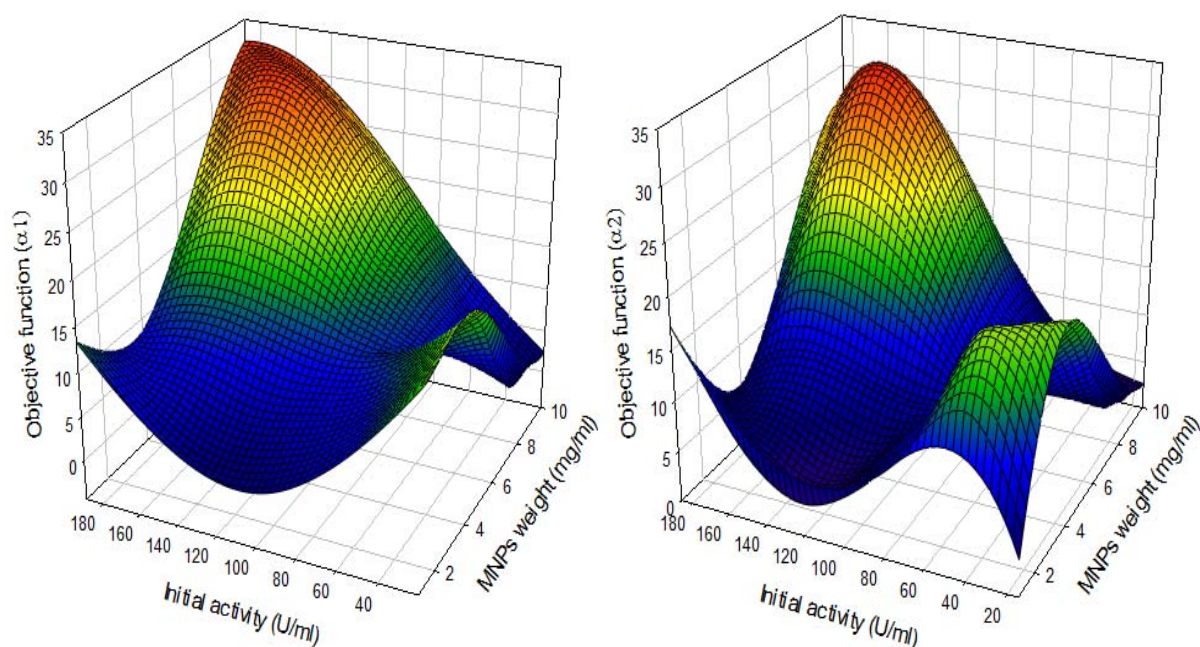


**Fig. 5.19** 3D mesh plot of proteases loading on MNPs as a carrier according to Box-Hunter experimental design with objective function  $(0.25F_1 + 0.75F_2)$

**Table 5.5** Experimental design of proteases loading per carrier (MNPs) according to Box-Hunter experimental design

Run	X1 (coded)	X2 (coded)	X1 (actual) (mg/ml)	X2_initial Phw (actual) (U/ml)	X2_initial Psr (actual) (U/ml)	A	B	F1_h (% IY)	F1_s (% IY)	F2_h (U/mg)	F2_s (U/mg)	$\alpha_1$	$\alpha_2$	$\alpha_3$
1	0	0	5	87	75	27	14	31	19	6.0	3.1	12	7	10
2	0	0	5	87	75	13	17	15	22	2.9	3.7	6	8	7
3	0	0	5	87	75	25	21	28	28	5.5	4.7	11	11	11
4	0	0	5	87	75	19	14	22	19	4.3	3.1	9	7	8
5	1	1	10	189	186	159	136	84	73	15.9	13.6	33	28	31
6	-1	-1	1	21	15	9	2	43	10	9.0	1.5	17	4	11
7	1	-1	10	21	15	2	2	9	10	0.2	0.2	2	3	3
8	-1	1	1	189	186	15	20	8	10	15.1	19.5	13	17	15
9	-1	0	1	87	75	3	9	3	11	2.6	8.6	3	9	6
10	1	0	10	87	75	45	23	52	31	4.5	2.3	16	9	13
11	0	-1	5	21	15	13	10	64	69	3.0	2.3	18	19	19
12	0	1	5	189	186	32	22	17	12	7.1	5.0	10	7	8
13	-0.71	-0.71	1	24	24	10	8	43	31	7.9	5.8	17	12	14
14	-0.71	0.71	1	150	144	6	6	4	4	4.5	4.3	4	4	4
15	0.71	-0.71	8	24	24	2	4	10	15	0.3	0.5	3	4	3
16	0.71	0.71	8	150	144	114	120	76	83	14.8	15.5	30	32	31

A: immobilised activity of Phw (U/ml); B: immobilised activity of Psr (U/ml);

F1\_h & F1\_s: immobilisation yield of Phw and Psr as objective function 1;

F2\_h & F2\_s: enzyme Phw and Psr loading per carrier as objective function 2;

$\alpha_1$ : objective function of  $(0.25 \cdot F1) + (0.75 \cdot F2)$  for Phw;

$\alpha_2$ : objective function of  $(0.25 \cdot F1) + (0.75 \cdot F2)$  for Psr;

$\alpha_3$ : objective function of  $(0.5 \cdot \alpha_1) + (0.5 \cdot \alpha_2)$ ;

All experimental run were carried out with 3 ml as a total volume

It is known that during immobilisation an excessive load on the support can reduce the activity due to a large enzymatic chain that can act as a steric barrier against the substrate (Tavano, 2013). As observed in Table 5.5, the optimum value obtained from  $\alpha_3$  was similar for condition (X1: 1, X2: 1 and X1: 0.71, X2: 0.71) where both of them were at higher range tested in this experiment. Since there was no effect of the excessive load, which can reduce the activity, we decided to carry forward the condition with X1: 1, X2: 1 (10 mg/ml MNPs, 100 mg/ml) for further study.

## **Conclusion**

To sum up, the work done in this chapter was to prepare and develop the most suitable condition for proteases (Phw and Psr) immobilisation using an appropriate support/carrier. For the beginning, we started with the most compatible support which was gold nanoparticles (AuNps). However, AuNps alone was difficult to separate from the substrate after each reaction, unless it was coupled with other larger materials. Thus other materials were investigated for the sake of reusability, reproducibility, feasibility, and cost effective. Of all the materials considered in this study for the carrier, magnetic nanoparticles (MNPs) are shown the most appropriate for immobilisation of proteases derived from hair waste and soy waste. Also, the characteristic of MNPs that ease the separation process with only use magnetic drive without the requirement of other mechanical apparatus seems the most compelling and promising mean. Therefore, MNPs was chosen to be the support for further experiments and reaction (specifically in Chapter 6) with NaOH as a precipitating agent during the nanoparticles synthesis and optimum enzyme loading obtained from the Box-Hunter experimental design.

## Chapter 6

*Immobilisation of protease produced from SSF on magnetic nanoparticles and its application in protein hydrolysis*

*Part of this chapter has been published in Journal of Molecular Catalysis B: Enzymatic (2017) – ARTICLE IN PRESS.*

*The immobilisation of proteases produced by SSF onto functionalized magnetic nanoparticles: Application in the hydrolysis of different protein sources.*

*Noraziah Abu Yazid, Raquel Barrena, Antoni Sánchez.*

<http://dx.doi.org/10.1016/j.molcatb.2017.01.009>



Graphical abstract

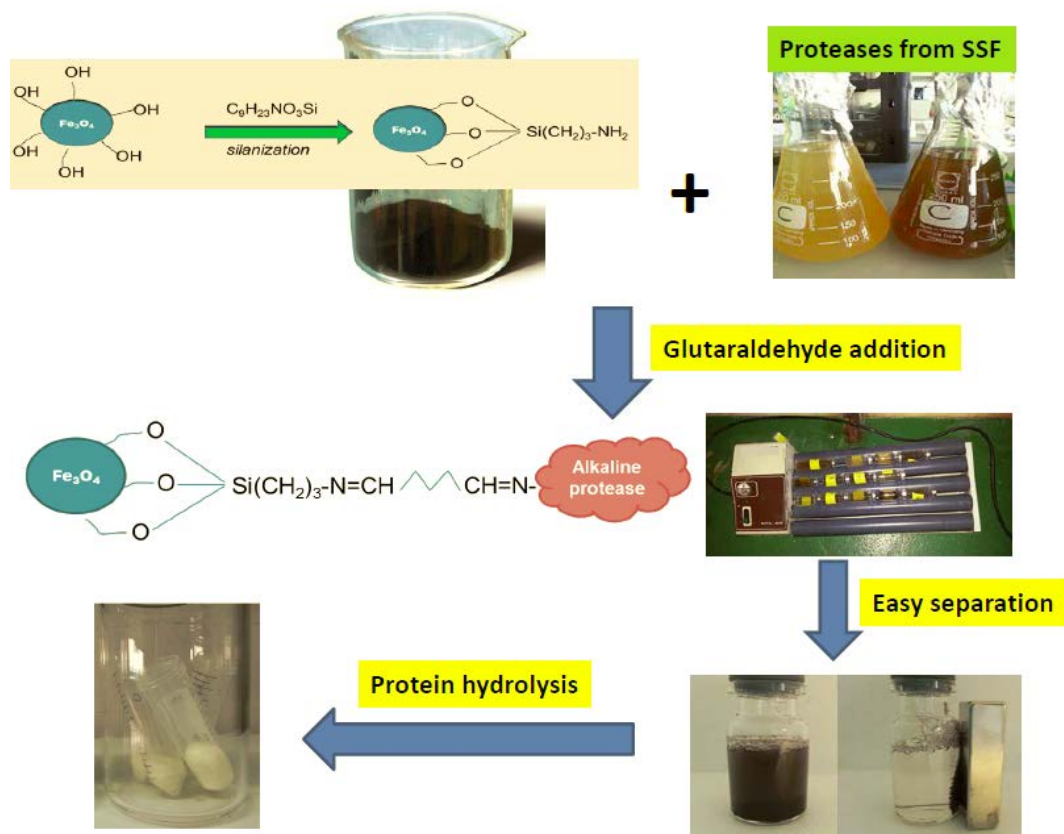


**Fig. 6.1** Graphical abstract of immobilisation of protease on magnetic nanoparticles and its application in protein hydrolysis

## **Summary**

This chapter demonstrated the application of the immobilised protease on a promising support/carrier obtained from Chapter 5. In this work, the use of relatively inexpensive enzyme preparative for immobilisation onto functionalized MNPs and crosslinking with glutaraldehyde was assessed. The goal was to test the viability of using low-cost proteases derived from an animal (hair waste) and vegetable (soy fibre residues) protein-rich wastes that were produced by SSF after being immobilised onto functionalized MNPs in the hydrolysis of different type of proteins. The relative differences regarding stability and reusability between the free and immobilised enzymes were significant, exhibiting the feasibility of the immobilised enzymes produced in this work. Also, the magnetic properties of the support render a convenient separation between the substrate and the enzymes within the catalytic system. The whole processes involve in this experimental has been illustrated in Fig. 6.1.

Briefly, alkaline proteases produced from protein-rich waste (hair waste and soy fibre residues) by solid state fermentation (SSF) were immobilised onto functionalised magnetic iron oxide nanoparticles (MNPs) using glutaraldehyde as a crosslinking agent. The covalent binding method had a better immobilisation yield compared to simple adsorption, retaining 93%-96% ( $45.9 \pm 10.6$  U/mg nanoparticles,  $31.9 \pm 34$  U/mg nanoparticles) of hair waste and soy residues proteases, respectively after crosslinking with 5% glutaraldehyde for 6 h. However, the adsorption immobilisation yield was 47%-54% after 8 h for both proteases. MNPs and immobilised proteases were characterised using transmission electron microscopy (TEM), scanning electron microscopy (SEM), Fourier transforms infrared spectroscopy (FT-IR) and electron diffraction. The results indicated successful crosslinking between the proteases and amino-functionalised MNPs. The operational stability (pH and temperature) and storage stability of free and immobilised enzyme were also analysed. Despite the fact that

the optimum pH of free and immobilised proteases was identical in the alkaline region, the immobilised proteases reached their optimum condition at higher temperatures (40 °C – 60 °C). After 2 months of storage at 4 °C, the immobilised proteases showed excellent stability, retaining more than 85% of their initial activity. The high magnetic response of MNPs renders an ease of separation and reusability, which contributes to the residual activity of both immobilised proteases on MNPs retaining more than 60% of their initial values after seven hydrolytic cycles. These results showed the enhancement of the stability of the crosslinking interactions between the proteases and nanoparticles. The immobilised proteases were capable of hydrolysing selected proteins (casein, oat bran protein isolate, and egg white albumin). However, differences in the degree of hydrolysis were observed, depending on the combination of the protease and type of substrate used.

### **6.1 Production of proteases from hair waste and soy fibre residue in SSF**

In this work, the protease was produced from SSF using a mixture of anaerobically digested sludge (ADS) and hair waste or soy fibre residue as substrate. The proteases were produced in the 10 L reactors according to Section 3.1. The characterisation of all substrates used to produce proteases was tabulated in Table 6.1. The initial dynamic respiration index (DRI) for both mixtures; hair waste and soy fibre residue were  $8.80 \pm 1.8 \text{ g O}_2 \text{ kg}^{-1} \text{ DM h}^{-1}$  and  $6.94 \pm 0.04 \text{ g O}_2 \text{ kg}^{-1} \text{ DM h}^{-1}$  which can be considered as highly degradable (Ponsá et al., 2010) and high enough to initiate the aerobic fermentation. Protein content from each waste was appropriate to produce protease in SSF.

Fig. 6.2 shows the typical fermentation profile of protease from both sources where the maximum temperature achieved in hair waste was in the range of 60 °C– 63 °C, whereas the maximum temperature achieved in soy fibre residue fermentation was in the range of 55 °C– 60 °C. The pH at the production of the protease was similar (pH 8.87–pH 8.96) for both

of the sources during the production of protease. The fermentation of hair waste was continued until 23 days, and the fermentation of soy fibre residue was continued until 12 days for stabilisation of the residues. The stabilisation of final mixtures for hair waste and soy fibre residue were sufficient with DRI less than  $1.0 \text{ g O}_2 \text{ kg OM h}^{-1}$  as suggested by others (Adani et al., 2004).

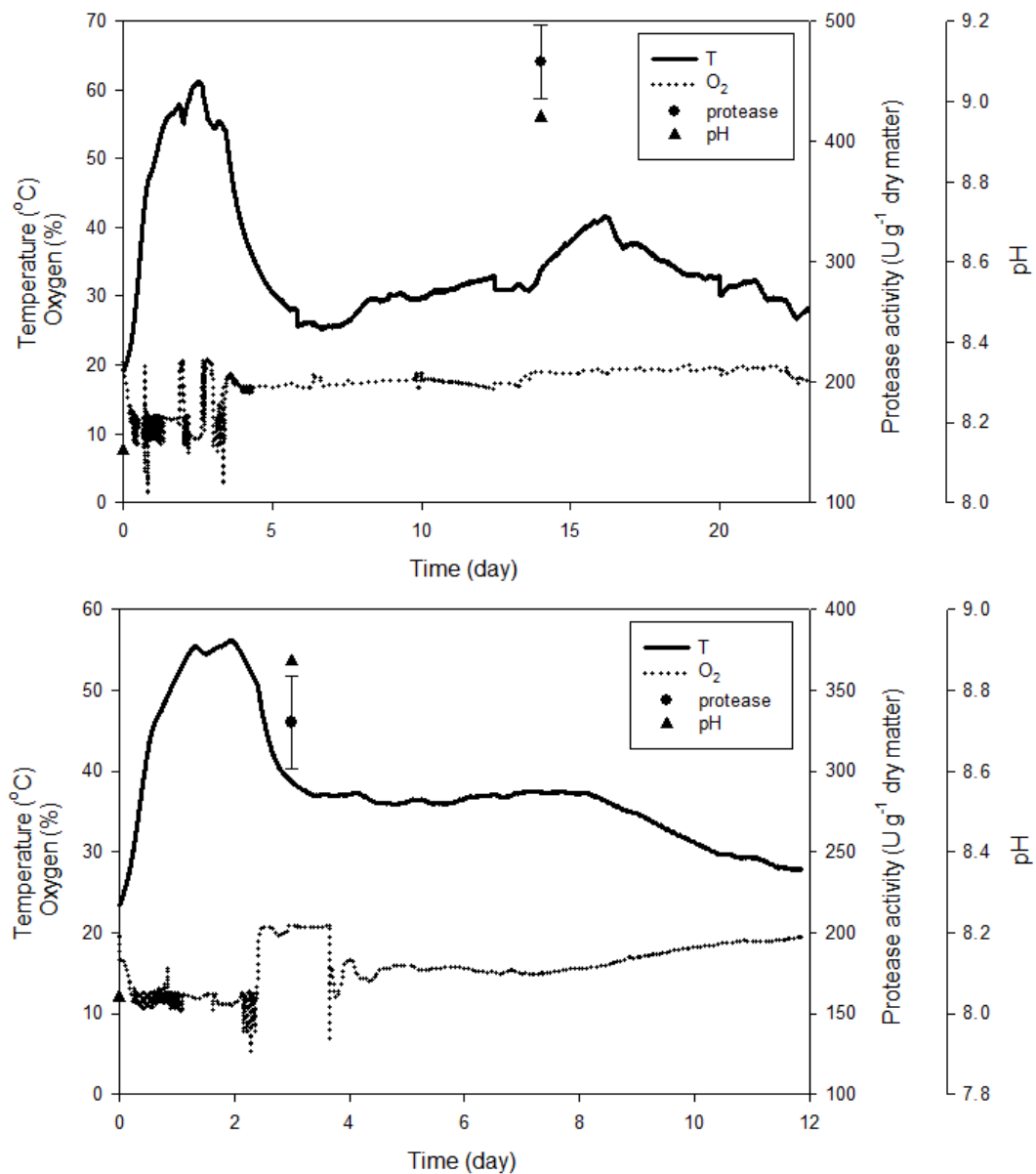


**Fig. 6.2** Fermentation profile of protease production in SSF using different substrate (a) hair waste and ADS; (b) soy fibre residue and ADS.

**Table 6.1** Characterisation of hair waste, soy fibre residue, anaerobically digested sludge (ADS), and an initial mixture of for SSF process.

Characteristics	Hair waste	Soy fibre residue	ADS	Mixture <sup>a</sup>	Mixture <sup>b</sup>
<i>Physical characteristics</i>					
Organic matter (% db)	86.9 ± 0.6	90.9 ± 0.4	76.3 ± 0.3	88.1 ± 0.5	89.3 ± 0.4
Water content (% db)	66.1 ± 7.3	85.4 ± 5.5	85.4 ± 4.2	69.7 ± 9.1	76.7 ± 5.4
Dynamic respiration index (DRI) (g O <sub>2</sub> kg <sup>-1</sup> DM h <sup>-1</sup> )	N.D.	N.D.	N.D.	8.80 ± 1.8	6.94 ± 0.04
Stabilisation DRI (g O <sub>2</sub> kg <sup>-1</sup> OM h <sup>-1</sup> )	N.D.	N.D.	N.D.	0.83 ± 0.4	0.71 ± 0.5
Electrical conductivity (mS cm <sup>-1</sup> )	2.27 ± 0.3	1.57 ± 0.2	1.59 ± 0.4	2.79 ± 0.2	1.54 ± 0.3
pH	9.13	6.43	8.34	8.38	8.04
<i>Chemical characteristics</i>					
Total carbon (% db)	57.6 ± 0.9	48.7 ± 0.6	45.1 ± 0.3	40.2 ± 1.4	40 ± 0.6
Total nitrogen (% db)	10.1 ± 0.1	4.8 ± 0.4	8.2 ± 0.6	9.3 ± 1.1	4.6 ± 0.2
C/N ratio	5.7	10.1	5.5	4.3	8.7

db: dry basis; DM: dry matter; OM: organic matter; N.D.: not determined.

<sup>a</sup>Ratio 1:2 (sludge: hair waste)

<sup>b</sup>Ratio 1:2 (sludge: soy fibre residue)

The substrate mixture for fermentation was prepared by adding ADS at a constant ratio (1:2 w/w) to standardise the condition of the substrate for protease production for this work, which the different factor was only hair waste (from animal) and soy fibre residue (from plant). This factor will be evaluated for protein hydrolysis efficiency of various sources. Also, by adding ADS to soy fibre residue can alter the initial pH from slightly acidic to an alkaline condition to produce alkaline protease (Table 6.1). The protease production from different source distinctively from animal and plant was an attempt to investigate the reaction of each protease. Since it is necessary to select the source for protease production as the same protease can present a distinct behaviour which could influence the choice of the enzyme for a given application particularly in industrial level (Tavano, 2013).

In view of the fact that different source of residues will result in various protease production pattern (Pandey et al., 1999), the protease was extracted at day 14<sup>th</sup> for hair waste

as a substrate (Fig. 6.2a), while for soy fibre residue, the protease was extracted after the thermophilic phase based on the fermentation profile (Fig 6.2b). The protease from soy fibre residue was extracted just after the thermophilic phase. Since the protease was considered to be produced during active phase with the substance that readily degraded such as soy fibre residue compared to hair waste that required more time to be degraded to produce more protease based on the previous study (Abraham et al., 2013). Afterwards, the protease extracts were collected and lyophilised before immobilisation process.

## **6.2 Immobilisation of protease onto functionalised magnetic nanoparticles (MNPs)**

The Phw and Psr enzymes from SSF were immobilised onto magnetic nanoparticles via simple adsorption and crosslinking with glutaraldehyde (GA). Both methods were carried out for 8 h with the aim of investigating the effect of time and crosslinker concentration on immobilisation (Fig. 6.3 and Fig. 6.4). The simple adsorption yielded a maximum activity recovery of 28% with an activity loading of  $8.7 \pm 2.2$  U/mg NP for Phw and 33% Psr (activity loading of  $7.0 \pm 1.7$  U/mg NP) after 8 h of immobilisation (Fig. 6.3a and Fig. 6.4 a). The immobilisation efficiency for both Phw and Psr in simple adsorption increased during 8 h with a maximum of 60-61% efficiency yield, while the maximum immobilisation yield in simple adsorption for both Phw and Psr were 47% and 54%, respectively (Fig. 6.3b and Fig. 6.4b). The surfaces of naked MNPs likely possess high reactivity, which makes them susceptible to degradation under particular environmental conditions. This fact could involve weaker binding forces that contribute to the poor stability of the protein attachments to the surface (Cowan and Fernandez-Lafuente, 2011; Xu et al., 2014). Immobilisation via the crosslinker showed good results for both enzymes studied (Phw and Psr).

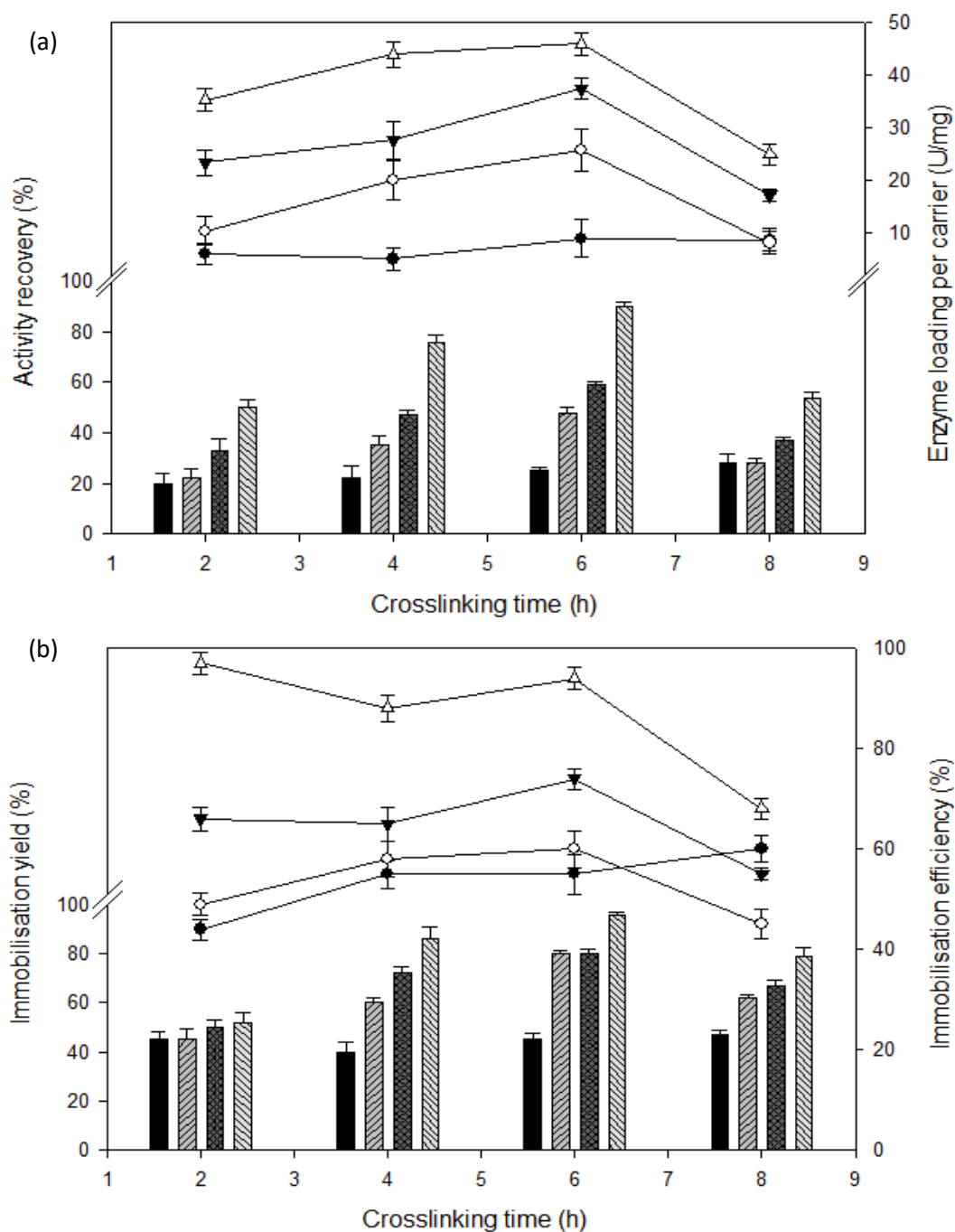


**Fig. 6.3** The effect of the glutaraldehyde (GA) concentration and crosslinking time on (a) the activity recovery of Phw with 0% GA (simple adsorption) (■), 1% GA (▨), 2.5% GA (■), 5% GA (▨) and enzyme loading per carrier of Phw with 0% GA (simple adsorption) (—●—), 1% GA (—○—), 2.5% GA (—▼—), 5% GA (—△—); (b) immobilisation yield of Phw with 0% GA (simple adsorption) (■), 1% GA (▨), 2.5% GA (■), 5% GA (▨), immobilisation efficiency of Phw with 0% GA (simple adsorption) (—●—), 1% GA (—○—), 2.5% GA (—▼—), 5% GA (—△—) onto amino-functionalized MNPs.

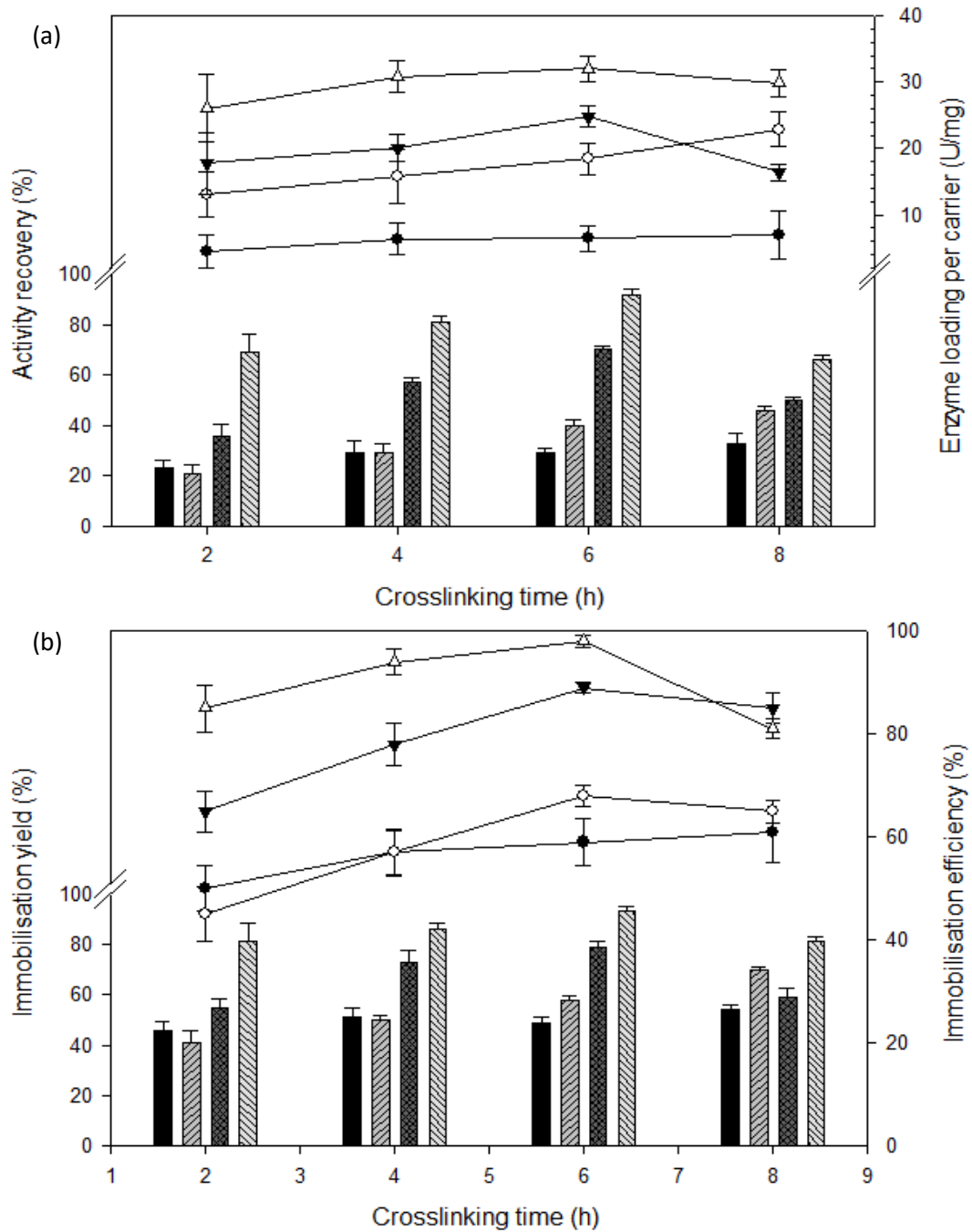


**Fig. 6.4** The effect of the glutaraldehyde (GA) concentration and crosslinking time on (a) the activity recovery of Psr with 0% GA (simple adsorption) (■), 1% GA (▨), 2.5% GA (▩), 5% GA (▧) and enzyme loading per carrier of Psr with 0% GA (simple adsorption) (●), 1% GA (○), 2.5% GA (▼), 5% GA (△); (b) immobilisation yield of Psr with 0% GA (simple adsorption) (■), 1% GA (▨), 2.5% GA (▩), 5% GA (▧) and immobilisation efficiency of Psr with 0% GA (simple adsorption) (●), 1% GA (○), 2.5% GA (▼), and 5% GA (△) onto amino-functionalized MNPs.



The immobilisation yield increased according to the increase in the GA concentration from 1%-5% up to 6 h; then, it decreased abruptly for Phw (Fig. 6.3b). Only when using Psr with 1% GA, the immobilisation yield continues increasing (Fig. 6.4b). Maximum activity recovery and immobilisation yields were obtained after 6 h of crosslinking time, 90% and 96% respectively, which is (equivalent to an activity load of  $45.9 \pm 10.6$  U/mg NP) for Phw with 5% GA (Fig 6.3a and Fig. 6.3b).

Similarly in Psr with 5% GA the maximum activity recovery and immobilisation yields were 92% and 93%, respectively (equivalent to activity loading of  $31.9 \pm 34$  U/mg NP) (Fig. 6.4a and Fig. 6.4b). In addition, the immobilisation via crosslinker was superior to simple adsorption as both of the enzymes (Phw, Psr) showed good immobilisation efficiency in the range of 45% to 98% during 6 h of immobilisation time (Fig 6.3b and Fig. 6.4b). Correspondingly, it indicated that the crosslinking time and GA concentration play a major role during the immobilisation of enzymes in this study. As GA plays a role as a spacer arm for the carriers by providing aldehyde groups for coupling to free amine groups from the enzymes, forming imines, it can also act as a denaturing agent (Chae et al., 1998). Additionally, some studies obtained different crosslinking times (between 1 h to 4 h) and GA concentrations (from 1% to 6%), implying good biocompatibility for these specific enzymes (Chae et al., 1998; Hu et al., 2015; Prasertkittikul et al., 2013; Wang et al., 2014).

### **6.3 Characterisation of the functionalised magnetic nanoparticles (MNPs)**

#### **6.3.1 Characterisation of MNPs using TEM, electron diffraction, and SEM**

Transmission electronic microscopy (TEM) images of MNPs before and after modification with APTES and after the enzymes immobilisation onto the activated surface were compared (Fig. 6.5). The average particle size of naked MNPs slightly increased from 10.2 nm (Fig. 6.5a) to 16.1 nm (Fig. 6.5b) after surface modification with APTES. This effect

has been observed previously in other studies (Lopez et al., 2010; Quanguo et al., 2010). After surface modification with APTES, fewer nanoparticle aggregates formed. As suggested previously (Jin et al., 2010), surface modifications of magnetic nanoparticles can improve their solubility and help avoid aggregation of particles. In Fig. 6.5c and Fig. 6.5d, a layer covering the surface of MNPs upon immobilisation of the proteases (Phw and Psr) can be seen.

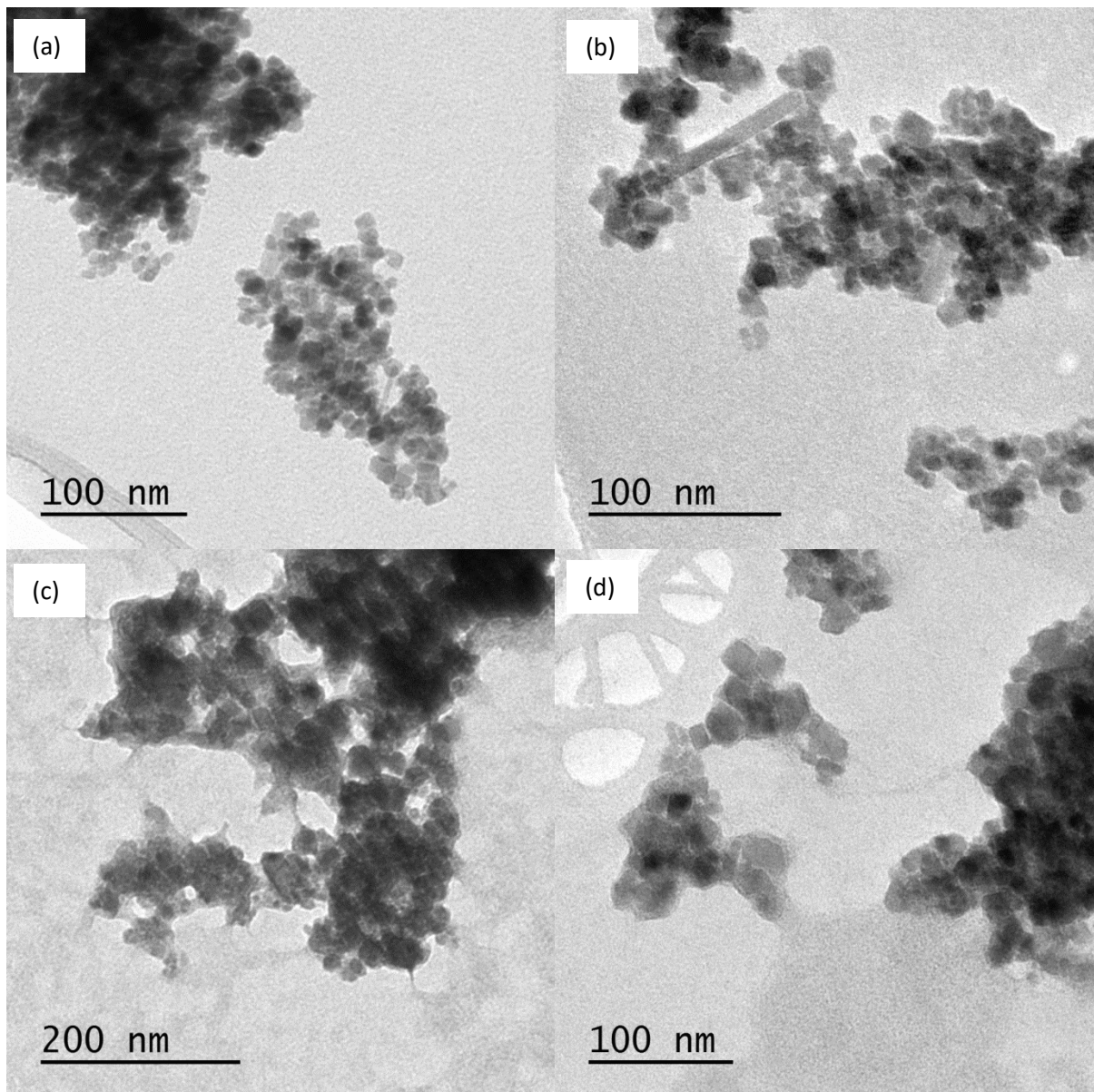


**Fig. 6.5** TEM images at a magnification of 30,000x of (a) naked MNPs, (b) amino-functionalized MNPs, (c) amino-functionalized MNPs after being immobilised with Phw, and (d) amino-functionalized MNPs after being immobilised with Psr.

The thickness of this layer covering the surface of MNPs was estimated to be approximately 5.1 nm for P<sub>sr</sub> and 8.4 nm for P<sub>hw</sub>, indicating an increase in the size of the particles. Based on electron diffraction analysis (Fig. 6.6) of the TEM images, the crystalline structure of the particles was not affected by surface modifications. Fig. 6.6a shows a clear loop, confirming the crystalline structure of MNPs. After surface modification by APTES or CTAB as a stabiliser, the crystalline structure was not modified; however, the size of some nanoparticles was enlarged, as observed in Fig. 6.6b and Fig. 6.6c. Once protease immobilisation was performed, the structure of the nanoparticles became an amorphous structure, confirming that the enzyme covered the surface of the nanoparticles (Fig. 6.6d).

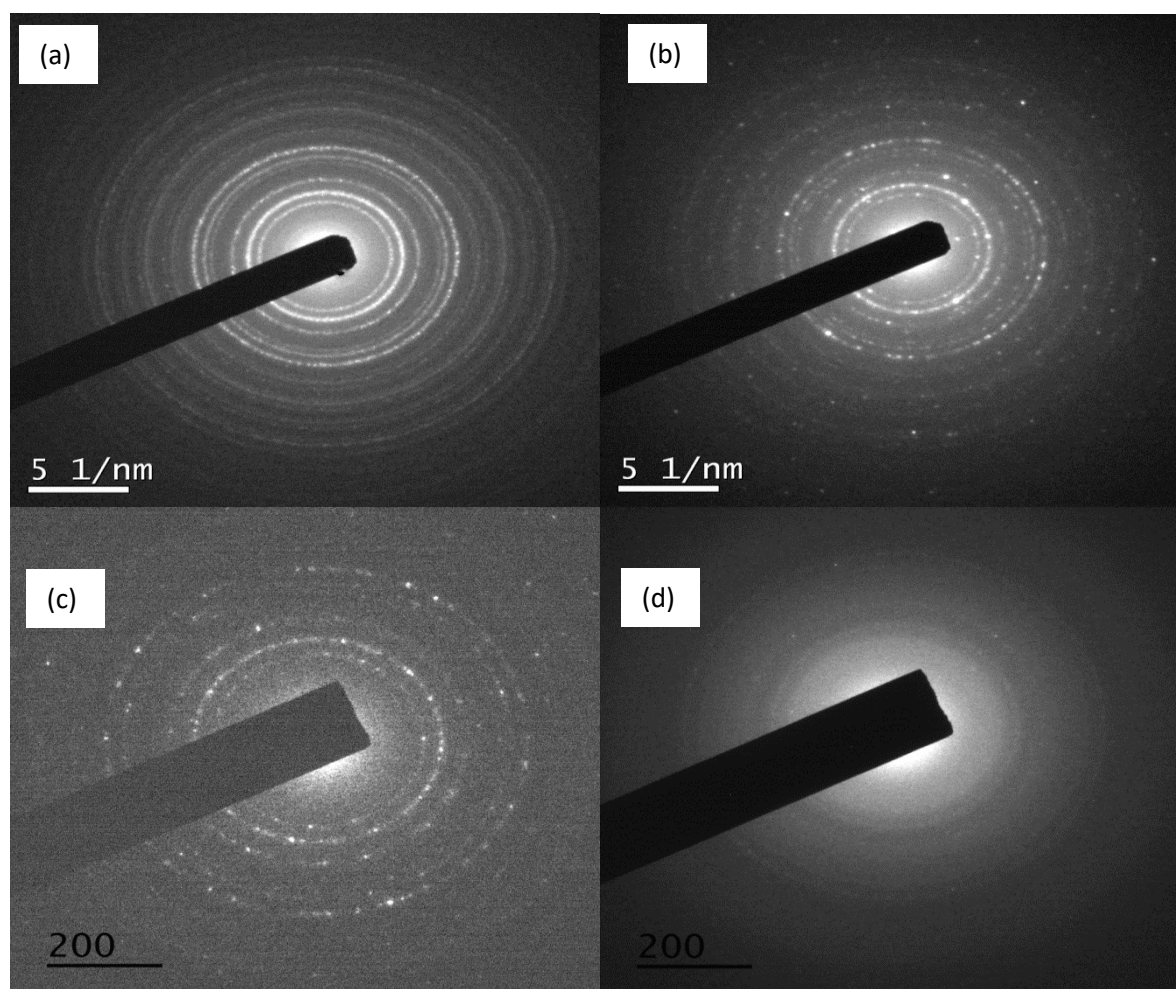


**Fig. 6.6** The electron diffraction images of (a) naked MNPs, (b) MNPs after the addition of CTAB, (c) MNPs after surface modification with APTES, and (d) MNPs after the immobilisation of the enzymes Phw and P<sub>sr</sub>.

The surface of the naked MNPs and functionalised MNPs can be observed in SEM images (Fig. 6.7a and Fig. 6.7b). The small and spherical particles with well-defined edges are observed as in other studies (Ladole et al., 2014). In contrast, in Fig. 6.7c and Fig. 6.7d, the edge surface of nanoparticles is smooth because they are covered by the enzymes, indicating that the immobilisation of proteases onto amino functionalised MNPs was successful.

Figure 6.7 also shows the element quantification using energy dispersive X-ray (EDX). For naked MNPs (Fig. 6.7a) the element carbon (C) was due to the holey carbon grid used during the analysis. As we can observe element silicon (Si) appeared after MNPs being functionalised by a silanisation reaction with APTES (Fig. 6.7b). While after the immobilisation of proteases (Phw and Psr) on MNPs, the element of C was enhanced and the nitrogen (N) element was quantified which can be indicated as enzyme protein appeared in the sample that demonstrated the successful of immobilisation process. The quantification of each element in naked MNPs, amino-functionalised MNPs, and immobilised proteases (Phw and Psr) on amino functionalised MNPs was tabulated in Table 6.2.

**Table 6.2** Energy dispersive X-ray analysis (EDX) element quantification

Element	Naked MNPs		Amino functionalised-MNPs		Amino functionalised-MNPs-Phw		Amino functionalised-MNPs-Psr	
	[wt%]	[At%]	[wt%]	[At%]	[wt%]	[At%]	[wt%]	[At%]
C	5.09	2.58	6.47	15.63	17.00	33.74	14.30	29.20
N	n.d.	n.d.	n.d.	n.d.	2.78	4.73	3.20	5.60
O	36.21	57.18	26.72	48.47	25.17	37.52	26.31	40.03
Si	n.d.	n.d.	2.3	2.38	1.22	1.04	1.00	0.85
Fe	58.70	40.24	64.51	33.52	53.83	22.98	55.19	24.32

n.d. not detected

no peak was omitted during the analysis

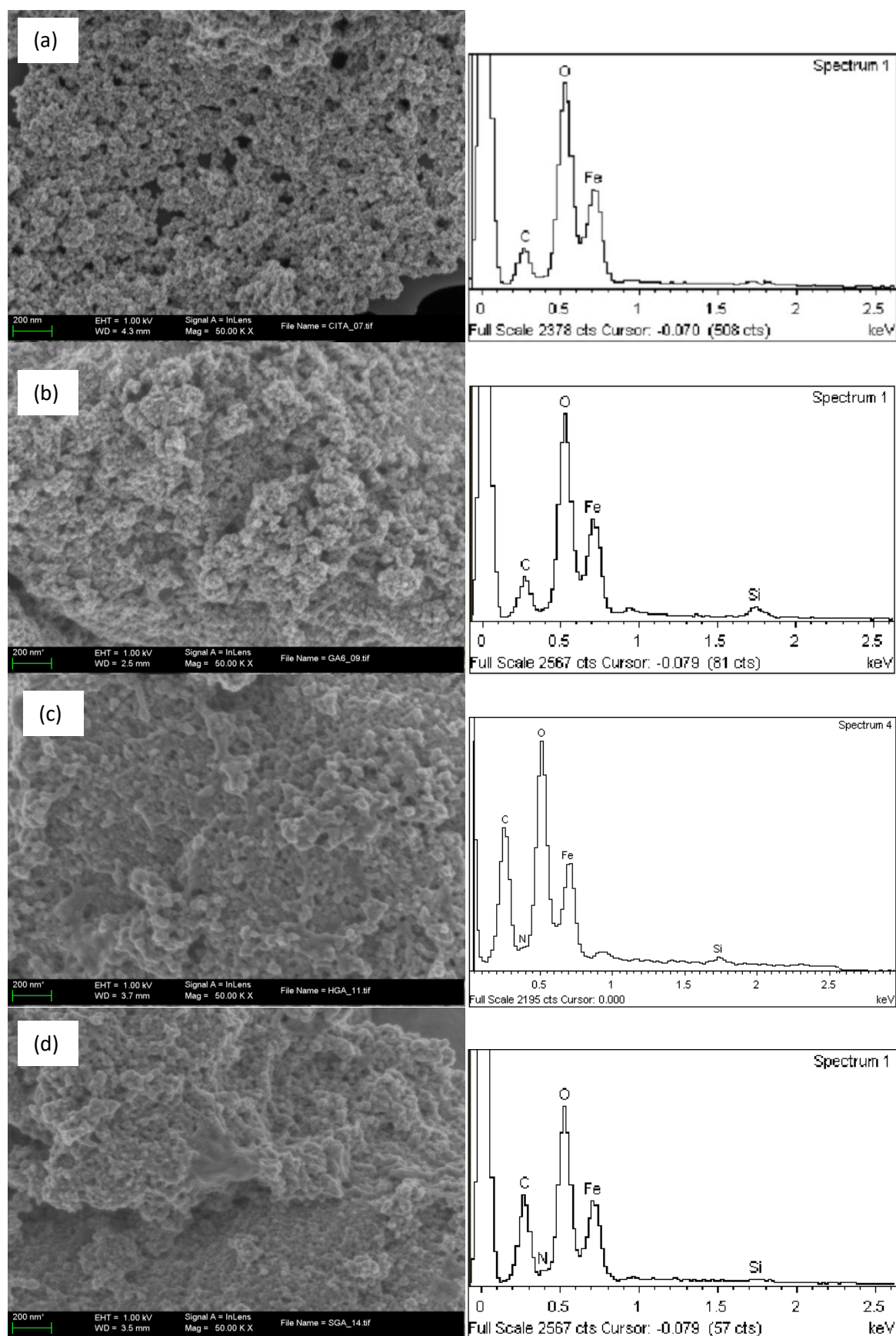


**Fig. 6.7** The SEM images at 50.00 KX magnification and EDX of (a) naked MNPs, (b) amino-functionalized MNPs, (c) amino-functionalized MNPs after being immobilised with Phw, and (d) amino-functionalized MNPs after being immobilised with Psr.

### **6.3.2 Characterisation of MNPs using FT-IR**

The surface modification and immobilisation of proteases (Phw and Psr) onto nanoparticles were confirmed by a comparison of the FT-IR spectra of naked MNPs, functionalised MNPs, and Phw and Psr immobilised onto functionalised MNPs. The FT-IR spectrum in Fig. 6.8A shows a strong absorption peak at  $584\text{ cm}^{-1}$ , which could correspond to Fe-O, as indicated in other studies (Bruce and Sen, 2005; Yamaura et al., 2004). It has been suggested that this strong peak could be due to the stretching vibration mode associated with metal-oxygen absorption. In this region, the stretching vibration peaks related to metal (ferrites in particular) in the octahedral and tetrahedral sites of the oxide structure were found (Lopez et al., 2010). In Fig. 6.8A, the peaks at  $1,662\text{ cm}^{-1}$  and  $3,444\text{ cm}^{-1}$  were due to the bending and stretching vibration of -OH, respectively (Pavia et al., 2015). After grafting with APTES, the characteristic peak of the Fe-O bond shifted from  $584\text{ cm}^{-1}$  to  $638\text{ cm}^{-1}$  and  $640\text{ cm}^{-1}$  because of the formation of the Fe-O-Si bond (Fig. 6.8B, Fig. 6.8C and Fig. 6.8D). The shifting of the absorption peaks to high wavenumbers is due to the greater electronegativity of -Si(O-) compared to H, which contributes to the bond forces for Fe-O bonds (Bini et al., 2012).

Additional strong peaks at  $1,039\text{ cm}^{-1}$ ,  $1,035\text{ cm}^{-1}$ , and  $1,034\text{ cm}^{-1}$  correspond to the Fe-O-Si bending vibrations, indicating that alkyl silanes are successfully attached to functionalised MNPs (Fig. 6.8B, Fig. 6.8C, and Fig. 6.8D). Additionally, the presence of silane groups was observed at  $995\text{ cm}^{-1}$ ,  $893\text{ cm}^{-1}$ , and  $896\text{ cm}^{-1}$  and was from the stretching vibrations of the Si-OH and Si-O-Si groups from APTES (Bini et al., 2012; Pavia et al., 2015).

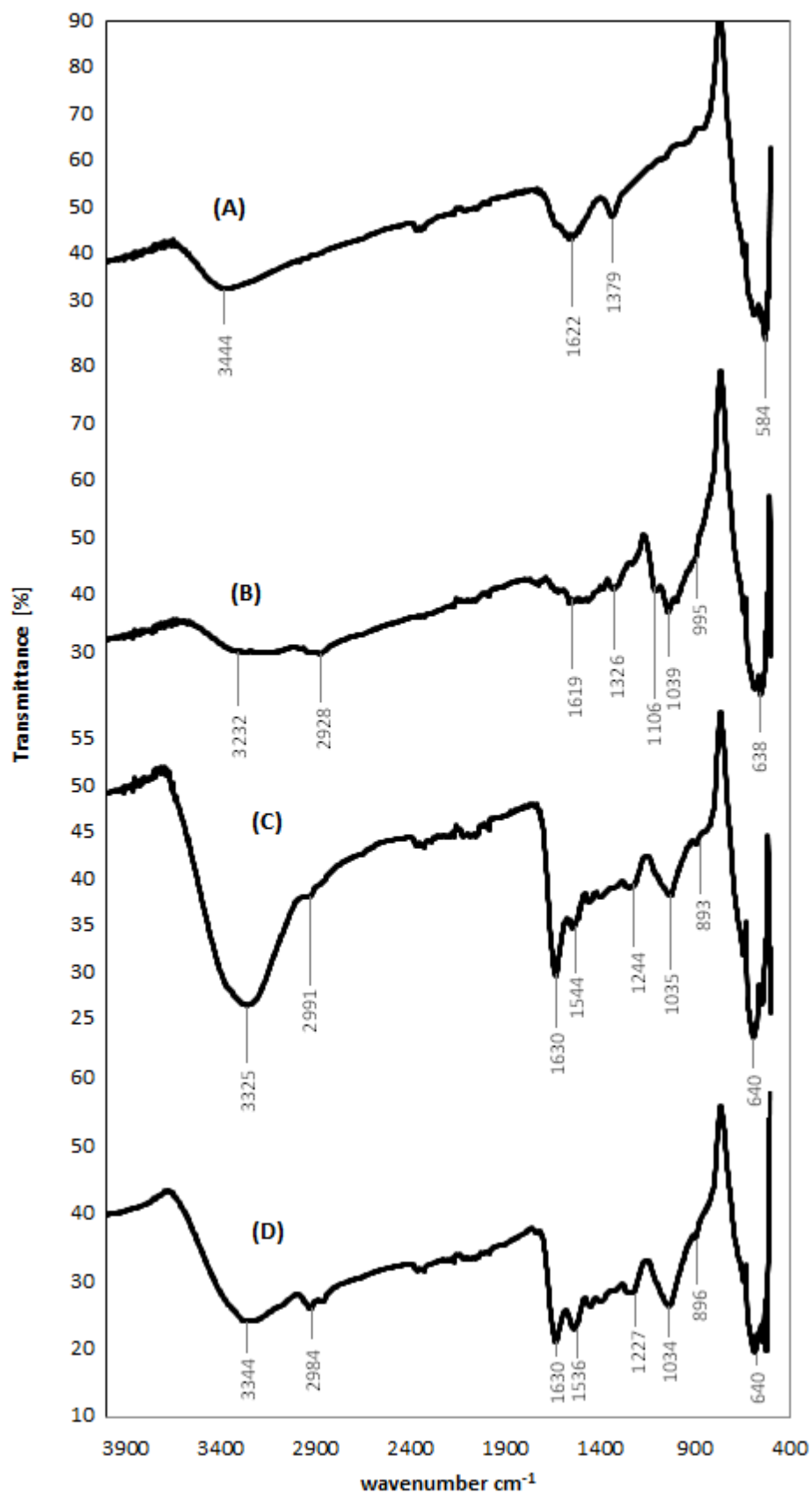


**Fig. 6.8** The FT-IR spectra of (A) naked MNPs, (B) amino-functionalized MNPs, (C) amino-functionalized MNPs after immobilisation of Phw, and (D) amino-functionalized MNPs after immobilisation of Psr.

Characteristic peaks of the immobilised enzymes attached via the crosslinker (Fig. 6.8C and Fig. 6.8D) were observed at  $1,536\text{ cm}^{-1}$ ,  $1,544\text{ cm}^{-1}$  and  $1,630\text{ cm}^{-1}$  because of the C=N and C=O absorption from the glutaraldehyde and  $\text{NH}_2$  from the enzyme (Wang et al., 2014). Small shifts in intensity from  $2,928\text{ cm}^{-1}$  (Fig. 6.8B) to  $2,991\text{ cm}^{-1}$  (Fig. 6.8C) and  $2,984\text{ cm}^{-1}$  (Fig. 6.8D) correspond to the C-H stretching vibration from the methyl group (Casillas et al., 2012), which illustrated the effect before and after the immobilisation of the enzymes. Additionally, in Fig. 6.8C and Fig. 6.8D, there were broad and strong peaks at  $3,325\text{ cm}^{-1}$  and  $3,344\text{ cm}^{-1}$ , which indicated the vibration modes of the O-H and -NH groups from enzymes that interact with nanoparticles, which has been suggested previously (Sinha and Khare, 2015).

## **6.4 Biochemical characterisation of immobilised proteases (Phw, Psr)**

### **6.4.1 Operational stability of immobilised Phw and Psr**

The operational stability regarding temperature and pH is an important criterion in the application of immobilised enzymes (De Castro and Sato, 2014; Tavano, 2013). Various pH values (5-11) and temperatures ( $30\text{ }^\circ\text{C}$ - $70\text{ }^\circ\text{C}$ ) were tested, and the results were compared with those of free enzymes (Phw\_free, Psr\_free) to check the operational stability of the immobilised proteases. The results were analysed using analysis of variance (ANOVA) to indicate the significant factor influencing the stability of both enzymes. The ANOVA results in Table 6.3 shows that the regression coefficients had a high statistical significance ( $p < 0.05$ ) and show the values obtained for the coefficient of determination for both Phw\_im and Psr\_im ( $R^2\ 0.9730$  and  $R^2\ 0.9733$ ) and Phw\_free and Psr\_free ( $R^2\ 0.9723$  and  $R^2\ 0.9712$ , respectively). The values indicated that the model of the immobilised enzymes could not explain only 2.7% of the variables behaviour, while with the free enzymes the value was 2.8-2.9%.



**Table 6.3** Analysis of variance (ANOVA) for the response surface quadratic model for immobilised (Phw\_im and Psr\_im) and free (Phw\_free and Psr\_free) enzymes

Protease	Source of variation	Sums of square	Degree of freedom	Mean square	F-value	Prob>F
Phw_im	Regression	12107.4	5	2421.5	50.47	<0.0001
	Residual	335.9	7	47.98		
	Pure error	150	4	37.5		
	Lack of fit	185.9	3	61.95	1.65	
	Total	12443.2	12			
Psr_im	Regression	5108.7	5	1021.7	50.99	<0.0001
	Residual	140.3	7	20		
	Pure error	58.8	4	14.7		
	Lack of fit	81.5	3	27.2	1.85	
	Total	5248.9	12			
Phw_free	Regression	3382.4	3	1127.5	105.4	<0.0001
	Residual	96.3	9	10.7		
	Pure error	20.8	4	5.2		
	Lack of fit	75.5	5	15.1	2.9	
	Total	3478.7	12			
Psr_free	Regression	6452.3	3	2150.8	101.1	<0.0001
	Residual	191.5	9	21.3		
	Pure error	32.3	4	8.1		
	Lack of fit	159.2	5	31.8	3.94	
	Total	6643.8	12			

Phw\_im:  $R^2$  0.9730, adj  $R^2$  0.9537, pred  $R^2$  0.8519

Psr\_im:  $R^2$  0.9733, adj  $R^2$  0.9542, pred  $R^2$  0.8260

Phw\_free:  $R^2$  0.9723, adj  $R^2$  0.9631, pred  $R^2$  0.9315

Psr\_free:  $R^2$  0.9712, adj  $R^2$  0.9616, pred  $R^2$  0.9224

For immobilised enzymes, the calculated F-value ( $\alpha=0.05$ , DOF=4,3) was 9.12 for the regression. This value was higher than the tabulated F-values (1.65, 1.85), indicating that the treatment differences were highly significant. Similarly, in free enzymes, the obtained F-values (2.90, 3.94) were less than the critical F-value ( $F_{0.05(4,5)} = 5.19$ ), reflecting the significance of the model. The following Equations (6.1-6.4) represent the second order polynomial model of the residual activity for the experimental data:

$$\text{Residual Phw\_im(\%)} = -407.2 + 56.5\text{pH} + 10.1\text{T} - 2.6\text{pH}^2 - 0.1\text{T}^2 - 0.16\text{pHT} \quad (6.1)$$

$$\text{Residual Psr\_im(\%)} = -275.9 + 41.8\text{pH} + 6.3\text{T} - 1.8\text{pH}^2 - 0.05\text{T}^2 - 0.17\text{pHT} \quad (6.2)$$

$$\text{Residual Phw\_free(\%)} = 22.2 + 2.5\text{pH} + 1.5\text{T} - 0.026\text{T}^2 \quad (6.3)$$

$$\text{Residual Psr\_free(\%)} = 66.4 + 1.04\text{pH} + 0.54\text{T} - 0.021\text{T}^2 \quad (6.4)$$

For free enzymes, the models (Eqs. 6.3-6.4) were reduced by removing the interaction between pH and temperature, as it was not significant to the stability of the free enzymes. Contour plots of the second order polynomial model were generated as a function of the independent variables of pH and temperature for immobilised and free enzymes.

The contour plots of free Phw and Psr exhibited their stability under mesophilic conditions (30 °C to 40 °C). Free enzymes were stable over a broad range of pH values (Fig. 6.9b and Fig. 6.9d), with no optimum condition obtained in the range tested (pH 5-11). However, both of the immobilised enzymes had improved the stability by achieving their optimum condition in the alkaline region (pH 8 to 11) with thermophilic temperature stability ranging from 40 °C to 60 °C for immobilised Phw (Fig. 6.9a) and 40 °C to 55 °C for immobilised Psr (Fig. 6.9c).

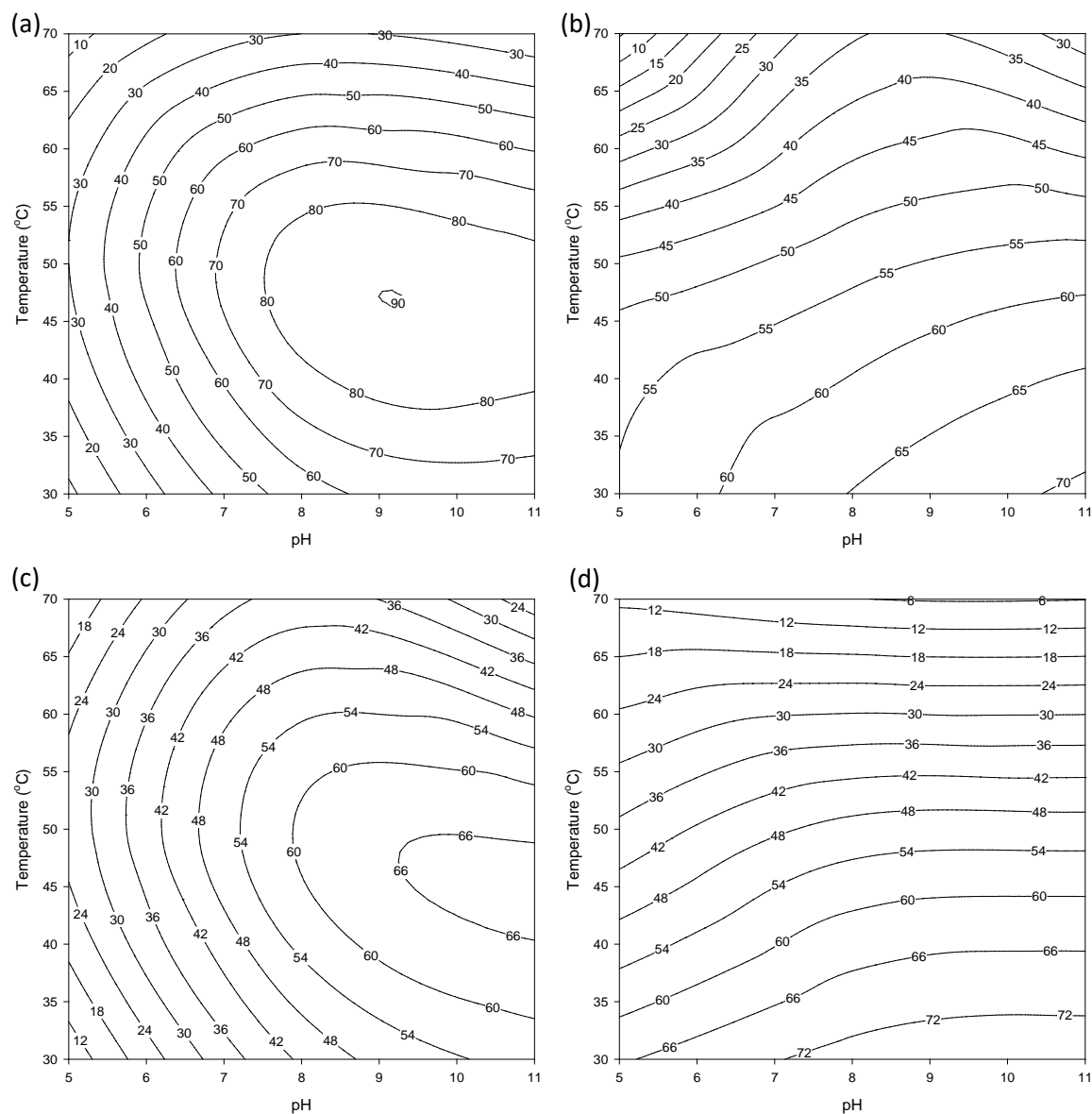


**Fig. 6.9** Contour plots of the residual activity (%) of the enzymes regarding their operation stability as a function of pH and temperature of (a) immobilised Phw, (b) free Phw, (c) immobilised Psr, and (d) free Psr

#### 6.4.2 Storage stability of immobilised Phw and Psr

Storage stability plays a crucial role in the use immobilised proteases, as the shelf life determines the viability of an immobilised enzyme over time (Kumar et al., 2009). The storage stabilities of enzymes immobilised via a crosslinker (Phw\_GA and Psr\_GA) and adsorption (Phw\_adsorp and Psr\_adsorp) were tested by dispersing the immobilised enzymes

in Tris buffer and maintaining them at 4 °C for 60 days. Free enzymes (Phw\_free and Psr\_free) were used as controls to monitor the durability of enzyme activity. Phw\_free and Psr\_free were not stable in solution, as their activity decreased over time. This fact could be related to the behaviour of the proteases, as they tend to autolyse themselves by nucleophilic attack on the intermediate in the presence of water (Beynon and Bond, 2001; Rao et al., 1998). After 7 days of storage at 4 °C, the residual activity of Phw\_free and Psr\_free was less than 17% (Table 6.4).

**Table 6.4** The storage stability of free and immobilised enzymes created via crosslinking with glutaraldehyde (GA) and via adsorption (adsorp) during 60 days of storage.

Enzymes	Initial activity (U/ml)	Final activity (U/ml)	Residual activity (%)
Phw_GA	501 ± 72	458 ± 51	91
Psr_GA	346 ± 69	297 ± 84	86
Phw_adsorp	190 ± 15	77 ± 9	41
Psr_adsorp	152 ± 9	46 ± 5	30
Phw_free	537 ± 26	91 ± 21 <sup>a</sup>	17
Psr_free	358 ± 29	42 ± 3 <sup>a</sup>	12

<sup>a</sup> The final activity was determined after 7 days of storage.  
The standard deviation was calculated from 3 replicates.

There was a significant decrease in the activity of the immobilised enzyme via adsorption over 60 days of storage, with a residual activity of less than 45%. The weak bonding between the enzyme and nanoparticles could induce partial desorption during the period of storage. Immobilisation via adsorption involves relatively weak interactions, such as electrostatic interactions, hydrogen bonds, van der Waals forces and hydrophobic interactions, which tend to strip off enzymes from the carrier easily, thus leading to a loss of activity and contamination of the reaction media (Xu et al., 2014). However, the enzymes

immobilised via crosslinking (Phw\_GA and Psr\_GA) retained 91% and 86% of their residual activity, respectively, after 60 days of storage at 4 °C (Table 6.4). These results show that enzymes immobilised created by crosslinking provide a distinctive advantage in stability over immobilised enzymes created by adsorption at a longer duration of storage.

### 6.4.3 Reusability of immobilised Phw and Psr

For the sake of the cost-effective use of enzymes, reusability is a critical factor to consider (Chen et al., 2014). The reusability of immobilised Phw and Psr created using crosslinking was evaluated in a repeated batch process using fresh casein as a model protein in each batch cycle (Fig. 6.10). Both immobilised Phw and Psr retained 66% and 64% of their activity, respectively, after 7 cycles, indicating a significant enhancement of the stability of the crosslinking interaction between the proteases and nanoparticles. In this work, testing the reusability was feasible, as the immobilised enzymes were easily separated by a magnetic force.

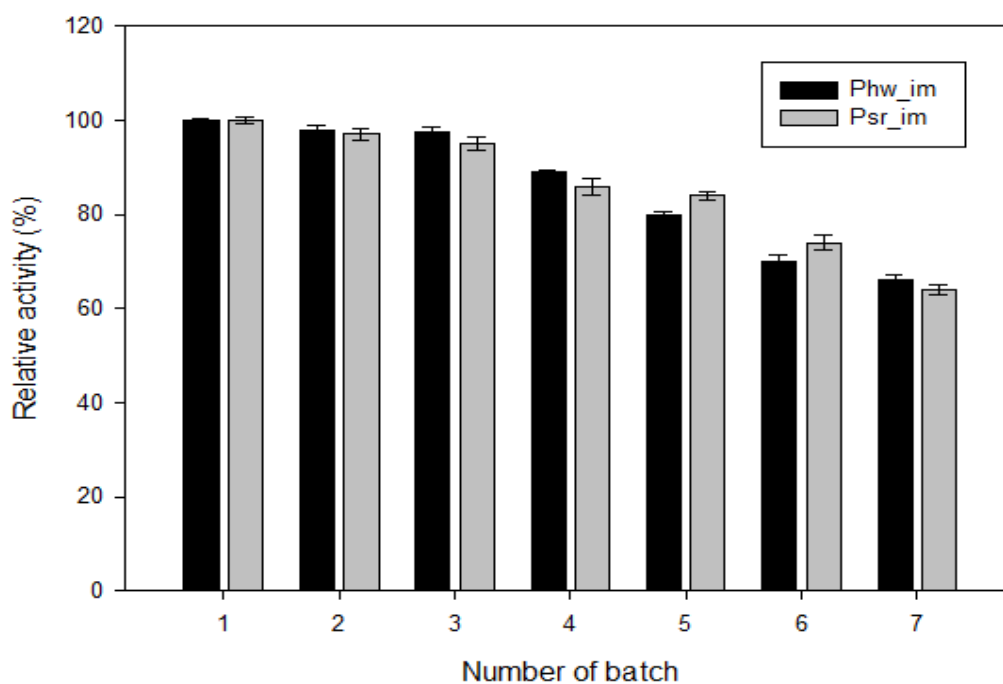


**Fig. 6.10** The reusability of immobilised Phw and immobilised Psr onto amino-functionalized MNPs using casein as a model substrate for the hydrolysis reaction

## **6.5 Application of immobilised proteases in the hydrolysis of proteins**

### **6.5.1 Degree of hydrolysis**

The degree of hydrolysis was determined by calculating the percentage of solubilised protein in 10% of trichloroacetic acid (TCA) in relation to the total protein content of the sample as mentioned in Section 3.4.5. Casein has been used as a model protein to evaluate the degree of hydrolysis (DH) of immobilised enzymes created via crosslinking and free Phw or Psr. While egg white albumin was chosen as protein source from animal and oat bran protein isolate was selected for protein source from vegetal. The different sources of protein were exploited to investigate the effect of protease from hair waste (Phw) and soy fibre residue (Psr). The results of the hydrolysis are shown in Fig. 6.11a.

The DH of immobilised Phw (24%) was higher than that of free Phw (15%) during the first 30 min of reaction time (Fig. 6.11a). The maximum DH was achieved after 24 h and was 80% for immobilised Phw and 40% for free Phw. Besides, the residual activity of both immobilised Phw and Psr were stable for 24 h whereas the residual activity of free Phw and Psr had decreased pronouncedly after 24 h at 50 °C indicating an improvement of process efficiency and thermal stability of the immobilised enzymes (Sinha and Khare, 2015). The higher stability may be possibly due to the multipoint covalent binding of protease to the solid support that limits the flexibility and conformational mobility of the enzyme, hence inhibits unfolding or denaturation of the enzyme (Singh et al., 2011).

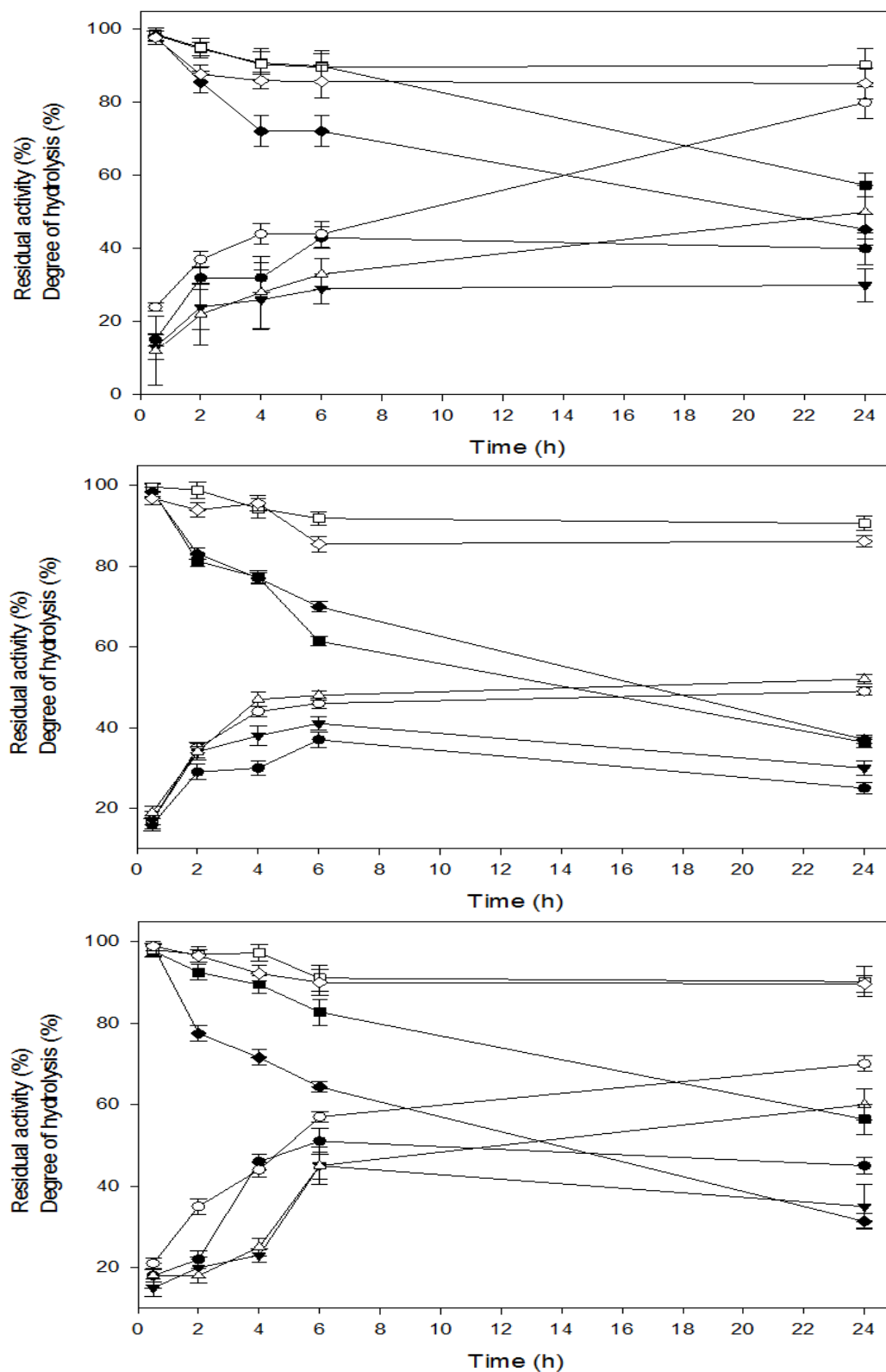


**Fig. 6.11** The degree of hydrolysis of the selected protein hydrolysates obtained from the hydrolysis of immobilised Phw (—□—), free Phw (—■—), immobilised Psr (—◇—), and free Psr (—◆—) with (a) casein; (b) oat bran protein isolate (OBPI); and (c) egg white albumin. The residual activity of immobilised Phw (—□—), free Phw (—■—), immobilised Psr (—◇—) and free Psr (—◆—) in 50 °C during 24h.

Likewise, the DH of immobilised Psr (12%) showed the same rate as that of free Psr (13%) and continued to increase over time with a similar profile, reaching the maximum DH 30% in free Psr and 50% in immobilised Psr after 24 h of reaction time. Thus, the immobilised enzymes in the present study could enhance the ability of free enzymes to hydrolyse protein, as shown by the model protein, reflecting that the active enzymes were successfully immobilised. The effect of both proteases (Phw and Psr) was also evaluated in the hydrolysis of the protein source from animals (egg white albumin) and vegetables (oat bran protein isolate). The hydrolysis of oat bran protein isolate (OBPI) corroborated the efficiency of immobilised Phw and Psr, as they had a higher DH compared to free Phw and Psr over a longer duration (Fig. 6.11b).

These results agree with those obtained using functionalised magnetite nanoparticles to hydrolyse soy protein isolates and whey protein isolates (Lamas et al., 2001; Wang et al., 2014). It seems that Psr exhibited a higher DH than (free and immobilised) Phw when using a vegetable protein source. In the hydrolysis of egg white albumin, immobilised Psr reached a maximum DH 60% after 24 h, and free Psr achieved maximum DH 45% after 6 h, while Phw reached a maximum DH of 70% and 51% for immobilised and free Phw, respectively (Fig. 6.11c). Hence, the different source of the proteases seems to be a distinct behaviour that depends on the substrate source; in fact, it could determine the choice of enzymes according to the application, as suggested by others (Tavano, 2013).

### **6.5.2 Peptide and amino acid analysis after treated with immobilised proteases**

SDS-PAGE of the hydrolysates from selected proteins (casein, OBPI, egg white albumin) is shown in Fig. 6.12. The presence of several smaller peptides with low molecular weights supports the idea that proteins were hydrolysed by immobilised protease derived from an animal source (Phw) and vegetable source (Psr). Similar profiles were obtained for



both immobilised enzymes (Phw and Psr), showing their ability to perform the reaction after being grafted on nanoparticle surfaces created by crosslinking with glutaraldehyde.

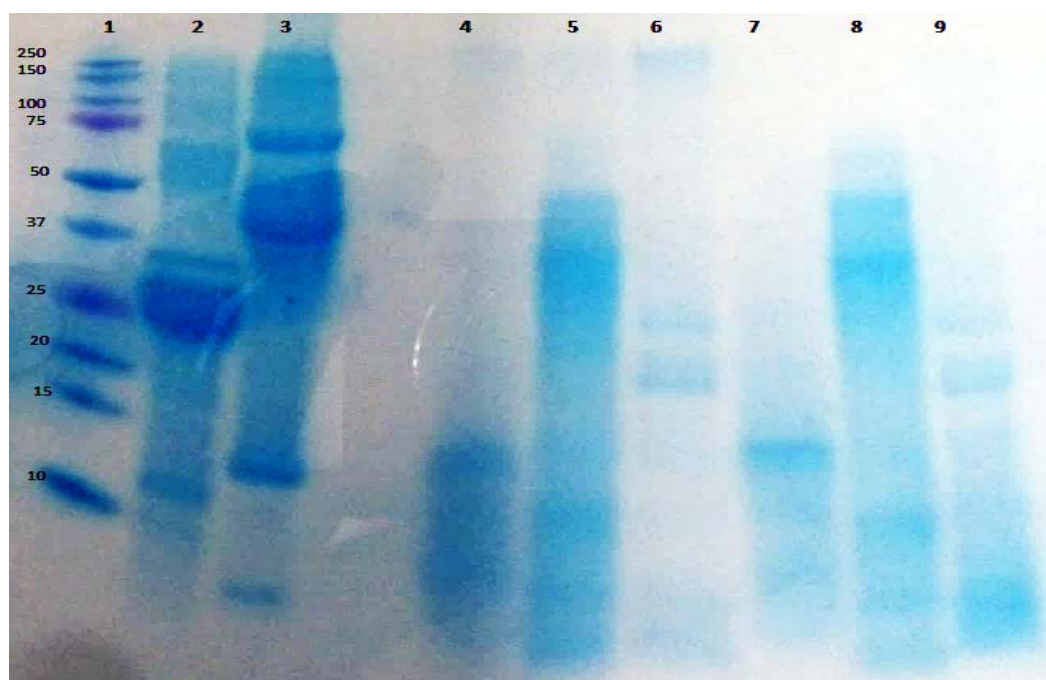


**Fig. 6.12** SDS-PAGE of the hydrolysates after reduction using 2-mercaptoethanol for selected proteins before and after treatment with the immobilised proteases; (1) Molecular mass marker; (2) casein; (3) egg white albumin; (4) hydrolysate from casein after treated with immobilised Phw; (5) hydrolysate from egg white albumin after treatment with immobilised Phw; (6) hydrolysate from OBPI after treatment with immobilised Phw; (7) hydrolysate from casein after treatment with immobilised Psr; (8) hydrolysate from egg white albumin after treatment with immobilised Psr; (9) hydrolysate from OBPI after treatment with Psr.

The hydrolysis of proteins was initiated with 4% (w/v) of proteins as substrate (casein, OBPI, and egg albumin) using immobilised proteases (Phw and Psr). The amino acids of the hydrolysates were analysed without derivatisation using LC-MS following the method in Section 3.4.6 for 30 minutes, and 20 amino acids were correlated with their standards as in A.5 – A.21, except for tryptophan. The amino acids were quantified according to Table 3.1 (Section 3.4.6) using positive APCI ionisation mode in SIM mode. The amino acids composition of the hydrolysates was shown in Table 6.5.

**Table 6.5** Amino acids distribution (% w/w) in protein hydrolysates of 100 mg of dried protein after treated with immobilised proteases for 24 hours.

Casein	0.5h		2h		4h		6h		24h	
	Psr	Phw	Psr	Phw	Psr	Phw	Psr	Phw	Psr	Phw
ala		0.21							0.31	0.83
val		1.22				0.46	0.12		1.12	7.39
thr	14.81					3.53		7.10		6.78
cys	21.29	33.78	25.18	37.11	26.75	39.00	29.80	31.24	31.64	32.26
hyp-leu-ile <sup>a</sup>		1.04				1.19	0.46		0.67	9.41
asn		3.54	0.49	1.88	1.23	3.60	3.38	1.73	4.00	15.13
gln-lys <sup>b</sup>									0.17	4.91
met						0.53	0.28		0.28	5.71
phe	9.59	0.36	0.41	0.54	1.40	3.01	2.72	5.09	4.26	3.11
arg		0.21								
tyr		2.21	0.29	1.26	1.40	3.39	2.80	2.16	1.08	13.96
OBPI	0.5h		2h		4h		6h		24h	
	Psr	Phw	Psr	Phw	Psr	Phw	Psr	Phw	Psr	Phw
ala						0.21				
val				0.28		1.29	1.91	1.84	3.50	2.16
thr	4.82	2.90								5.40
cys	31.67	25.39	32.76	29.50	31.65	34.47	35.31	38.33	39.79	32.61
hyp-leu-ile <sup>a</sup>				0.25		1.13	0.91	0.57	2.62	1.94
asn		0.30	0.99	2.74	5.55	4.02	3.91	3.03	6.31	4.19
gln-lys <sup>b</sup>				0.47						
met									0.17	0.18
phe	3.70	2.69	0.51	0.67	2.03	1.98	2.48	4.12	1.49	1.67
arg						0.20	0.27			
tyr			0.71	1.39	1.61	2.21	2.79	3.59	5.33	3.17
Egg albumin	0.5h		2h		4h		6h		24h	
	Psr	Phw	Psr	Phw	Psr	Phw	Psr	Phw	Psr	Phw
ala										0.98
val						0.24		0.57	0.57	4.31
thr		4.44								0.95
cys	16.59	23.16	21.73	27.86	22.68	29.39	22.22	29.89	24.17	28.11
hyp-leu-ile <sup>a</sup>								0.41	1.22	4.15
asn		0.42		1.55	0.37	2.37	1.37	3.32	4.85	9.72
gln-lys <sup>b</sup>										0.36
met						0.21		0.19	0.56	2.08
phe	4.63	3.57	0.37	0.56	0.49	1.33	0.55	1.34	1.19	2.15
arg										1.07
tyr				0.17		1.82		2.77	3.08	3.04

OBPI: oat bran protein isolate;

hyp-leu-ile<sup>a</sup>: hydroxyproline, leucine, and isoleucine were determined at the same mass ion (132 m/z) in Table 3.1

gln-lys<sup>b</sup>: glutamine and lysine were determined at the same mass ion (147 m/z) in Table 3.1

The total nitrogen content (N %) of each unhydrolysed proteins were 13.6%  $\pm$ 0.2, 12.9%  $\pm$ 1.5, and 10.5%  $\pm$ 3.5 in casein, egg albumin, and oat bran protein isolate (OBPI), respectively determined using the Kjeldahl method in Section 3.3.5. The N factors used for the conversion from total N content to proteins were 6.38, 6.25, and 5.38 for casein, egg albumin, and OBPI, respectively (Who/Fao, 2002). Out of 20 amino acids detected from the sample hydrolysates, only the residues with significant amount were tabulated in Table 6.5. The amino acids composition released was well balanced with the degree of hydrolysis (Fig. 6.11) and was different in each protein substrates which had treated with different proteases (Phw and Psr) due to the different nature of these proteins. There are a significant amount of tyrosine, phenylalanine, and leucine residues signify that these proteases probably belongs to alkaline serine which has broad substrate specificities and hydrolyses a peptide bond which has tyrosine, phenylalanine, or leucine at the carboxyl side of the splitting bond (Rao et al., 1998).

Furthermore, in Table 6.5, amino acids composition from hydrolysate obtained from different proteases hydrolysis showed high cysteine content (>30%) during 24 h of hydrolysis reaction and more prominent when hydrolysis of OBPI using Psr which both were from vegetal/plant source. This finding was corresponding to the study with the hydrolysate from defatted soy flakes which were a vegetal source protein (Ding et al., 2015). As a matter of fact, in plants/vegetal there are the peptides with the abundance of cysteine (cys) residues that called phytochelatins (PC) that have general structure (glu-cys)<sub>n</sub> which known to bind heavy metals.

Normally, hard metals such as Ca<sup>2+</sup> and Mg<sup>2+</sup> will bind to acidic amino acid residues such as aspartic acid (asp) and glutamic acid (glu), while soft metals such as Zn<sup>2+</sup>, Cu<sup>2+</sup>, and Fe<sup>2+</sup> rather bind to cys and histidine (his) residues (Viswanathan et al., 2012). However, in

this study, the cys residue was found in abundance which not binding to the  $\text{Fe}^{2+}$  ions in the nanoparticles indicated the successful of amino functionalised magnetite with covalent binding to the proteases and denoted the irreversible immobilisation as suggested in iron magnetic nanoparticles immobilisation (Xu et al., 2014). In this case, protease immobilised on amino functionalised magnetic nanoparticles can be used without affecting the reaction or residues of amino acids during the protein hydrolysis.

## **Conclusion**

Low-cost proteases obtained through the SSF of protein-rich wastes (hair waste and soy fibre residues) were successfully immobilised onto functionalised MNPs over a relatively short time. The ease of the separation and reusability of these enzymes in comparison with free enzymes could be considered an advantage of their use in industrial processes. Additionally, stability was enhanced from mesophilic to thermophilic conditions under alkaline conditions, preventing autolysis of the enzymes and maintaining their initial activities for 2 months with only 9%-14% activity loss. Immobilised Phw and Psr were able to hydrolyse some proteins derived from plant and animal sources with a high degree of hydrolysis, indicating that they are promising for immobilised enzyme applications in a wide range of industrial processes.

All in all, the degree of hydrolysis of the protein can be a determiner to produce certain amino acids and the hydrolysates produced in the present work can be further used in peptide synthesis for heavy metal sequestration scheme.



## Chapter 7

*Conclusions and suggestions for future work*



From the findings obtained in this study, in general, we can conclude that the extraction, immobilisation and utilisation of proteases produced by SSF using organic waste were successful. Apart from the general conclusion, several specific issues can be withdrawn from the results obtained in this research study as presented as following:

- Most of the studies involved solid residues in SSF dealing with small scale and barely explore the reproducibility of the process. In this study, the SSF of protein-rich solid waste and anaerobically digested sludge has demonstrated a reproducibility process with the similar protease production profile generated from several batch fermentations in 10 L reactors. Furthermore, statistically, the coefficients of variation (CV) for all fermentations were lower than 5% validating the process and confirming that there were non-significant differences between replicates.
- Since SSF is a process occurred in a limited of water activity, therefore extraction of bio-product has become a significant downstream processing in SSF. Downstream processing in SSF is scarcely reported in the literature and commonly treated in a lower scale, which hampers the up-scaling process. This study successfully demonstrated an extraction process using the whole material in 10 L reactors, that enables the utilisation of the whole material to yield maximum recovery of the protease from SSF.
- The reutilisation of the remaining residues after solid state fermentation was accomplished by stabilisation process in the reactor until a compost-like material was obtained which is stable and easy to handle and could be applied for agricultural purpose.



- The protease produced from hair waste was classified as an alkaline serine protease that has broad substrate specificities which suitable for dehairing process, coupled with its stability at the alkaline condition with moderate heat stability (30°C – 50°C), suitable for the industrial application.
- Even though the lyophilised protease extracts has lost its activity about 21% after lyophilisation process, it still exhibited a promising alternative for chemical methods in dehairing of cowhides with the result was comparable with the commercial enzyme and chemical methods.
- The selection of suitable support has become a key consideration for enzyme immobilisation. In this work, out of 10 materials screened for immobilisation support, magnetic nanoparticles seem appropriate for immobilisation of proteases from hair waste and soy waste.
- Nanoparticles have exhibited ideal characteristics as a support for proteases immobilisation with high biocatalysts efficiency and sufficient enzyme loading. Besides, immobilisation of proteases on nanoparticles has improved the stability and performance of the enzymes. Additionally, the magnetic nanoparticles as a support for enzyme immobilisation have an extra advantage on reusability, reproducibility, feasibility and cost effective. Not only inexpensive but also offer an easy preparation and separation processes.
- Box-hunter experimental design technique has been used to determine the optimal load of protease activity on magnetic nanoparticles. The optimisation was carried out taking into account the maximum enzymatic load and the possibility of reuse.

- In this work, it has been demonstrated that the characterisation of the support for protease immobilisation can be an important aspect as it can provide a visual interpretation regarding enzyme attachment and chemical and physical modification occurred after and before immobilisation.
- Immobilisation via covalent binding is an excellent method for the produced proteases. It provides higher stability regarding operation that enhanced from mesophilic to thermophilic conditions under alkaline conditions. In addition, the storage stability was maintained for 2 months with only 9%-14% activity loss. The stability improvement is very useful for industrial application mainly associated with the hydrolytic reaction.
- Enzyme immobilisation on magnetic nanoparticles not only can provide enzyme stabilisation but also eliminate the step of enzyme inactivation at the end of reaction as it can be easily removed, subsequently, can be reused for the next reaction. The activity of immobilised enzyme was maintained above 60% for both proteases after seven consecutive cycles of reaction indicating a high stability of the immobilised enzyme. Also, the biocompatibility of this method of immobilisation with magnetic nanoparticles as a support is demonstrated for enzyme immobilisation.
- The immobilised proteases exhibited an enhanced performance with their ability to hydrolyse different protein substrates with a high degree of hydrolysis, which is useful for industrial applications.
- As observed in this study, the same protein substrate can produce different hydrolysates using different proteases, as proteases produced from various sources (animal and vegetal sources) may present distinct behaviour. Therefore the sources of the enzyme could influence the production of protease for a given application.

Finally, from this research work, several suggestions for future studies should be considered as follows:

- In an effort to impart the sustainability concept in wastes utilisation via SSF, the use of solid waste should be investigated with a particular focus on biorefinery concepts. Hence, the viability to produce other valuable products in the same process could be an interesting approach. In addition, economic and environmental studies of the complete process are needed, since there is a lack of information available involving SSF.
- The identification of microorganisms directly involved in the production of proteases through SSF would be very useful in the optimisation of the protease production. The enrichment with protease producing microorganisms could achieve higher productivity. In this sense, the use of 16S rDNA gene sequencing could be conducted to identify the consortia involved in this work.
- New uses of immobilised proteases could be explored, for example in the improvement of the hydrolysis of the anaerobic digestion process.
- The hydrolysates produced from reaction with immobilised proteases can be further utilised for peptide synthesis for heavy metal sequestration.

## References

## *References*

- Abdullah, J.J., Greetham, D., Pensupa, N., Tucker, G.A., Du, C., 2016. Optimizing Cellulase Production from Municipal Solid Waste (MSW) using Solid State Fermentation (SSF). *J. Fundam. Renew. Energy Appl.* 6, 206.
- Abo Markeb, A., Alonso, A., Dorado, A.D.A.D., Sánchez, A., Font, X., 2016. Phosphate removal and recovery from water using nanocomposite of immobilized magnetite nanoparticles on cationic polymer. *Environ. Technol.* 3330, 1–14.
- Abraham, J., Gea, T., Sánchez, A., 2014. Substitution of chemical dehairing by proteases from solid-state fermentation of hair wastes. *J. Clean. Prod.* 74, 191–198.
- Abraham, J., Gea, T., Sánchez, A., 2013. Potential of the solid-state fermentation of soy fibre residues by native microbial populations for bench-scale alkaline protease production. *Biochem. Eng. J.* 74, 15–19.
- Adams, T.T., Eiteman, M.A., Hanel, B.M., 2002. Solid state fermentation of broiler litter for production of biocontrol agents. *Bioresour. Technol.* 82, 33–41.
- Adani, F., Confalonieri, R., Tambone, F., 2004. Dynamic respiration index as a descriptor of the biological stability of organic wastes. *J. Environ. Qual.* 33, 1866–1876.
- Adani, F., Ubbiali, C., Generini, P., 2006. The determination of biological stability of composts using the Dynamic Respiration Index: The results of experience after two years. *Waste Manag.* 26, 41–48.
- Afrisham, S., Badoei-Dalfard, A., Namaki-Shoushtari, A., Karami, Z., 2016. Characterization of a thermostable, CaCl<sub>2</sub>-activated and raw-starch hydrolyzing alpha-amylase from *Bacillus licheniformis* AT70: Production under solid state fermentation by utilizing agricultural wastes. *J. Mol. Catal. B Enzym.* 132, 98–106.
- Ahmed, S.A., Mostafa, F.A., 2013. Utilization of orange bagasse and molokhia stalk for production of pectinase enzyme. *Brazilian J. Chem. Eng.* 30, 449–456.
- Aikat, K., Bhattacharyya, B.C., 2000. Protease extraction in solid state fermentation of wheat bran by a local strain of *Rhizopus oryzae* and growth studies by the soft gel technique. *Process Biochem.* 35, 907–914.
- Alef, K., Nannipieri, P., 1995. *Methods in applied soil microbiology and biochemistry - Enzyme activities, Methods in applied soil microbiology and biochemistry.* Academic Press, San Diego.
- Alonso, A., Muñoz-Berbel, X., Vigués, N., Rodríguez-Rodríguez, R., Macanás, J., Mas, J., Muñoz, M., Muraviev, D.N., 2012. Intermatrix synthesis of monometallic and magnetic metal/metal oxide nanoparticles with bactericidal activity on anionic exchange polymers. *RSC Adv.* 2, 4596–4599.
- Amini, M., Younesi, H., Bahramifar, N., Lorestani, A.A.Z., Ghorbani, F., Daneshi, A., Sharifzadeh, M., 2008. Application of response surface methodology for optimization of lead biosorption in an aqueous solution by *Aspergillus niger*. *J. Hazard. Mater.* 154, 694–702.
- Amira, H.A.A., Eida, M.A.K., 2016. Recovery of silver from used X-ray film using alkaline protease from *Bacillus subtilis* sub sp. *subtilis*. *African J. Biotechnol.* 15, 1413–1416.
- Andrade, Â.L., Fabris, J.D., Ardisson, J.D., Valente, M.A., Ferreira, J.M.F., 2012. Effect of Tetramethylammonium Hydroxide on Nucleation, Surface Modification and Growth of Magnetic Nanoparticles. *J. Nanomater.* 1–10.
- Anto, H., Trivedi, U.B., Patel, K.C., 2006. Glucoamylase production by solid-state fermentation using rice flake manufacturing waste products as substrate. *Bioresour. Technol.* 97, 1161–1166.
- Arantes, V., Silva, E.M., Milagres, A.M.F., 2011. Optimal recovery process conditions for manganese-peroxidase obtained by solid-state fermentation of eucalyptus residue using *Lentinula edodes*. *Biomass and Bioenergy* 35, 4040–4044.

## References

- Ardao, I., Comenge, J., Benaiges, M.D., Álvaro, G., Puentes, V.F., 2012. Rational nanoconjugation improves biocatalytic performance of enzymes: Aldol addition catalyzed by immobilized rhamnulose-1-phosphate aldolase. *Langmuir* 28, 6461–6467.
- Asgher, M., Shahid, M., Kamal, S., Iqbal, H.M.N., 2014. Recent trends and valorization of immobilization strategies and ligninolytic enzymes by industrial biotechnology. *J. Mol. Catal. B Enzym.* 101, 56–66.
- Asha Poorna, C., Prema, P., 2007. Production of cellulase-free endoxylanase from novel alkalophilic thermotolerant *Bacillus pumilus* by solid-state fermentation and its application in wastepaper recycling. *Bioresour. Technol.* 98, 485–490.
- Asker, M.M.S., Mahmoud, M.G., El Shebwy, K., Abd el Aziz, M.S., 2013. Purification and characterization of two thermostable protease fractions from *Bacillus megaterium*. *J. Genet. Eng. Biotechnol.* 11, 103–109.
- Ávila-Cisneros, N., Velasco-Lozano, S., Huerta-Ochoa, S., Córdova-López, J., Gimeno, M., Favela-Torres, E., 2014. Production of Thermostable Lipase by *Thermomyces lanuginosus* on Solid-State Fermentation: Selective Hydrolysis of Sardine Oil. *Appl. Biochem. Biotechnol.* 174, 1859–1872.
- Bansal, N., Janveja, C., Tewari, R., Soni, R., Soni, S.K., 2014. Highly thermostable and pH-stable cellulases from *Aspergillus niger* NS-2: Properties and application for cellulose hydrolysis. *Appl. Biochem. Biotechnol.* 172, 141–156.
- Barreiro-Iglesias, R., Coronilla, R., Concheiro, a., Alvarez-Lorenzo, C., 2005. Preparation of chitosan beads by simultaneous cross-linking/ insolubilisation in basic pH: Rheological optimisation and drug loading/release behaviour. *Eur. J. Pharm. Sci.* 24, 77–84.
- Barrena, R., d'Imporzano, G., Ponsá, S., Gea, T., Artola, A., Vázquez, F., Sánchez, A., Adani, F., 2009. In search of a reliable technique for the determination of the biological stability of the organic matter in the mechanical-biological treated waste. *J. Hazard. Mater.* 162, 1065–1072.
- Barrena, R., Pagans, E. I., Vasquez, F., Artola, A., Sanchez, A., 2007a. Full-scale cocomposting of hair wastes from the leather manufacturing industry and sewage sludge. *Compost Sci. Util.* 15, 16–21.
- Barrena, R., Pagans, E. La, Artola, A., Vázquez, F., Sánchez, A., 2007b. Co-composting of hair waste from the tanning industry with de-inking and municipal wastewater sludges. *Biodegradation* 18, 257–268.
- Bas, A.D., Yazici, E.Y., Devenci, H., 2012. Recovery of silver from X-ray film processing effluents by hydrogen peroxide treatment. *Hydrometallurgy* 121-124, 22–27.
- Bastus, N.G., Comenge, J., Puentes, V., 2011. Kinetically Controlled Seeded Growth Synthesis of Citrate-Stabilized Gold Nanoparticles of up to 200 nm : Size Focusing versus Ostwald Ripening Kinetically Controlled Seeded Growth Synthesis of Citrate-Stabilized Gold Nanoparticles of up to 200 nm : Size. *Langmuir* 27, 11098–11105.
- Behera, S.S., Ray, R.C., 2016. Solid state fermentation for production of microbial cellulases: Recent advances and improvement strategies. *Int. J. Biol. Macromol.* 86, 656–669.
- Beynon, R., Bond, J.S. (Eds.), 2001. *Proteolytic enzymes: a practical approach*, 3rd ed. Oxford University Press.
- Bezawada, J., Yan, S., John, R.P., Tyagi, R.D., Surampalli, R.Y., 2011. Recovery of *Bacillus licheniformis* Alkaline Protease from Supernatant of Fermented Wastewater Sludge Using Ultrafiltration and Its Characterization. *Biotechnol. Res. Int.* 1-11.
- Bhalkar, B.N., Bedekar, P.A., Kshirsagar, S.D., Govindwar, S.P., 2016. Solid state fermentation of soybean waste and an up-flow column bioreactor for continuous production of camptothecin by an endophytic fungus: *Fusarium oxysporum*. *RSC Adv.* 6, 56527–56536.

- Bhavsar, K., Ravi Kumar, V., Khire, J.M., 2012. Downstream processing of extracellular phytase from *Aspergillus niger*: Chromatography process vs. aqueous two phase extraction for its simultaneous partitioning and purification. *Process Biochem.* 47, 1066–1072.
- Bio-Rad, 2012. A Guide to Polyacrylamide Gel Electrophoresis and Detection Part I : Theory and Product Selection Part II : Methods Part III : Troubleshooting Part IV : Appendices, Bio-Rad.
- Bini, R.A., Marques, R.F.C., Santos, F.J., Chaker, J.A., Jafelicci, M., 2012. Synthesis and functionalization of magnetite nanoparticles with different amino-functional alkoxy silanes. *J. Magn. Mater.* 324, 534–539.
- Botella, C., Diaz, A., de Ory, I., Webb, C., Blandino, A., 2007. Xylanase and pectinase production by *Aspergillus awamori* on grape pomace in solid state fermentation. *Process Biochem.* 42, 98–101.
- Bruce, I.J., Sen, T., 2005. Surface modification of magnetic nanoparticles with alkoxy silanes and their application in magnetic bioseparations. *Langmuir* 21, 7029–7035.
- Casillas, P.E.G., Gonzalez, C.A.R., Pérez, C.A.M., 2012. Infrared Spectroscopy of Functionalized Magnetic Nanoparticles, in: Theophile, T. (Ed.), *Infrared Spectroscopy - Materials Science, Engineering and Technology*. InTech, pp. 405–420.
- Castro, A.M. De, Carvalho, D.F., Freire, D.M.G., Castilho, L.D.R., 2010. Economic analysis of the production of amylases and other hydrolases by *Aspergillus awamori* in solid-state fermentation of Babassu Cake. *Enzyme Res.* 2010, 1–9.
- Cerda, A., El-Bakry, M., Gea, T., Sánchez, A., 2016. Long term enhanced solid-state fermentation: Inoculation strategies for amylase production from soy and bread wastes by *Thermomyces* sp. in a sequential batch operation. *J. Environ. Chem. Eng.* 4, 2394–2401.
- Chae, H.J., In, M.J., Kim, E.Y., 1998. Optimization of protease immobilization by covalent binding using glutaraldehyde. *Appl. Biochem. Biotechnol.* 73, 195–204.
- Chang, J., Cheng, W., Yin, Q., Zuo, R., Song, A., Zheng, Q., Wang, P., Wang, X., Liu, J., 2012. Effect of steam explosion and microbial fermentation on cellulose and lignin degradation of corn stover. *Bioresour. Technol.* 104, 587–592.
- Chaplin, M., 2014, August 6. *Enzyme Technology. Methods of immobilisation*. Retrieved from <http://www1.lsbu.ac.uk/water/enztech/immmethod.html>.
- Chen, H.Q., Chen, X.M., Chen, T.X., Xu, X.M., Jin, Z.Y., 2011. Extraction optimization of inulinase obtained by solid state fermentation of *Aspergillus ficuum* JNSP5-06. *Carbohydr. Polym.* 85, 446–451.
- Chen, H.Z., He, Q., 2012. Value-added bioconversion of biomass by solid-state fermentation. *J. Chem. Technol. Biotechnol.* 87, 1619–1625.
- Chen, T., Yang, W., Guo, Y., Yuan, R., Xu, L., Yan, Y., 2014. Enhancing catalytic performance of  $\beta$ -glucosidase via immobilization on metal ions chelated magnetic nanoparticles. *Enzyme Microb. Technol.* 63, 50–57.
- Cipolatti, E.P., Silva, M.J.A., Klein, M., Feddern, V., Feltes, M.M.C., Oliveira, J.V., Ninow, J.L., De Oliveira, D., 2014. Current status and trends in enzymatic nanoimmobilization. *J. Mol. Catal. B Enzym.* 99, 56–67.
- Cîrcu, M., Nan, A., Borodi, G., Liebscher, J., Turcu, R., 2016. Refinement of Magnetite Nanoparticles by Coating with Organic Stabilizers. *Nanomaterials* 6, 228.
- Cowan, D.A., Fernandez-Lafuente, R., 2011. Enhancing the functional properties of thermophilic enzymes by chemical modification and immobilization. *Enzyme Microb. Technol.* 49, 326–346.



## References

- Da Silva, R.R., de Freitas Cabral, T.P., Rodrigues, A., Cabral, H., 2013. Production and partial characterization of serine and metallo peptidases secreted by *Aspergillus fumigatus Fresenius* in submerged and solid state fermentation. *Brazilian J. Microbiol.* 44, 235–243.
- Daâssi, D., Zouari-Mechichi, H., Frikha, F., Rodríguez-Couto, S., Nasri, M., Mechichi, T., 2016. Sawdust waste as a low-cost support-substrate for laccases production and adsorbent for azo dyes decolorization. *J. Environ. Heal. Sci. Eng.* 14, 1–12.
- Das, R.K., Brar, S.K., Verma, M., 2016. Potential use of pulp and paper solid waste for the bio-production of fumaric acid through submerged and solid state fermentation. *J. Clean. Prod.* 112, 4435–4444.
- Datta, S., Christena, L.R., Rajaram, Y.R.S., 2012. Enzyme immobilization: an overview on techniques and support materials. *3 Biotech* 1–9.
- Dave, B.R., Parmar, P., Sudhir, A., Singal, N., Subramanian, R.B., 2015. Cellulases production under solid state fermentation using agro waste as a substrate and its application in saccharification by *Trametes hirsuta* NCIM. *J. Microbiol. Biotechnol. Food Sci.* 4, 203–208.
- Dave, B.R., Sudhir, A.P., Pansuriya, M., Raykundaliya, D.P., Subramanian, R.B., 2012. Utilization of *Jatropha* deoiled seed cake for production of cellulases under solid-state fermentation. *Bioprocess Biosyst. Eng.* 35, 1343–1353.
- Dayanandan, A., Kanagaraj, J., Sounderraj, L., Govindaraju, R., Suseela Rajkumar, G., 2003. Application of an alkaline protease in leather processing: An ecofriendly approach. *J. Clean. Prod.* 11, 533–536.
- De Castro, R.J.S., Ohara, A., Nishide, T.G., Bagagli, M.P., Gonçalves Dias, F.F., Sato, H.H., 2015. A versatile system based on substrate formulation using agroindustrial wastes for protease production by *Aspergillus niger* under solid state fermentation. *Biocatal. Agric. Biotechnol.* 4, 678–684.
- De Castro, R.J.S., Sato, H.H., 2015. Enzyme Production by Solid State Fermentation: General Aspects and an Analysis of the Physicochemical Characteristics of Substrates for Agro-industrial Wastes Valorization. *Waste and Biomass Valorization* 6, 1085–1093.
- De Castro, R.J.S., Sato, H.H., 2014. Production and biochemical characterization of protease from *Aspergillus oryzae*: An evaluation of the physical-chemical parameters using agroindustrial wastes as supports. *Biocatal. Agric. Biotechnol.* 3, 20–25.
- De Guardia, A., Mallard, P., Teglia, C., Marin, A., Le Pape, C., Launay, M., Benoist, J.C., Petiot, C., 2010. Comparison of five organic wastes regarding their behaviour during composting: Part 1, biodegradability, stabilization kinetics and temperature rise. *Waste Manag.* 30, 402–414.
- De la Cruz Quiroz, R., Roussos, S., Hernández, D., Rodríguez, R., Castillo, F., Aguilar, C.N., 2015. Challenges and opportunities of the bio-pesticides production by solid-state fermentation: filamentous fungi as a model. *Crit. Rev. Biotechnol.* 35, 326–333.
- Demiral, H., Demiral, İ., 2008. Surface properties of activated carbon prepared from wastes. *Surf. Interface Anal.* 40, 612–615.
- Dhillon, G.S., Brar, S.K., Kaur, S., Verma, M., 2013a. Bioproduction and extraction optimization of citric acid from *Aspergillus niger* by rotating drum type solid-state bioreactor. *Ind. Crops Prod.* 41, 78–84.
- Dhillon, G.S., Kaur, S., Sarma, S.J., Brar, S.K., 2013b. Integrated process for fungal citric acid fermentation using apple processing wastes and sequential extraction of chitosan from waste stream. *Ind. Crops Prod.* 50, 346–351.
- Ding, X., Hua, Y., Chen, Y., Zhang, C., Kong, X., 2015. Heavy metal complexation of thiol-containing peptides from soy glycinin hydrolysates. *Int. J. Mol. Sci.* 16, 8040–8058.

- Do-Myoung, K., Eun, J.C., Ji, W.K., Yong-Woog, L., Hwa-Jee, C., 2014. Production of cellulases by *Penicillium* sp. in a solid-state fermentation of oil palm empty fruit bunch. *African J. Biotechnol.* 13, 145–155.
- Du, C., Lin, S.K.C., Koutinas, A., Wang, R., Dorado, P., Webb, C., 2008. A wheat biorefining strategy based on solid-state fermentation for fermentative production of succinic acid. *Bioresour. Technol.* 99, 8310–8315.
- Eijsink, V.G.H., Bjørk, A., Gåseidnes, S., Sirevåg, R., Synstad, B., Burg, B., Van Den, Vriend, G., 2004. Rational engineering of enzyme stability. *J. Biotechnol.* 113, 105–120.
- El-Bakry, M., Abraham, J., Cerda, a., Barrena, R., Ponsá, S., Gea, T., Sánchez, a., 2015. From Wastes to High Value Added Products: Novel Aspects of SSF in the Production of Enzymes. *Crit. Rev. Environ. Sci. Technol.* 45, 1999–2042.
- El-Bakry, M., Gea, T., Sánchez, A., 2016. Inoculation effect of thermophilic microorganisms on protease production through solid-state fermentation under non-sterile conditions at lab and bench scale (SSF). *Bioprocess Biosyst. Eng.* 39, 585–592.
- El-Gindy, A.A., Saad, R.R., Fawzi, E.M., 2015. Purification of  $\beta$ -xylosidase from *Aspergillus tamarii* using ground oats and a possible application on the fermented hydrolysate by *Pichia stipitis*. *Ann. Microbiol.* 65, 965–974.
- Ellaiyah, P., Srinivasulu, B., Adinarayana, K., 2002. A review on microbial alkaline proteases. *J. Sci. Ind. Res. (India)*. 61, 690–704.
- Elmekawy, A., Diels, L., De Wever, H., Pant, D., 2013. Valorization of cereal based biorefinery byproducts: Reality and expectations. *Environ. Sci. Technol.* 47, 9014–9027.
- Embaby, A.M., Masoud, A. a, Marey, H.S., Shaban, N.Z., Ghonaim, T.M., 2014. Raw agro-industrial orange peel waste as a low cost effective inducer for alkaline polygalacturonase production from *Bacillus licheniformis* SHG10. *Springerplus* 3, 327–340.
- Esakkiraj, P., Usha, R., Palavesam, A., Immanuel, G., 2012. Solid-state production of esterase using fish processing wastes by *Bacillus altitudinis* AP-MSU. *Food Bioprod. Process.* 90, 370–376.
- Ezejiolor, T.I.N., Duru, C.I., Asagbra, A.E., Ezejiolor, A.N., Orisakwe, O.E., Afonne, J.O., Obi, E., 2012. Waste to wealth: Production of oxytetracycline using *Streptomyces* species from household kitchen wastes of agricultural produce. *African J. Biotechnol.* 11, 10115–10124.
- Gabelle, J.C., Jourdir, E., Licht, R.B., Ben Chaabane, F., Henaut, I., Morchain, J., Augier, F., 2012. Impact of rheology on the mass transfer coefficient during the growth phase of *Trichoderma reesei* in stirred bioreactors. *Chem. Eng. Sci.* 75, 408–417.
- Garcia-Carreno, F.L., 1992. Protease inhibition in theory and practice. *Biotechnol. Educ.* 3, 145–150.
- Garcia-Galan, C., Berenguer-Murcia, Á., Fernandez-Lafuente, R., Rodrigues, R.C., 2011. Potential of different enzyme immobilization strategies to improve enzyme performance. *Adv. Synth. Catal.* 353, 2885–2904.
- Gasparotto, J.M., Werle, L.B., Foletto, E.L., Kuhn, R.C., Jahn, S.L., Mazutti, M.A., 2015. Production of Cellulolytic Enzymes and Application of Crude Enzymatic Extract for Saccharification of Lignocellulosic Biomass. *Appl. Biochem. Biotechnol.* 175, 560–572.
- Gea, T., Barrena, R., Artola, A., Sánchez, A., 2004. Monitoring the biological activity of the composting process: Oxygen uptake rate (OUR), respirometric index (RI), and respiratory quotient (RQ). *Biotechnol. Bioeng.* 88, 520–527.

## References

- Ghazi, I., Fernandez-Arrojo, L., Gomez De Segura, A., Alcalde, M., Plou, F.J., Ballesteros, A., 2006. Beet sugar syrup and molasses as low-cost feedstock for the enzymatic production of fructo-oligosaccharides. *J. Agric. Food Chem.* 54, 2964–2968.
- Gilmour, S.G., 2006. Response surface designs for experiments in bioprocessing. *Biometrics* 62, 323–331.
- Giuntini, E., Bazzicalupo, M., Castaldini, M., Fabiani, A., Miclaus, N., Piccolo, R., Ranalli, G., Santomassimo, F., Zanobini, S., Mengoni, A., 2006. Genetic diversity of dinitrogen-fixing bacterial communities in soil amended with olive husks. *Ann. Microbiol.* 56, 83–88.
- Gnanaprakash, G., Philip, J., Jayakumar, T., Raj, B., 2007. Effect of digestion time and alkali addition rate on physical properties of magnetite nanoparticles. *J. Phys. Chem. B* 111, 7978–7986.
- Gohel, V., Vyas, P., Chhatpar, H.S., Zitouni, M., Fortin, M., Thibeault, J.-S., Brzezinski, R., Muzzarelli, R.A., Larionova, N.I., Zubaerova, D.K., Guranda, D.T., Pechyonkin, M.A., Balabushevich, N.G., Prochazkova, S., Vårum, K.M., Ostgaard, K., Wischke, C., Borchert, H.H., 2006. Quantitative determination of chitosans by ninhydrin. *Carbohydr. Polym.* 38, 255–257.
- Gole, A., Dash, C., Ramakrishnan, V., Sainkar, S.R., Mandale, A.B., Rao, M., Sastry, M., 2001. Pepsin-gold colloid conjugates: Preparation, characterization, and enzymatic activity. *Langmuir* 17, 1674–1679.
- Govumoni, S.P., Gentela, J., Koti, S., Haragopal, V., Venkateshwar, S., Rao, L.V., 2015. Original Research Article Extracellular Lignocellulolytic Enzymes by *Phanerochaete chrysosporium* ( MTCC 787 ) Under Solid-State Fermentation of Agro Wastes. *Int. J. Curr. Microbiol. Appl. Sci.* 4, 700–710.
- Graminha, E.B.N., Gonçalves, A.Z.L., Pirota, R.D.P.B., Balsalobre, M.A.A., Da Silva, R., Gomes, E., 2008. Enzyme production by solid-state fermentation: Application to animal nutrition. *Anim. Feed Sci. Technol.* 144, 1–22.
- Gratisito, M.K.B., Panyathanmaporn, T., Chumnanklang, R.A., Sirinuntawittaya, N., Dutta, A., 2008. Production of activated carbon from coconut shell: Optimization using response surface methodology. *Bioresour. Technol.* 99, 4887–4895.
- Gupta, R., Beg, Q., Lorenz, P., 2002. Bacterial alkaline proteases: Molecular approaches and industrial applications. *Appl. Microbiol. Biotechnol.* 59, 15–32.
- Hai-Yan Sun, Li, J., Zhao, P., Peng, M., 2011. Banana peel: A novel substrate for cellulase production under solid-state fermentation. *African J. Biotechnol.* 10, 17887–17890.
- Herculano, P.N., Moreira, K.A., Bezerra, R.P., Porto, T.S., de Souza-Motta, C.M., Porto, A.L.F., 2016. Potential application of waste from castor bean (*Ricinus communis* L.) for production for xylanase of interest in the industry. *3 Biotech* 6, 144–154.
- Hölker, U., Höfer, M., Lenz, J., 2004. Biotechnological advantages of laboratory-scale solid-state fermentation with fungi. *Appl. Microbiol. Biotechnol.* 64, 175–186.
- Hölker, U., Lenz, J., 2005. Solid-state fermentation - Are there any biotechnological advantages? *Curr. Opin. Microbiol.* 8, 301–306.
- Hongzhang, C., Hongqiang, L., Liying, L., 2011. The inhomogeneity of corn stover and its effects on bioconversion. *Biomass and Bioenergy* 35, 1940–1945.
- Hu, T.G., Cheng, J.H., Zhang, B.B., Lou, W.Y., Zong, M.H., 2015. Immobilization of alkaline protease on amino-functionalized magnetic nanoparticles and its efficient use for preparation of oat polypeptides. *Ind. Eng. Chem. Res.* 54, 4689–4698.
- Hu, Y., Ju, L.K., 2001. Purification of lactonic sophorolipids by crystallization. *J. Biotechnol.* 87, 263–272.

- Huang, Q., Peng, Y., Li, X., Wang, H., Zhang, Y., 2003. Purification and characterization of an extracellular alkaline serine protease with dehairing function from *Bacillus pumilus*. *Curr. Microbiol.* 46, 169–173.
- Iborra, F.J., Kimura, H., Cook, P.R., Hermann, G., Shaw, J., Yaffe, M., Otsuga, et. al., 2004. The functional organization of mitochondrial genomes in human cells. *BMC Biol.* 2, 1-14.
- Iannotti, D.A., Pang, T., Toth, B.L., Elwell, D.L., Keener, H.M., Hoitink, H.A.J., 1993. A Quantitative Respirometric Method for Monitoring Compost Stability. *Compost Sci. Util.* 1, 52–65.
- Ito, M., Yamada, T., Makimura, K., Ishihara, Y., Satoh, K., 2010. Intracellular Serine Protease from *Candida glabrata* Species Detected and Analyzed by Zymography. *Med. Mycol.* 1, 29–35.
- Jacobson, J.W., Glick, L.J., Madello, K.L., 1987. Composition for cleaning drain clogged with deposits containing hair. EP 0125801 B1.
- Janveja, C., Rana, S.S., Soni, S.K., 2014. Optimization of valorization of biodegradable kitchen waste biomass for production of fungal cellulase system by statistical modeling. *Waste and Biomass Valorization* 5, 807–821.
- Jayathilakan, K., Sultana, K., Radhakrishna, K., Bawa, A.S., 2012. Utilization of byproducts and waste materials from meat, poultry and fish processing industries: A review. *J. Food Sci. Technol.* 49, 278–293.
- Jia, H., Zhu, G., Wang, P., 2003. Catalytic Behaviors of Enzymes Attached to Nanoparticles: The Effect of Particle Mobility. *Biotechnol. Bioeng.* 84, 406–414.
- Jin, X., Li, J.F., Huang, P.Y., Dong, X.Y., Guo, L.L., Yang, L., Cao, Y.C., Wei, F., Zhao, Y. Di, Chen, H., 2010. Immobilized protease on the magnetic nanoparticles used for the hydrolysis of rapeseed meals. *J. Magn. Magn. Mater.* 322, 2031–2037.
- Jodayree, S., 2014. Antioxidant activity of oat bran hydrolyzed proteins in vitro and in vivo. Carleton University, Ottawa, Ontario.
- Jooste, T., García-Aparicio, M.P., Brienza, M., Van Zyl, W.H., Görgens, J.F., 2013. Enzymatic hydrolysis of spent coffee ground. *Appl. Biochem. Biotechnol.* 169, 2248–2262.
- Jørgensen, H., Sanadi, A.R., Felby, C., Lange, N.E.K., Fischer, M., Ernst, S., 2010. Production of ethanol and feed by high dry matter hydrolysis and fermentation of Palm kernel press cake. *Appl. Biochem. Biotechnol.* 161, 318–332.
- Kachrimanidou, V., Kopsahelis, N., Vlysidis, A., Papanikolaou, S., Kookos, I.K., Monje Martinez, B., Escrig Rondan, M.C., Koutinas, A.A., 2016. Downstream separation of poly(hydroxyalkanoates) using crude enzyme consortia produced via solid state fermentation integrated in a biorefinery concept. *Food Bioprod. Process.* 100, 323–334.
- Kanagaraj, J., Velappan, K.C., Chandra Babu, N.K., Sadulla, S., 2006. Solid wastes generation in the leather industry and its utilization for cleaner environment - A review. *J. Sci. Ind. Res. (India)*. 65, 541–548.
- Kandra, P., Challa, M.M., Kalangi Padma Jyothi, H., 2012. Efficient use of shrimp waste: Present and future trends. *Appl. Microbiol. Biotechnol.* 93, 17–29.
- Kanwar, S., Kumar, G., Sahgal, M., Singh, A., 2012. Ethanol Production Through *Saccharomyces* Based Fermentation Using Apple Pomace Amended with Molasses. *Sugar Tech* 14, 304–311.
- Khandelwal, H.B., More, S. V, Kalal, K.M., Laxman, R.S., 2014. Eco-friendly enzymatic dehairing of skins and hides by *C. breffeldianus* protease. *Clean Technol. Environ. Policy* 17, 393–405.

## References

- Kim, S.K., Mendis, E., 2006. Bioactive compounds from marine processing byproducts - A review. *Food Res. Int.* 39, 383–393.
- Kobayashi, M., Tomita, S., Sawada, K., Shiba, K., Yanagi, H., Yamashita, I., Uraoka, Y., 2012. Chiral meta-molecules consisting of gold nanoparticles and genetically engineered tobacco mosaic virus. *Opt. Express* 20, 1-8.
- Koller, M., Mahl, D., Greulich, C., Meyer-Zaika, W., Epple, M., Köller, M., Epple, M., 2010. Gold nanoparticles: dispersibility in biological media and cell-biological effect. *J. Mater. Chem.* 20, 6176–6181.
- Krajewska, B., 2004. Application of chitin- and chitosan-based materials for enzyme immobilizations : a review. *Enzyme Microb. Technol.* 35, 126–139.
- Kriaa, M., Kammoun, R., 2016. Producing *Aspergillus tubingensis* CTM507 Glucose oxidase by Solid state fermentation versus submerged fermentation: Process optimization and enzyme stability by an intermediary metabolite in relation with diauxic growth. *J. Chem. Technol. Biotechnol.* 91, 1540–1550.
- Kumar, A., Dutt, D., Gautam, A., 2016. Production of crude enzyme from *Aspergillus nidulans* AKB-25 using black gram residue as the substrate and its industrial applications. *J. Genet. Eng. Biotechnol.* 14, 107–118.
- Kumar, A.G., Swarnalatha, S., Kamatchi, P., Sekaran, G., 2009. Immobilization of high catalytic acid protease on functionalized mesoporous activated carbon particles. *Biochem. Eng. J.* 43, 185–190.
- Kumar, C.G., Tiwari, M.P., Jany, K.D., 1999. Novel alkaline serine proteases from alkalophilic *Bacillus* spp.: Purification and some properties. *Process Biochem.* 34, 441–449.
- Kumar, D., Lavanya, S., Priya, P., 2012. Production of Feather Protein Concentrate from Feathers by In vitro Enzymatic Treatment, its Biochemical Characterization and Antioxidant Nature. *Middle-East J. Sci. Res.* 11, 881–886.
- Kumar, V., Singh, D., Sangwan, P., Gill, P.K., 2014. Global market scenario of industrial enzymes. *Ind. Enzym. Trends, Scope Relev.* 173 – 196.
- Ladole, M.R., Muley, A.B., Patil, I.D., Talib, M.I., Parate, R., 2014. Immobilization of tropizyme-P on amino-functionalized magnetic nanoparticles for fruit juice clarification 5, 838–845.
- Laemmli, U. K. 1970. Cleavage of structural proteins during the assembly of the head of bacteriophage T4. *Nature* 227, 680-685.
- Lamas, E.M., Barros, R.M., Balcao, V.M., Malcata, F.X., 2001. Hydrolysis of whey proteins by proteases extracted from *Cynara cardunculus* and immobilized onto highly activated supports. *Enzyme Microb. Technol.* 28, 642–652.
- Lio, J., Wang, T., 2012. Solid-state fermentation of soybean and corn processing coproducts for potential feed improvement. *J. Agric. Food Chem.* 60, 7702–7709.
- Liu, D., Zhang, R., Yang, X., Wu, H., Xu, D., Tang, Z., Shen, Q., 2011. Thermostable cellulase production of *Aspergillus fumigatus* Z5 under solid-state fermentation and its application in degradation of agricultural wastes. *Int. Biodeterior. Biodegrad.* 65, 717–725.
- Liu, H., Chen, D., Zhang, R., Hang, X., Li, R., Shen, Q., 2016. Amino Acids Hydrolyzed from Animal Carcasses Are a Good Additive for the Production of Bio-organic Fertilizer. *Front Microbiol* 7, 1–10.
- Lopez, J.A., González, F., Bonilla, F.A., Zambrano, G., Gómez, M.E., 2010. Synthesis and characterization of Fe<sub>3</sub>O<sub>4</sub> magnetic nanofluid. *Rev. Latinoam. Metal. y Mater.* 30, 60–66.

- López, J.A., Lázaro, C.D.C., Castilho, L.D.R., Freire, D.M.G., Castro, A.M.H. De, 2013. Characterization of multienzyme solutions produced by solid-state fermentation of babassu cake, for use in cold hydrolysis of raw biomass. *Biochem. Eng. J.* 77, 231–239.
- López-Gallego, F., Betancor, L., Hidalgo, A., Alonso, N., Fernández-Lafuente, R., Guisán, J.M., 2005. Co-aggregation of enzymes and polyethyleneimine: A simple method to prepare stable and immobilized derivatives of glutaryl acylase. *Biomacromolecules* 6, 1839–1842.
- López-Pérez, M., Viniestra-González, G., 2016. Production of protein and metabolites by yeast grown in solid state fermentation: Present status and perspectives. *J. Chem. Technol. Biotechnol.* 91, 1224–1231.
- Lowry, O.H., Rosebrough, N.J., Farr, A.L., Randall, R.J., 1951. Protein measurement with the Folin phenol reagent. *J. Biol. Chem.* 193, 265–275.
- Lu, A.H., Salabas, E.L., Schüth, F., 2007. Magnetic nanoparticles: Synthesis, protection, functionalization, and application. *Angew. Chemie - Int. Ed.* 46, 1222–1244.
- Madhavi, J., Srilakshmi, J., Raghavendra Rao, M. V., Sambasiva Rao, K.R.S., 2011. Efficient leather dehairing by bacterial thermostable protease. *Int. J. Bio-Science Bio-Technology* 3, 11–26.
- Mahanta, N., Gupta, A., Khare, S.K., 2008. Production of protease and lipase by solvent tolerant *Pseudomonas aeruginosa* PseA in solid-state fermentation using *Jatropha curcas* seed cake as substrate. *Bioresour. Technol.* 99, 1729–1735.
- Mandalari, G., Bisignano, G., Lo Curto, R.B., Waldron, K.W., Faulds, C.B., 2008. Production of feruloyl esterases and xylanases by *Talaromyces stipitatus* and *Humicola grisea* var. thermoidea on industrial food processing by-products. *Bioresour. Technol.* 99, 5130–5133.
- Mansour, A.A., Arnaud, T., Lu-Chau, T.A., Fdz-Polanco, M., Moreira, M.T., Rivero, J.A.C., 2016. Review of solid state fermentation for lignocellulolytic enzyme production: challenges for environmental applications. *Rev. Environ. Sci. Biotechnol.* 15, 31–46.
- Mantzouridou, F.T., Paraskevopoulou, A., Lalou, S., 2015. Yeast flavour production by solid state fermentation of orange peel waste. *Biochem. Eng. J.* 101, 1–8.
- Martínez-Morales, F., Bertrand, B., Pasi3n Nava, A.A., Tinoco, R., Acosta-Urdapilleta, L., Trejo-Hernández, M.R., 2015. Production, purification and biochemical characterization of two laccase isoforms produced by *Trametes versicolor* grown on oak sawdust. *Biotechnol. Lett.* 37, 391–396.
- Martins, S., Mussatto, S.I., Martínez-Avila, G., Montañez-Saenz, J., Aguilar, C.N., Teixeira, J.A., 2011. Bioactive phenolic compounds: Production and extraction by solid-state fermentation. A review. *Biotechnol. Adv.* 29, 365–373.
- Matsakas, L., Christakopoulos, P., 2015. Ethanol production from enzymatically treated dried food waste using enzymes produced on-site. *Sustain.* 7, 1446–1458.
- Matsakas, L., Kekos, D., Loizidou, M., Christakopoulos, P., 2014. Utilization of household food waste for the production of ethanol at high dry material content. *Biotechnol. Biofuels* 7, 4–13.
- Mazutti, M., Bender, J.P., Treichel, H., Luccio, M. Di, 2006. Optimization of inulinase production by solid-state fermentation using sugarcane bagasse as substrate. *Enzyme Microb. Technol.* 39, 56–59.
- Mehboob, N., Asad, M.J., Imran, M., Gulfraz, M., Wattoo, F.H., Hadri, S.H., Asghar, M., 2011. Production of lignin peroxidase by *Ganoderma leucidum* using solid state fermentation. *African J. Biotechnol.* 10, 9880–9887.

## References

- Melikoglu, M., Lin, C.S.K., Webb, C., 2015. Solid state fermentation of waste bread pieces by *Aspergillus awamori*: Analysing the effects of airflow rate on enzyme production in packed bed bioreactors. *Food Bioprod. Process.* 95, 63–75.
- Melikoglu, M., Lin, C.S.K., Webb, C., 2013. Stepwise optimisation of enzyme production in solid state fermentation of waste bread pieces. *Food Bioprod. Process.* 91, 638–646.
- Mohamad, N.R., Marzuki, N.H.C., Buang, N.A., Huyop, F., Wahab, R.A., 2015. An overview of technologies for immobilization of enzymes and surface analysis techniques for immobilized enzymes. *Biotechnol. Biotechnol. Equip.* 29, 205–220.
- Motta, F.L., Santana, M.H. A., 2014. Solid-state fermentation for humic acids production by a *Trichoderma reesei* strain using an oil palm empty fruit bunch as the substrate. *Appl. Biochem. Biotechnol.* 172, 2205–2217.
- Mtui, G.Y.S., 2009. Recent advances in pretreatment of lignocellulosic wastes and production of value added products. *African J. Biotechnol.* 8, 1398–1415.
- Mussatto, S.I., Ballesteros, L.F., Martins, S., Teixeira, J.A., 2012. Use of Agro-Industrial Wastes in Solid-State Fermentation Processes, in: *Industrial Waste*. pp. 121–141.
- Myers, R.H., Montgomery, D.C., Vining, G.G., Borrer, C.M., Kowalski, S.M., 2004. Response Surface Methodology: A Retrospective and Literature Survey. *J. Qual. Technol.* 36, 53–78.
- Nakiboğlu, N., Toscali, D., Yaşa, I., 2001. Silver recovery from waste photographic films by an enzymatic method. *Turkish J. Chem.* 25, 349–353.
- Narra, M., Balasubramanian, V., 2015. Utilization of solid and liquid waste generated during ethanol fermentation process for production of gaseous fuel through anaerobic digestion - A zero waste approach. *Bioresour. Technol.* 180, 376–380.
- Nguyen, M.V., Lee, B.K., 2015. Removal of dimethyl sulfide from aqueous solution using cost-effective modified chicken manure biochar produced from slow pyrolysis. *Sustainability* 7, 15057–15072.
- Nidheesh, T., Pal, G.K., Suresh, P. V., 2015. Chitooligomers preparation by chitosanase produced under solid state fermentation using shrimp by-products as substrate. *Carbohydr. Polym.* 121, 1–9.
- Nigam, S., Barick, K.C., Bahadur, D., 2011. Development of citrate-stabilized Fe<sub>3</sub>O<sub>4</sub> nanoparticles: Conjugation and release of doxorubicin for therapeutic applications. *J. Magn. Magn. Mater.* 323, 237–243.
- Novelli, P.K., Barros, M.M., Fleuri, L.F., 2016. Novel inexpensive fungi proteases: Production by solid state fermentation and characterization. *Food Chem.* 198, 119–124.
- Ohkouchi, Y., Inoue, Y., 2007. Impact of chemical components of organic wastes on l(+)-lactic acid production. *Bioresour. Technol.* 98, 546–553.
- Onyuka, A., 2010. Sustainable management of tannery hair waste through composting. The University of Northampton.
- Ortiz, G.E., Guitart, M.E., Cavalitto, S.F., Albertó, E.O., Fernández-Lahore, M., Blasco, M., 2015. Characterization, optimization, and scale-up of cellulases production by *Trichoderma reesei* cbs 836.91 in solid-state fermentation using agro-industrial products. *Bioprocess Biosyst. Eng.* 38, 2117–2128.
- Orzua, M.C., Mussatto, S.I., Contreras-Esquivel, J.C., Rodriguez, R., de la Garza, H., Teixeira, J.A., Aguilar, C.N., 2009. Exploitation of agro industrial wastes as immobilization carrier for solid-state fermentation. *Ind. Crops Prod.* 30, 24–27.

- Özdemir, S., Matpan, F., Okumus, V., Dündar, A., Ulutas, M.S., Kumru, M., 2012. Isolation of a thermophilic *Anoxybacillus flavithermus* sp. nov. and production of thermostable  $\alpha$ -amylase under solid-state fermentation (SSF). *Ann. Microbiol.* 62, 1367–1375.
- Panda, S.K., Mishra, S.S., Kayitesi, E., Ray, R.C., 2016. Microbial-processing of fruit and vegetable wastes for production of vital enzymes and organic acids: Biotechnology and scopes. *Environ. Res.* 146, 161–172.
- Pandey, A., 2003. Solid-state fermentation. *Biochem. Eng. J.* 13, 81–84.
- Pandey, A., Selvakumar, P., Soccol, C.R., Nigam, P., 1999. Solid state fermentation for the production of industrial enzymes. *Curr. Sci.* 77, 149–162.
- Pandey, A., Soccol, C.R., Mitchell, D., 2000. New developments in solid state fermentation: I-bioprocesses and products. *Process Biochem.* 35, 1153–1169.
- Pandey, P., Singh, S.P., Arya, S.K., Gupta, V., Datta, M., Singh, S., Malhotra, B.D., 2007. Application of thiolated gold nanoparticles for the enhancement of glucose oxidase activity. *Langmuir* 23, 3333–3337.
- Pandi, A., Ramalingam, S., Rao, R., 2016. Inexpensive  $\alpha$ -amylase production and application for fiber splitting in leather processing. *RSC Adv.* 6, 33170–33176.
- Pandya, J.J., Gupte, A., 2012. Production of xylanase under solid-state fermentation by *Aspergillus tubingensis* JP-1 and its application. *Bioprocess Biosyst. Eng.* 35, 769–779.
- Pathak, P., Bhardwaj, N.K., Singh, A.K., 2014. Production of crude cellulase and xylanase from *Trichoderma harzianum* PPDDN10 NFCCI-2925 and its application in photocopier waste paper recycling. *Appl. Biochem. Biotechnol.* 172, 3776–3797.
- Paul, T., Das, A., Mandal, A., Jana, A., Maity, C., Adak, A., Halder, S.K., DasMohapatra, P.K., Pati, B.R., Mondal, K.C., 2014. Effective dehairing properties of keratinase from *Paenibacillus woosongensis* TKB2 obtained under solid state fermentation. *Waste and Biomass Valorization* 5, 97–107.
- Pavia, D.L., Lampman, G.M., Kriz, G.S., Vyvyan, J.A. (Eds.), 2015. Introduction to spectroscopy, 5th ed. Cengage Learning, United State of America.
- Peternele, W.S., Monge Fuentes, V., Fascineli, M.L., Rodrigues Da Silva, J., Silva, R.C., Lucci, C.M., Bentes De Azevedo, R., 2014. Experimental investigation of the coprecipitation method: An approach to obtain magnetite and maghemite nanoparticles with improved properties. *J. Nanomater.* 1–11.
- Phadtare, S., Vinod, V.P., Mukhopadhyay, K., Kumar, A., Rao, M., Chaudhari, R. V., Sastry, M., 2004. Immobilization and Biocatalytic Activity of Fungal Protease on Gold Nanoparticle-Loaded Zeolite Microspheres. *Biotechnol. Bioeng.* 85, 629–637.
- Pirota, R.D.P.B., Delabona, P.S., Farinas, C.S., 2014. Simplification of the Biomass to Ethanol Conversion Process by Using the Whole Medium of Filamentous Fungi Cultivated Under Solid-State Fermentation. *Bioenergy Res.* 7, 744–752.
- Pirota, R.D.P.B., Miotto, L.S., Delabona, P.S., Farinas, C.S., 2013. Improving the extraction conditions of endoglucanase produced by *Aspergillus niger* under solid-state fermentation. *Brazilian J. Chem. Eng.* 30, 117–123.
- Pleissner, D., Lam, W.C., Han, W., Lau, K.Y., Cheung, L.C., Lee, M.W., Lei, H.M., Lo, K.Y., Ng, W.Y., Sun, Z., Melikoglu, M., Lin, C.S.K., 2014. Fermentative polyhydroxybutyrate production from a novel feedstock derived from bakery waste. *Biomed Res. Int.* 2014, 1–8.



## References

- Poletto, P., Borsóí, C., Zeni, M., Moura, M., 2015. Downstream processing of pectinase produced by *Aspergillus niger* in solid state cultivation and its application to fruit juices clarification. *Food Sci. Technol.* 35, 391–397.
- Ponsá, S., Gea, T., Sánchez, A., 2010. Different indices to express biodegradability in organic solid wastes. *J. Environ. Qual.* 39, 706–712.
- Pottier, A., Cassaignon, S., Chanéac, C., Villain, F., Tronc, E., Jolivet, J.-P., 2003. Size tailoring of TiO<sub>2</sub> anatase nanoparticles in aqueous medium and synthesis of nanocomposites. Characterization by Raman spectroscopy. *J. Mater. Chem.* 13, 877–882.
- Prajapati, V.S., Trivedi, U.B., Patel, K.C., 2015. A statistical approach for the production of thermostable and alkophilic alpha-amylase from *Bacillus amyloliquefaciens* KCP2 under solid-state fermentation. *3 Biotech* 5, 211–220.
- Prakasham, R.S., Rao, C.S., Sarma, P.N., 2006. Green gram husk-an inexpensive substrate for alkaline protease production by *Bacillus* sp. in solid-state fermentation. *Bioresour. Technol.* 97, 1449–1454.
- Prasertkittikul, S., Chisti, Y., Hansupalak, N., 2013. Deproteinization of natural rubber using protease immobilized on epichlorohydrin cross-linked chitosan beads. *Ind. Eng. Chem. Res.* 52, 11723–11731.
- Puyuelo, B., Gea, T., Sánchez, A., 2010. A new control strategy for the composting process based on the oxygen uptake rate. *Chem. Eng. J.* 165, 161–169.
- Quanguo, H., Lei, Z., Wei, W., Rong, H., Jingke, H., 2010. Preparation and Magnetic Comparison of Silane-Functionalized Magnetite Nanoparticles. *Sensors Mater.* 22, 285–295.
- Radha, K. V., Arun, C., 2010. Recycling of exposed photographic X-ray films and recovery of silver using Bromelain. *WIT Trans. Ecol. Environ.* 142, 421–430.
- Raghavarao, K.S.M., Ranganathan, T., Karanth, N., 2003. Some engineering aspects of solid-state fermentation. *Biochem. Eng. J.* 13, 127–135.
- Raghuwanshi, S., Deswal, D., Karp, M., Kuhad, R.C., 2014. Bioprocessing of enhanced cellulase production from a mutant of *Trichoderma asperellum* RCK2011 and its application in hydrolysis of cellulose. *Fuel* 124, 183–189.
- Rahardjo, Y.S.P., Korona, D., Haemers, S., Weber, F.J., Tramper, J., Rinzema, A., 2004. Limitations of membrane cultures as a model solid-state fermentation system. *Lett. Appl. Microbiol.* 39, 504–508.
- Ramos Guivar, J.A., Sanches, E.A., Magon, C.J., Ramos Fernandes, E.G., 2015. Preparation and characterization of cetyltrimethylammonium bromide (CTAB)-stabilized Fe<sub>3</sub>O<sub>4</sub> nanoparticles for electrochemistry detection of citric acid. *J. Electroanal. Chem.* 755, 158–166.
- Rao, M.B., Tanksale, A.M., Ghatge, M.S., Deshpande, V. V, 1998. Molecular and biotechnological aspects of microbial proteases. *Microbiol. Mol. Biol. Rev.* 62, 597–635.
- Rathna, G.S., Saranya, R., Kalaiselvam, M., 2014. Original Research Article Bioethanol from sawdust using cellulase hydrolysis of *Aspergillus ochraceus* and fermentation by *Saccharomyces cerevisiae*. *Int. J. Curr. Microbiol. Appl. Sci.* 3, 733–742.
- Ravindran, B., Ganesh Kumar, a., Aruna Bhavani, P.S., Sekaran, G., 2011. Solid-state fermentation for the production of alkaline protease by *Bacillus cereus* 1173900 using proteinaceous tannery solid waste. *Curr. Sci.* 100, 726–730.
- Reckinger, N., Seim, J., 2016. Sources and Opportunities in Organic Waste Transformation.

- Ribeiro, R.R., Vitolo, M., 2005. Anion exchange resin as support for invertase immobilization. *Rev. Ciencias Farm. Basica e Apl.* 26, 175–179.
- Rocha, M.V.P., de Matos, L.J.B.L., Lima, L.P. De, Figueiredo, P.M.D.S., Lucena, I.L., Fernandes, F.A.N., Gonçalves, L.R.B., 2014. Ultrasound-assisted production of biodiesel and ethanol from spent coffee grounds. *Bioresour. Technol.* 167, 343–348.
- Rodríguez-Fernández, D.E., Rodríguez-León, J.A., de Carvalho, J.C., Thomaz-Soccol, V., Parada, J.L., Soccol, C.R., 2010. Recovery of phytase produced by solid-state fermentation on citrus peel. *Brazilian Arch. Biol. Technol.* 53, 1487–1496.
- S, S.K., Vinay, D.R., Saviraj, A.S., Naik, P.K., 2015. Flexural Behaviour of Coconut Shell / Epoxy Composites Subjected to Accelerated Ageing. *Am. J. Mater. Sci.* 5, 126–132.
- Salariato, D., Diorio, L.A., Mouso, N., Forchiassin, F., 2010. Extraction and characterization of polygalacturonase of fomes sclerodermeus produced by solid-state fermentation. *Rev. Argent. Microbiol.* 42, 57–62.
- Salihu, A., Sallau, A.B., Adamu, A., Kudu, F.A., Tajo, M.M., Bala, T.F., Yashim, W.D., 2014. Utilization of Groundnut Husk as a Solid Substrate for Cellulase Production by *Aspergillus niger* Using Response Surface Methodology. *Waste and Biomass Valorization* 5, 585–593.
- Sánchez, A., Artola, A., Font, X., Gea, T., Barrena, R., Gabriel, D., Sánchez-Monedero, M.Á., Roig, A., Cayuela, M.L., Mondini, C., 2015. Greenhouse gas emissions from organic waste composting. *Environ. Chem. Lett.* 13, 223–238.
- Sánchez, A., del Río, J.L., Valero, F., Lafuente, J., Faus, I., Solà, C., 2000. Continuous enantioselective esterification of trans-2-phenyl-1-cyclohexanol using a new *Candida rugosa* lipase in a packed bed bioreactor. *J. Biotechnol.* 84, 1–12.
- Sandhu, S.K., Oberoi, H.S., Babbar, N., Miglani, K., Chadha, B.S., Nanda, D.K., 2013. Two-Stage Statistical Medium Optimization for Augmented Cellulase Production via Solid-State Fermentation by Newly Isolated *Aspergillus niger* HN - 1 and Application of Crude Cellulase Consortium in Hydrolysis of Rice Straw. *J. Agric. Food Chem.* 61, 12653–12661.
- Santis-Navarro, A., Gea, T., Barrena, R., Sánchez, A., 2011. Production of lipases by solid state fermentation using vegetable oil-refining wastes. *Bioresour. Technol.* 102, 10080–10084.
- Sapuan, S.M., Harimi, M., Maleque, M.A., 2003. Mechanical Properties of Epoxy / Coconut Shell Filler Particle Composites. *Arab. J. Sci. Eng.* 28, 171–181.
- Saqib, A.A.N., Farooq, A., Iqbal, M., Hassan, J.U., Hayat, U., Baig, S., 2012. A thermostable crude endoglucanase produced by *Aspergillus fumigatus* in a novel solid state fermentation process using isolated free water. *Enzyme Res.* 2012, 1–6.
- Saratale, G.D., Kshirsagar, S.D., Sampange, V.T., Saratale, R.G., Oh, S.E., Govindwar, S.P., Oh, M.K., 2014. Cellulolytic Enzymes Production by Utilizing Agricultural Wastes Under Solid State Fermentation and its Application for Biohydrogen Production. *Appl. Biochem. Biotechnol.* 174, 2801–2817.
- Saravanan, P., Shiny Renitha, T., Gowthaman, M.K., Kamini, N.R., 2014. Understanding the chemical free enzyme based cleaner unhairing process in leather manufacturing. *J. Clean. Prod.* 79, 258–264.
- Sathiyarayanan, G., Kiran, G.S., Selvin, J., Saibaba, G., 2013. Optimization of polyhydroxybutyrate production by marine *Bacillus megaterium* MSBN04 under solid state culture. *Int. J. Biol. Macromol.* 60, 253–261.

## References

- Sawant, R., Saraswathy, N., 2014. Protease: an enzyme with multiple industrial applications. *World J. Pharm. Pharm. Sci.* 3, 568–579.
- Saxena, R., Singh, R., 2011. Amylase production by solid-state fermentation of agro-industrial wastes using *Bacillus* sp. *Brazilian J. Microbiol.* 42, 1334–1342.
- Sebola, M.R., Tesfagiorgis, H.B., Muzenda, E., 2015. Methane Production from Anaerobic Co- digestion of Cow Dung , Chicken Manure , Pig Manure and Sewage Waste, in: *Proceedings of the World Congress on Engineering.* pp. 1–7.
- Shankar, S., More, S., Laxman, R.S., 2010. Recovery of Silver from Waste X-Ray Film by Alkaline Protease from *Conidiobolus coronatus*. *Kathmandu Univ. J. Sci. Eng. Technol.* 6, 60–69.
- Sheldon, R.A., 2011. Characteristic features and biotechnological applications of cross-linked enzyme aggregates (CLEAs). *Appl. Microbiol. Biotechnol.* 92, 467–477.
- Sheldon, R.A., Van Pelt, S., 2013. Enzyme immobilisation in biocatalysis: why, what and how. *Chem. Soc. Rev.* 42, 6223–6235.
- Sigma-Aldrich, 2012. Technical bulletin - Bradford Reagent (B6916). Missouri, USA.
- Silveira, E. a., Tardioli, P.W., Farinas, C.S., 2016. Valorization of Palm Oil Industrial Waste as Feedstock for Lipase Production. *Appl. Biochem. Biotechnol.* 179, 558–571.
- Silvestre, M.P.C., Morais, H.A., Silva, V.D.M., Silva, M.R., 2013. Degree of hydrolysis and peptide profile of whey proteins using pancreatin. *Brazilian Soc. Food Nutr.* 38, 278–290.
- Sindhu, R., Pandey, a., Binod, P., 2015. Solid-state Fermentation for the Production of Poly(hydroxyalkanoates). *Chem. Biochem. Eng. Q.* 29, 173–181.
- Singh, A., Kuila, A., Adak, S., Bishai, M., Banerjee, R., 2012. Utilization of Vegetable Wastes for Bioenergy Generation. *Agric. Res.* 1, 213–222.
- Singh, R.K., Zhang, Y.W., Nguyen, N.P.T., Jeya, M., Lee, J.K., 2011. Covalent immobilization of beta-1,4-glucosidase from *Agaricus arvensis* onto functionalized silicon oxide nanoparticles. *Appl. Microbiol. Biotechnol.* 89, 337–344.
- Singh, S., Singh, S., Bali, V., Sharma, L., Mangla, J., 2014. Production of fungal amylases using cheap, readily available agriresidues, for potential application in textile industry. *Biomed Res. Int.* 2014, 1–9.
- Singhania, R.R., Patel, A.K., Soccol, C.R., Pandey, A., 2009. Recent advances in solid-state fermentation. *Biochem. Eng. J.* 44, 13–18.
- Sinha, R., Khare, S.K., 2015. Immobilization of halophilic *Bacillus* sp. EMB9 protease on functionalized silica nanoparticles and application in whey protein hydrolysis. *Bioprocess Biosyst. Eng.* 38, 739–748.
- Sivasubramanian, S., Murali Manohar, B., Rajaram, A., Puvanakrishnan, R., 2008. Ecofriendly lime and sulfide free enzymatic dehairing of skins and hides using a bacterial alkaline protease. *Chemosphere* 70, 1015–1024.
- Song, G.J.-, Feng, X.Y.-, 2011. Review of Enzymatic Sludge Hydrolysis. *J. Bioremediation Biodegrad.* 02, 130.
- Sun, Z., Li, M., Qi, Q., Gao, C., Lin, C.S.K., 2014. Mixed Food Waste as Renewable Feedstock in Succinic Acid Fermentation. *Appl. Biochem. Biotechnol.* 174, 1822–1833.

- Sundararajan, S., Kannan, C.N., Chittibabu, S., 2011. Alkaline protease from *Bacillus cereus* VITSN04: Potential application as a dehairing agent. *J. Biosci. Bioeng.* 111, 128–133.
- Suresh, P. V., Anil Kumar, P.K., 2012. Enhanced degradation of a-chitin materials prepared from shrimp processing byproduct and production of N-acetyl-d-glucosamine by thermoactive chitinases from soil mesophilic fungi. *Biodegradation* 23, 597–607.
- Szabo, O.E., Csiszar, E., Koczka, B., Kiss, K., 2015. Ultrasonically assisted single stage and multiple extraction of enzymes produced by *Aspergillus oryzae* on a lignocellulosic substrate with solid-state fermentation. *Biomass and Bioenergy* 75, 161–169.
- Takami, H., Nakamura, S., Aono, R., Horikoshi, K., 1992. Degradation of human hair by a Thermostable alkaline protease from alkaliphilic *Bacillus* sp. No.AH-101. *Biosci. Biotech. Biochem* 56, 1667–1669.
- Talbert, J.N., Goddard, J.M., 2012. Enzymes on material surfaces. *Colloids Surfaces B Biointerfaces* 93, 8–19.
- Tavano, O.L., 2013. Protein hydrolysis using proteases: An important tool for food biotechnology. *J. Mol. Catal. B Enzym.* 90, 1–11.
- Thomas, L., Larroche, C., Pandey, A., 2013. Current developments in solid-state fermentation. *Biochem. Eng. J.* 81, 146–161.
- The USDA and the US Composting Council, 2001. Test methods for the examination of composting and compost. Edaphos International, Houston.
- Tsegaye, K.N., Gessesse, A., 2014. Amylase production under solid state fermentation by a bacterial isolate W74. *African J. Biotechnol.* 13, 2145–2153.
- Uçkun Kiran, E., Trzcinski, A.P., Liu, Y., 2014. Glucoamylase production from food waste by solid state fermentation and its evaluation in the hydrolysis of domestic food waste. *Biofuel Res. J.* 3, 98–105.
- Ukpai, P.A., Nnabuchi, M.N., 2012. Comparative study of biogas production from cow dung, cow pea and cassava peeling using 45 litres biogas digester. *Adv. Appl. Sci. Res.* 3, 1864–1869.
- Veana, F., Martínez-Hernández, J.L., Aguilar, C.N., Rodríguez-Herrera, R., Michelena, G., 2014. Utilization of molasses and sugar cane bagasse for production of fungal invertase in solid state fermentation using *Aspergillus niger* GH1. *Brazilian J. Microbiol.* 45, 373–377.
- Verma, A., Ansari, M.W., Anwar, M.S., Agrawal, R., Agrawal, S., 2014. Alkaline protease from *Thermoactinomyces* sp. RS1 mitigates industrial pollution. *Protoplasma* 251, 711–718.
- Vigneshwaran, C., Shanmugam, S., Kumar, T.S., 2010. Screening and characterization of keratinase from *Bacillus licheniformis* isolated from namakkal poultry farm. *Researcher* 2, 89–96.
- Vijayaraghavan, P., Lazarus, S., Vincent, S.G.P., 2014. De-hairing protease production by an isolated *Bacillus cereus* strain AT under solid-state fermentation using cow dung: Biosynthesis and properties. *Saudi J. Biol. Sci.* 21, 27–34.
- Viniegra-González, G., Favela-Torres, E., Aguilar, C.N., Romero-Gomez, S.D.J., Díaz-Godínez, G., Augur, C., 2003. Advantages of fungal enzyme production in solid state over liquid fermentation systems. *Biochem. Eng. J.* 13, 157–167.
- Viswanathan, K., Schofield, M.H., Teraoka, I., Gross, R.A., 2012. Surprising metal binding properties of phytochelatin-like peptides prepared by protease-catalysis. *Green Chem.* 14, 1020–1029.

## References

- Wang, L., Yang, S.-T., 2007. Chapter 18 - Solid State Fermentation and Its Applications, in: *Bioprocessing for Value-Added Products from Renewable Resources: New Technologies and Applications*. Elsevier B.V., pp. 465–489.
- Wang, H.Y., Liu, D.M., Liu, Y., Cheng, C.F., Ma, Q.Y., Huang, Q., Zhang, Y.Z., 2007. Screening and mutagenesis of a novel *Bacillus pumilus* strain producing alkaline protease for dehairing. *Let. Appl. Microbiol.* 44, 1–6.
- Wang, S.N., Zhang, C.R., Qi, B.K., Sui, X.N., Jiang, L.Z., Li, Y., Wang, Z.J., Feng, H.X., Wang, R., Zhang, Q.Z., 2014. Immobilized alcalase alkaline protease on the magnetic chitosan nanoparticles used for soy protein isolate hydrolysis. *Eur. Food Res. Technol.* 239, 1051–1059.
- Who/Fao, 2002. Food energy – methods of analysis and conversion factors. Food and agriculture organization of the united nation (FAO). *Food Nutr. Pap.* 93.
- Wiradimadja, R., Rusmana, D., Widjastuti, T., Mushawwir, A., 2014. Chicken Slaughterhouse Waste Utilization ( Chicken Feather Meal Treated ) As a Source of Protein Animal Feed Ingredients in Broiler Chickens. *Lucr. Stiint. - Ser. Zooteh.* 62, 120–124.
- Xu, J., Sun, J., Wang, Y., Sheng, J., Wang, F., Sun, M., 2014. Application of iron magnetic nanoparticles in protein immobilization. *Molecules* 19, 11465–11486.
- Yamaura, M., Camilo, R.L., Sampaio, L.C., Macedo, M.A., Nakamura, M., Toma, H.E., 2004. Preparation and characterization of (3-aminopropyl)triethoxysilane-coated magnetite nanoparticles. *J. Magn. Magn. Mater.* 279, 210–217.
- Yazid, N.A., Barrena, R., Sánchez, A., 2016. Assessment of protease activity in hydrolysed extracts from SSF of hair waste by and indigenous consortium of microorganisms. *Waste Manag.* 49, 420–426.
- Zambare, V.P., Nilegaonkar, S.S., Kanekar, P.P., 2007. Production of an alkaline protease by *Bacillus cereus* MCM B-326 and its application as a dehairing agent. *World J. Microbiol. Biotechnol.* 23, 1569–1574.
- Zhang, D., Neumann, O., Wang, H., Yuwono, V.M., Barhoumi, A., Perham, M., Hartgerink, J.D., Wittung-Stafshede, P., Halas, N.J., 2009. Gold nanoparticles can induce the formation of protein-based aggregates at physiological pH. *Nano Lett.* 9, 666–671.
- Zhang, W., Zou, H., Jiang, L., Yao, J., Liang, J., Wang, Q., 2015. Semi-solid state fermentation of food waste for production of *Bacillus thuringiensis* biopesticide. *Biotechnol. Bioprocess Eng.* 20, 1123–1132.
- Zhang, Z.Y., Jin, B., Kelly, J.M., 2007. Production of lactic acid from renewable materials by *Rhizopus* fungi. *Biochem. Eng. J.* 35, 251–263.
- Zhou, H., Wang, C.Z., Ye, J.Z., Chen, H.X., Tao, R., Zhang, Y.S., 2015. Solid-state fermentation of *Ginkgo biloba* L. residue for optimal production of cellulase, protease and the simultaneous detoxification of *Ginkgo biloba* L. residue using *Candida tropicalis* and *Aspergillus oryzae*. *Eur. Food Res. Technol.* 240, 379–388.
- Zhuang, J., Marchant, M.A., Nokes, S.E., Strobel, H.J., 2007. Economic analysis of cellulase production methods for bio-ethanol. *Appl. Eng. Agric.* 23, 679–687.
- Zidehsaraei, A.Z., Moshkelani, M., Amiri, M.C., 2009. An innovative simultaneous glucoamylase extraction and recovery using colloidal gas aphrons. *Sep. Purif. Technol.* 67, 8–13.
- Zimbardi, A.L.R.L., Sehn, C., Meleiro, L.P., Souza, F.H.M., Masui, D.C., Nozawa, M.S.F., Guimarães, L.H.S., Jorge, J.A., Furiel, R.P.M., 2013. Optimization of  $\beta$ -Glucosidase,  $\beta$ -Xylosidase and Xylanase Production by *Colletotrichum graminicola* under Solid-State Fermentation and Application in Raw Sugarcane Trash Saccharification. *Int. J. Mol. Sci.* 14, 2875–2902.

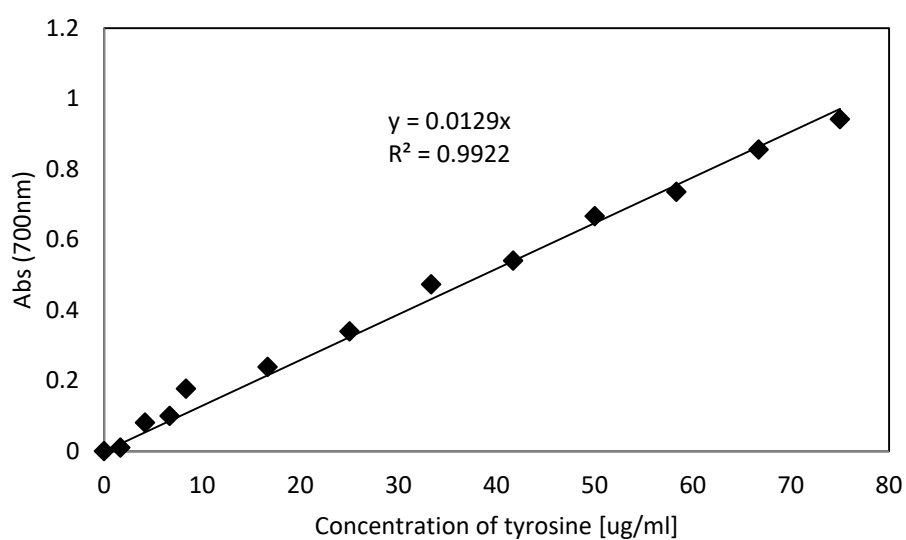
## Annexe 1: Calibration curve



### A.1 Standard curve for protease activity determination

The protease activity obtained from the assay in Section 3.4.2 was correlated with the standard curve. The standard curve was constructed using L-tyrosine (500 µg/ml) as a standard protein.

No	Std (ml)	Buffer (ml)	Concentration [µg/ml]
0	0	5	0
1	0.05	4.95	1.67
2	0.125	4.875	4.17
3	0.2	4.8	6.67
4	0.25	4.75	8.33
5	0.5	4.5	16.67
6	0.75	4.25	25
7	1	4	33.33
8	1.25	3.75	41.67
9	1.5	3.5	50
10	1.75	3.25	58.33
11	2	3	66.7
12	2.25	2.75	75
13	2.5	2.5	83.3



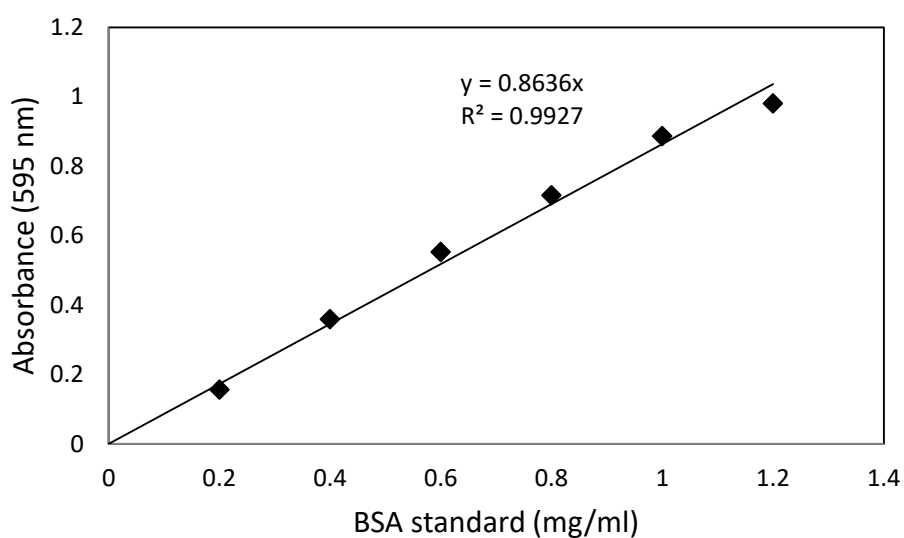
$$\text{Absorbance (700 nm)} = 0.0129 \times \text{concentration } (\mu\text{g/ml})$$



## A.2 Standard curve Bradford method

Total soluble protein content was determined using Bradford method assay in Section 3.4.3 was correlated with the standard curve. The standard curve was constructed using 2 mg/ml bovine serum albumin (BSA) as a standard protein.

No	Std (ml)	dH <sub>2</sub> O (ml)	Protein concentration [mg/ml]
0	0	0.3	0
1	0.03	0.27	0.2
2	0.06	0.24	0.4
3	0.09	0.21	0.6
4	0.12	0.18	0.8
5	0.15	0.15	1
6	0.18	0.12	1.2
7	0.21	0.09	1.4

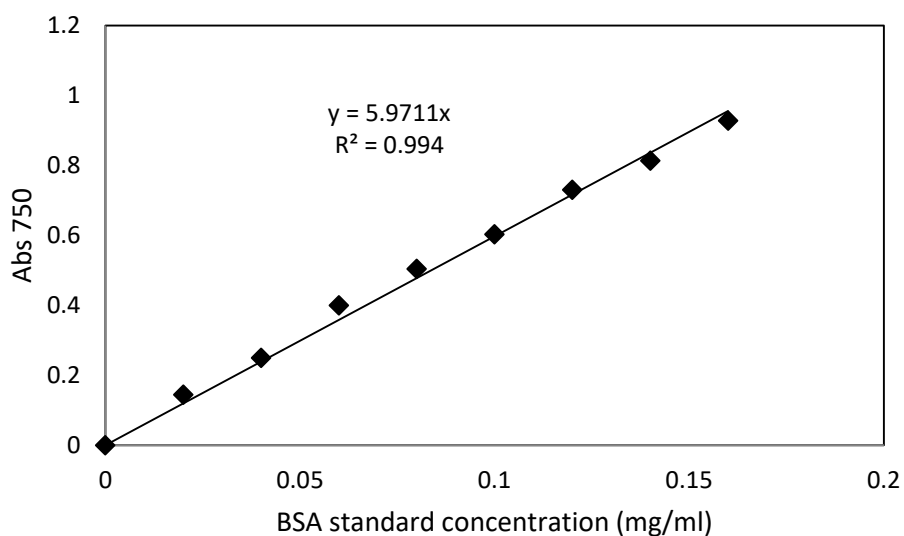


$$\text{Absorbance (700 nm)} = 0.8636 \times \text{concentration (mg/ml)}$$

### A.3 Standard curve Lowry method

Total soluble protein content was determined using Lowry method assay in Section 3.4.3 was correlated with the standard curve. The standard curve was constructed using 0.2 mg/ml bovine serum albumin (BSA) as a standard protein.

No	Std (ml)	dH <sub>2</sub> O (ml)	Protein concentration [mg/ml]
0	0	0.5	0.00
1	0.05	0.45	0.02
2	0.1	0.4	0.04
3	0.15	0.35	0.06
4	0.2	0.3	0.08
5	0.25	0.25	0.10
6	0.3	0.2	0.12
7	0.35	0.15	0.14
8	0.4	0.1	0.16
9	0.45	0.05	0.18
10	0.5	0	0.20



$$\text{Absorbance (750 nm)} = 5.9711 \times \text{concentration (mg/ml)}$$

#### A.4 Determination of molecular weight (MW) of unknown protein by SDS-PAGE

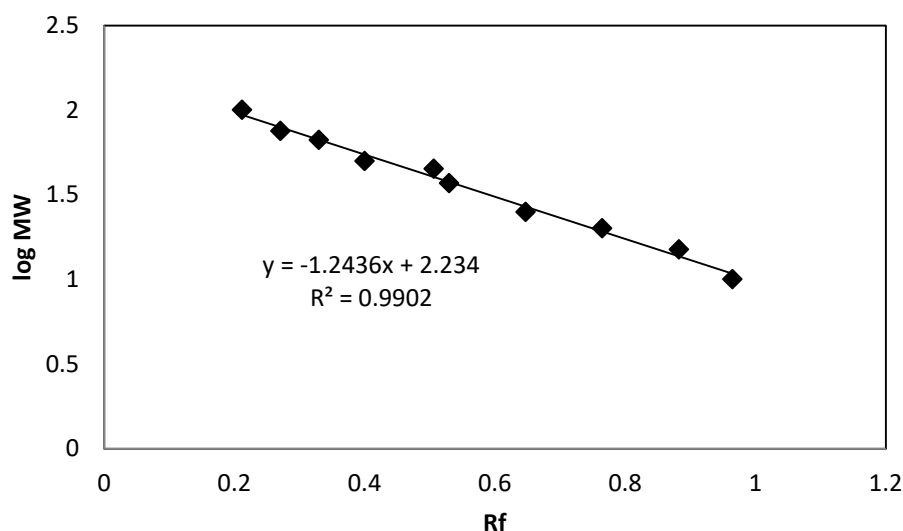
To determine the molecular weight (MW) of an unknown protein by SDS-PAGE, a standard curve of the log (MW) versus  $R_f$  was generated using the Precision Plus Protein standards. The strong linear relationship ( $R^2 = 0.9902$ ) between the protein MW and migration distances indicated the reliability in predicting MW.

**Table A.4** Data to establish the standard curve for molecular weight (MW) determination

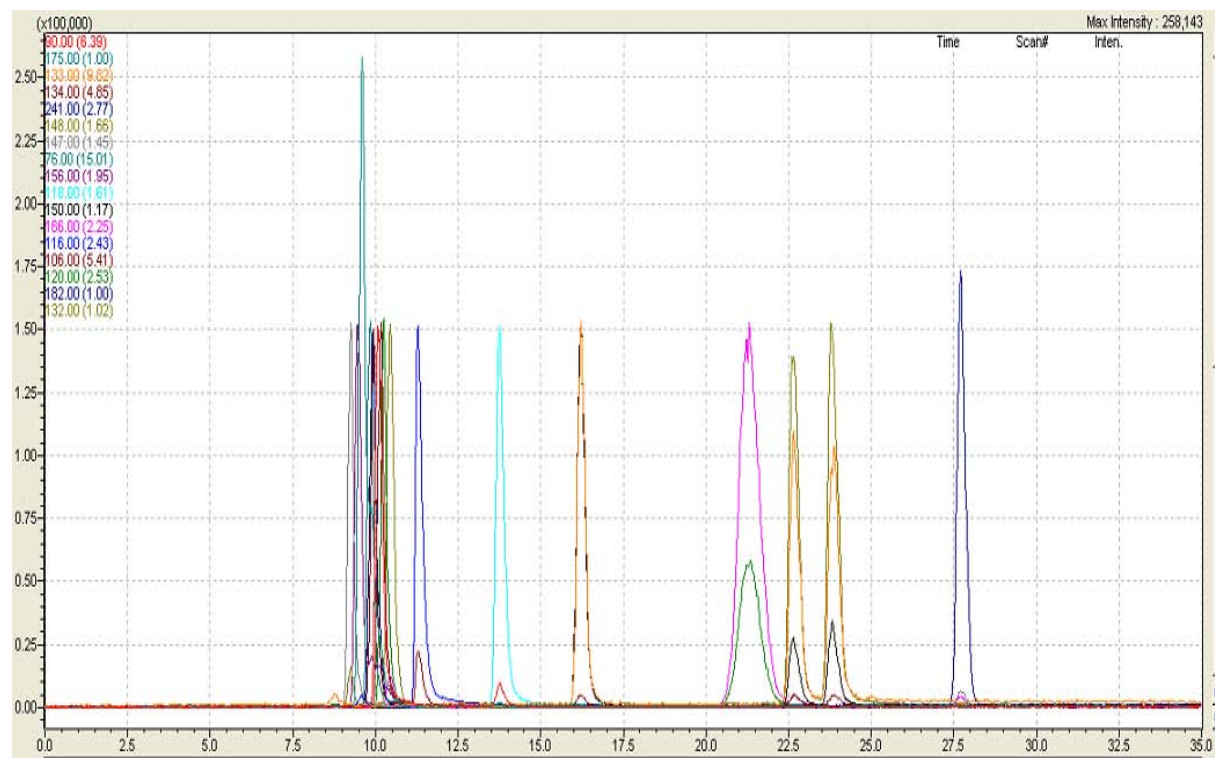
No	MW	$R_b$	$R_f$	Log MW
1	10	8.2	0.964706	1
2	15	7.5	0.882353	1.176091
3	20	6.5	0.764706	1.30103
4	25	5.5	0.647059	1.39794
5	37	4.5	0.529412	1.568202
6	45	4.3	0.505882	1.653213
7	50	3.4	0.4	1.69897
8	66.5	2.8	0.329412	1.822822
9	75	2.3	0.270588	1.875061
10	100	1.8	0.211765	2
11	150	1.3	0.152941	2.176091
12	250	1	0.117647	2.39794

$R_b$  = migration distance of the protein

$R_f$  = migration distance of the protein/migration distance of the dye front

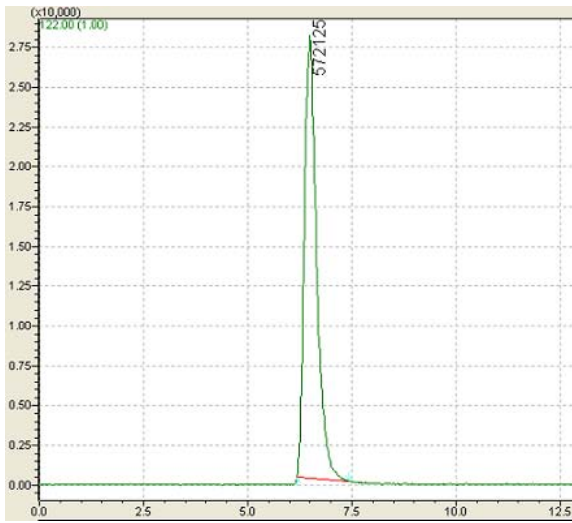


Amino acids calibration curve analysed with LC-MS using Aeris Peptide 5U XB-C18 column (Micron-Phenomenex, USA) with core-shell of 3.6  $\mu\text{m}$  (100  $\text{\AA}$ , 250 x 4.6 mm). The mobile phase is 0.1% formic acid in deionized water. All the standards were obtained from Sigma-Aldrich, Spain.

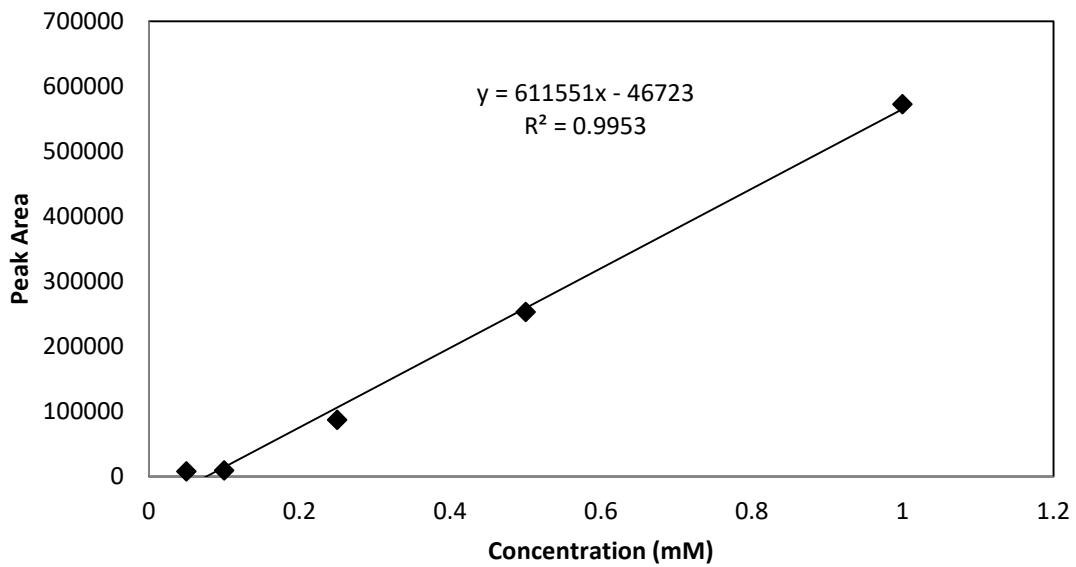


**A.5** Chromatograph 21 amino acids analysed using LC-MS with positive APCI ionisation mode in SIM mode

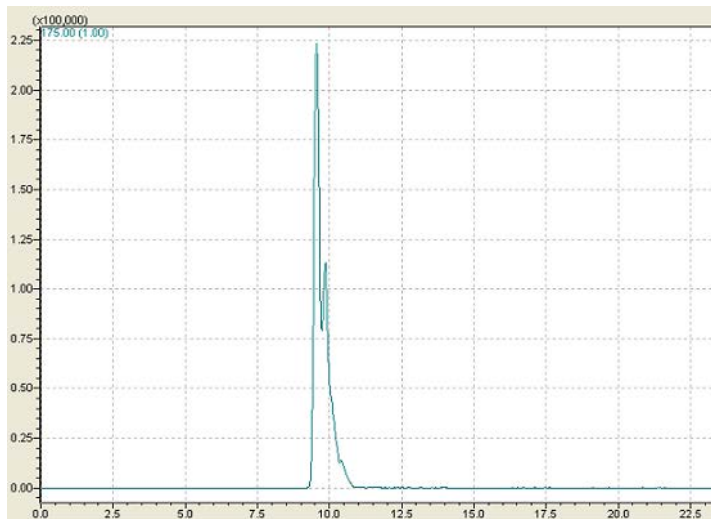
### A.6 Amino acid – Cysteine



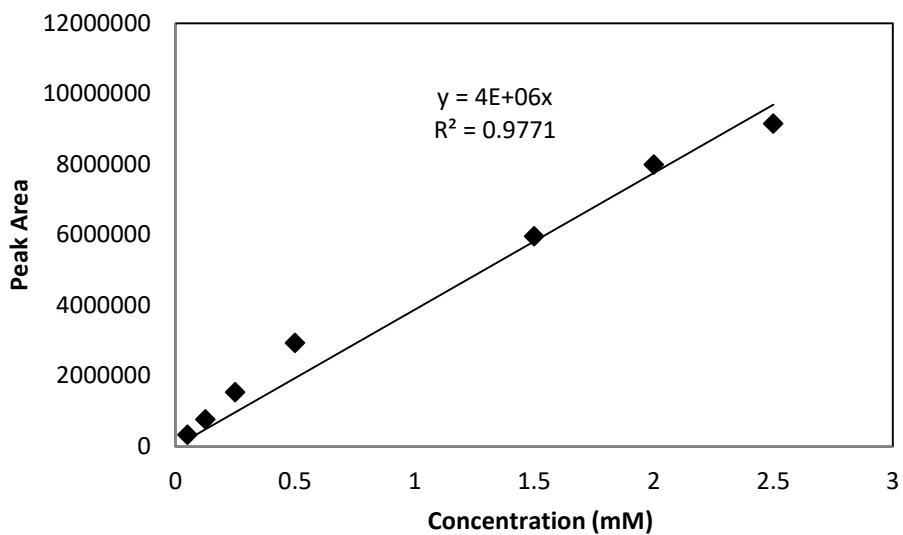
no	area	concentration (mM)
1	7590	0.05
2	8885	0.1
3	86910	0.25
4	252821	0.5
5	572125	1



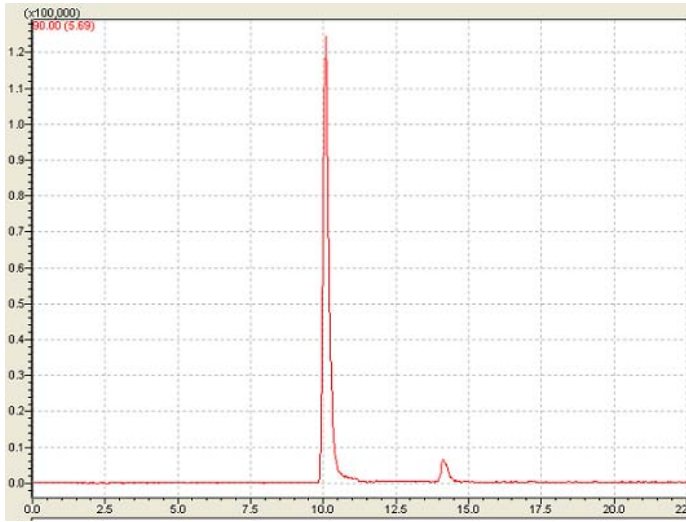
**A.7 Amino acid – Arginine**



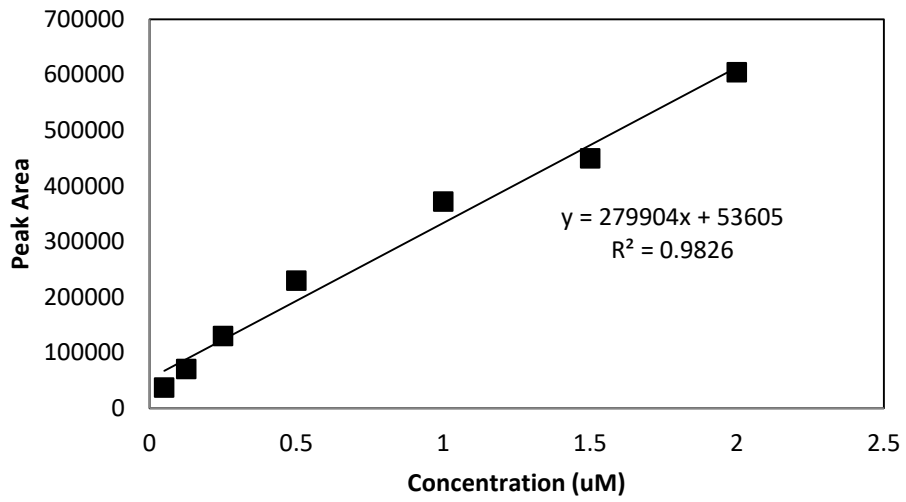
no	area	concentration (mM)
1	325893	0.05
2	763818	0.125
3	1531745	0.25
4	2934466	0.5
5	5953897	1.5
6	7986993	2
7	9149772	2.5



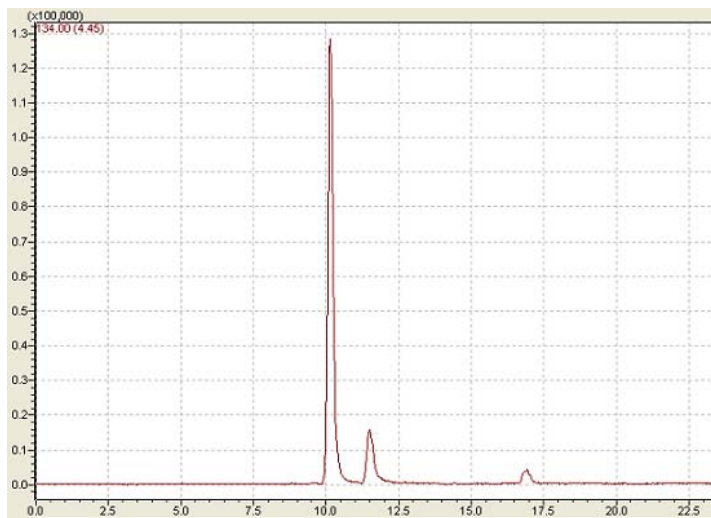
**A.8 Amino acid – Alanine**



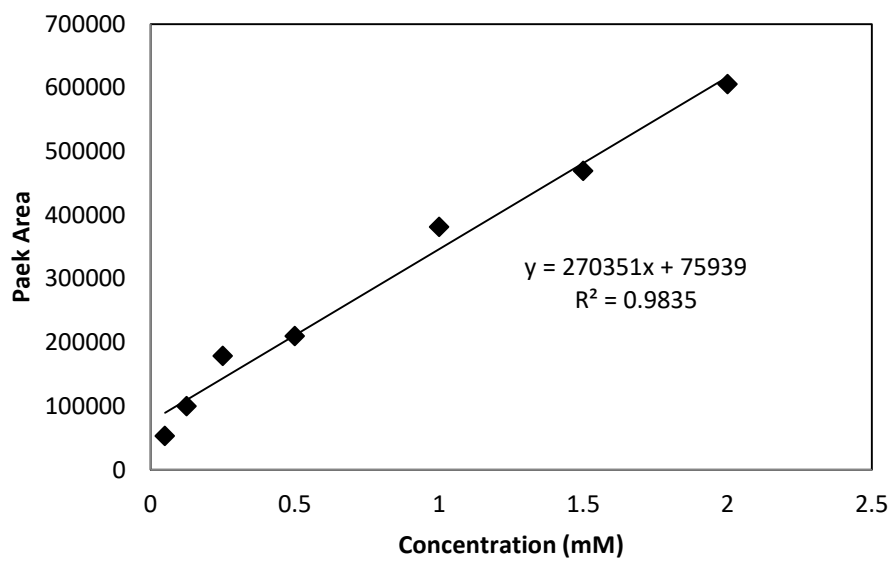
no	area	concentration (uM)
1	37438	0.05
2	70964	0.125
3	130227	0.25
4	229346	0.5
5	372085	1
6	449425	1.5
7	604229	2



## A.9 Amino acid – Aspartic acid

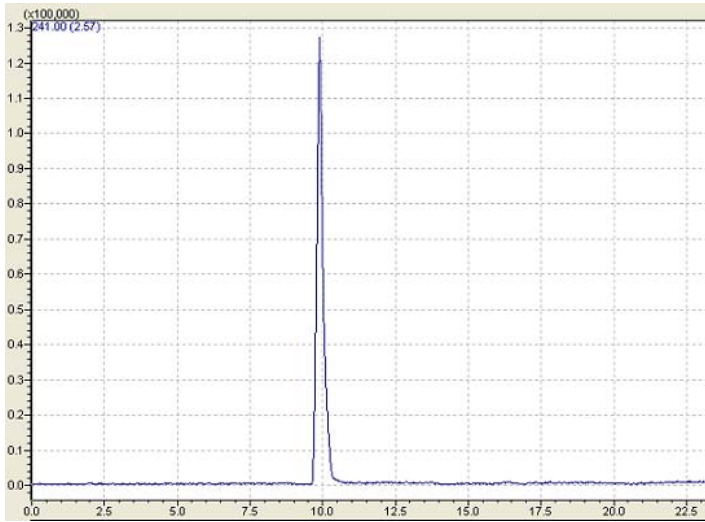


no	area	concentration (mM)
1	53423	0.05
2	99813	0.125
3	178914	0.25
4	209811	0.5
5	381337	1
6	469161	1.5
7	605769	2

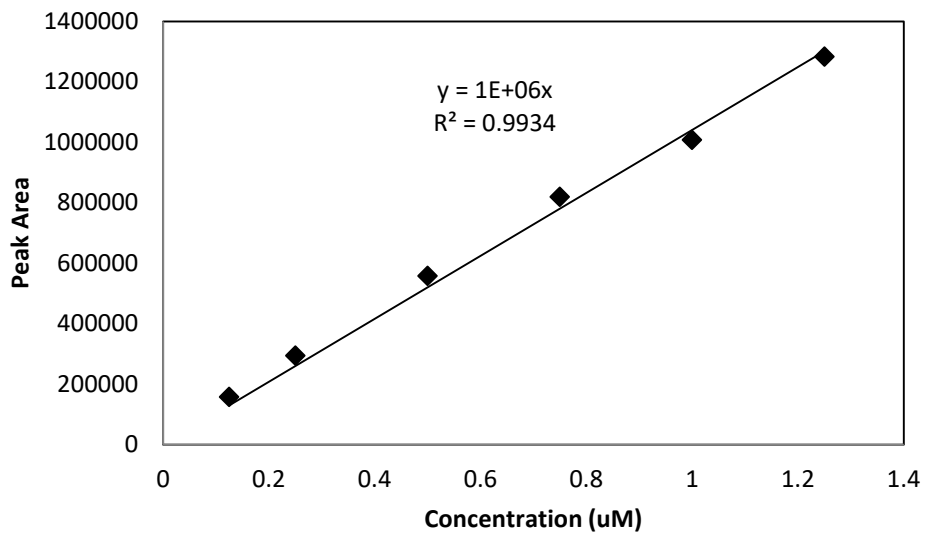




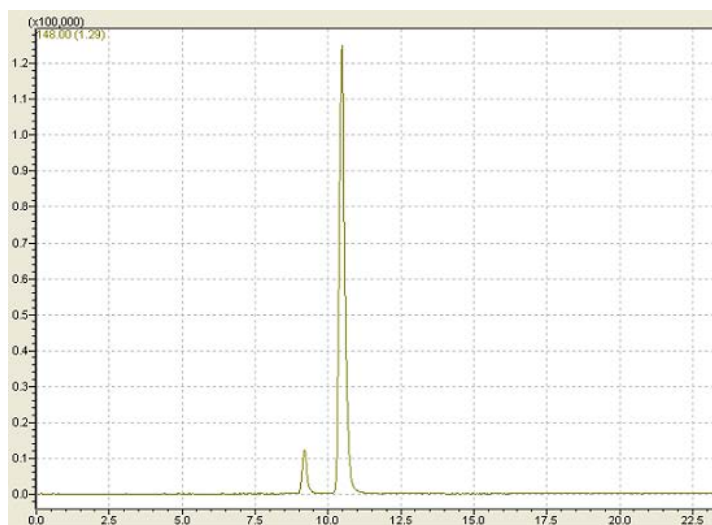
**A.10 Amino acid – Cystine**



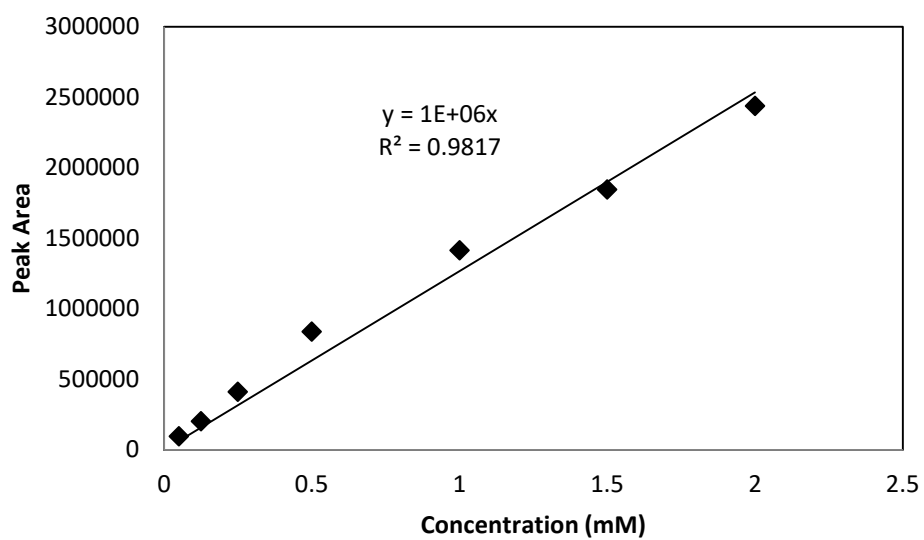
no	area	concentration (uM)
1	293373	0.125
2	557148	0.25
3	818399	0.5
4	1006908	0.75
5	1282469	1
6	1420061	1.25



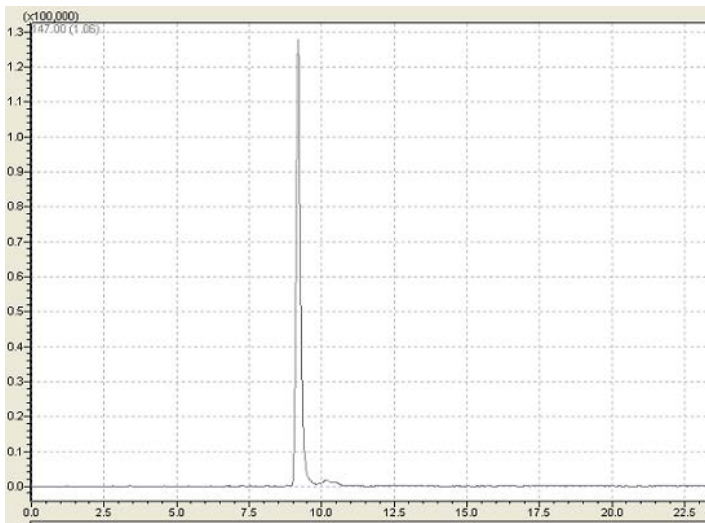
## A.11 Amino acid – Glutamic acid



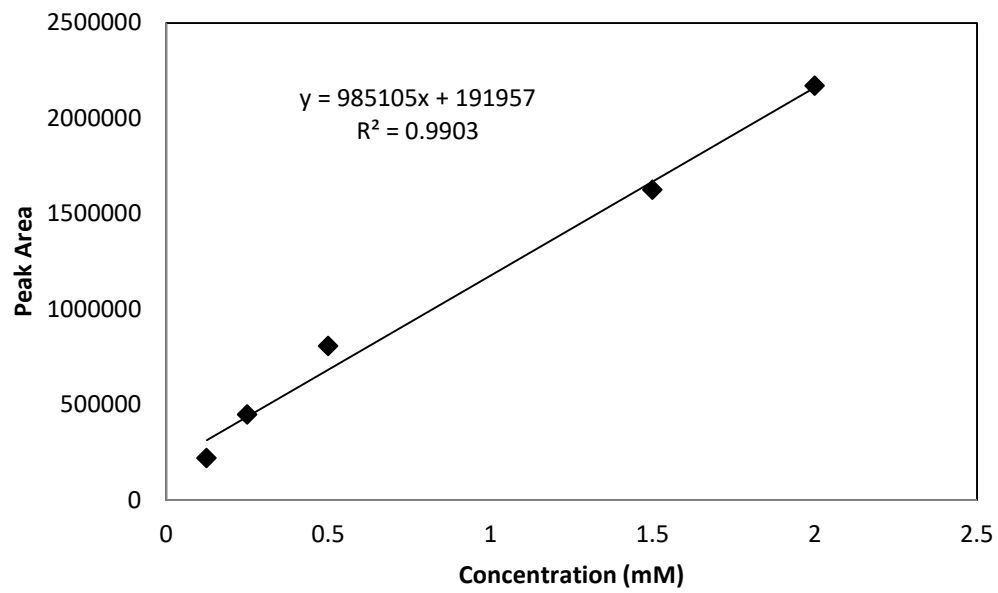
no	area	concentration (mM)
1	94508	0.05
2	202082	0.125
3	409950	0.25
4	838443	0.5
5	1413732	1
6	1845097	1.5
7	2437053	2



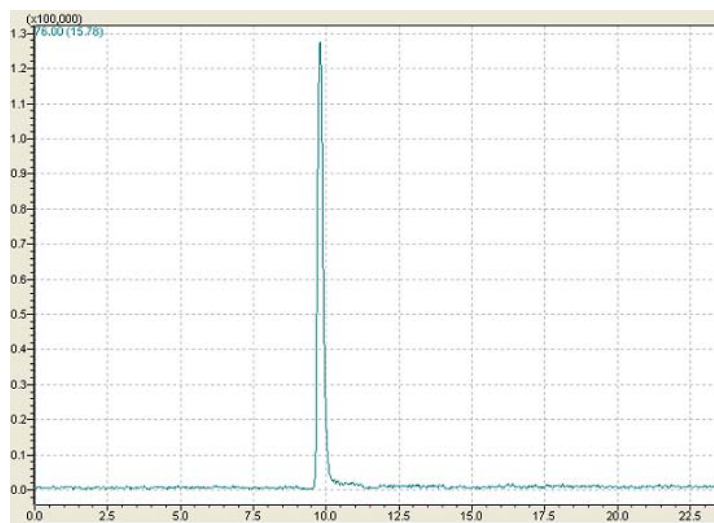
**A.12 Amino acid – Glutamine-lysine**



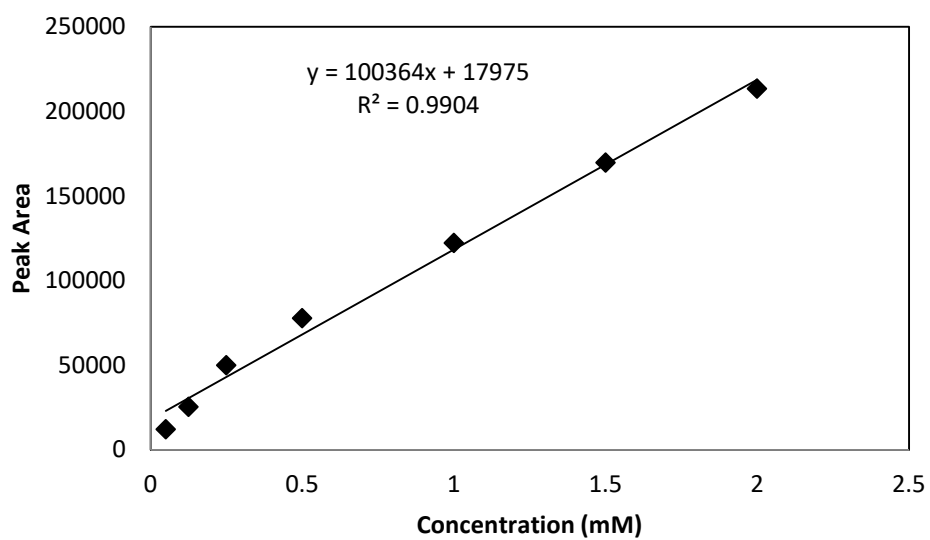
no	area	concentration (mM)
1	220237	0.125
2	447783	0.25
3	806774	0.5
5	1625109	1.5
6	2169713	2



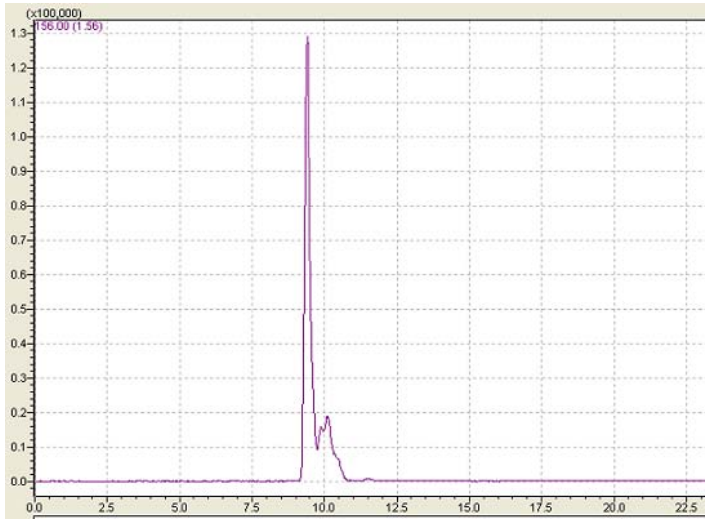
## A.13 Amino acid – Glycine



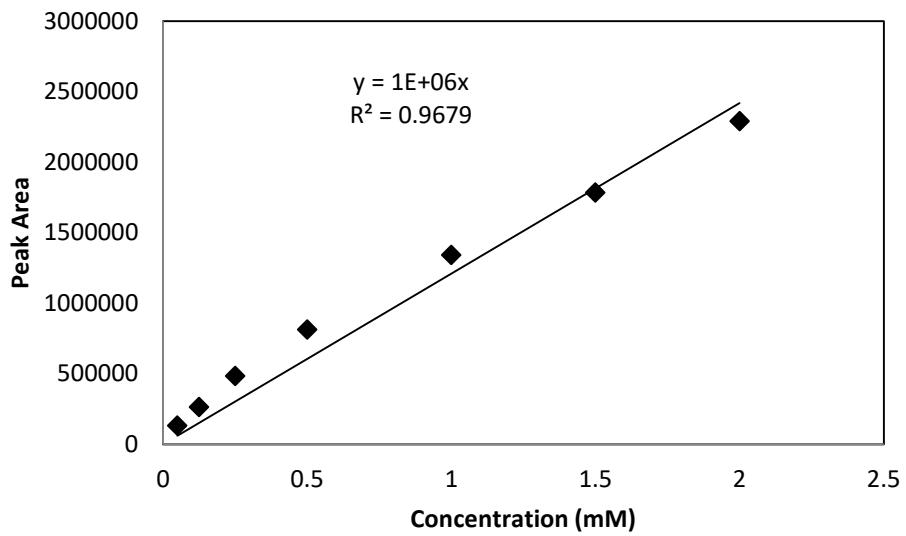
no	area	concentration (mM)
1	12163	0.05
2	25280	0.125
3	49975	0.25
4	77811	0.5
5	122198	1
6	169552	1.5
7	213323	2



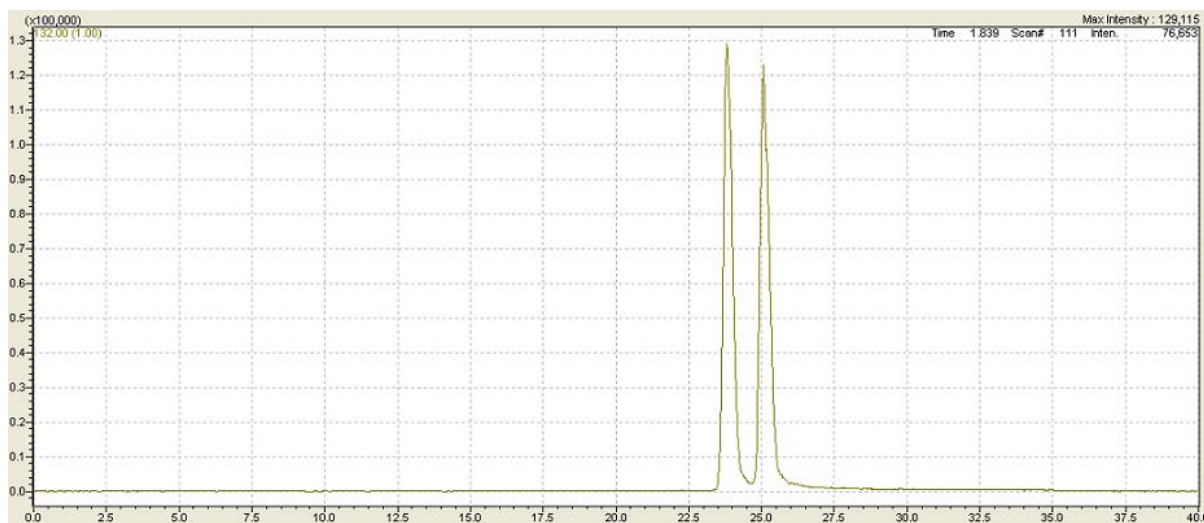
**A.14 Amino acid – Histidine**



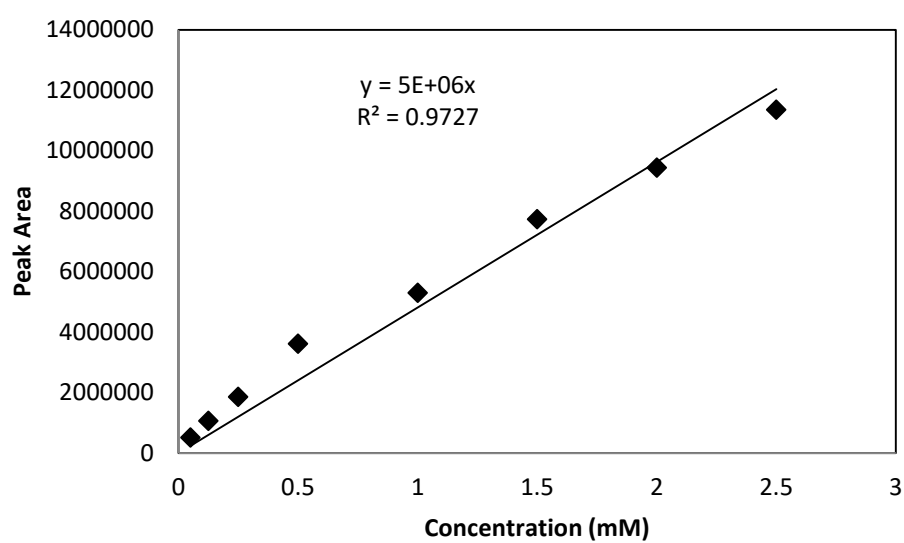
no	area	concentration (mM)
1	131616	0.05
2	263830	0.125
3	482644	0.25
4	812372	0.5
5	1340648	1
6	1783984	1.5
7	2290319	2



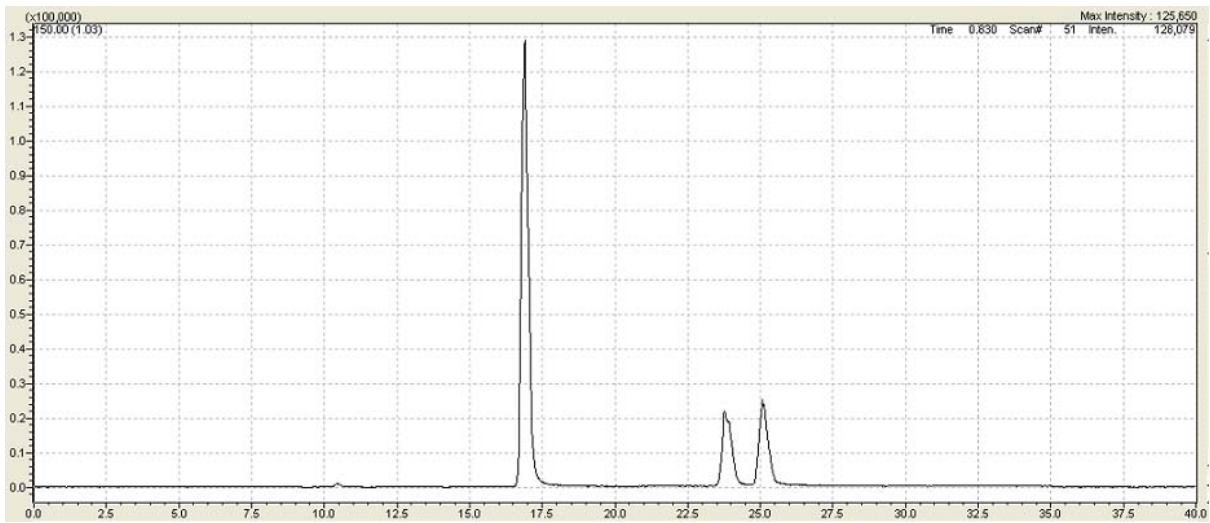
## A.15 Amino acid – Leucine-Isoleucine



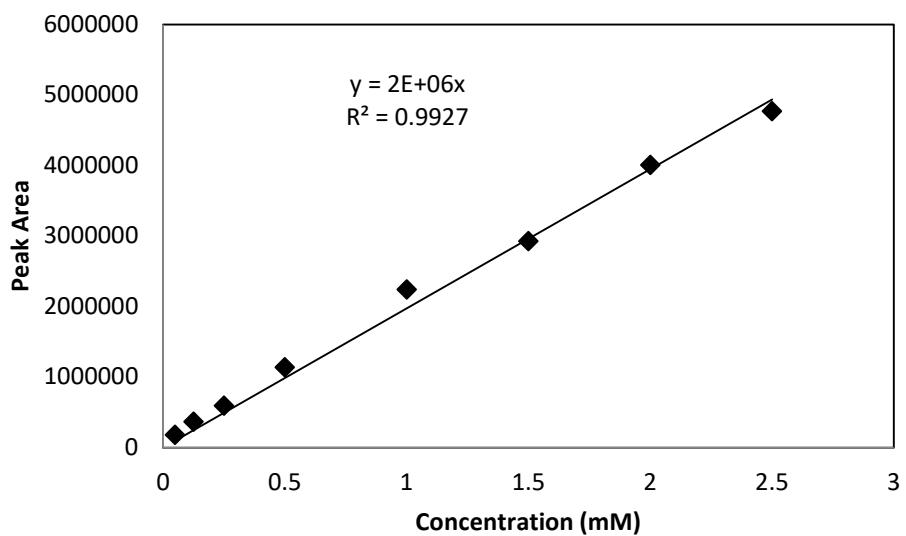
no	area	concentration (mM)
1	511651	0.05
2	1054313	0.125
3	1855582	0.25
4	3610125	0.5
5	5292785	1
6	7734384	1.5
7	9437810	2
8	11355657	2.5



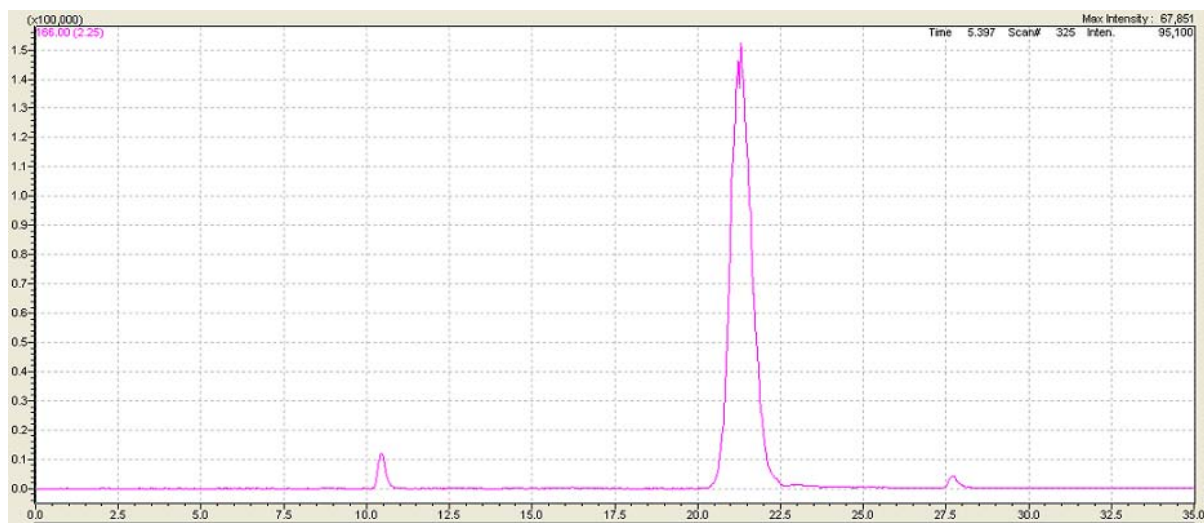
**A.16 Amino acid – Methionine**



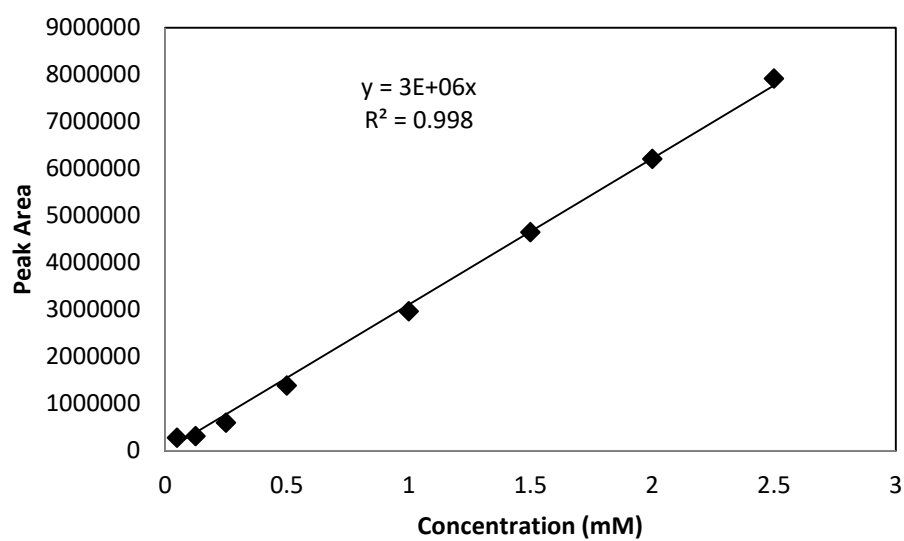
no	area	concentration (mM)
1	175051	0.05
2	364132	0.125
3	588783	0.25
4	1135797	0.5
5	2239424	1
6	2923669	1.5
7	4003742	2
8	4763617	2.5



## A.17 Amino acid – Phenylalanine

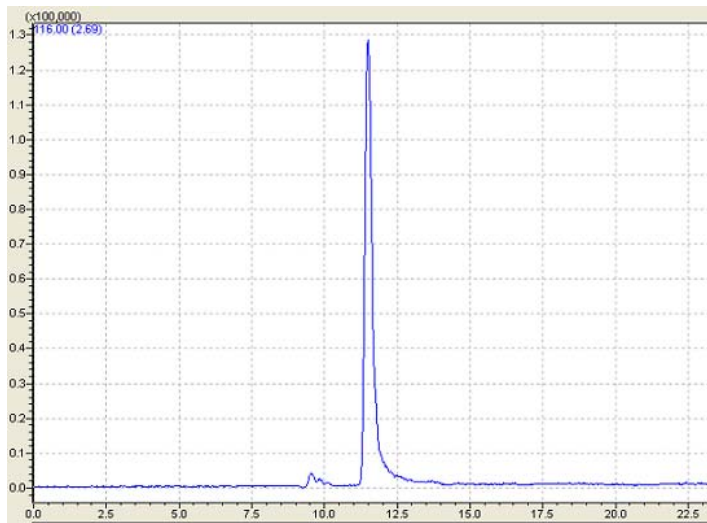


no	area	concentration (mM)
1	275459	0.05
2	313779	0.125
3	600037	0.25
4	1389010	0.5
5	2965813	1
6	4645518	1.5
7	6204381	2
8	7918052	2.5

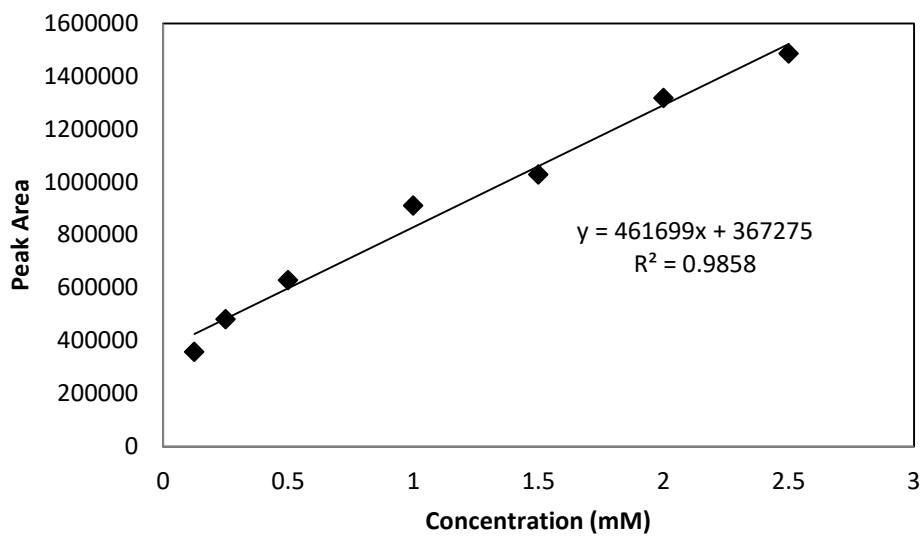




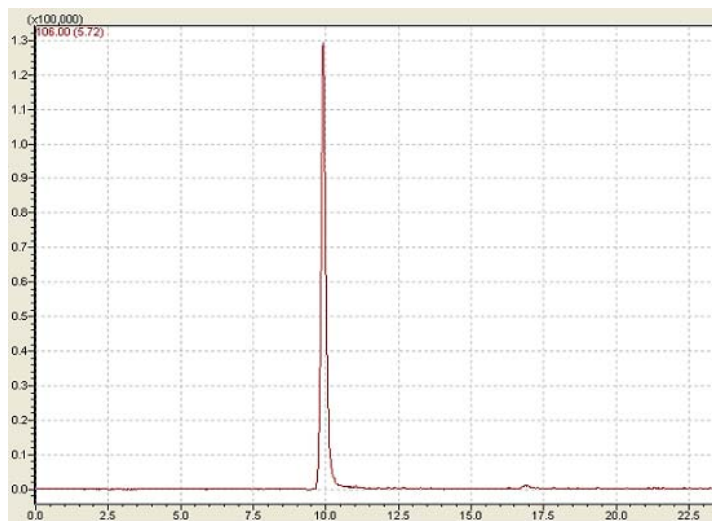
**A.18 Amino acid – Proline**



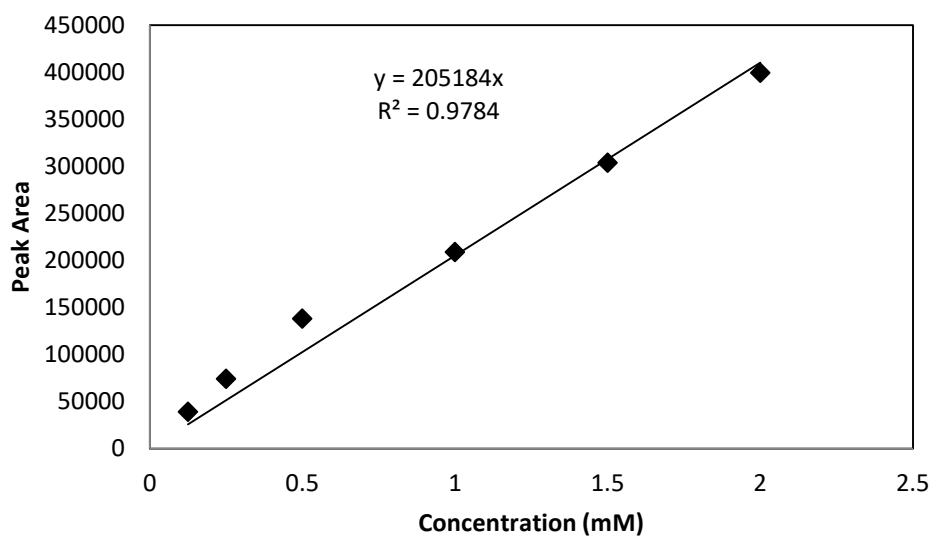
no	area	concentration (mM)
1	357406	0.125
2	481118	0.25
3	628518	0.5
4	910749	1
5	1027612	1.5
6	1316331	2
7	1485072	2.5



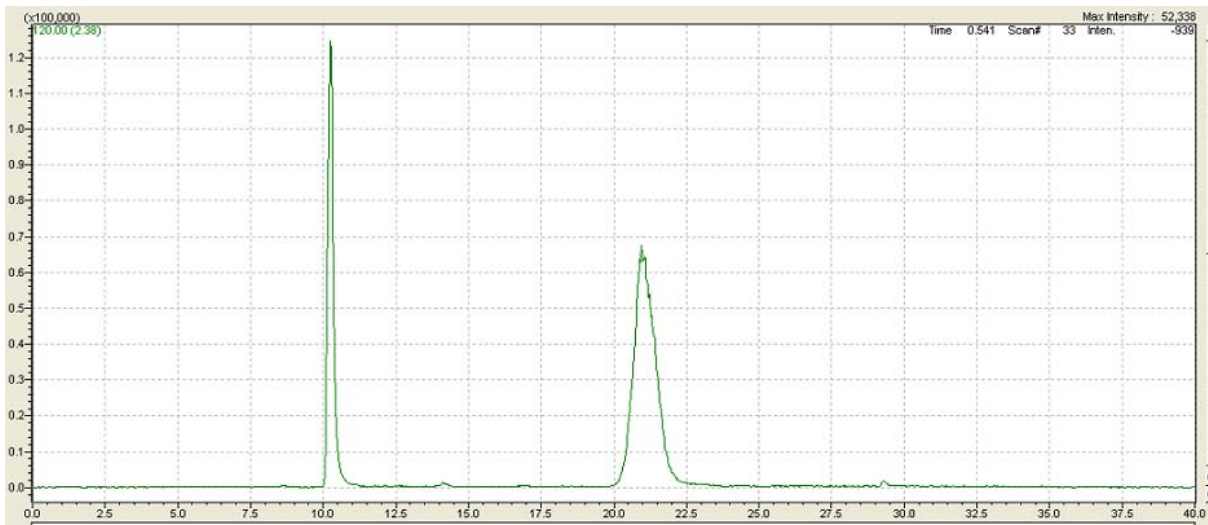
## A.19 Amino acid – Serine



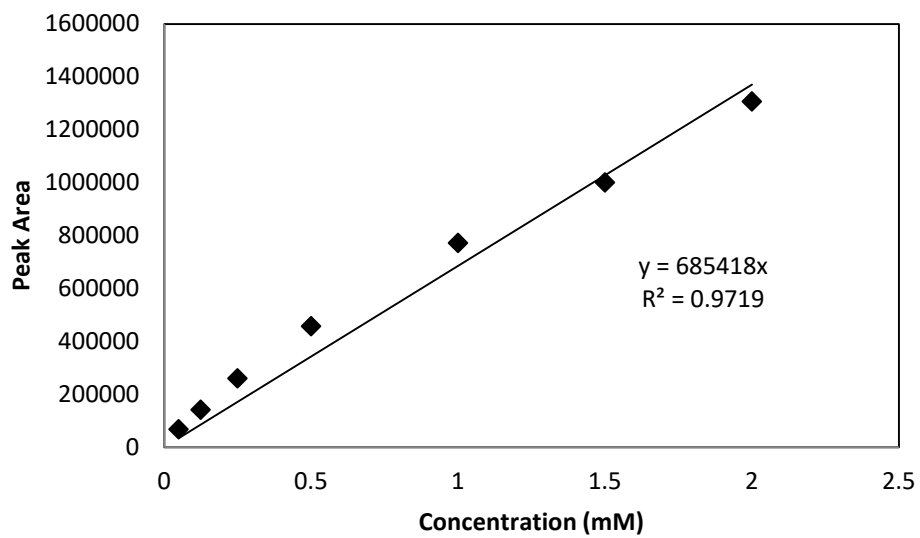
no	area	concentration (mM)
1	73711	0.125
2	137921	0.25
3	208641	0.5
4	303574	1
5	399332	1.5
6	501201	2



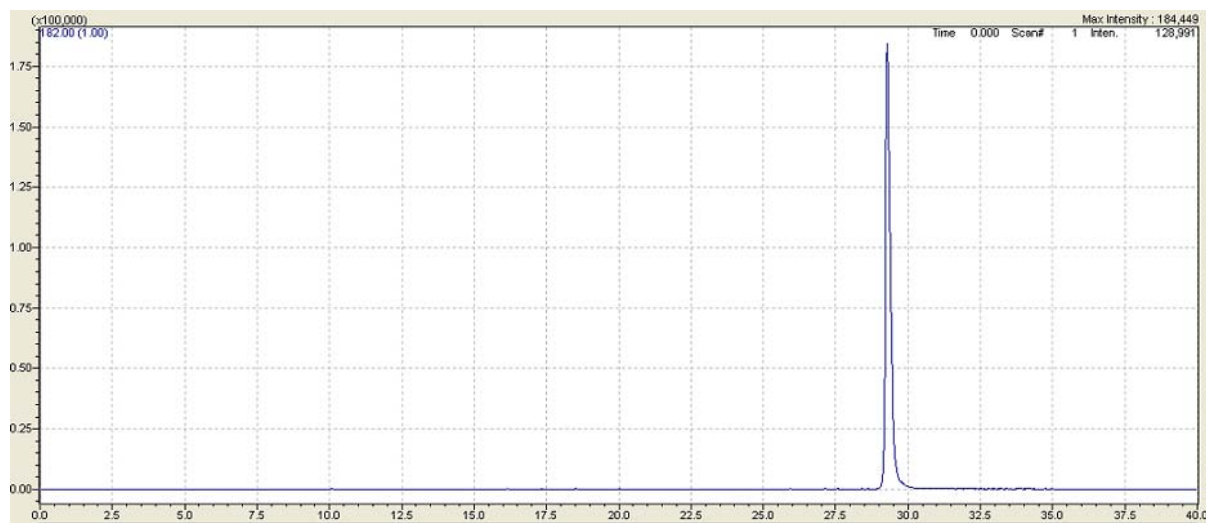
**A.20 Amino acid – Threonine**



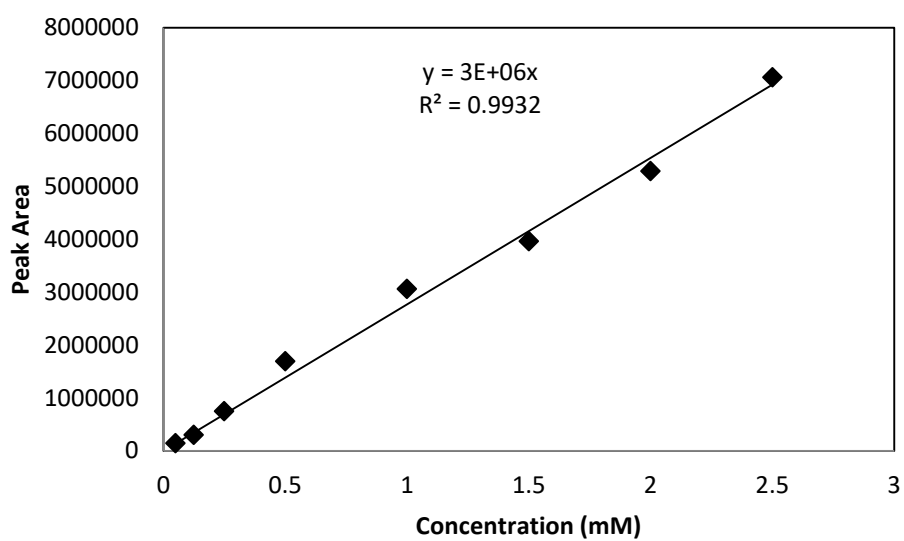
no	area	concentration (mM)
1	66309	0.05
2	139979	0.125
3	259122	0.25
4	455853	0.5
5	771311	1
6	999435	1.5
7	1305955	2



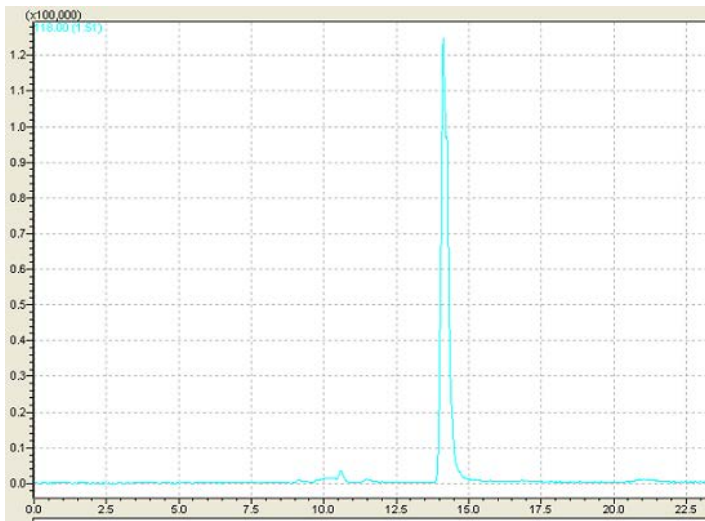
## A.21 Amino acid – Tyrosine



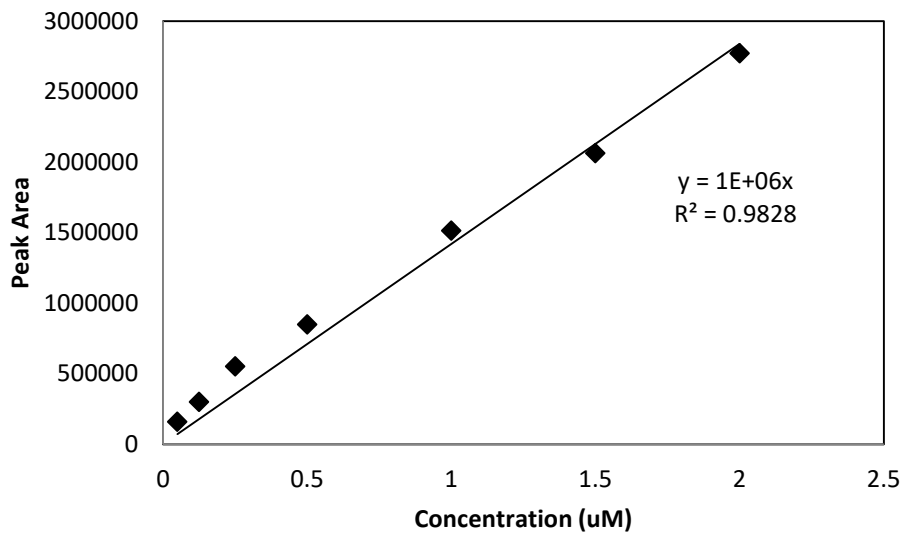
no	area	concentration (mM)
1	146178	0.05
2	299811	0.125
3	745539	0.25
4	1693707	0.5
5	3057486	1
6	3964759	1.5
7	5284322	2
8	7060084	2.5



**A.22 Amino acid – Valine**



no	area	concentration (uM)
1	159002	0.05
2	299284	0.125
3	551556	0.25
4	848378	0.5
5	1514325	1
6	2062749	1.5
7	2770579	2



## Annexe 2: Publications



Review

# Solid-State Fermentation as a Novel Paradigm for Organic Waste Valorization: A Review

Noraziah Abu Yazid <sup>1</sup>, Raquel Barrena <sup>1</sup>, Dimitrios Komilis <sup>1,2</sup> and Antoni Sánchez <sup>1,\*</sup>

<sup>1</sup> Composting Research Group, Department of Chemical, Biological and Environmental Engineering, Universitat Autònoma de Barcelona, 08193 Bellaterra, Barcelona, Spain; noraziah.abuyazid@uab.cat (N.A.Y.); raquel.barrena@uab.cat (R.B.); dkomilis@env.duth.gr (D.K.)

<sup>2</sup> Department of Environmental Engineering, Democritus University of Thrace, University Campus, 69100 Komotini, Greece

\* Correspondence: antoni.sanchez@uab.cat; Tel.: +34-935-811-019; Fax: +34-935-812-013

Academic Editor: Vincenzo Torretta

Received: 29 November 2016; Accepted: 31 January 2017; Published: 8 February 2017

**Abstract:** The abundance of organic solid waste throughout the world has become a common issue that needs complete management at every level. Also, the scarcity of fuel and the competition between food and substance as an alternative to a petroleum-based product has become a major problem that needs to be properly handled. An urge to find renewable substances for sustainable development results in a strategy to valorize organic solid waste using solid state fermentation (SSF) and to manage the issue of solid wastes in a green approach. This paper reviews management of solid wastes using SSF, with regard to its current application, advantages and challenges, downstream processing in SSF, economic viewpoint, and future perspectives.

**Keywords:** solid state fermentation (SSF); downstream processing; organic wastes; value-added; enzymes; organic acids; biopesticides; biosurfactants; aroma compounds

## 1. Introduction

The generation of organic solid waste is dramatically increasing each year. The problems related to organic solid waste disposal have become more pronounced in recent years due to the rapid pace of development towards modernization throughout the world. Most of the organic waste is composed of household food waste, agricultural waste, human and animal wastes, etc. which are normally used as animal feed, incinerated or go to landfill sites [1]. However, incineration is an expensive disposal method and causes air pollution, while in landfills the organic waste is broken down by microorganisms and forms leachate that can contaminate the groundwater [2]. In addition, the degradation of organics in these conditions produces methane, which is 25 times more harmful greenhouse gas compared to carbon dioxide [3]. Incorrect waste management practices can result in public health and environmental problems, regarding issues such as odors and diseases [4]. Nevertheless, organic wastes are comprised of materials rich in sugars, minerals, and proteins that could be used for other processes as substrates or raw materials. Since the cultivation of microorganism requires carbon, nutrient, and moisture, organic waste could be a good candidate to provide the appropriate conditions for the development of microorganisms.

In this view, solid state fermentation (SSF) is presented as a promising technology for waste valorization through the bioconversion of organic wastes used as either substrate or inert support [5], whilst microorganisms will play a role in the degradation of organic wastes into its constituents to convert them into high value-added products. SSF shows sustainable characteristics in the bioconversion of solid wastes that have been proved to be able to give high efficiency in terms of product yields and productivities, low energy consumption, and solving disposal problems [1,6].



SSF is a process carried out with microorganisms growing on solid and moist substrates that act as nutrient sources and support the microbial growth in the absence or near absence of water [7,8]. SSF is not a new technology in bioprocessing since it has been mainly applied in the Asian region from ancient time, but recently it is gaining a lot of attention due to the increasing use of different types of organic wastes and the larger production of added-value products [5,9]. The search for sustainable and green processes to transform traditional chemical processes also highlights the potential of SSF. Thus, the bioconversion of organic wastes into valuable bio-products could substitute non-renewable materials and transform chemical processes into cleaner practices in the industrial sector. The particular interest of SSF is due to its relatively simple as a process that uses abundant low-cost biomaterials with minimal or no pre-treatment for bioconversion, less waste water generation, and the capacity for simulating similar microenvironments favorable to microorganism growth [10]. Similarly, SSF simulates natural microbiological processes such as composting and ensiling [11].

The present paper attempts to present routes for organic waste valorization using SSF technology with regard to recent applications and developments in SSF.

## 2. Organic Waste and Its Potential

Organic waste can be practically defined as any material or unused by-product from a process that is biodegradable and comes from either plant or animal. The main forms of organic waste are household food waste, agricultural waste, industrial waste, and human and animal waste. Organic waste tends to be degraded over time by other organisms depending on its composition and moisture content. The composition of organic waste varies from the nature of the original material. Depending on the type of organic waste, SSF can be applied with the aim of producing different valuable bio-products [9,12–14]. In this sense, Table 1 summarizes the use of different organic wastes with their potential to produce bio-products.

**Table 1.** List of organic wastes and their potential use in solid state fermentation (SSF) to obtain value-added bio-products.

Category of Organic Waste	Type of Products/Processes	Waste Materials/Residues	Potential Use	References
Municipal/domestic food waste	Kitchen waste	Preparation waste, leftover food, sludge, cocoyam peels	Biopesticides, animal feedstuff, organic acids, antibiotics	[15,16]
	Commercial/marke/hotel	Used coffee grounds, used tea bags, waste bread, leftover, expired foods, sludge	Enzymes, animal feedstuff, biopesticides, bioethanol, bioplastics	[17,18]
Industrial organic waste	Animal products/tannery/slaughterhouse	Skin, hides, fleshing wastes, fats, horns, shaving wastes, bones, liver, intestines	Enzymes, animal feedstuff, glues, surfactants, lubricants, fillers	[19–22]
	Paper/wood industry	Pulp, sawdust	Enzymes, bioethanol, biofuels	[23]
	Sugar industry	Molasses	Enzymes, fructo-oligosaccharides	[24]
	Poultry processing	Skin, blood, fats, hairs, feathers, bones, liver, intestines, wings, trimmed organs	Enzymes, animal feedstuff, biofertilizers	[25]
	Marine products processing	Shells, roes, pincers, trimmed parts	Enzymes, bioactive compounds	[26,27]
	Cereals and spices processing	Husk, hull, chaff, stalks, residues	Enzymes, activated carbon	[28]
	Fruits and vegetables processing	Skin, peels, pomace, fiber, kernel, stones, seeds	Pectinolytic enzymes, biofuels, animal feed, organic acids	[29,30]

Table 1. Cont.

Category of Organic Waste	Type of Products/Processes	Waste Materials/Residues	Potential Use	References
	Nuts processing	Shells, coir, pith	Biopulping, biochar, activated carbon	[31]
Agricultural organic waste	Corn, wheat, rice, soya, coffee, sugarcane, barley	Fiber, meal, straw, bran, husk, pulp, bagasse	Enzymes, animal feedstuff, biofuels, bioethanol, furfural, chemical feedstock, biopolymers, organic acids	[1,32]
	Cattle, broiler	Fleshing wastes, dung, litter	Animal glue, animal feed supplement, methane production, biochar, activated carbon, biofertilizers, biopesticide	[33–35]
	Fruits and vegetables	Seeds, peels, pomace, husks	Enzymes, animal feed, biofuels, compost	[31,36]
	Oils and oil seeds	Shells, husks, fibers, sludge, presscake	Bioethanol, enzymes, biofuels, biofertilizers, activated carbon	[37]
	Coconuts	Fibers, shell, kernel	Resins, pigments, fillers, mats, activated carbon, tanning materials	[38–40]

### 2.1. Agricultural Organic Waste

Agricultural and agro-industrial activities generate a large amount of lignocellulosic by-products such as bagasse, straw, stem, stalk, cobs, fruit peel and husk, among others. These wastes are mainly composed of cellulose (35%–50%), hemicellulose (25%–30%), and lignin (25%–30%) [41]. Typically, in lignocellulosic materials, the cellulose main constituent is glucose; hemicellulose is a heterogeneous polymer that is mainly comprised of five different sugars (L-arabinose, D-galactose, D-glucose, D-mannose, and D-xylose) and some organic acids; whereas lignin is formed by a complex three-dimensional structure of phenylpropane units [1].

Despite the complex structure and composition of agricultural organic wastes, SSF has been successfully applied to the production of hydrolytic and ligninolytic enzymes [31,42,43]. Lignin peroxidase has been produced using corn cobs as a substrate in SSF [44]. Furthermore, considering the rising price and shortage of grains as a custom animal feed, lignocellulosic materials have a great potential to produce edible animal feedstuff [45]. However, the direct application for animal feedstuff is limited because of the presence of lignin that reduces its digestibility. Several pre-treatments of straw have been made using SSF for cellulose and lignin degradation to increase the digestibility of the feed [46]. In this sense, SSF can have a great potential in producing enzymes to improve the digestibility of rich fiber materials such as soybean cotyledon [47]. *Jatropha* seed cake has been reported for the production of cellulases through SSF without any pre-treatment [13]. Several authors present other uses for similar materials such as the reinforcement of composite materials for application in building materials, furniture, fishnet, etc. [39,40] or as activated carbons [38]. Agricultural organic wastes also include livestock manure. Cow dung was reported to have a high nitrogen content that made it suitable for methane production [33,34]. The production of biochar and activated carbon were favored by utilization of chicken manure and cow dung [48,49]. Furthermore, high-quality biofertilizer was produced employing liquid amino acid hydrolyzed from animal carcasses as an additive to mature compost of chicken or pig manure by SSF [50].

### 2.2. Industrial Organic Waste

Industrial organic wastes include any organic by-product from a large variety of industries such as slaughterhouses, fruit and vegetable processing plants, poultry processing, paper and pulp manufacturing, the sugar industry, and the dairy industry, among others. Most of these wastes have the potential to be used as a substrate or support in SSF processes to produce high value products.

For instance, sawdust, which is an easily available by-product of the wood industry, has been used as a support substrate in SSF to obtain high laccase production by white rot fungi *Coriolopsis gallica* [51]. The leather industry and slaughterhouses generate many organic wastes containing protein such as animal fleshing, hair wastes, skin trimming, keratin wastes, chrome shaving, and buffing wastes that are being underutilized. Several authors have reported the utilization of animal fleshing as a substrate in SSF for protease production [52]. The mixture of hair wastes with activated sludge or anaerobically digested sludge showed a high yield of protease production [19,20]. By-products of the sugar industry such as molasses and sugarcane bagasse have been reported in the production of invertase by SSF [53]. Molasses also was chosen as a low-cost substrate to replace an expensive feedstock (cane sugar) in ethanol production [54]. Additionally, tapioca industry waste which contains considerable organic matter with a strong odor that could cause environmental pollution has been successfully converted into poly-3-hydroxybutyrate (PHB) via SSF, thus possibly becoming an alternative process and reducing the total production cost [55]. Food processing industries generate many by-products able to be used in SSF for producing valuable bio-products [28,56]. The use of fruits and vegetable waste for production of organic acid and vital enzymes has been widely reported [30]. Due to its high and easily degradable organic content, vegetable wastes show a great potential for energy bioconversion, particularly in biofuel production [57]. Crustacean by-products, generated in industrial seafood processing, have been reported in the production of chitinase and chitosanase with a wide range of applications in biomedical, food and agrochemical sectors [58,59]. Fish processing wastes in SSF are favorable since the waste is easy to obtain at low-cost and provides appropriate conditions for microorganism cultivation. Fish processing wastes, rich in lipids and proteins, have been found suitable to produce esterase, a product with a versatile industrial application in organic chemical processing, in detergent formulations, and in the surfactant and oleochemical industry [60].

### 2.3. Municipal/Domestic Food Waste

Most countries around the world are facing a great challenge to manage domestic food waste as it is wet, putrescible, and sometimes mixed with inorganic waste (impurities). Generally, the composition of domestic food waste is complex and includes oil, water, as well as spoiled and leftover foods from kitchen wastes and markets. These substances are chemically comprised of starch, cellulose, protein, fats, lipids, and other organic matter. High moisture and salt contents lead to rapid decomposition of the organic wastes and produce unpleasant odors that can attract flies and bugs, which are vectors for various diseases. Apart from being perishable, municipal solid waste including household kitchen waste and domestic food waste from restaurants and markets contains high lignocellulosic materials that could be exploited to produce valuable bio-products. Domestic food wastes such as waste bread, savory, waste cakes, cafeteria waste, fruits, vegetables and potato peel wastes have been reported as a suitable substrate for glucoamylase enzymes production by *Aspergillus awamori* via SSF technology [61,62]. Bread waste has been used to produce amylase [63], whereas municipal solid waste and kitchen waste residues principally composed of potato peel, orange peel, onion peel, carrot peel, cauliflower leaves, banana stalks and pea pods have been used to produce cellulase by SSF [64,65]. The cultivation of selected industrial yeast strains using orange peel as a substrate resulted in a high yield of aroma esters [66]. The utilization of household food wastes with high dry content to produce high yields of ethanol by SSF has also been reported in several studies [67,68]. Likewise, mixed food wastes collected from restaurants and inoculated with fungal inoculum can produce glucoamylase-rich media and protease-rich media by SSF, suitable to be used as a feedstock to produce succinic acid which has a wide range of applications including laundry detergents, plastics, and medicine production [69]. Cocoyam peel is a common household kitchen waste in Nigeria presenting a capability to become a very useful substrate for oxytetracyclines, which are an important antibiotic to treat many infections [70]. The complex composition of food wastes also makes them suitable for microbial growth, having potential to produce *Bacillus thuringiensis* (Bt) biopesticide through SSF [16].

### 3. General Aspects of Solid State Fermentation

Solid state fermentation (SSF) has received great attention in the past years. The successful development of bioprocesses in SSF is linked to several general aspects including the suitability of different types of microorganisms, substrates, and process parameters. There are various types of microorganisms used in the SSF process including fungi, yeasts, and bacteria. However, fungi and yeast are the most commonly reported for the reason that SSF can provide a similar natural habitat, which has low water activity in the fermentation media. The most common yeast genera reported in SSF are *Candida*, *Saccharomyces* and *Aureobasidium* [71], while common fungal genera are *Aspergillus*, *Penicillium*, and *Rhizopus*, which have a broad range of species for the production of a wide number of valuable bio-products through SSF [12]. Despite SSF seeming to be more favorable for fungi and yeast growth, there is also increasing evidence of bacteria successfully used in producing bio-products in SSF. The most common bacteria genera used are *Bacillus* and *Streptomyces* [11,72]. There are a lot of studies reporting the use of filamentous fungi, mainly chosen in SSF because of their ability to produce thermostable enzymes of high commercial value [72–75]. However, there are also several studies reporting that thermostable enzymes can be produced by bacteria strains especially from *Bacillus* species [76–79].

Selection of suitable substrates also plays a key role in an efficient and economical production of the desired product. In selecting proper substrates for the SSF process, it is important to ensure the availability and cost of the substrates. They can supply appropriate nutrients and physical support for the development of microorganisms in SSF. Organic wastes from agricultural, industrial processing, and domestic food waste are the most suitable substrates to be used due to their abundance at low or no cost and their chemical composition. Additionally, by using these organic wastes as substrates their environmental pollution problems can be minimized. However, in some cases, an additional supplement has to be added to the organic wastes. In other cases, a chemical or mechanical pretreatment (especially for lignocellulosic materials) is necessary due to the inaccessibility of certain nutrients for microorganisms. For example, a chemical pre-treatment of municipal solid waste was performed to prepare the solid fraction for an easier microbial uptake in the production of cellulase [65]. Pulp and paper solid waste were pre-treated with acid hydrolysis in a microwave prior to SSF as a substrate to produce fumaric acid [80]. In the production of an anti-cancer pro-drug, camptothecin (CPT), by SSF, complex protein sources (whey concentrate powder) were added to soybean waste to enhance the productivity of *Fusarium oxysporum* producing a secondary metabolite [81].

Other important aspects to enhance the efficiency of SSF are the selection and optimization of process variables including initial moisture, particle size, pH, temperature, media composition, sterilization, water activity, inoculum density, agitation, aeration, extraction of product and its downstream process [7]. Among these aspects, particle size and moisture content have been mainly studied, reported and reviewed by others [9,11,72,82]. Ideally, it is apparent that small substrate particles could provide a large surface area for microbial attachment. Yet, extremely small particles would result in substrate agglomeration that could affect oxygen transfer, thus retarding microorganism development. However, although a large particle size of the substrate provides better aeration efficiency, it can limit the surface area for microbial attachment [6,7,82]. Hence, the conditions that are favorable in a particular process are an aspect that needs to be thoroughly assessed. Moisture content also has a significant role in SSF as bacteria and fungi have different moisture content requirements. Fungi need lower moisture content around 40%–60% [11] whereas bacteria can require high moisture content (60%–85%) [72]. The optimum moisture content in a solid substrate is closely related to the correct nutrient and oxygen/carbon dioxide diffusion during fermentation [83]. High moisture content would decrease porosity, with the loss of the structure of the particles and interfere in oxygen diffusion. On the contrary, low moisture content can limit nutrient solubility hindering microorganism development. An increase of temperature during the fermentation will indicate the growth of the microorganism. In aerobic fermentation, oxygen is supplied and exchanged with carbon dioxide and heat is generated by microorganisms, leading to a temperature increase. In some cases, high

temperatures will negatively affect the growth of microorganisms and product formation [7]. However, in other cases, high temperatures increase the yield of the enzyme produced [19,20,84].

These general aspects are relevant to point out a general idea to design an efficient strategy using organic wastes in SSF according to the product required and considering the cost and waste availability. Figure 1 summarizes the whole general processes involved in the valorization of organic waste via SSF.

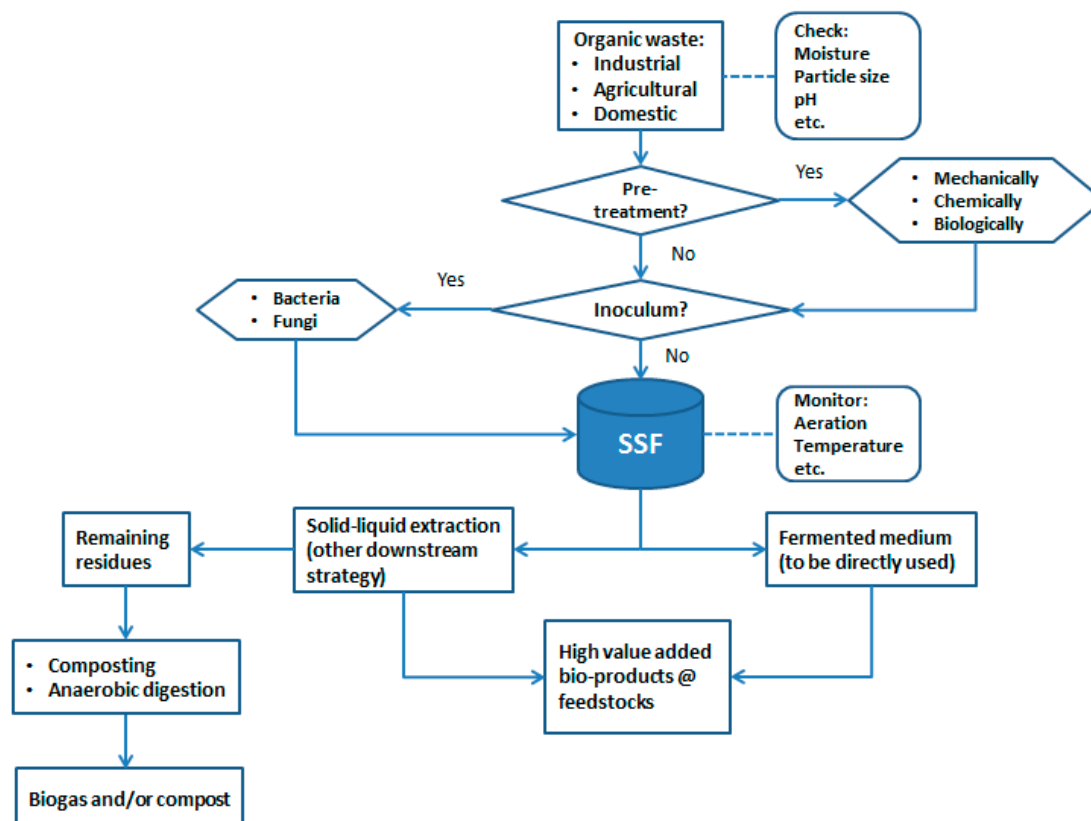


**Figure 1.** Flowchart of valorization of organic waste to produce valuable bio-products using solid state fermentation (SSF).

#### 4. Advantages and Challenges of Solid State Fermentation

In recent years, there has been an increasing trend for using SSF in the biotechnology field due to its simplicity and ability to perform the bioconversion of low-cost solid substrates, in some cases achieving higher productivity than that of submerged fermentation (SmF) [85,86], due to broth rheology problems that affect the transport phenomena and mass transfer in a SmF reactor [87]. In addition, the lack of a liquid phase in SSF reduces waste water and lower down the risk of bacterial contamination. In this sense, SSF offers an advantage by using unsterilized substrates and creates non-strict sterile conditions for the process [88]. Also, SSF provides a simple media preparation with the reduction of reagents use, since the media normally contain the appropriate nutrient for the process and present negligible foaming problems during the process. As a matter of fact, the process requires low consumption of energy since agitation and sterilization are not always necessary. Similarly, this process reduces purification costs due to higher end product concentration or by using the product in a crude form [71].

In spite of these advantages, SSF also faces several challenges such as mass and heat transfer, scale-up, biomass estimation, and recovery and operational control. In addition, the utilization of natural substrates is often limited by their poor reproducibility and heterogeneity [89]. Also, the heterogeneity of the substrate related to porosity can lead to mass and heat transfer problems

in SSF [90]. Moreover, the diffusion of mass and heat in SSF depends on aeration which may differ according to the substrate types. In the small scale, an appropriate aeration allows heat dissipation and a regulation of the mass moisture level. However, the removal of heat generated during metabolic growth can be a problem at the large scale. The high solid concentration requires a large quantity of air [91]. Furthermore, biomass determination is quite a challenge in SSF, especially involving fungi that usually develop a tight interaction between mycelia and solid substrate making difficult the complete recovery of biomass [92]. Due to this difficulty in biomass quantification, a lack of important basic scientific engineering and fermentation operational control is often found in publications and only a qualitative or empirical characterization is done [93]. The same happens when establishing kinetics of reactions in SSF.

## 5. Applications of Solid State Fermentation

SSF has opened a new paradigm of bioconversion of organic solid wastes through the production of biologically active metabolites both at the lab and industrial scale. The application of SSF in the production of different bio-products has been widely reported including enzymes, organic acids, biofertilizers, biopesticides, biosurfactants, bioethanol, aroma compounds, animal feed, pigments, vitamins, antibiotics, etc.

### 5.1. Enzymes Production

In search of green technology, enzyme production has received a lot of attention in industrial biotechnology processes with the objective of replacement of chemical processes having potentially negative effects on humans and the environment. Various enzymes emerging from biotechnology processes, mainly from submerged fermentation, are playing a key role in a large number of industrial processes. In recent years, the production of enzymes from SSF has gained attention due to the simplicity, high productivity, and stability that make them suitable for industrial processes. Several reviews on the production of enzymes from SSF have been published in recent years [5,9,11,12]. Fungi, yeasts, and bacteria are capable of producing various enzymes through SSF, as the environment in SSF is favorable for most microorganisms. In Table 2, a compilation of several organic solid wastes used as substrates for enzyme production with or without inoculation of specific strains is shown.

**Table 2.** List of several enzymes produced and organic waste used as substrates in SSF.

Enzyme	Microorganism	Substrate	Reference
cellulase	<i>T. reesei</i>	Municipal solid waste	[65]
	<i>Thermoascus aurantiacus</i>	Jatropha deoiled seed cake	[13]
	<i>A. niger</i>	kitchen waste	[64]
	<i>Penicillium</i> sp.	empty fruit bunches	[43]
	<i>T. reesei</i>	wheat bran	[94]
	<i>A. niger</i>	groundnut husks	[95]
	<i>Trichoderma viridae</i>	banana peel	[96]
	<i>Candida tropicalis</i> ,	Ginkgo biloba residues	[97]
	<i>A. oryzae</i>		
	<i>A. niger</i>		
	<i>Trametes hirsuta</i>	wheat bran	[99]
	<i>T. reesei</i>	soybean bran	[100]
	<i>A. fumigatus</i>	lignocellulosic materials	[73]
	<i>T. harzianum</i>	wheat bran	[101]
	<i>T. asperellum</i>	lignocellulosic materials	[102]
	<i>A. niger</i>	rice straw and wheat bran	[103]
	glucoamylase	<i>Phanerochaete chrysosporium</i>	grass powder
<i>A.nidulans</i>		black gram residues	[105]
<i>Aspergillus</i> sp.		banana peel, pineapple peel	[106]
<i>A. awamori</i>		domestic food waste	[61]
amylase	<i>A. awamori</i>	bread waste	[62,107]
	<i>Bacillus</i> sp.	mustard oil seed cake	[108]
	<i>Thermomyces</i> sp.	soy and bread waste	[63]

Table 2. Cont.

Enzyme	Microorganism	Substrate	Reference
protease	<i>Bacillus subtilis</i>	wheat bran and wheat rava	[109]
	<i>A. fumigatus</i>	wheat bran	[110]
	<i>A. niger</i>	wheat bran, soybean meal, cottonseed meal, orange peel	[111]
	<i>Pseudomonas aeruginosa</i>	<i>Jatropha curcas</i> seed cake	[112]
	<i>A. awamori</i>	bread waste	[62,107]
	<i>A. oryzae</i>	wheat bran, soya bran	[113]
	<i>Bacillus</i> sp.	green gram husk	[114]
	<i>A. fumigatus</i>	wheat bran	[115]
	<i>B. cereus</i>	cow dung	[116]
	<i>Candida tropicalis</i> , <i>A. oryzae</i>	Ginkgo biloba residues	[97]
	<i>Thermus</i> sp.	soy fiber	[117]
	N.S.	hair waste, activated wastewater sludge	[19]
	<i>Thermoactinomyces</i> sp.	agricultural and household waste	[118]
	N.S.	hair waste, anaerobic digested wastewater sludge	[20]
keratinase	<i>Paenibacillus woosongensis</i>	dry feathers	[119]
lipase	<i>Pseudomonas aeruginosa</i>	<i>Jatropha curcas</i> seed cake	[112]
	N.S.	vegetable oil refining waste	[120]
xylanase	<i>A. niger</i>	oil palm waste residues	[121]
	<i>A. japonicus</i>	castor bean waste	[122]
	<i>A. tubingensis</i>	wheat straw	[123]
	<i>B. pumilus</i>	wheat bran	[124]
	<i>T. harzianum</i>	wheat bran	[101]
	<i>Colletotrichum graminicola</i>	wheat bran	[125]
inulinase	<i>A. nidulans</i>	black gram residues	[105]
	<i>A. ficuum</i>	wheat bran	[126]
laccase	<i>Kluyveromyces marxianus</i>	sugarcane bagasse	[127]
	<i>Coriolopsis gallica</i>	sawdust waste	[51]
	<i>Trametes versicolor</i>	oak sawdust	[128]
esterase	<i>B. altitudinis</i>	fish processing waste	[60]
lignin peroxidase	<i>Ganoderma leucidum</i>	waste corn cob	[44]
invertase	<i>A. niger</i>	molasses and sugarcane bagasse	[53]
$\beta$ -xylosidase	<i>A. tamarii</i>	ground oats	[129]
$\beta$ -glucosidase	<i>Colletotrichum graminicola</i>	wheat bran	[125]
	<i>Colletotrichum graminicola</i>	wheat bran	[125]
multienzyme protease, xylanase, cellulase, endomyrase	<i>A. awamori</i>	babassu cake	[130]

N.S.: non-specified.

In SSF, non-sterilized and non-inoculated media are often suitable. This aspect can positively affect the economic feasibility for the production of enzymes at the industrial scale. For example, protease production from hair waste and waste water sludge in a 4.5 L reactor ( $469 \text{ U}\cdot\text{g}^{-1} \text{ DM}$ ) has been successfully scaled up to a 10 L reactor resulting in a stable proteolytic activity of  $435 \text{ U}\cdot\text{g}^{-1} \text{ DM}$  [20]. Also, the production of lipase from the mixture of winterization residue and waste water sludge in a 4.5 L SSF reactor under non-sterilized conditions resulted in a high lipolytic activity ( $120,000 \text{ U}\cdot\text{g}^{-1} \text{ DM}$ ) [120]. It has been proved that non-sterilized conditions are applicable in the production of enzymes by SSF even without specific inoculation [117].

Kriaa and Kammoun [131] compared the production of glucose oxidase by *Aspergillus tubingensis* in SSF and SmF. Preliminarily, both conditions were compared using glucose and gluconic acid as substrates which led to higher activity of glucose oxidase in SSF ( $170.59 \text{ U}\cdot\text{mL}^{-1}$ ) compared to SmF ( $43.73 \text{ U}\cdot\text{mL}^{-1}$ ). Then, the production of glucose oxidase was carried out using a mixture of agro-residues such as wheat bran, molasses and fish meal. An enhanced yield was observed, 74% higher than preliminary SSF and SmF. Similarly, peptidase production by *Aspergillus fumigatus* in

SSF using wheat bran and SmF using casein as a substrate was compared. An improved yield of peptidase production, approximately 30 times higher, was obtained through SSF compared to SmF [115]. In another comparative study among SSF, slurry state fermentation (SISF) and SmF, revealed that maximum  $\beta$ -xylosidase was obtained in SSF ( $33.7 \text{ U}\cdot\text{mL}^{-1}$ ) followed by SISF ( $24.9 \text{ U}\cdot\text{mL}^{-1}$ ) and SmF ( $5.5 \text{ U}\cdot\text{mL}^{-1}$ ) [129].

The enzymes produced by SSF maintain a similar or enhanced capability for chemical processes or commercial enzymes normally produced by SmF. Several studies have been successfully applied to the crude enzymes produced from SSF to industrial processes such as dehairing of hides, hydrolysis of lignocellulosic materials, detergent formulation, deinking and biobleaching paper waste, bioethanol production, xylitol production, silver recovery from X-ray films, etc.

Tanning and leather industries release a lot of hazardous chemicals. In this sense, some authors have explored the use of crude enzymes such as protease, keratinase, and amylase from SSF in leather processing as an alternative to chemical processes. Crude protease produced from hair waste and waste water sludge in SSF showed a high potential to substitute chemical dehairing [19,20]. The results in cowhide dehairing were as efficient as using chemical and commercial powder enzymes, indicating the economic viability of the process. Likewise, the crude protease produced by *Bacillus cereus* from agro-industrial residues and cow dung as substrates in SSF were effectively used for the dehairing of goat hides for 18 h at  $30 \text{ }^\circ\text{C}$  [116]. In other studies, the use of crude keratinase in dehairing of goat skins has been also reported [119]. The keratinase produced by *Paenibacillus woosongensis* by SSF employing chicken feather and rice straw as substrates, showed similar or improved characteristics to using chemical treatments, without causing damage to the collagen layers after the dehairing process. Integrated bioprocessing in leather processing including detaining and fiber opening normally needs a commercial enzyme. This enzyme is expensive for the regular processes of tanning and contains some added stabilizers that could contribute to the pollution of the effluent. Correspondingly, amylase produced by *Bacillus subtilis* on wheat bran through SSF showed a good performance in the fiber opening process developed on goat skins in comparison to chemicals and commercial enzymes. Besides, the employment of crude amylase during the process showed a lower pollution load (COD, TS) [109].

Crude cellulase produced from agricultural residues under SSF has been used in the saccharification of lignocellulosic materials such as rice straw, sugarcane bagasse, corn cob, fruits peel, and wheat bran enhanced the sugar yield for bioethanol production [98–100,102,103]. The utilization of grass powder as a carbon source in the production of cellulase and hemicellulase by *Phanerochaete chrysosporium* by SSF yielded an efficient enzyme complex which could be employed for hydrolysis of rice husk. Then, the hydrolysate was used by *Clostridium beijerinckii* and resulted in higher biohydrogen production, which was superior to other values reported [104]. Production of cellulase and xylanase by SSF inoculating *Trichoderma harzianum* showed a better activity and stability at optimum pH and temperature. The crude enzyme complex produced by SSF enhanced the toner removal of photocopier waste papers with superior strength properties (fiber and microfibrils) compared to chemical treatment, and the enzyme complex improved the brightness and drainage as well [101]. Similarly, the crude enzyme complex (cellulase, xylanase,  $\beta$ -glucosidase) by *Aspergillus nidulans* cultivated on low-cost crop residues as a substrate under SSF was efficiently used in the saccharification of pearl millet stover and bio-deinking of mixed office waste paper with enhanced physical properties [105]. Verma et al. [118] reported the use of crude protease produced from low cost agricultural and household waste by *Thermoactinomyces* sp. via SSF. The enzyme was used as an additive to commercial detergents as an alternative to caustic soda. Interestingly, the crude enzyme also showed gelatinase activity capable of hydrolyzing the gelatine layer locking the silver salt on used X-ray film, for silver recovery.

## 5.2. Organic Acids Production

Organic acids are categorized as the third largest products among biologically produced compounds [132] and their application has been continuously increasing. Organic acids are known



to hold extensive and versatile applications in many industries such as those for food and beverage preservation, animal feed production, soap manufacturing, medicines and pharmaceutical products, industrial solvents, perfumes preparation, oil and gas stimulation treatments, among others. Organic acids such as citric acid, lactic acid, succinic acid, fumaric acid, humic acid, oxalic acid, gluconic acid, and gallic acid have been produced commercially both by chemical synthesis and biological fermentation. Over the past years, several attempts have been made to develop and produce organic acids using SSF. Several authors have evaluated the potential use of organic solid waste such as sugarcane bagasse, cassava bagasse, coffee husk, kiwi fruit peel, wheat bran, rice bran, pineapple waste or apple pomace in organic acid production by SSF [1,9,30].

Citric acid is a weak acid that plays an important role in several industries such as food, cosmetics, pharmaceutical, and chemical products, etc. presenting an increase in its global demand over the last years. *Aspergillus niger* is a well-known citric acid producer, capable of using a wide variety of raw materials and achieving high yields. This acid has been mainly produced using SmF by *A. niger* using starch or sucrose-based media. However, the use of non-food materials (agro-industrial residues, fruit wastes, and other solid by-products) by SSF would be a greener approach for citric acid production. Fruit wastes such as pineapple pulp waste [133], grape peel [134], mixed fruit waste [135], apple pomace [136], orange peel [137], or banana peel [138,139] have been extensively studied to produce citric acid by SSF. When comparing SSF and SmF with *A. niger* growing on orange peel, the production of citric acid increased about 3-fold in SSF ( $193.2 \text{ g}\cdot\text{kg}^{-1}$ ) compared to SmF ( $73.6 \text{ g}\cdot\text{kg}^{-1}$ ) [140]. The addition of methanol, ethanol, isopropanol or methyl acetate, copper, and zinc has been related to the enhancement of the production of citric acid [141]. The amount of citric acid ( $640 \text{ g}\cdot\text{kg}^{-1}$  orange peels) by *A. niger* grown on orange peels supplemented with molasses and 3.5% methanol in the medium after 72 h fermentation [137] and with pineapple pulp as substrate showed higher yield in a medium with methanol ( $5.25 \text{ g}\cdot\text{kg}^{-1}$ ) compared to medium without methanol ( $3.25 \text{ g}\cdot\text{kg}^{-1}$ ) [133]. Similarly, the addition of 3% ( $\text{v}\cdot\text{w}^{-1}$ ) ethanol and 4% ( $\text{v}\cdot\text{w}^{-1}$ ) methanol to apple pomace as substrate increased the citric acid concentration up to 90% compared to the control study [136]. Likewise, the high amount of citric acid ( $82 \text{ g}\cdot\text{kg}^{-1}$ ) obtained after 72 h was reported with banana peel as substrate supplemented with 1% ( $\text{v}\cdot\text{w}^{-1}$ ) methanol and 10 ppm of copper ions [139]. However, other studies found that the addition of methanol was detrimental for citric acid production [140]. Goud et al. [134] reported that a higher yield of citric acid was obtained with a particle size of 0.63 mm compared to 0.25 mm and 0.15 mm particle size of grape peel in the medium, indicated that the production of citric acid by SSF was also influenced by this parameter.

Apart from fruit wastes, citric acid can also be produced from agro-industrial wastes such as oil palm empty fruit bunches [142], sugarcane bagasse [143], cassava bagasse [144], and biodiesel by-products [145] through SSF. Yadegary et al. [143] optimized citric acid production using sugarcane bagasse as a substrate by SSF using the Taguchi statistical method. Alkaline and acid pretreatment showed an increase in the yield production of  $97.81 \text{ g}\cdot\text{kg}^{-1}$  and  $87.32 \text{ g}\cdot\text{kg}^{-1}$  respectively, compared with untreated sugarcane bagasse yield of  $75.45 \text{ g}\cdot\text{kg}^{-1}$ . The production and scale up of citric acid can be influenced by operation parameters such as pH, inoculum development, substrate concentration, incubation temperature, and bioconversion time as reported in the study with oil palm empty fruit bunches as a substrate under SSF [142]. The bioconversion of biodiesel by-product (tung cake and glycerine) by *A. niger* under SSF for the production of citric acid has also been reported. The high yield of citric acid obtained ( $350 \text{ g}\cdot\text{kg}^{-1}$ ) provides a feasible way to manage the solid waste economically [145].

Lactic acid is another organic acid that has many applications in food, pharmaceutical, cosmetics, and chemical industries. The demand is increasing as it acts as a precursor to produce poly-lactic acid (PLA) for biodegradable plastic production. It is commonly produced from fungi (*Rhizopus* sp.) and bacterial strains (*Lactobacillus* sp.) in fermentation. A study of comparison between a wild and mutant strain of *Rhizopus* sp. for lactic acid production from cassava peel using SSF, indicated that the mutant strain subjected to mutation by UV radiation yielded the highest production ( $57.6 \text{ mg}\cdot\text{g}^{-1}$ ) while the

wild strain only yielded  $32.4 \text{ mg}\cdot\text{g}^{-1}$  [146]. In an effort to reduce the production costs, several low-cost materials were used as a carbon source or support for L-lactic acid production by *Lactobacillus* sp. in SSF such as cassava bagasse [147], sugarcane bagasse [148], rice straw [149], wheat bran [150], tea waste [151], pine needles [152], etc. During the production of lactic acid, the nitrogen source also plays an important role in improving the yield. Several authors reported the utilization of wheat bran as substrate impregnated with low-cost nitrogen sources such as red lentil flour and baker's yeast substituting peptone and yeast extracts during the SSF process. As a result, higher yields up to 96% of lactic acid efficiency (g lactic acid produced per g substrate utilized) have been reported [150,153].

El-Naggar et al. [154] investigated five cellulosic wastes included rice husks, wheat bran, corn cobs, wheat straw, and rice straw by *A. glaucus*, *A. oryzae*, and *Penicillium purpurogenum*. Through SSF, the production of high concentrations of levulinic acid ( $46.15 \text{ mg}\cdot\text{g}^{-1}$ ) on corn cobs and oxalic acid ( $43.20 \text{ mg}\cdot\text{g}^{-1}$ ) on rice husks by *P. purpurogenum* were studied. The production of oxalic acid was enhanced by the optimization of inoculum size and the initial substrate concentration. *A. niger* ( $10^6 \text{ spores}\cdot\text{g}^{-1}$  dry weight) and 5% ( $\text{w}\cdot\text{v}^{-1}$ ) corn cob as a substrate in 0.1 N NaOH solution which contributed to a maximum yield ( $123 \text{ g}\cdot\text{kg}^{-1}$  DM) [155]. Another remarkable route of waste valorization via SSF is the production of fumaric acid from pulp and paper solid waste from the paper industry. Das et al. [80] compared the production of fumaric acid by *Rhizopus oryzae* through SmF and SSF. The highest fumaric acid production was obtained from SSF ( $41.45 \text{ g}\cdot\text{kg}^{-1}$  DM) after 21 days with  $75 \mu\text{m} < x < 300 \mu\text{m}$  particle size, whereas  $23.47 \text{ g}\cdot\text{L}^{-1}$  of fumaric acid were produced through SmF after 48 days. Furthermore, humic acid that has a diverse application in agriculture, industry, the environment, and biomedicine has been commercially produced from non-renewable materials. Utilization of empty fruit bunches from oil palm processing by *T. reesei* for humic acid production by SSF provides an alternative for humic acid production [14].

### 5.3. Biopesticides Production

It is widely known that the use of chemical insecticides can cause harmful effects on human health as well as give environmental problems. The shift towards biopesticides has become more attractive in recent years. SSF was found to be the most suitable platform for biopesticide production as the spores produced in SSF are more stable and resistant to stress than those produced in SmF [8,88]. Both fungi and bacteria are able to produce biopesticides.

De Vrije [156] reviewed the development of fungal biopesticides produced by *Coniothyrium minitans* through SSF and its viable application on oilseed rape and lettuce, which were the most susceptible crops to have problems with the parasite *Sclerotinia sclerotiorum*. Employing continuous slow mixing (0.2 rpm) in a scraped-drum reactor during biopesticide production by *C. minitans* on oats can overcome heat accumulation in the large scale with high spore yields  $5 \times 10^{12}$  spores per kg of dry oats [157]. Production of spores from *Clonostachys rosea* on white rice grain in polyethylene bags ( $20.5 \text{ cm} \times 25 \text{ cm}$ ) using SSF showed no significant effect on mixing yield with  $1.1 \times 10^8 \text{ spores}\cdot\text{g}^{-1}$  DM with 15 days of fermentation [158]. Contrarily, spore production of a biocontrol agent *C. rosea* on wheat bran and maize meal in a new developed SSF reactor showed an efficient yield of  $3.36 \times 10^{10} \text{ spores}\cdot\text{g}^{-1}$  DM, which was 10 times higher than in a conventional tray reactor [159]. Several agricultural wastes such as rice husk, tea leaf waste, and wheat bran have revealed great sporulation of *Beauveria bassiana* in SSF that presents pathogenicity towards the larvae *M. domestica* [160].

*Bacillus thuringiensis* is a common producer of biopesticides releasing a crystalline protein known as  $\delta$ -endotoxin. Several studies compared the production of  $\delta$ -endotoxin by *B. thuringiensis* by SSF and SmF. Higher biomass production and induced early sporulation were achieved using several agricultural products. In addition, this process led to a reduction in the batch time for the economical production of biopesticides [161–163]. Zhuang et al. [164] demonstrated a cost-effective production of *B. thuringiensis* biopesticides using a mixture of waste water sludge and wheat bran by SSF that yielded a high number of viable cells ( $5.98 \times 10^{10} \text{ CFU}\cdot\text{g}^{-1}$ ), spore counts ( $5.26 \times 10^{10} \text{ CFU}\cdot\text{g}^{-1}$ ), toxin production ( $7.14 \text{ mg}\cdot\text{g}^{-1}$   $\delta$ -endotoxin) and entomotoxicity ( $4758 \text{ IU}\cdot\text{mg}^{-1}$ ). In other studies, kitchen

waste ( $5.01 \times 10^{10}$  CFU·g<sup>-1</sup>; 15,200 IU·mg<sup>-1</sup>) was found to be efficient to produce *B. thuringiensis* biopesticides compared to conventional medium ( $2.51 \times 10^{10}$  CFU·g<sup>-1</sup>; 12,900 IU·mg<sup>-1</sup>) during 48 h of SSF. This study showed kitchen waste as an alternative medium to reduce production costs [165]. Utilization of soy fiber residue as substrate at lab scale for production of viable cells ( $3.8 \times 10^9$  CFU·g<sup>-1</sup> DM) and spores ( $1.3 \times 10^8$  spores·g<sup>-1</sup> DM) of *B. thuringiensis* under non-sterile condition eased the scale up to 10 L SSF reactors ( $9.5 \times 10^7$  CFU·g<sup>-1</sup> DM;  $1.1 \times 10^8$  spores·g<sup>-1</sup> DM) and substantially reduced the production costs and facilitated the waste management [166].

#### 5.4. Biosurfactant Production

The production of biosurfactants during recent years has received great attention due to their eco-friendly features such as low toxicity, highly efficiency, and high biodegradability, contrary to the chemical synthesis of surfactants that mainly come from petroleum [167]. They are involved in various applications including environmental, food, household, agricultural, biomedical, cosmetics and the pharmaceutical industries. Since the emergence of biosurfactants, submerged fermentation has been a dominant research field in the manufacture of biosurfactants. However, during SmF, apart from having low yields and diluted product streams, severe foaming and a gradual increase in viscosity can occur [5]. The addition of chemical antifoams to overcome the problem implies a negative effect on the production of biosurfactants [168]. However, SSF can avoid the foaming problems during biosurfactant production, among other advantages such as low production costs, reduced waste water effluent, and no dilution problems.

Fungi, yeasts, and bacteria are able to produce biosurfactants (e.g., rhamnolipids, surfactin, sophorolipids, and peptidolipids) as secondary metabolites during their growth. Production of biosurfactants (surfactin and rhamnolipids) by *Pleurotus djamor* on sunflower seed shells as substrates supplemented with sunflower seed oil as carbon source has been reported under SSF [169]. A reduction in water surface tension from 72 to 29 mN·m<sup>-1</sup> with 10.2 g·L<sup>-1</sup> of biosurfactants was produced. Also, their ability to remove 77% of waste frying oil from contaminated sand was demonstrated. A mixture of two by-products of olive mill factory (olive leaf residues and olive cake flour) was utilized as a substrate for *Bacillus subtilis* cultivation in SSF [170]. The results showed a potential to produce lipopeptides as 30.67 mg·g<sup>-1</sup> dry substrate within 48 h, while at the same duration higher production of lipopeptides (50.01 mg·g<sup>-1</sup> dry substrate) by *Bacillus amyloliquefaciens* on rice straw and soybean flour by SSF was obtained [171]. Additionally, in a 1000-fold scale up of surfactin production by *B. amyloliquefaciens* on rice straw and soybean mixtures reached 15.03 mg·g<sup>-1</sup> dry substrate [172], which was higher than the production by *Bacillus pumilus* in SSF using okara and sugarcane bagasse that yielded about 3.3 g·kg<sup>-1</sup> dry substrate [173].

Various organic solid wastes can be utilized in SSF to produce diverse biosurfactants. For instance, soy processing waste cultivated with two different microorganisms showed that *Candida guilliermondii* produced a glycolipids complex while *B. subtilis* produced lipoprotein and glycolipids [174]. Also, *B. subtilis* was reported to yield lipopeptide biosurfactants when cultivated on potato peel from kitchen organic wastes [175]. Maximum yield of sophorolipids (18 g·mg<sup>-1</sup> dry substrate) was attained by the cultivation of *Starmerella bombicola* on a mixture of wheat bran, glucose and oleic acid [176]. It was reported that by employing an intermittent mixing in SSF during the fermentation the production of sophorolipids increased in a 31% [177]. Moreover, the cultivation of *Pseudomonas aeruginosa* on a mixture of sugarcane bagasse and corn bran supplemented with glycerol and soybean oil in SSF produced 45 g·L<sup>-1</sup> of rhamnolipids [178].

In general, the utilization of low-cost materials such as solid organic wastes impregnated with appropriate carbon and nitrogen sources together with a suitable microorganism play a key factor towards efficient biosurfactant production by SSF.

### 5.5. Bioethanol Production

Bioconversion of organic solid wastes instead of food source using SSF for bioethanol production is suitable and attractive for sustainability and renewable energy production. Several authors have proved the efficiency of SSF in the reduction of capital costs and consumption of energy and water during bioethanol production. The process also offers a valorization of organic solid wastes, the elimination of sugar extraction and additional separation steps, a production of higher yield and a simplification of the operation by carrying out the hydrolysis and the fermentation together.

Both yeast and fungi are the most reported microorganisms involved in bioethanol production due to their convenient environment in SSF. *Saccharomyces cerevisiae* yeast has been extensively reported as a responsible organism for the bioconversion of solid wastes (apple pomace, grape pomace, sugar beet pomace, potato peel, sweet sorghum stalks, sugarcane bagasse, food waste, etc.) into bioethanol production under SSF [54,179–183]. Du et al. [181] confirmed the feasibility of scaling up the bioconversion of sweet sorghum stalks by *S. cerevisiae* from 500 mL to a 127 m<sup>3</sup> rotary drum fermenter and subsequently in a 550 m<sup>3</sup> rotary drum fermenter with 88% of relative theoretical ethanol yield in less than 20 h. Anjani et al. [180] presented an interesting integrated bioconversion of potato peel by SSF for the production of bioethanol and manure by employing yeast and fungi (*Aspergillus niger*, *A. variabilis* and *S. cerevisiae*) in an effort to achieve zero waste generation. In Asian regions, palm oil trunk [184], rice straw [185,186], and banana pseudo stem [187] were successfully utilized to produce bioethanol with high yield (84%) by *Aspergillus* sp. and *T. reesei* through SSF.

Production of bioethanol in SSF has proved to achieve higher yields compared to SmF. For instance, the ethanol yield in a bioconversion of grape and sugar beet pomace was more than 82% obtained at 48 h and was higher than in liquid fermentations [179]. Also, the ethanol obtained was more concentrated than in SmF reducing the recovery costs. The utilization of the whole fermented medium containing an enzyme cocktail from *Trichoderma reesei*, *A. niger*, *A. oryzae* [188], and *Kluyveromyces marxianus* [189] evidenced an efficient cost reduction by reducing enzyme extraction that enables the use of a single reactor system in SSF. Likewise, a consolidated bioprocess integrating enzyme production, saccharification, and fermentation for bioethanol production in SSF by *Trichoderma* sp., *Penicillium* sp., and *S. cerevisiae* avoided enzyme preparation, and reduced energy consumption and equipment investment [183].

Apart from yeast and fungi, other attempts have been made using bacterial strains to produce bioethanol that resulted in efficient bioconversion. In fact, an integrated bioconversion process of organic solid wastes (switchgrass and sweet sorghum bagasse) by *Clostridium phytofermentans* [190] and *Zymomonas mobilis* [191,192] competently resulted in a high bioethanol yield through SSF.

### 5.6. Aroma Compounds Production

There is a wide spectrum of application of aroma compounds in food, cosmetic, chemical, and pharmaceutical fields. Normally, aroma compounds have been produced by steam distillation and extraction of natural sources (e.g., plants, fruits, herbs, spices). Yet, the extraction of natural sources often gives various problems and low yields of the desired compounds that increase the downstream costs [193]. Although chemical synthesis may offer an economical price compared to natural extraction, environmental problems due to the manufacturing processes and the resolution of racemic mixtures are difficult to solve [194].

The range of aroma compounds such as fruit-like or flower-like depends largely on the strains and conditions [1]. Various fungi, yeast, and bacteria have the capability to produce aroma compounds such as *Ceratocystis fimbriata*, *Aspergillus* sp., *Neurospora* sp., *Kluyveromyces marxianus*, *Bacillus subtilis*, etc. [194]. The use of different yeast strains promotes the formation of the desired aroma compounds. Apple pomace inoculated with *Saccharomyces cerevisiae*, *Hanseniaspora valbyensis*, and *Hanseniaspora uvarum* indicated that a high level of fatty acids and their corresponding ethyl esters could be obtained with *Saccharomyces* strains. Also, substrate inoculated with *Hanseniaspora* sp. gave a high level of acetic esters and 132 volatile compounds belonging to different chemical families were

identified by chromatographic analysis [195]. Apart from that, in the SSF process with food industry waste mixtures as a substrate for cultivation of *S. cerevisiae*, *K. marxianus* and kefir respectively, the production of  $\epsilon$ -pinene was only observed as a product of kefir fermentation yielding a high amount (4208 mg·kg<sup>-1</sup> of SSF product) [196]. Several authors have demonstrated the production of fruity aroma compounds by *C. fimbriata* in SSF using coffee residues (coffee husk, coffee pulp) as substrates [197,198]. Steam treated coffee husk is appropriate for aroma production by *C. fimbriata* supplemented with 20% of glucose concentration, while the addition of leucine improves the aroma intensity by 58%, especially by increasing the ester production [199]. The production of fruity aroma compounds was increased (99.60  $\mu\text{mol}\cdot\text{g}^{-1}$ ) using waste from citric juice production industry (citric pulp) cultivated with *C. fimbriata* by SSF supplemented with 50% of soya bran as a nitrogen source and 25% of sugarcane molasses as a carbon source [200]. This yield is higher than other ones reported in previous studies using other solid substrates [197]. The influence of oxygen on the total volatile compounds was demonstrated in studies carried out using cassava bagasse as a substrate for *K. marxianus* in SSF using packed bed reactors. Nine major fruity aroma compounds were identified, the lower aeration rates (0.06 L·h<sup>-1</sup>·g<sup>-1</sup> of initial dry matter) being responsible for an increase in total volatile compound production [201].

SSF has become a preferable method to produce aroma compounds as it can supply a natural condition for microbials to grow and also yields a higher concentration of aroma compounds compared to SmF. For instance, the production of 6-pentyl- $\alpha$ -pyrone (6-PP), which is related to coconut smells, by *Trichoderma* sp. was compared in SSF and SmF. Sugarcane bagasse was used as a solid support for SSF reaching a higher yield of 6-PP concentration (3.0  $\pm$  0.5 mg·g<sup>-1</sup> DM) with no evidence of growth inhibition compared to that reported in the literature for SmF [202]. Other studies using *T. viridae* showed that increasing the concentration of sugarcane bagasse produced a significant increase in the 6-PP production (3.62 mg·g<sup>-1</sup> DM) after five days of fermentation. This production was higher than those reported in previous studies under the same fermentation conditions [203], whereas less 6-PP production by *T. harzianum* IOC 4042 using the same support was reported (0.093 mg·g<sup>-1</sup> DM) after seven days of fermentation [204]. Comparative analysis of production of aroma compounds by *Pleurotus ostreatus* JMO 95 fruit body and its mycelium obtained under SmF and SSF (agar and sugarcane bagasse) showed that the main aromatic compounds octan-3-one (sweet and fruity odor), octan-3-ol (hazelnut and sweet herbaceous odor) were produced in the same proportions on the agar surface and on the solid support culture. However, in liquid fermentation, the aromatic intensity produced was very low [205]. The cultivation of *P. ostreatus* and *Favolus tenuiculus* by SSF using eucalyptus waste from the essential oil industry as a substrate was able to transform 1,8-cineole to new aroma compounds which were 1,3,3-trimethyl-2-oxabicyclo[2.2.2]octan-6-ol and 1,3,3-trimethyl-2-oxabicyclo[2.2.2] octan-6-one [206].

## 6. Downstream Processing in SSF and Residue Reutilization

Downstream processing is the processes involved after the fermentation process mainly bioseparations such as extraction, purification, and recovery. There are few studies reporting on downstream processing in SSF which hampers the process development in up-scaling. Not to mention the downstream processing that usually implies the need for additional processes and facilities that represent a cost up to 70% of production cost [207]. Since SSF is performed in limited or absence of liquid, an extraction with an appropriate solvent is necessary to recover secreted products that bind to the solid substrates. For this reason, extraction efficiency is crucial in order to obtain the maximum product-recovery from SSF. Dhillon et al. [208] achieved higher citric acid extraction from the SSF process using response surface methodology involving process parameters such as extraction time, agitation rate, and solvent volume. Solid-liquid ratio, solvent or buffer type, pH, temperature, stirring rate, repeated extraction, and extraction time are process parameters that also have been studied to optimize the extraction of products from SSF [209–214]. However, in these studies usually a small amount of solid substrate ranging from 1–20 g in a shake flask was used for the extraction, and only

some of them reported the extraction using the whole substrate fermented (in kg) with the aim of knowing the total recovery of the product [20]. This assessment is considerably important since it affects the extraction efficiency and product recovery from SSF. To point out, it was reported in a scale up system, there was a reduction of product activity per gram of dry substrate of about 60% compared to the activity obtained at the lab scale, yet the total product activity obtained was high [215].

Szabo et al. [216] found that sonication has a significant effect on enzyme extraction. They observed that multiple extractions with sonication improved the recovery of enzymes from SSF with an increment of enzyme yield more than twice that of conventional single stage extraction. Furthermore, in order to improve the enzyme recovery from SSF, it has been observed that extraction followed by diafiltration can enhance the activity recovery by removing inhibitory phenolic compounds from extracts [217]. Since the recovery and concentration steps are significant in enzyme production, employing ultrafiltration with 10 kDa cut off after solid–liquid extraction can improve the rate of enzyme recovery by about 74% [20,218]. Moreover, the recovery of biosurfactant such as sophorolipid from SSF can be improved by employing solid–liquid extraction using methanol followed by multiple re-extractions of the fermented material with ethyl acetate with continuous mixing for 1 h, subsequently filtered using 0.2  $\mu\text{m}$  membrane filtration [219]. The resulting crude extracts were further purified using a rotary evaporator at 40 °C to remove any solvent. Then, hexane was used to wash the remaining hydrophobic residue after vacuum drying and the partially purified sophorolipid was obtained after vaporizing the residual hexane at 40 °C under vacuum [220].

An innovation of downstream processing in SSF has been proposed using a simultaneous extraction and recovery of products scheme [207]. In this method, the enzyme was produced through SSF followed by a combined separation method (simultaneous extraction and recovery) based on aphron flotation. Briefly, the colloidal gas aphron (CGA) was generated by mixing solid biomass from SSF with distilled water and aluminum sulfate as a flocculating agent. Then the purified enzyme was recovered by filtration (Figure 2b). This method was considered straightforward by eliminating the extraction step in conventional SSF (Figure 2a) and producing a relatively pure enzyme. Furthermore, an efficient employment of single step aqueous two-phase extraction (ATPE) for downstream processing of enzyme produced from SSF (Figure 2c) has been reported, avoiding the conventional multi-step procedures involving salt precipitation, dialysis, and chromatography processes [221]. In addition, the high recovery of the enzyme within a short time (3 h) shows the potential commercial interest of this technique.

A novel simplified configuration for conversion of biomass to ethanol using the whole SSF cultivation medium for the hydrolysis of steam-exploded sugarcane bagasse [188]. This configuration would allow a single reactor system thus avoiding additional separation steps. The industrial production of biopolymers such as PHA (polyhydroxyalkanoate) are normally hampered by the high cost of production which involves capital investment in fermentation media and downstream processing. In this sense, SSF has been proposed as an alternative to SmF for more feasible PHA production using agro-industrial waste instead of using expensive defined media [93]. While in downstream processing an enzymatic method is more favorable compared to a chemical method due to the high recovery rate, the implementation has been limited by the high cost of the enzyme. A novel downstream separation processing using crude enzyme produced via SSF using sunflower meal as the main substrate has been proposed to reduce the high cost of PHA recovery [222]. The enzymatic lysis of bacterial cells facilitated a high recovery (98%) and purity (96.7%) of poly(3-hydroxybutyrate-co-3-hydroxyvalerate) showing that enzymatic digestion can be used as an alternative process to PHA recovery.

After the recovery of products, a solid waste with different level of biodegradability still remains once SSF processing is finished. Late work by our research group (data not published yet) indicates the possibility to reutilizing the remaining solid by composting and anaerobic digestion. The stabilization of the remaining organic matter was done by composting in the same reactors, and continuing the process until no increment in temperature was observed; the stability measured by means of the

dynamic respiration index (DRI) was lower than  $1 \text{ g O}_2 \cdot \text{kg}^{-1} \text{ OM} \cdot \text{h}^{-1}$  [20]. Solid and liquid wastes generated after enzyme extraction of SSF during the ethanol fermentation process were reutilized as a substrate for anaerobic digestion to generate biogas in a zero waste approach [223]. Moreover, it has been observed that solid residues remained after production of citric acid in SSF can be reutilized in a sequential extraction process to produce fungal chitosan as an eco-friendly alternative to the chitosan derived from marine shells [224].

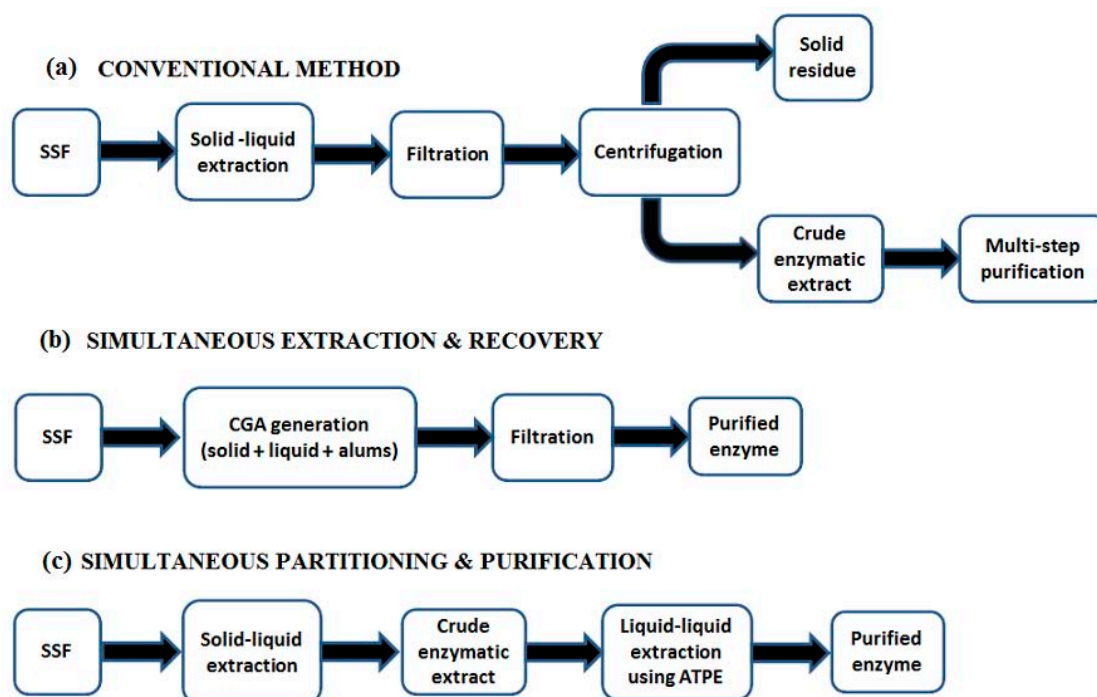


**Figure 2.** Schematic diagram of the downstream processing in SSF (a) conventional method; (b) simultaneous extraction and recovery based on aphron flotation; (c) simultaneous partitioning and purification using the ATPE system.

## 7. Economic Viewpoint

Solid state fermentation has proved to yield high biomolecules concentrations making further additional downstream processes easier than in SmF. Consequently, SSF minimized the requirements for additional equipment as well as energy and water consumption. Since the cost of substrates represents 30%–40% of total production costs [225], the valorization of organic solid waste as a substrate in SSF effectively reduces the operational costs. The superiority of SSF over SmF in several biotechnological processes poses an attractive economic feasibility. For instance, Zhuang et al. [226] compared an economic analysis of cellulase for bioethanol production through SSF and SmF. The analysis reported the unit costs for the cellulase production in SSF ( $\$15.67 \text{ kg} \cdot \text{cellulase}^{-1}$ ) and SmF ( $\$40.36 \text{ kg} \cdot \text{cellulase}^{-1}$ ), while the market price for cellulase was approximate  $\$90 \text{ kg} \cdot \text{cellulase}^{-1}$ . Comparatively, a sensitivity analysis was performed indicating that the production cost using SSF was lower than SmF with an efficiency of 99.6%. Furthermore, another report studied the economic analysis of hydrolases enzyme cocktails (amylase, cellulase, xylanase, protease) by *A. awamori* on babassu cake in SSF suggesting that solid residues or fermented cake generated after enzyme extraction can be sold as animal feed, which in turn compensates the enzyme production costs [227].

However, it does seem evident that there is an important lack of economical systematic studies on SSF economics, especially those related to the comparison between SSF and SmF.

## 8. Future Perspectives and Concluding Remarks

The use of SSF in various biotechnological processes and in the production of value-added bio-products seems very appealing and promising as reported in this review. As SSF valorizes organic solid waste, it leads to the reduction of operational and production costs, concurrently contributes to solid waste management, and decreases environmental pollution. There are various types of organic solid waste that can be easily used and converted into valuable bio-products such as enzymes, organic acids, bioethanol, biopesticides, biosurfactants, etc. by means of SSF. Apart from these evident advantages, SSF presents limited application at industrial level due to several technical aspects that need to be improved and well established, such as scientific engineering and fermentation operational control. However, with the uprising of studies related to SSF that are being currently explored, it is believed that there are numerous aspects of bioreactor technology suitable to enhance processes to compensate for the lack of application at the industrial level. With the understanding of SSF theory and the development of current SSF technology for the production of biomolecules, SSF can be considered a novel paradigm for organic solid waste valorization.

**Acknowledgments:** The authors thank the Spanish Ministerio de Economía y Competitividad (Project CTM2015-69513-R) for their financial support. N.A. Yazid thanks the Government of Malaysia and University Malaysia Pahang for their financial support. Raquel Barrena is grateful to TECNIOspring fellowship programme (no. TECSPR15-1-0051) co-financed by the European Union through the Marie Curie Actions and Acció (Generalitat de Catalunya).

**Author Contributions:** Noraziah Abu Yazid and Antoni Sánchez conceived and designed the review; Raquel Barrena, Dimitrios Komilis, and Antoni Sánchez analyzed the data and revised the paper; Noraziah Abu Yazid wrote the paper draft.

**Conflicts of Interest:** The authors declare no conflict of interest. The funding sponsors had no role in the design of the study; in the collection, analyses, or interpretation of data; in the writing of the manuscript, and in the decision to publish the results.

## References

1. Mussatto, S.I.; Ballesteros, L.F.; Martins, S.; Teixeira, J.A. Use of Agro-Industrial Wastes in Solid-State Fermentation Processes. In *Industrial Waste*; InTech: Rijeka, Croatia, 2012; pp. 121–141.
2. Eco-Cycle. *Waste of Energy-Why Incineration Is Bad for Our Economy, Environment and Community*; Eco-Cycle: Boulder County, CO, USA, 2011; pp. 1–20.
3. Sánchez, A.; Artola, A.; Font, X.; Gea, T.; Barrena, R.; Gabriel, D.; Sánchez-Monedero, M.Á.; Roig, A.; Cayuela, M.L.; Mondini, C. Greenhouse gas emissions from organic waste composting. *Environ. Chem. Lett.* **2015**, *13*, 223–238. [[CrossRef](#)]
4. Giuntini, E.; Bazzicalupo, M.; Castaldini, M.; Fabiani, A.; Miclaus, N.; Piccolo, R.; Ranalli, G.; Santomassimo, F.; Zanobini, S.; Mengoni, A. Genetic diversity of dinitrogen-fixing bacterial communities in soil amended with olive husks. *Ann. Microbiol.* **2006**, *56*, 83–88. [[CrossRef](#)]
5. Thomas, L.; Larroche, C.; Pandey, A. Current developments in solid-state fermentation. *Biochem. Eng. J.* **2013**, *81*, 146–161. [[CrossRef](#)]
6. Chen, H.Z.; He, Q. Value-added bioconversion of biomass by solid-state fermentation. *J. Chem. Technol. Biotechnol.* **2012**, *87*, 1619–1625. [[CrossRef](#)]
7. Pandey, A. Solid-state fermentation. *Biochem. Eng. J.* **2003**, *13*, 81–84. [[CrossRef](#)]
8. Hölker, U.; Lenz, J. Solid-state fermentation—Are there any biotechnological advantages? *Curr. Opin. Microbiol.* **2005**, *8*, 301–306. [[CrossRef](#)] [[PubMed](#)]
9. Pandey, A.; Soccol, C.R.; Mitchell, D. New developments in solid state fermentation: I-bioprocesses and products. *Process Biochem.* **2000**, *35*, 1153–1169. [[CrossRef](#)]
10. Wang, L.; Yang, S.-T. Chapter 18—Solid State Fermentation and Its Applications. In *Bioprocessing for Value-Added Products from Renewable Resources: New Technologies and Applications*; Elsevier B.V.: Amsterdam, The Netherlands, 2007; pp. 465–489.
11. Singhanian, R.R.; Patel, A.K.; Soccol, C.R.; Pandey, A. Recent advances in solid-state fermentation. *Biochem. Eng. J.* **2009**, *44*, 13–18. [[CrossRef](#)]



12. El-Bakry, M.; Abraham, J.; Cerda, A.; Barrena, R.; Ponsá, S.; Gea, T.; Sánchez, A. From Wastes to High Value Added Products: Novel Aspects of SSF in the Production of Enzymes. *Crit. Rev. Environ. Sci. Technol.* **2015**, *45*, 1999–2042. [[CrossRef](#)]
13. Dave, B.R.; Sudhir, A.P.; Pansuriya, M.; Raykundaliya, D.P.; Subramanian, R.B. Utilization of *Jatropha* deoiled seed cake for production of cellulases under solid-state fermentation. *Bioprocess Biosyst. Eng.* **2012**, *35*, 1343–1353. [[CrossRef](#)] [[PubMed](#)]
14. Motta, F.L.; Santana, M.H. Solid-state fermentation for humic acids production by a *Trichoderma reesei* strain using an oil palm empty fruit bunch as the substrate. *Appl. Biochem. Biotechnol.* **2014**, *172*, 2205–2217. [[CrossRef](#)] [[PubMed](#)]
15. Ohkouchi, Y.; Inoue, Y. Impact of chemical components of organic wastes on l(+)-lactic acid production. *Bioresour. Technol.* **2007**, *98*, 546–553. [[CrossRef](#)] [[PubMed](#)]
16. Zhang, W.; Zou, H.; Jiang, L.; Yao, J.; Liang, J.; Wang, Q. Semi-solid state fermentation of food waste for production of *Bacillus thuringiensis* biopesticide. *Biotechnol. Bioprocess Eng.* **2015**, *20*, 1123–1132. [[CrossRef](#)]
17. Jooste, T.; García-Aparicio, M.P.; Brienza, M.; Van Zyl, W.H.; Görgens, J.F. Enzymatic hydrolysis of spent coffee ground. *Appl. Biochem. Biotechnol.* **2013**, *169*, 2248–2262. [[CrossRef](#)] [[PubMed](#)]
18. Rocha, M.V.P.; de Matos, L.J.B.L.; De Lima, L.P.; Figueiredo, P.M.D.S.; Lucena, I.L.; Fernandes, F.A.N.; Gonçalves, L.R.B. Ultrasound-assisted production of biodiesel and ethanol from spent coffee grounds. *Bioresour. Technol.* **2014**, *167*, 343–348. [[CrossRef](#)] [[PubMed](#)]
19. Abraham, J.; Gea, T.; Sánchez, A. Substitution of chemical dehairing by proteases from solid-state fermentation of hair wastes. *J. Clean. Prod.* **2014**, *74*, 191–198. [[CrossRef](#)]
20. Yazid, N.A.; Barrena, R.; Sánchez, A. Assessment of protease activity in hydrolysed extracts from SSF of hair waste by and indigenous consortium of microorganisms. *Waste Manag.* **2016**, *49*, 420–426. [[CrossRef](#)] [[PubMed](#)]
21. Wiradimadja, R.; Rusmana, D.; Widjastuti, T.; Mushawwir, A. Chicken Slaughterhouse Waste Utilization (Chicken Feather Meal Treated) as a Source of Protein Animal Feed Ingredients in Broiler Chickens. *Lucr. Stiint.—Ser. Zooteh.* **2014**, *62*, 120–124.
22. Kanagaraj, J.; Velappan, K.C.; Chandra Babu, N.K.; Sadulla, S. Solid wastes generation in the leather industry and its utilization for cleaner environment—A review. *J. Sci. Ind. Res. (India)* **2006**, *65*, 541–548.
23. Rathna, G.S.; Saranya, R.; Kalaiselvam, M. Original Research Article Bioethanol from sawdust using cellulase hydrolysis of *Aspergillus ochraceus* and fermentation by *Saccharomyces cerevisiae*. *Int. J. Curr. Microbiol. Appl. Sci.* **2014**, *3*, 733–742.
24. Ghazi, I.; Fernandez-Arrojo, L.; Gomez De Segura, A.; Alcalde, M.; Plou, F.J.; Ballesteros, A. Beet sugar syrup and molasses as low-cost feedstock for the enzymatic production of fructo-oligosaccharides. *J. Agric. Food Chem.* **2006**, *54*, 2964–2968. [[CrossRef](#)] [[PubMed](#)]
25. Jayathilakan, K.; Sultana, K.; Radhakrishna, K.; Bawa, A.S. Utilization of byproducts and waste materials from meat, poultry and fish processing industries: A review. *J. Food Sci. Technol.* **2012**, *49*, 278–293. [[CrossRef](#)] [[PubMed](#)]
26. Kim, S.K.; Mendis, E. Bioactive compounds from marine processing byproducts—A review. *Food Res. Int.* **2006**, *39*, 383–393. [[CrossRef](#)]
27. Kandra, P.; Challa, M.M.; Kalangi Padma Jyothi, H. Efficient use of shrimp waste: Present and future trends. *Appl. Microbiol. Biotechnol.* **2012**, *93*, 17–29. [[CrossRef](#)] [[PubMed](#)]
28. Elmekawy, A.; Diels, L.; De Wever, H.; Pant, D. Valorization of cereal based biorefinery byproducts: Reality and expectations. *Environ. Sci. Technol.* **2013**, *47*, 9014–9027. [[CrossRef](#)] [[PubMed](#)]
29. Embaby, A.M.; Masoud, A.A.; Marey, H.S.; Shaban, N.Z.; Ghonaim, T.M. Raw agro-industrial orange peel waste as a low cost effective inducer for alkaline polygalacturonase production from *Bacillus licheniformis* SHG10. *Springerplus* **2014**, *3*, 327–340. [[CrossRef](#)] [[PubMed](#)]
30. Panda, S.K.; Mishra, S.S.; Kayitesi, E.; Ray, R.C. Microbial-processing of fruit and vegetable wastes for production of vital enzymes and organic acids: Biotechnology and scopes. *Environ. Res.* **2016**, *146*, 161–172. [[CrossRef](#)] [[PubMed](#)]
31. Mtui, G.Y.S. Recent advances in pretreatment of lignocellulosic wastes and production of value added products. *Afr. J. Biotechnol.* **2009**, *8*, 1398–1415.

32. Govumoni, S.P.; Gentela, J.; Koti, S.; Haragopal, V.; Venkateshwar, S.; Rao, L.V. Original Research Article Extracellular Lignocellulolytic Enzymes by *Phanerochaete chrysosporium* (MTCC 787) Under Solid-State Fermentation of Agro Wastes. *Int. J. Curr. Microbiol. Appl. Sci.* **2015**, *4*, 700–710.
33. Ukpai, P.A.; Nnabuchi, M.N. Comparative study of biogas production from cow dung, cow pea and cassava peeling using 45 litres biogas digester. *Adv. Appl. Sci. Res.* **2012**, *3*, 1864–1869.
34. Sebola, M.R.; Tesfagiorgis, H.B.; Muzenda, E. Methane Production from Anaerobic Co-digestion of Cow Dung, Chicken Manure, Pig Manure and Sewage Waste. In Proceedings of the World Congress on Engineering, London, UK, 1–3 July 2015; Volume I, pp. 1–7.
35. Adams, T.T.; Eiteman, M.A.; Hanel, B.M. Solid state fermentation of broiler litter for production of biocontrol agents. *Bioresour. Technol.* **2002**, *82*, 33–41. [[CrossRef](#)]
36. Botella, C.; Diaz, A.; de Ory, I.; Webb, C.; Blandino, A. Xylanase and pectinase production by *Aspergillus awamori* on grape pomace in solid state fermentation. *Process Biochem.* **2007**, *42*, 98–101. [[CrossRef](#)]
37. Jørgensen, H.; Sanadi, A.R.; Felby, C.; Lange, N.E.K.; Fischer, M.; Ernst, S. Production of ethanol and feed by high dry matter hydrolysis and fermentation of Palm kernel press cake. *Appl. Biochem. Biotechnol.* **2010**, *161*, 318–332. [[CrossRef](#)] [[PubMed](#)]
38. Gratuito, M.K.B.; Panyathanmaporn, T.; Chumnanklang, R.A.; Sirinuntawittaya, N.; Dutta, A. Production of activated carbon from coconut shell: Optimization using response surface methodology. *Bioresour. Technol.* **2008**, *99*, 4887–4895. [[CrossRef](#)] [[PubMed](#)]
39. Sapuan, S.M.; Harimi, M.; Maleque, M.A. Mechanical Properties of Epoxy/Coconut Shell Filler Particle Composites. *Arab. J. Sci. Eng.* **2003**, *28*, 171–181.
40. Sunil, K.S.; Vinay, D.R.; Saviraj, A.S.; Naik, P.K. Flexural Behaviour of Coconut Shell/Epoxy Composites Subjected to Accelerated Ageing. *Am. J. Mater. Sci.* **2015**, *5*, 126–132.
41. Behera, S.S.; Ray, R.C. Solid state fermentation for production of microbial cellulases: Recent advances and improvement strategies. *Int. J. Biol. Macromol.* **2016**, *86*, 656–669. [[CrossRef](#)] [[PubMed](#)]
42. De Castro, R.J.S.; Ohara, A.; Nishide, T.G.; Bagagli, M.P.; Gonçalves Dias, F.F.; Sato, H.H. A versatile system based on substrate formulation using agroindustrial wastes for protease production by *Aspergillus niger* under solid state fermentation. *Biocatal. Agric. Biotechnol.* **2015**, *4*, 678–684. [[CrossRef](#)]
43. Do-Myoung, K.; Eun, J.C.; Ji, W.K.; Yong-Woog, L.; Hwa-Jee, C. Production of cellulases by *Penicillium* sp. in a solid-state fermentation of oil palm empty fruit bunch. *Afr. J. Biotechnol.* **2014**, *13*, 145–155.
44. Mehboob, N.; Asad, M.J.; Imran, M.; Gulfray, M.; Wattoo, F.H.; Hadri, S.H.; Asghar, M. Production of lignin peroxidase by *Ganoderma leucidum* using solid state fermentation. *Afr. J. Biotechnol.* **2011**, *10*, 9880–9887.
45. Graminha, E.B.N.; Gonçalves, A.Z.L.; Pirota, R.D.P.B.; Balsalobre, M.A.A.; Da Silva, R.; Gomes, E. Enzyme production by solid-state fermentation: Application to animal nutrition. *Anim. Feed Sci. Technol.* **2008**, *144*, 1–22. [[CrossRef](#)]
46. Chang, J.; Cheng, W.; Yin, Q.; Zuo, R.; Song, A.; Zheng, Q.; Wang, P.; Wang, X.; Liu, J. Effect of steam explosion and microbial fermentation on cellulose and lignin degradation of corn stover. *Bioresour. Technol.* **2012**, *104*, 587–592. [[CrossRef](#)] [[PubMed](#)]
47. Lio, J.; Wang, T. Solid-state fermentation of soybean and corn processing coproducts for potential feed improvement. *J. Agric. Food Chem.* **2012**, *60*, 7702–7709. [[CrossRef](#)] [[PubMed](#)]
48. Nguyen, M.V.; Lee, B.K. Removal of dimethyl sulfide from aqueous solution using cost-effective modified chicken manure biochar produced from slow pyrolysis. *Sustainability* **2015**, *7*, 15057–15072. [[CrossRef](#)]
49. Demiral, H.; Demiral, İ. Surface properties of activated carbon prepared from wastes. *Surf. Interface Anal.* **2008**, *40*, 612–615. [[CrossRef](#)]
50. Liu, H.; Chen, D.; Zhang, R.; Hang, X.; Li, R.; Shen, Q. Amino Acids Hydrolyzed from Animal Carcasses Are a Good Additive for the Production of Bio-organic Fertilizer. *Front. Microbiol.* **2016**, *7*, 1–10. [[CrossRef](#)] [[PubMed](#)]
51. Daâssi, D.; Zouari-Mechichi, H.; Frikha, F.; Rodríguez-Couto, S.; Nasri, M.; Mechichi, T. Sawdust waste as a low-cost support-substrate for laccases production and adsorbent for azo dyes decolorization. *J. Environ. Heal. Sci. Eng.* **2016**, *14*, 1–12. [[CrossRef](#)] [[PubMed](#)]
52. Ravindran, B.; Kumar, A.G.; Bhavani, P.S.A.; Sekaran, G. Solid-state fermentation for the production of alkaline protease by *Bacillus cereus* 1173900 using proteinaceous tannery solid waste. *Current* **2011**, *100*, 726–730.

53. Veana, F.; Martínez-Hernández, J.L.; Aguilar, C.N.; Rodríguez-Herrera, R.; Michelena, G. Utilization of molasses and sugar cane bagasse for production of fungal invertase in solid state fermentation using *Aspergillus niger* GH1. *Braz. J. Microbiol.* **2014**, *45*, 373–377. [[CrossRef](#)] [[PubMed](#)]
54. Kanwar, S.; Kumar, G.; Sahgal, M.; Singh, A. Ethanol Production through *Saccharomyces* Based Fermentation Using Apple Pomace Amended with Molasses. *Sugar Tech.* **2012**, *14*, 304–311. [[CrossRef](#)]
55. Sathiyarayanan, G.; Kiran, G.S.; Selvin, J.; Saibaba, G. Optimization of polyhydroxybutyrate production by marine *Bacillus megaterium* MSBN04 under solid state culture. *Int. J. Biol. Macromol.* **2013**, *60*, 253–261. [[CrossRef](#)] [[PubMed](#)]
56. Mandalari, G.; Bisignano, G.; Lo Curto, R.B.; Waldron, K.W.; Faulds, C.B. Production of feruloyl esterases and xylanases by *Talaromyces stipitatus* and *Humicola grisea* var. *thermoidea* on industrial food processing by-products. *Bioresour. Technol.* **2008**, *99*, 5130–5133. [[PubMed](#)]
57. Singh, A.; Kuila, A.; Adak, S.; Bishai, M.; Banerjee, R. Utilization of Vegetable Wastes for Bioenergy Generation. *Agric. Res.* **2012**, *1*, 213–222. [[CrossRef](#)]
58. Suresh, P.V.; Anil Kumar, P.K. Enhanced degradation of a-chitin materials prepared from shrimp processing byproduct and production of *N*-acetyl-D-glucosamine by thermoactive chitinases from soil mesophilic fungi. *Biodegradation* **2012**, *23*, 597–607. [[CrossRef](#)] [[PubMed](#)]
59. Nidheesh, T.; Pal, G.K.; Suresh, P.V. Chitooligomers preparation by chitosanase produced under solid state fermentation using shrimp by-products as substrate. *Carbohydr. Polym.* **2015**, *121*, 1–9. [[CrossRef](#)] [[PubMed](#)]
60. Esakkiraj, P.; Usha, R.; Palavesam, A.; Immanuel, G. Solid-state production of esterase using fish processing wastes by *Bacillus altitudinis* AP-MSU. *Food Bioprod. Process.* **2012**, *90*, 370–376. [[CrossRef](#)]
61. Uçkun Kiran, E.; Trzcinski, A.P.; Liu, Y. Glucoamylase production from food waste by solid state fermentation and its evaluation in the hydrolysis of domestic food waste. *Biofuel Res. J.* **2014**, *3*, 98–105. [[CrossRef](#)]
62. Melikoglu, M.; Lin, C.S.K.; Webb, C. Solid state fermentation of waste bread pieces by *Aspergillus awamori*: Analysing the effects of airflow rate on enzyme production in packed bed bioreactors. *Food Bioprod. Process.* **2015**, *95*, 63–75. [[CrossRef](#)]
63. Cerda, A.; El-Bakry, M.; Gea, T.; Sánchez, A. Long term enhanced solid-state fermentation: Inoculation strategies for amylase production from soy and bread wastes by *Thermomyces* sp. in a sequential batch operation. *J. Environ. Chem. Eng.* **2016**, *4*, 2394–2401. [[CrossRef](#)]
64. Janveja, C.; Rana, S.S.; Soni, S.K. Optimization of valorization of biodegradable kitchen waste biomass for production of fungal cellulase system by statistical modeling. *Waste Biomass Valoriz.* **2014**, *5*, 807–821. [[CrossRef](#)]
65. Abdullah, J.J.; Greetham, D.; Pensupa, N.; Tucker, G.A.; Du, C. Optimizing Cellulase Production from Municipal Solid Waste (MSW) using Solid State Fermentation (SSF). *J. Fundam. Renew. Energy Appl.* **2016**, *6*, 206. [[CrossRef](#)]
66. Mantzouridou, F.T.; Paraskevopoulou, A.; Lalou, S. Yeast flavour production by solid state fermentation of orange peel waste. *Biochem. Eng. J.* **2015**, *101*, 1–8. [[CrossRef](#)]
67. Matsakas, L.; Kekos, D.; Loizidou, M.; Christakopoulos, P. Utilization of household food waste for the production of ethanol at high dry material content. *Biotechnol. Biofuels* **2014**, *7*, 4–13. [[CrossRef](#)] [[PubMed](#)]
68. Matsakas, L.; Christakopoulos, P. Ethanol production from enzymatically treated dried food waste using enzymes produced on-site. *Sustainability* **2015**, *7*, 1446–1458. [[CrossRef](#)]
69. Sun, Z.; Li, M.; Qi, Q.; Gao, C.; Lin, C.S.K. Mixed Food Waste as Renewable Feedstock in Succinic Acid Fermentation. *Appl. Biochem. Biotechnol.* **2014**, *174*, 1822–1833. [[CrossRef](#)] [[PubMed](#)]
70. Ezejiolor, T.I.N.; Duru, C.I.; Asagbra, A.E.; Ezejiolor, A.N.; Orisakwe, O.E.; Afonne, J.O.; Obi, E. Waste to wealth: Production of oxytetracycline using streptomyces species from household kitchen wastes of agricultural produce. *Afr. J. Biotechnol.* **2012**, *11*, 10115–10124.
71. López-Pérez, M.; Viniegra-González, G. Production of protein and metabolites by yeast grown in solid state fermentation: Present status and perspectives. *J. Chem. Technol. Biotechnol.* **2016**, *91*, 1224–1231. [[CrossRef](#)]
72. Martins, S.; Mussatto, S.I.; Martínez-Avila, G.; Montañez-Saenz, J.; Aguilar, C.N.; Teixeira, J.A. Bioactive phenolic compounds: Production and extraction by solid-state fermentation. A review. *Biotechnol. Adv.* **2011**, *29*, 365–373. [[CrossRef](#)] [[PubMed](#)]
73. Liu, D.; Zhang, R.; Yang, X.; Wu, H.; Xu, D.; Tang, Z.; Shen, Q. Thermostable cellulase production of *Aspergillus fumigatus* Z5 under solid-state fermentation and its application in degradation of agricultural wastes. *Int. Biodeterior. Biodegrad.* **2011**, *65*, 717–725. [[CrossRef](#)]

74. Ávila-Cisneros, N.; Velasco-Lozano, S.; Huerta-Ochoa, S.; Córdova-López, J.; Gimeno, M.; Favela-Torres, E. Production of Thermostable Lipase by *Thermomyces lanuginosus* on Solid-State Fermentation: Selective Hydrolysis of Sardine Oil. *Appl. Biochem. Biotechnol.* **2014**, *174*, 1859–1872. [[CrossRef](#)] [[PubMed](#)]
75. Saqib, A.A.N.; Farooq, A.; Iqbal, M.; Hassan, J.U.; Hayat, U.; Baig, S. A thermostable crude endoglucanase produced by *aspergillus fumigatus* in a novel solid state fermentation process using isolated free water. *Enzyme Res.* **2012**, *2012*, 1–6. [[CrossRef](#)] [[PubMed](#)]
76. Tsegaye, K.N.; Gessesse, A. Amylase production under solid state fermentation by a bacterial isolate W74. *Afr. J. Biotechnol.* **2014**, *13*, 2145–2153.
77. Afrisham, S.; Badoei-Dalfard, A.; Namaki-Shoushtari, A.; Karami, Z. Characterization of a thermostable, CaCl<sub>2</sub>-activated and raw-starch hydrolyzing alpha-amylase from *Bacillus licheniformis* AT70: Production under solid state fermentation by utilizing agricultural wastes. *J. Mol. Catal. B Enzym.* **2016**, *132*, 98–106. [[CrossRef](#)]
78. Özdemir, S.; Matpan, F.; Okumus, V.; DüNDAR, A.; Ulutas, M.S.; Kumru, M. Isolation of a thermophilic *Anoxybacillus flavithermus* sp. nov. and production of thermostable  $\alpha$ -amylase under solid-state fermentation (SSF). *Ann. Microbiol.* **2012**, *62*, 1367–1375.
79. Prajapati, V.S.; Trivedi, U.B.; Patel, K.C. A statistical approach for the production of thermostable and alklophilic alpha-amylase from *Bacillus amyloliquefaciens* KCP2 under solid-state fermentation. *3 Biotech* **2015**, *5*, 211–220. [[CrossRef](#)]
80. Das, R.K.; Brar, S.K.; Verma, M. Potential use of pulp and paper solid waste for the bio-production of fumaric acid through submerged and solid state fermentation. *J. Clean. Prod.* **2016**, *112*, 4435–4444. [[CrossRef](#)]
81. Bhalkar, B.N.; Bedekar, P.A.; Kshirsagar, S.D.; Govindwar, S.P. Solid state fermentation of soybean waste and an up-flow column bioreactor for continuous production of camptothecine by an endophytic fungus: *Fusarium oxysporum*. *RSC Adv.* **2016**, *6*, 56527–56536. [[CrossRef](#)]
82. De Castro, R.J.S.; Sato, H.H. Enzyme Production by Solid State Fermentation: General Aspects and an Analysis of the Physicochemical Characteristics of Substrates for Agro-industrial Wastes Valorization. *Waste Biomass Valoriz.* **2015**, *6*, 1085–1093. [[CrossRef](#)]
83. Orzua, M.C.; Mussatto, S.I.; Contreras-Esquível, J.C.; Rodriguez, R.; de la Garza, H.; Teixeira, J.A.; Aguilar, C.N. Exploitation of agro industrial wastes as immobilization carrier for solid-state fermentation. *Ind. Crops Prod.* **2009**, *30*, 24–27. [[CrossRef](#)]
84. Abraham, J.; Gea, T.; Sánchez, A. Potential of the solid-state fermentation of soy fiber residues by native microbial populations for bench-scale alkaline protease production. *Biochem. Eng. J.* **2013**, *74*, 15–19. [[CrossRef](#)]
85. Viniegra-González, G.; Favela-Torres, E.; Aguilar, C.N.; Romero-Gomez, S.D.J.; Díaz-Godínez, G.; Augur, C. Advantages of fungal enzyme production in solid state over liquid fermentation systems. *Biochem. Eng. J.* **2003**, *13*, 157–167. [[CrossRef](#)]
86. Hölker, U.; Höfer, M.; Lenz, J. Biotechnological advantages of laboratory-scale solid-state fermentation with fungi. *Appl. Microbiol. Biotechnol.* **2004**, *64*, 175–186. [[CrossRef](#)] [[PubMed](#)]
87. Gabelle, J.C.; Jourdir, E.; Licht, R.B.; Ben Chaabane, F.; Henaut, I.; Morchain, J.; Augier, F. Impact of rheology on the mass transfer coefficient during the growth phase of *Trichoderma reesei* in stirred bioreactors. *Chem. Eng. Sci.* **2012**, *75*, 408–417. [[CrossRef](#)]
88. De la Cruz Quiroz, R.; Roussos, S.; Hernández, D.; Rodríguez, R.; Castillo, F.; Aguilar, C.N. Challenges and opportunities of the bio-pesticides production by solid-state fermentation: *Filamentous fungi* as a model. *Crit. Rev. Biotechnol.* **2015**, *35*, 326–333. [[CrossRef](#)] [[PubMed](#)]
89. Hongzhang, C.; Hongqiang, L.; Liying, L. The inhomogeneity of corn stover and its effects on bioconversion. *Biomass Bioenergy* **2011**, *35*, 1940–1945. [[CrossRef](#)]
90. Raghavarao, K.S.M.; Ranganathan, T.; Karanth, N. Some engineering aspects of solid-state fermentation. *Biochem. Eng. J.* **2003**, *13*, 127–135. [[CrossRef](#)]
91. Mansour, A.A.; Arnaud, T.; Lu-Chau, T.A.; Fdz-Polanco, M.; Moreira, M.T.; Rivero, J.A.C. Review of solid state fermentation for lignocellulolytic enzyme production: Challenges for environmental applications. *Rev. Environ. Sci. Biotechnol.* **2016**, *15*, 31–46. [[CrossRef](#)]
92. Rahardjo, Y.S.P.; Korona, D.; Haemers, S.; Weber, F.J.; Tramper, J.; Rinzema, A. Limitations of membrane cultures as a model solid-state fermentation system. *Lett. Appl. Microbiol.* **2004**, *39*, 504–508. [[CrossRef](#)] [[PubMed](#)]

93. Sindhu, R.; Pandey, A.; Binod, P. Solid-state Fermentation for the Production of Poly(hydroxyalkanoates). *Chem. Biochem. Eng. Q.* **2015**, *29*, 173–181. [[CrossRef](#)]
94. Ortiz, G.E.; Guitart, M.E.; Cavalitto, S.F.; Albertó, E.O.; Fernández-Lahore, M.; Blasco, M. Characterization, optimization, and scale-up of cellulases production by *trichoderma reesei* cbs 836.91 in solid-state fermentation using agro-industrial products. *Bioprocess Biosyst. Eng.* **2015**, *38*, 2117–2128. [[PubMed](#)]
95. Salihu, A.; Sallau, A.B.; Adamu, A.; Kudu, F.A.; Tajo, M.M.; Bala, T.F.; Yashim, W.D. Utilization of Groundnut Husk as a Solid Substrate for Cellulase Production by *Aspergillus niger* Using Response Surface Methodology. *Waste Biomass Valoriz.* **2014**, *5*, 585–593. [[CrossRef](#)]
96. Sun, H.-Y.; Li, J.; Zhao, P.; Peng, M. Banana peel: A novel substrate for cellulase production under solid-state fermentation. *Afr. J. Biotechnol.* **2011**, *10*, 17887–17890.
97. Zhou, H.; Wang, C.Z.; Ye, J.Z.; Chen, H.X.; Tao, R.; Zhang, Y.S. Solid-state fermentation of *Ginkgo biloba* L. residue for optimal production of cellulase, protease and the simultaneous detoxification of *Ginkgo biloba* L. residue using *Candida tropicalis* and *Aspergillus oryzae*. *Eur. Food Res. Technol.* **2015**, *240*, 379–388.
98. Bansal, N.; Janveja, C.; Tewari, R.; Soni, R.; Soni, S.K. Highly thermostable and pH-stable cellulases from *Aspergillus niger* NS-2: Properties and application for cellulose hydrolysis. *Appl. Biochem. Biotechnol.* **2014**, *172*, 141–156. [[CrossRef](#)] [[PubMed](#)]
99. Dave, B.R.; Parmar, P.; Sudhir, A.; Singal, N.; Subramanian, R.B. Cellulases production under solid state fermentation using agro waste as a substrate and its application in saccharification by *Trametes hirsuta* NCIM. *J. Microbiol. Biotechnol. Food Sci.* **2015**, *4*, 203–208. [[CrossRef](#)]
100. Gasparotto, J.M.; Werle, L.B.; Foletto, E.L.; Kuhn, R.C.; Jahn, S.L.; Mazutti, M.A. Production of Cellulolytic Enzymes and Application of Crude Enzymatic Extract for Saccharification of Lignocellulosic Biomass. *Appl. Biochem. Biotechnol.* **2015**, *175*, 560–572. [[CrossRef](#)] [[PubMed](#)]
101. Pathak, P.; Bhardwaj, N.K.; Singh, A.K. Production of crude cellulase and xylanase from *Trichoderma harzianum* PPDDN10 NFCCI-2925 and its application in photocopier waste paper recycling. *Appl. Biochem. Biotechnol.* **2014**, *172*, 3776–3797. [[CrossRef](#)] [[PubMed](#)]
102. Raghuwanshi, S.; Deswal, D.; Karp, M.; Kuhad, R.C. Bioprocessing of enhanced cellulase production from a mutant of *Trichoderma asperellum* RCK2011 and its application in hydrolysis of cellulose. *Fuel* **2014**, *124*, 183–189. [[CrossRef](#)]
103. Sandhu, S.K.; Oberoi, H.S.; Babbar, N.; Miglani, K.; Chadha, B.S.; Nanda, D.K. Two-Stage Statistical Medium Optimization for Augmented Cellulase Production via Solid-State Fermentation by Newly Isolated *Aspergillus niger* HN-1 and Application of Crude Cellulase Consortium in Hydrolysis of Rice Straw. *J. Agric. Food Chem.* **2013**, *61*, 12653–12661. [[CrossRef](#)] [[PubMed](#)]
104. Saratale, G.D.; Kshirsagar, S.D.; Sampange, V.T.; Saratale, R.G.; Oh, S.E.; Govindwar, S.P.; Oh, M.K. Cellulolytic Enzymes Production by Utilizing Agricultural Wastes Under Solid State Fermentation and its Application for Biohydrogen Production. *Appl. Biochem. Biotechnol.* **2014**, *174*, 2801–2817. [[CrossRef](#)] [[PubMed](#)]
105. Kumar, A.; Dutt, D.; Gautam, A. Production of crude enzyme from *Aspergillus nidulans* AKB-25 using black gram residue as the substrate and its industrial applications. *J. Genet. Eng. Biotechnol.* **2016**, *14*, 107–118. [[CrossRef](#)]
106. Anto, H.; Trivedi, U.B.; Patel, K.C. Glucoamylase production by solid-state fermentation using rice flake manufacturing waste products as substrate. *Bioresour. Technol.* **2006**, *97*, 1161–1166. [[CrossRef](#)] [[PubMed](#)]
107. Melikoglu, M.; Lin, C.S.K.; Webb, C. Stepwise optimisation of enzyme production in solid state fermentation of waste bread pieces. *Food Bioprod. Process.* **2013**, *91*, 638–646. [[CrossRef](#)]
108. Saxena, R.; Singh, R. Amylase production by solid-state fermentation of agro-industrial wastes using *Bacillus* sp. *Braz. J. Microbiol.* **2011**, *42*, 1334–1342. [[CrossRef](#)] [[PubMed](#)]
109. Pandi, A.; Ramalingam, S.; Rao, R. Inexpensive  $\alpha$ -amylase production and application for fiber splitting in leather processing. *RSC Adv.* **2016**, *6*, 33170–33176. [[CrossRef](#)]
110. Singh, S.; Singh, S.; Bali, V.; Sharma, L.; Mangla, J. Production of fungal amylases using cheap, readily available agriresidues, for potential application in textile industry. *BioMed Res. Int.* **2014**, *2014*, 1–9. [[CrossRef](#)] [[PubMed](#)]
111. De Castro, R.J.S.; Sato, H.H. Production and biochemical characterization of protease from *Aspergillus oryzae*: An evaluation of the physical-chemical parameters using agroindustrial wastes as supports. *Biocatal. Agric. Biotechnol.* **2014**, *3*, 20–25. [[CrossRef](#)]

112. Mahanta, N.; Gupta, A.; Khare, S.K. Production of protease and lipase by solvent tolerant *Pseudomonas aeruginosa* PseA in solid-state fermentation using *Jatropha curcas* seed cake as substrate. *Bioresour. Technol.* **2008**, *99*, 1729–1735. [[CrossRef](#)] [[PubMed](#)]
113. Novelli, P.K.; Barros, M.M.; Fleuri, L.F. Novel inexpensive fungi proteases: Production by solid state fermentation and characterization. *Food Chem.* **2016**, *198*, 119–124. [[CrossRef](#)] [[PubMed](#)]
114. Prakasham, R.S.; Rao, C.S.; Sarma, P.N. Green gram husk-an inexpensive substrate for alkaline protease production by *Bacillus* sp. in solid-state fermentation. *Bioresour. Technol.* **2006**, *97*, 1449–1454. [[PubMed](#)]
115. Da Silva, R.R.; de Freitas Cabral, T.P.; Rodrigues, A.; Cabral, H. Production and partial characterization of serine and metallo peptidases secreted by *Aspergillus fumigatus* Fresenius in submerged and solid state fermentation. *Braz. J. Microbiol.* **2013**, *44*, 235–243. [[CrossRef](#)] [[PubMed](#)]
116. Vijayaraghavan, P.; Lazarus, S.; Vincent, S.G.P. De-hairing protease production by an isolated *Bacillus cereus* strain AT under solid-state fermentation using cow dung: Biosynthesis and properties. *Saudi J. Biol. Sci.* **2014**, *21*, 27–34. [[CrossRef](#)] [[PubMed](#)]
117. El-Bakry, M.; Gea, T.; Sánchez, A. Inoculation effect of thermophilic microorganisms on protease production through solid-state fermentation under non-sterile conditions at lab and bench scale (SSF). *Bioprocess Biosyst. Eng.* **2016**, *39*, 585–592. [[CrossRef](#)] [[PubMed](#)]
118. Verma, A.; Ansari, M.W.; Anwar, M.S.; Agrawal, R.; Agrawal, S. Alkaline protease from *Thermoactinomyces* sp. RS1 mitigates industrial pollution. *Protoplasma* **2014**, *251*, 711–718. [[PubMed](#)]
119. Paul, T.; Das, A.; Mandal, A.; Jana, A.; Maity, C.; Adak, A.; Halder, S.K.; DasMohapatra, P.K.; Pati, B.R.; Mondal, K.C. Effective dehairing properties of keratinase from *Paenibacillus woosongensis* TKB2 obtained under solid state fermentation. *Waste Biomass Valoriz.* **2014**, *5*, 97–107. [[CrossRef](#)]
120. Santis-Navarro, A.; Gea, T.; Barrena, R.; Sánchez, A. Production of lipases by solid state fermentation using vegetable oil-refining wastes. *Bioresour. Technol.* **2011**, *102*, 10080–10084. [[CrossRef](#)] [[PubMed](#)]
121. Silveira, E.A.; Tardioli, P.W.; Farinas, C.S. Valorization of Palm Oil Industrial Waste as Feedstock for Lipase Production. *Appl. Biochem. Biotechnol.* **2016**, *179*, 558–571. [[CrossRef](#)] [[PubMed](#)]
122. Herculano, P.N.; Moreira, K.A.; Bezerra, R.P.; Porto, T.S.; de Souza-Motta, C.M.; Porto, A.L.F. Potential application of waste from castor bean (*Ricinus communis* L.) for production for xylanase of interest in the industry. *3 Biotech* **2016**, *6*, 144–154.
123. Pandya, J.J.; Gupte, A. Production of xylanase under solid-state fermentation by *Aspergillus tubingensis* JP-1 and its application. *Bioprocess Biosyst. Eng.* **2012**, *35*, 769–779. [[CrossRef](#)] [[PubMed](#)]
124. Asha Poorna, C.; Prema, P. Production of cellulase-free endoxylanase from novel alkalophilic thermotolerant *Bacillus pumilus* by solid-state fermentation and its application in wastepaper recycling. *Bioresour. Technol.* **2007**, *98*, 485–490. [[CrossRef](#)] [[PubMed](#)]
125. Zimbaridi, A.L.R.L.; Sehn, C.; Meleiro, L.P.; Souza, F.H.M.; Masui, D.C.; Nozawa, M.S.F.; Guimarães, L.H.S.; Jorge, J.A.; Furriel, R.P.M. Optimization of  $\beta$ -Glucosidase,  $\beta$ -Xylosidase and Xylanase Production by *Colletotrichum graminicola* under Solid-State Fermentation and Application in Raw Sugarcane Trash Saccharification. *Int. J. Mol. Sci.* **2013**, *14*, 2875–2902. [[CrossRef](#)] [[PubMed](#)]
126. Chen, H.Q.; Chen, X.M.; Chen, T.X.; Xu, X.M.; Jin, Z.Y. Extraction optimization of inulinase obtained by solid state fermentation of *Aspergillus ficuum* JNSP5-06. *Carbohydr. Polym.* **2011**, *85*, 446–451. [[CrossRef](#)]
127. Mazutti, M.; Bender, J.P.; Treichel, H.; Luccio, M. Di Optimization of inulinase production by solid-state fermentation using sugarcane bagasse as substrate. *Enzyme Microb. Technol.* **2006**, *39*, 56–59. [[CrossRef](#)]
128. Martínez-Morales, F.; Bertrand, B.; Pasi3n Nava, A.A.; Tinoco, R.; Acosta-Urdapilleta, L.; Trejo-Hernández, M.R. Production, purification and biochemical characterization of two laccase isoforms produced by *Trametes versicolor* grown on oak sawdust. *Biotechnol. Lett.* **2015**, *37*, 391–396. [[CrossRef](#)] [[PubMed](#)]
129. El-Gindy, A.A.; Saad, R.R.; Fawzi, E.M. Purification of  $\beta$ -xylosidase from *Aspergillus tamaritii* using ground oats and a possible application on the fermented hydrolysate by *Pichia stipitis*. *Ann. Microbiol.* **2015**, *65*, 965–974. [[CrossRef](#)]
130. L3pez, J.A.; L3zaro, C.D.C.; Castilho, L.D.R.; Freire, D.M.G.; Castro, A.M.H. De Characterization of multienzyme solutions produced by solid-state fermentation of babassu cake, for use in cold hydrolysis of raw biomass. *Biochem. Eng. J.* **2013**, *77*, 231–239. [[CrossRef](#)]

131. Kriaa, M.; Kammoun, R. Producing *Aspergillus tubingensis* CTM507 Glucose oxidase by Solid state fermentation versus submerged fermentation: Process optimization and enzyme stability by an intermediary metabolite in relation with diauxic growth. *J. Chem. Technol. Biotechnol.* **2016**, *91*, 1540–1550. [[CrossRef](#)]
132. Ali, H.K.Q.; Zulkali, M.M.D. Utilization of Agro-Residual Ligno-Cellulosic Substances by Using Solid State Fermentation: A Review. *Croat. J. Food Technol. Biotechnol. Nutr.* **2011**, *6*, 5–12.
133. Bezalwar, P.; Gomashe, A.V.; Sanap, H.M.; Gulhane, P.A. Original Research Article Production and Optimization of Citric Acid by *Aspergillus niger* using Fruit Pulp Waste *Aspergillus niger* culture maintenance. *Int. J. Curr. Microbiol. Appl. Sci.* **2013**, *2*, 347–352.
134. Goud, K.H.; Srilakshmi, A.; Kumar, P.A.; Narasimha, G. Citric acid production by *aspergillus niger* through solid state fermentation using fruit wastes. *Biotechnol. Indian J.* **2012**, *6*, 93–96.
135. Kumar, D.; Jain, V.K.; Shanker, G.; Srivastava, A. Utilization of fruits waste for citric acid production by solid state fermentation. *Process Biochem.* **2003**, *38*, 1725–1729. [[CrossRef](#)]
136. Dhillon, G.S.; Brar, S.K.; Verma, M.; Tyagi, R.D. Utilization of different agro-industrial wastes for sustainable bioproduction of citric acid by *Aspergillus niger*. *Biochem. Eng. J.* **2011**, *54*, 83–92. [[CrossRef](#)]
137. Hamdy, H.S. Citric acid production by *Aspergillus niger* grown on orange peel medium fortified with cane molasses. *Ann. Microbiol.* **2013**, *63*, 267–278. [[CrossRef](#)]
138. Karthikeyan, A.; Sivakumar, N. Citric acid production by *Koji fermentation* using banana peel as a novel substrate. *Bioresour. Technol.* **2010**, *101*, 5552–5556. [[CrossRef](#)] [[PubMed](#)]
139. Kareem, S.O.; Rahman, R.A. Utilization of banana peels for citric acid production by *Aspergillus niger*. *Agric. Biol. J. N. Am.* **2011**, *4*, 384–387. [[CrossRef](#)]
140. Torrado, A.M.; Cortes, S.; Salgado, J.M.; Max, B.; Rodriguez, N.; Bibbins, B.P.; Converti, A.; Dominguez, J.M. Citric acid production from orange peel wastes by solid-state fermentation. *Braz. J. Microbiol.* **2011**, *42*, 394–409. [[CrossRef](#)] [[PubMed](#)]
141. Krishna, C. Solid-State Fermentation Systems—An Overview. *Crit. Rev. Biotechnol.* **2005**, *25*, 1–30. [[CrossRef](#)] [[PubMed](#)]
142. Alam, M.Z.; Bari, M.N.; Muyibi, S.A.; Jamal, P.; Al-Mamun, A. Development of culture inoculum for scale-up production of citric acid from oil palm empty fruit bunches by *Aspergillus niger*. *Procedia Environ. Sci.* **2011**, *8*, 396–402. [[CrossRef](#)]
143. Yadegary, M.; Hamidi, A.; Alavi, S.A.; Khodaverdi, E.; Sattari, S.; Bagherpour, G.; Yahaghi, E. Citric acid production from sugarcane bagasse through solid state fermentation method using *Aspergillus niger* mold and optimization of citric acid production by taguchi method. *Jundishapur J. Microbiol.* **2013**, *6*, 1–6. [[CrossRef](#)]
144. Prado, F.C.; Vandenberghe, L.P.S.; Woiciechowski, A.L.; Rodrigues-Léon, J.A.; Soccol, C.R. Citric acid production by solid-state fermentation on a semi-pilot scale using different percentages of treated cassava bagasse. *Braz. J. Chem. Eng.* **2005**, *22*, 547–555. [[CrossRef](#)]
145. Schneider, M.; Zimmer, G.F.; Cremonese, E.B.; De, C.D.S.S.R.; Corbellini, V.A. By-products from the biodiesel chain as a substrate to citric acid production by solid-state fermentation. *Waste Manag. Res.* **2014**, *32*, 653–660. [[CrossRef](#)] [[PubMed](#)]
146. Hayihama, S.; Suwazono, W. The Use of *Rhizopus* sp. mutant for Lactic Acid Production by Solid State Fermentation. *KKU Res. J.* **2016**, *22*, 52–58.
147. John, R.P.; Nampoothiri, K.M.; Pandey, A. Solid-state fermentation for L-lactic acid production from agro wastes using *Lactobacillus delbrueckii*. *Process Biochem.* **2006**, *41*, 759–763. [[CrossRef](#)]
148. Rojan, P.J.; Nampoothiri, K.M.; Nair, A.S.; Pandey, A. L(+)-lactic acid production using *Lactobacillus casei* in solid-state fermentation. *Biotechnol. Lett.* **2005**, *27*, 1685–1688. [[CrossRef](#)] [[PubMed](#)]
149. Qi, B.; Yao, R. L-Lactic acid production from *Lactobacillus casei* by solid state fermentation using rice straw. *BioResources* **2007**, *2*, 419–429.
150. Altaf, M.; Naveena, B.J.; Venkateshwar, M.; Kumar, E.V.; Reddy, G. Single step fermentation of starch to L(+) lactic acid by *Lactobacillus amylophilus* GV6 in SSF using inexpensive nitrogen sources to replace peptone and yeast extract—Optimization by RSM. *Process Biochem.* **2006**, *41*, 465–472. [[CrossRef](#)]
151. Gowdhaman, D.; Sugumaran, K.R.; Ponnusami, V. Optimization of lactic acid production from tea waste by *lactobacillus plantarum* MTCC 6161 in solid state fermentation by central composite design. *Int. J. ChemTech Res.* **2012**, *4*, 143–148.
152. Ghosh, M.K.; Ghosh, U.K. Utilization of Pine needles as bed material in solid state fermentation for production of Lactic acid by *Lactobacillus* strains. *BioResources* **2011**, *6*, 1556–1575.

153. Ghosh, U.K.; Ghosh, M.K. Utilization of Wheat Bran as Bed Material in Solid State Bacterial Production of Lactic Acid with Various Nitrogen Sources. *Int. J. Biol. Biomol. Agric. Food Biotechnol. Eng.* **2012**, *6*, 90–93.
154. El-Naggar, N.E.A.; El-Hersh, M.S. Organic acids associated with saccharification of cellulosic wastes during solid-state fermentation. *J. Microbiol.* **2011**, *49*, 58–65. [[CrossRef](#)] [[PubMed](#)]
155. Mai, H.T.N.; Lee, K.M.; Choi, S.S. Enhanced oxalic acid production from corncob by a methanol-resistant strain of *Aspergillus niger* using semi solid-state fermentation. *Process Biochem.* **2016**, *51*, 9–15. [[CrossRef](#)]
156. De Vrije, T.; Antoine, N.; Buitelaar, R.M.; Bruckner, S.; Dissevelt, M.; Durand, A.; Gerlagh, M.; Jones, E.E.; Lüth, P.; Oostra, J.; et al. The fungal biocontrol agent *Coniothyrium minitans*: Production by solid-state fermentation, application and marketing. *Appl. Microbiol. Biotechnol.* **2001**, *56*, 58–68. [[CrossRef](#)] [[PubMed](#)]
157. Oostra, J.; Tramper, J.; Rinzema, A. Model-based bioreactor selection for large-scale solid-state cultivation of *Coniothyrium minitans* spores on oats. *Enzyme Microb. Technol.* **2000**, *27*, 652–663. [[CrossRef](#)]
158. Viccini, G.; Mannich, M.; Capalbo, D.M.F.; Valdebenito-Sanhueza, R.; Mitchell, D.A. Spore production in solid-state fermentation of rice by *Clonostachys rosea*, a biopesticide for gray mold of strawberries. *Process Biochem.* **2007**, *42*, 275–278. [[CrossRef](#)]
159. Zhang, Y.; Liu, J.; Zhou, Y.; Ge, Y. Spore Production of *Clonostachys rosea* in a New Solid-state Fermentation Reactor. *Appl. Biochem. Biotechnol.* **2014**, *174*, 2951–2959. [[CrossRef](#)] [[PubMed](#)]
160. Mishra, S.; Kumar, P.; Malik, A. Suitability of agricultural by-products as production medium for spore production by *Beauveria bassiana* HQ917687. *Int. J. Recycl. Org. Waste Agric.* **2016**, *5*, 179–184. [[CrossRef](#)]
161. Vijith, C.C.; Thota, S.G.; Vivek, A.T.; Gopinathan, C. Improved *Bacillus thuringiensis*-based biopesticide production using cheap carbon and nitrogen sources by solid state fermentation technique. *IOSR J. Environ. Sci. Food Technol.* **2016**, *10*, 49–53.
162. Jisha, V.N.; Benjamin, S. Solid-State Fermentation for the Concomitant Production of  $\delta$ -Endotoxin and Endospore from *Bacillus thuringiensis* subsp. *kurstaki*. *Adv. Biosci. Biotechnol.* **2014**, *5*, 797–804. [[CrossRef](#)]
163. Smitha, R.B.; Jisha, V.N.; Pradeep, S.; Josh, M.S.; Benjamin, S. Potato flour mediated solid-state fermentation for the enhanced production of *Bacillus thuringiensis*-toxin. *J. Biosci. Bioeng.* **2013**, *116*, 595–601. [[CrossRef](#)] [[PubMed](#)]
164. Zhuang, L.; Zhou, S.; Wang, Y.; Liu, Z.; Xu, R. Cost-effective production of *Bacillus thuringiensis* biopesticides by solid-state fermentation using wastewater sludge: Effects of heavy metals. *Bioresour. Technol.* **2011**, *102*, 4820–4826. [[CrossRef](#)] [[PubMed](#)]
165. Zhang, W.; Qiu, L.; Gong, A.; Cao, Y.; Wang, B. Solid-state Fermentation of Kitchen Waste for Production of *Bacillus thuringiensis*-based Bio-pesticide. *BioResources* **2013**, *8*, 1124–1135. [[CrossRef](#)]
166. Ballardó, C.; Abraham, J.; Barrena, R.; Artola, A.; Gea, T.; Sánchez, A. Valorization of soy waste through SSF for the production of compost enriched with *Bacillus thuringiensis* with biopesticide properties. *J. Environ. Manag.* **2016**, *169*, 126–131. [[CrossRef](#)] [[PubMed](#)]
167. De, S.; Malik, S.; Ghosh, A.; Saha, R.; Saha, B. A Review on Natural Surfactants. *RSC Adv.* **2015**, *5*, 65757–65767. [[CrossRef](#)]
168. Winterburn, J.B.; Martin, P.J. Foam mitigation and exploitation in biosurfactant production. *Biotechnol. Lett.* **2012**, *34*, 187–195. [[CrossRef](#)] [[PubMed](#)]
169. Velioglu, Z.; Urek, R.O. Physicochemical and structural characterization of biosurfactant produced by *Pleurotus djamor* in solid-state fermentation. *Biotechnol. Bioprocess Eng.* **2016**, *21*, 430–438. [[CrossRef](#)]
170. Zouari, R.; Ellouze-Chaabouni, S.; Ghribi-Aydi, D. Optimization of *Bacillus subtilis* SPB1 Biosurfactant Production Under Solid-state Fermentation Using By-products of a Traditional Olive Mill Factory. *Achieve Life Sci.* **2014**, *8*, 162–169. [[CrossRef](#)]
171. Zhu, Z.; Zhang, G.; Luo, Y.; Ran, W.; Shen, Q. Production of lipopeptides by *Bacillus amyloliquefaciens* XZ-173 in solid state fermentation using soybean flour and rice straw as the substrate. *Bioresour. Technol.* **2012**, *112*, 254–260. [[CrossRef](#)] [[PubMed](#)]
172. Zhu, Z.; Zhang, F.; Wei, Z.; Ran, W.; Shen, Q. The usage of rice straw as a major substrate for the production of surfactin by *Bacillus amyloliquefaciens* XZ-173 in solid-state fermentation. *J. Environ. Manag.* **2013**, *127*, 96–102. [[CrossRef](#)] [[PubMed](#)]
173. Slivinski, C.T.; Mallmann, E.; De Araújo, J.M.; Mitchell, D.A.; Krieger, N. Production of surfactin by *Bacillus pumilus* UFPEDA 448 in solid-state fermentation using a medium based on okara with sugarcane bagasse as a bulking agent. *Process Biochem.* **2012**, *47*, 1848–1855. [[CrossRef](#)]



174. Sitohy, M.Z.; Rashad, M.M.; Sharobeem, S.F.; Mahmoud, A.E.; Nooman, M.U.; Kashef, A.S. Al Bioconversion of soy processing waste for production of surfactants. *J. Microbiol.* **2010**, *4*, 2811–2821.
175. Das, K.; Mukherjee, A.K. Comparison of lipopeptide biosurfactants production by *Bacillus subtilis* strains in submerged and solid state fermentation systems using a cheap carbon source: Some industrial applications of biosurfactants. *Process Biochem.* **2007**, *42*, 1191–1199. [[CrossRef](#)]
176. Parekh, V.J.; Pandit, A.B. Solid state fermentation (SSF) for the production of sophorolipids from *Starmerella bombicola* NRRL Y-17069 using glucose, wheat bran and oleic acid. *Curr. Trends Biotechnol. Pharm.* **2012**, *6*, 418–424.
177. Jiménez-Peñalver, P.; Gea, T.; Sánchez, A.; Font, X. Production of sophorolipids from winterization oil cake by Solid-state fermentation: Optimization, monitoring and effect of mixing. *Biochem. Eng. J.* **2016**, *115*, 93–100. [[CrossRef](#)]
178. Camilios-Neto, D.; Bugay, C.; De Santana-Filho, A.P.; Joslin, T.; De Souza, L.M.; Sasaki, G.L.; Mitchell, D.A.; Krieger, N. Production of rhamnolipids in solid-state cultivation using a mixture of sugarcane bagasse and corn bran supplemented with glycerol and soybean oil. *Appl. Microbiol. Biotechnol.* **2011**, *89*, 1395–1403. [[CrossRef](#)] [[PubMed](#)]
179. Rodríguez, L.A.; Toro, M.E.; Vazquez, F.; Correa-Daneri, M.L.; Gouiric, S.C.; Vallejo, M.D. Bioethanol production from grape and sugar beet pomaces by solid-state fermentation. *Int. J. Hydrogen Energy* **2010**, *35*, 5914–5917. [[CrossRef](#)]
180. Chintagunta, A.D.; Jacob, S.; Banerjee, R. Integrated bioethanol and biomanure production from potato waste. *Waste Manag.* **2016**, *49*, 320–325. [[CrossRef](#)] [[PubMed](#)]
181. Du, R.; Yan, J.; Feng, Q.; Li, P.; Zhang, L.; Chang, S.; Li, S. A novel wild-type *Saccharomyces cerevisiae* strain TSH1 in scaling-up of solid-state fermentation of ethanol from sweet sorghum stalks. *PLoS ONE* **2014**, *9*, 94480–94490. [[CrossRef](#)] [[PubMed](#)]
182. Uçkun Kiran, E.; Liu, Y. Bioethanol production from mixed food waste by an effective enzymatic pretreatment. *Fuel* **2015**, *159*, 463–469. [[CrossRef](#)]
183. Liu, Y.; Zhang, Y.; Xu, J.; Sun, Y.; Yuan, Z.; Xie, J. Consolidated bioprocess for bioethanol production with alkali-pretreated sugarcane bagasse. *Appl. Energy* **2015**, *157*, 517–522. [[CrossRef](#)]
184. Ang, S.K.; Adibah, Y.; Abd-Aziz, S.; Madihah, M.S. Potential Uses of Xylanase-Rich Lignocellulolytic Enzymes Cocktail for Oil Palm Trunk (OPT) Degradation and Lignocellulosic Ethanol Production. *Energy Fuels* **2015**, *29*, 5103–5116. [[CrossRef](#)]
185. Thomas, L.; Parameswaran, B.; Pandey, A. Hydrolysis of pretreated rice straw by an enzyme cocktail comprising acidic xylanase from *Aspergillus* sp. for bioethanol production. *Renew. Energy* **2016**, *98*, 9–15. [[CrossRef](#)]
186. Suresh, S.V.; Srujana, S.; Muralidharan, A. Production of bioethanol by Solid State Fermentation using paddy straw as a substrate. *Int. J. Adv. Res.* **2015**, *3*, 212–215.
187. Ingale, S.; Joshi, S.J.; Gupte, A. Production of bioethanol using agricultural waste: Banana pseudo stem. *Braz. J. Microbiol.* **2014**, *45*, 885–892. [[CrossRef](#)] [[PubMed](#)]
188. Pirota, R.D.P.B.; Delabona, P.S.; Farinas, C.S. Simplification of the Biomass to Ethanol Conversion Process by Using the Whole Medium of Filamentous Fungi Cultivated Under Solid-State Fermentation. *Bioenergy Res.* **2014**, *7*, 744–752. [[CrossRef](#)]
189. Singhanian, R.R.; Saini, R.; Adsul, M.; Saini, J.K.; Mathur, A.; Tuli, D. An integrative process for bio-ethanol production employing SSF produced cellulase without extraction. *Biochem. Eng. J.* **2015**, *102*, 45–48. [[CrossRef](#)]
190. Jain, A.; Morlok, C.K.; Henson, J.M. Comparison of solid-state and submerged-state fermentation for the bioprocessing of switchgrass to ethanol and acetate by *Clostridium phytofermentans*. *Appl. Microbiol. Biotechnol.* **2013**, *97*, 905–917. [[CrossRef](#)] [[PubMed](#)]
191. Yu, M.; Li, J.; Li, S.; Du, R.; Jiang, Y.; Fan, G.; Zhao, G.; Chang, S. A cost-effective integrated process to convert solid-state fermented sweet sorghum bagasse into cellulosic ethanol. *Appl. Energy* **2014**, *115*, 331–336. [[CrossRef](#)]
192. Yu, M.; Li, J.; Chang, S.; Zhang, L.; Mao, Y.; Cui, T.; Yan, Z.; Luo, C.; Li, S. Bioethanol production using the sodium hydroxide pretreated sweet sorghum bagasse without washing. *Fuel* **2016**, *175*, 20–25. [[CrossRef](#)]
193. Izawa, N.; Kudo, M.; Nakamura, Y.; Mizukoshi, H.; Kitada, T.; Sone, T. Production of aroma compounds from whey using *Wickerhamomyces pijperi*. *AMB Express* **2015**, *5*, 23. [[CrossRef](#)] [[PubMed](#)]

194. Ben Akacha, N.; Gargouri, M. Microbial and enzymatic technologies used for the production of natural aroma compounds: Synthesis, recovery modeling, and bioprocesses. *Food Bioprod. Process.* **2015**, *94*, 675–706. [[CrossRef](#)]
195. Madrera, R.R.; Bedriñana, R.P.; Valles, B.S. Production and characterization of aroma compounds from apple pomace by solid-state fermentation with selected yeasts. *LWT Food Sci. Technol.* **2015**, *64*, 1342–1353. [[CrossRef](#)]
196. Aggelopoulos, T.; Katsieris, K.; Bekatorou, A.; Pandey, A.; Banat, I.M.; Koutinas, A.A. Solid state fermentation of food waste mixtures for single cell protein, aroma volatiles and fat production. *Food Chem.* **2014**, *145*, 710–716. [[CrossRef](#)] [[PubMed](#)]
197. Pedroni Medeiros, A.B.; Christen, P.; Roussos, S.; Gern, J.C.; Soccol, C.R. Coffee residues as substrates for aroma production by *Ceratocystis fimbriata* in solid state fermentation. *Braz. J. Microbiol.* **2003**, *34*, 245–248. [[CrossRef](#)]
198. Medeiros, A.B.P.; Pandey, A.; Vandenberghe, L.P.S.; Pastorel, G.M.; Soccol, C.R. Production and recovery of aroma compounds produced by solid-state fermentation using different adsorbents. *Food Technol. Biotechnol.* **2006**, *44*, 47–52.
199. Soares, M.; Christen, P.; Pandey, A. Fruity flavor production by *Ceratocystis fimbriata* grown on coffee husk in solid-state fermentation. *Process Biochem.* **2000**, *35*, 857–861. [[CrossRef](#)]
200. Rossi, S.C.; Vandenberghe, L.P.S.; Pereira, B.M.P.; Gago, F.D.; Rizzolo, J.A.; Pandey, A.; Soccol, C.R.; Medeiros, A.B.P. Improving fruity aroma production by fungi in SSF using citric pulp. *Food Res. Int.* **2009**, *42*, 484–486. [[CrossRef](#)]
201. Medeiros, A.B.P.; Pandey, A.; Christen, P.; Fontoura, P.S.G.; de Freitas, R.J.S.; Soccol, C.R. Aroma compounds produced by *Kluyveromyces marxianus* in solid state fermentation on a packed bed column bioreactor. *World J. Microbiol. Biotechnol.* **2001**, *17*, 767–771. [[CrossRef](#)]
202. De Araújo, Á.; Pastore, G.M.; Berger, R.G. Production of coconut aroma by fungi cultivation in solid-state fermentation. *Appl. Biochem. Biotechnol.* **2002**, *98–100*, 747–751.
203. Fadel, H.H.M.; Mahmoud, M.G.; Asker, M.M.S.; Lotfy, S.N. Characterization and evaluation of coconut aroma produced by *Trichoderma viride* EMCC-107 in solid state fermentation on sugarcane bagasse. *Electron. J. Biotechnol.* **2015**, *18*, 5–9. [[CrossRef](#)]
204. Da Penha, M.P.; da Rocha Leão, M.H.M.; Leite, S.G.F. Sugarcane bagasse as support for the production of coconut aroma by solid state fermentation (SSF). *BioResources* **2012**, *7*, 2366–2375. [[CrossRef](#)]
205. Kabbaj, W.; Breheret, S.; Guimberteau, J.; Talou, T.; Olivier, J.-M.; Bensoussan, M.; Sobal, M.; Roussos, A.S. Comparison of Volatile Compound Production in Fruit Body and in Mycelium of *Pleurotus ostreatus* Identified by Submerged and Solid-State Cultures. *Appl. Biochem. Biotechnol.* **2002**, *102–103*, 463–469. [[CrossRef](#)]
206. Omarini, A.; Dambolena, J.S.; Lucini, E.; Jaramillo Mejía, S.; Albertó, E.; Zygadlo, J.A. Biotransformation of 1,8-cineole by solid-state fermentation of Eucalyptus waste from the essential oil industry using *Pleurotus ostreatus* and *Favolus tenuiculus*. *Folia Microbiol.* **2016**, *61*, 149–157. [[CrossRef](#)] [[PubMed](#)]
207. Zidehsaraei, A.Z.; Moshkelani, M.; Amiri, M.C. An innovative simultaneous glucoamylase extraction and recovery using colloidal gas apherons. *Sep. Purif. Technol.* **2009**, *67*, 8–13. [[CrossRef](#)]
208. Dhillon, G.S.; Brar, S.K.; Kaur, S.; Verma, M. Bioproduction and extraction optimization of citric acid from *Aspergillus niger* by rotating drum type solid-state bioreactor. *Ind. Crops Prod.* **2013**, *41*, 78–84. [[CrossRef](#)]
209. Pirota, R.D.P.B.; Miotto, L.S.; Delabona, P.S.; Farinas, C.S. Improving the extraction conditions of endoglucanase produced by *Aspergillus niger* under solid-state fermentation. *Braz. J. Chem. Eng.* **2013**, *30*, 117–123. [[CrossRef](#)]
210. Arantes, V.; Silva, E.M.; Milagres, A.M.F. Optimal recovery process conditions for manganese-peroxidase obtained by solid-state fermentation of eucalyptus residue using *Lentinula edodes*. *Biomass Bioenergy* **2011**, *35*, 4040–4044. [[CrossRef](#)]
211. Chandra, M.S.; Viswanath, B.; Reddy, B.R. Optimization of extraction of beta-endoglucanase from the fermented bran of *Aspergillus niger*. *Indian J. Microbiol.* **2010**, *50*, S122–S126. [[CrossRef](#)] [[PubMed](#)]
212. Ahmed, S.A.; Mostafa, F.A. Utilization of orange bagasse and molokhia stalk for production of pectinase enzyme. *Braz. J. Chem. Eng.* **2013**, *30*, 449–456. [[CrossRef](#)]

213. Rodríguez-Fernández, D.E.; Rodríguez-León, J.A.; de Carvalho, J.C.; Thomaz-Soccol, V.; Parada, J.L.; Soccol, C.R. Recovery of phytase produced by solid-state fermentation on citrus peel. *Braz. Arch. Biol. Technol.* **2010**, *53*, 1487–1496. [[CrossRef](#)]
214. Dey, T.B.; Kuhad, R.C. Enhanced production and extraction of phenolic compounds from wheat by solid-state fermentation with *Rhizopus oryzae* RCK2012. *Biotechnol. Rep.* **2014**, *4*, 120–127.
215. Salariato, D.; Diorio, L.A.; Mouso, N.; Forchiassin, F. Extraction and characterization of polygalacturonase of fomes sclerodermeus produced by solid-state fermentation. *Rev. Argent. Microbiol.* **2010**, *42*, 57–62. [[PubMed](#)]
216. Szabo, O.E.; Csiszar, E.; Koczka, B.; Kiss, K. Ultrasonically assisted single stage and multiple extraction of enzymes produced by *Aspergillus oryzae* on a lignocellulosic substrate with solid-state fermentation. *Biomass Bioenergy* **2015**, *75*, 161–169. [[CrossRef](#)]
217. Rezaei, F.; Joh, L.D.; Kashima, H.; Reddy, A.P.; Vandergheynst, J.S. Selection of conditions for cellulase and xylanase extraction from switchgrass colonized by acidothermus cellulolyticus. *Appl. Biochem. Biotechnol.* **2011**, *164*, 793–803. [[CrossRef](#)] [[PubMed](#)]
218. Poletto, P.; Borsói, C.; Zeni, M.; Moura, M. Downstream processing of pectinase produced by *Aspergillus niger* in solid state cultivation and its application to fruit juices clarification. *Food Sci. Technol.* **2015**, *35*, 391–397. [[CrossRef](#)]
219. Rashad, M.M.; Nooman, M.U.; Ali, M.M.; Mahmoud, A.E. Production, characterization and anticancer activity of *Candida bombicola* sophorolipids by means of solid state fermentation of sunflower oil cake and soybean oil. *Grasas Aceites* **2014**, *65*, 1–11. [[CrossRef](#)]
220. Hu, Y.; Ju, L.K. Purification of lactonic sophorolipids by crystallization. *J. Biotechnol.* **2001**, *87*, 263–272. [[CrossRef](#)]
221. Bhavsar, K.; Ravi Kumar, V.; Khire, J.M. Downstream processing of extracellular phytase from *Aspergillus niger*: Chromatography process vs. aqueous two phase extraction for its simultaneous partitioning and purification. *Process Biochem.* **2012**, *47*, 1066–1072.
222. Kachrimanidou, V.; Kopsahelis, N.; Vlysidis, A.; Papanikolaou, S.; Kookos, I.K.; Monje Martinez, B.; Escrig Rondan, M.C.; Koutinas, A.A. Downstream separation of poly(hydroxyalkanoates) using crude enzyme consortia produced via solid state fermentation integrated in a biorefinery concept. *Food Bioprod. Process.* **2016**, *100*, 323–334. [[CrossRef](#)]
223. Narra, M.; Balasubramanian, V. Utilization of solid and liquid waste generated during ethanol fermentation process for production of gaseous fuel through anaerobic digestion—A zero waste approach. *Bioresour. Technol.* **2015**, *180*, 376–380. [[CrossRef](#)] [[PubMed](#)]
224. Dhillon, G.S.; Kaur, S.; Sarma, S.J.; Brar, S.K. Integrated process for fungal citric acid fermentation using apple processing wastes and sequential extraction of chitosan from waste stream. *Ind. Crops Prod.* **2013**, *50*, 346–351. [[CrossRef](#)]
225. Zhang, Z.Y.; Jin, B.; Kelly, J.M. Production of lactic acid from renewable materials by *Rhizopus fungi*. *Biochem. Eng. J.* **2007**, *35*, 251–263. [[CrossRef](#)]
226. Zhuang, J.; Marchant, M.A.; Nokes, S.E.; Strobel, H.J. Economic analysis of cellulase production methods for bio-ethanol. *Appl. Eng. Agric.* **2007**, *23*, 679–687. [[CrossRef](#)]
227. De Castro, A.M.; Carvalho, D.F.; Freire, D.M.G.; Castilho, L.D.R. Economic analysis of the production of amylases and other hydrolases by *Aspergillus awamori* in solid-state fermentation of Babassu Cake. *Enzyme Res.* **2010**, *2010*, 1–9.





# Assessment of protease activity in hydrolysed extracts from SSF of hair waste by and indigenous consortium of microorganisms



Noraziah Abu Yazid, Raquel Barrena, Antoni Sánchez\*

Composting Research Group, Department of Chemical Engineering, Escola d'Enginyeria, Universitat Autònoma de Barcelona, 08193 Bellaterra, Barcelona, Spain

## ARTICLE INFO

### Article history:

Received 16 September 2015

Revised 20 January 2016

Accepted 31 January 2016

Available online 5 February 2016

### Keywords:

Protease

Dehairing

Protein purification

Solid-state fermentation

Hair waste

## ABSTRACT

Hair wastes from the tannery industry were assessed for its suitability as substrates for protease production by solid-state fermentation (SSF) using a pilot-batch mode operation and anaerobically digested sludge as co-substrate. Maximum protease activity ( $52,230 \pm 1601 \text{ U g}^{-1} \text{ DM}$ ) was observed at the 14th day of SSF. Single step purification resulted in 2 fold purification with 74% of recovery by ultrafiltration with 10 kDa cut-off. The recovered enzyme was stable at a temperature of 30 °C and pH 11; optimal conditions that were determined by a central composite full factorial experimental design. The enzyme activity was inhibited by phenylmethylsulfonyl fluoride, which indicates that it belongs to serine protease group. The remaining solid material after protease extraction could be easily stabilized to obtain a final good quality compost-like material as the final dynamic respiration index was lower than  $1 \text{ g O}_2 \text{ kg}^{-1} \text{ OM h}^{-1}$ . The lyophilized recovered enzymes were a good alternative in the process of cowhides dehairing with respect to the current chemical treatment, avoiding the production of solid wastes and highly polluted wastewaters. In conclusion, the entire process can be considered a low-cost sustainable technology for the dehairing process, closing the organic matter cycle in the form of value added product and a compost-like material from a waste.

© 2016 Elsevier Ltd. All rights reserved.

## 1. Introduction

Traditionally, the tanning industry has been always associated with high pollution of the environment, which is mainly related to the use of toxic chemicals and the production of huge amounts of highly polluted wastewaters and solid wastes that impart a great challenge to the environment (Ahmad and Ansari, 2013). Over the years a large quantity of solid waste is generated worldwide from tanning processes such as skin trimming, shaving, dehairing, fleshing and production of buffing waste, which are associated to the increasing of high oxygen demand in water, discharging of highly toxic metal salts and the emission of unpleasant odour and atmospheric pollutants (Kanagaraj et al., 2006). Consequently, these processes lead to health and safety issues due to the land, air, surface, and groundwater contamination.

Approximately 5–10% of dry hair per ton of animal is being disposed to land or sanitary landfills (Onyuka et al., 2012). The main composition of hair waste is protein that constitutes 65–95% of hair weight where the rest consists of water, lipids, pigments and trace elements (Dawber, 1996). Furthermore, keratin, which is a

constituent of protein in hair waste has a structure that take long time to degrade under natural environmental conditions, therefore landfill is not the best option to manage this material and it can cause severe environmental problems (Gupta and Ramnani, 2006).

Due to the environmental concern, EU tanners' environmental costs for hair waste disposal are estimated about 5% of their turnover (IPCC, 2003). Hence, any alternative treatment for hair waste would be attractive to tanning industry. In some cases, due to its high content of nitrogen, composting of hair waste has been proposed as a friendly environmental technology to produce a valuable organic amendment (Barrena et al., 2007a). However, for an efficient waste management the organic solid waste abundantly produced from tanneries could be recycled and exploited into other value added products. Currently, only few works regarding the recycle of hair waste into these products are reported. One of the preferable ways of hair waste valorisation is its bioconversion into proteolytic enzymes that could be used in the same tanneries for dehairing (Wang et al., 2007). This strategy demonstrated to be a viable technique through solid-state fermentation (SSF) (Abraham et al., 2013).

Due to this origin, hair waste are highly alkaline and do not present the appropriate characteristics to be degraded alone and the use of a co-substrate and an inoculum is necessary to activate the biological transformation and accomplish the biodegradation

\* Corresponding author.

E-mail address: [antoni.sanchez@uab.cat](mailto:antoni.sanchez@uab.cat) (A. Sánchez).

process of hair waste. Dewatered sewage sludge has been effectively tested as a co-substrate to biodegrade hair waste (Barrena et al., 2007a; Abraham et al., 2014). Other economical option is to use as co-substrate anaerobically digested sludge (ADS), which has been successfully used as a co-substrate for different organic wastes (Barrena et al., 2007b). Furthermore, ADS is available in sufficient quantity and can be easily obtained from local wastewater treatment plants. To date, the use of hair waste and ADS as co-substrates for the production of alkaline protease has not been studied.

Literature regarding the production of alkaline protease by SSF is relatively abundant (Haddar et al., 2010; Mukherjee et al., 2008; Uyar and Baysal, 2004). However, most of the protease production via SSF is carried out with few grams of material, which hampers the development of the process at industrial scale (Ravindran et al., 2011). Moreover, the information about the recovery yields of protease activity is very scarce. As alkaline proteases have numerous potential applications in detergent industries, food processing, tanning and leather processing, waste treatment, textile and pharmaceutical industry (Abidi et al., 2008; Gupta et al., 2002; Khan, 2013; Raj et al., 2012), it is essential to develop highly scalable process of SSF that could use wastes as substrates or the hydrolysed materials for applications as biofuels (Han et al., 2015a).

In this context, the present study highlighted the protease production and extraction using a pilot-batch mode operation presenting the yields and recovery achieved on an easily scalable low-cost downstream process. In addition, a first approach to the characterization of enzyme produced is also presented. It also examines the possibility to continue the SSF process after the protease extraction in the same reactor after final material stabilization.

## 2. Materials and methods

### 2.1. Materials

The main waste used for this research was hydrolysed hair produced during the dehairing of bovine hide and obtained from a local tanning industry located in Igualada (Barcelona, Spain). ADS from a local wastewater treatment plant were used as co-substrate for the SSF process. The complete characterization of substrates in terms of physical, chemical and overall biological activity is presented in Table 1. For the mixture, firstly, hair waste and ADS were mixed in a weight ratio of 1:2, as described in previous studies (Abraham et al., 2014; Barrena et al., 2007a). Afterwards, wood chips were used as bulking agent to the mixture

**Table 1**  
Characterization of anaerobically digested sludge, hair waste and initial mixture for SSF process.

Characteristics	Hair waste	Anaerobically digested sludge	Mixture <sup>a</sup>
<i>Physical characteristics</i>			
Organic matter (% db)	85.5 ± 0.7	71.3 ± 0.6	84.6 ± 0.4
Water content (% wb)	62 ± 3	86 ± 4	72 ± 4
Dynamic respiration index (DRI) (g O <sub>2</sub> kg <sup>-1</sup> OM h <sup>-1</sup> )	N.D.	2.4 ± 0.3	4.7 ± 0.7
Electrical conductivity (mS cm <sup>-1</sup> )	4.1 ± 0.9	1.2 ± 0.7	1.6 ± 0.8
pH	10.7 ± 0.1	8.32 ± 0.04	8.52 ± 0.01
<i>Chemical characteristics</i>			
Total carbon (% db)	57.2 ± 0.9	42.0 ± 0.1	68.3 ± 0.4
Total nitrogen (% db)	12.1 ± 0.1	7.2 ± 0.6	6.9 ± 0.1
C/N ratio	4.7	5.9	11

db: dry basis; wb: wet basis; OM: organic matter; N.D.: not determined.

<sup>a</sup> Ratio 1:2 (sludge:hair waste).

hair: sludge in a 1:1 volumetric ratio to create the proper porosity in the mixtures (Barrena et al., 2007b).

Protease inhibitors phenylmethylsulfonyl fluoride (PMSF), pepstatin A and trans-epoxysuccinyl-L-leucylamido-(4-guanidino) butane (e64) were purchased from Sigma–Aldrich (St. Louis).

### 2.2. Solid state fermentation

Several fermentations were carried out under – aerobic environment. A preliminary fermentation was done to establish a reference profile for protease production in SSF using the above-explained mixture. The mixtures (approximately 3.7 kg) were prepared in duplicate (C1 and C2) in 10-L air tight reactors and fermented for 23 days, which was considered the control experiment. Samples of 100 g were collected at 0, 3, 6, 14, 20 and 23 days after manual homogenization of the entire mass in all the reactors. SSF for protease extraction with the same mixture content was done in triplicate (R1, R2 and R3) using the same 10-L reactors. These reactors are used to produce the proteases and to extract them in the same reactor in the moment of higher protease activity detected in the control experiment. The extracts were purified, characterized and used in the dehairing process, as explained later.

The experiments were performed under near-adiabatic conditions with continuous aeration at a minimum rate of 0.1 L/min. The reactors included a data acquisition system with a PLC (programmable logic controllers), which allowed data reading every minute. Particularly, PLC system reads the values of oxygen, air-flow and temperature, which are connected to a personal computer, and it enables on-line complete monitoring. The oxygen was regulated by means of airflow manipulation in the exhaust gas to maintain the system in favourable aerobic conditions (oxygen content above 12%), as previously described (Puyuelo et al., 2010).

### 2.3. Enzyme extraction

For the control experiment, in which the protease activity was only monitored, about 10 g of homogenized solid samples were taken from the reactors at different days of SSF, as explained. The samples were mixed and extracted with 50 mM HCl–Tris buffer (pH 8.10) at 1:5 (w/v) ratios for 45 min at room temperature. Then the mixtures were separated by centrifugation at 10,000 rpm for 10 min. The supernatant was collected and filtered through a 0.45 µm filter and used as crude enzyme extract for further characterization and use. All the extractions were done in triplicates.

To ensure the reproducibility, extraction of the whole fermented mass was performed in triplicate 10-L reactors at day 14, which was the time when the control experiment showed the highest production of protease according to the protease profile. In this mode of extraction the entire batch was submerged in each reactor with 50 mM HCl–Tris buffer (pH 8.10) at 1:1 (v/v) ratio for 1 h. Then the extracts were sieved with 2.0 mm stainless steel sieve and centrifuged as aforementioned. The supernatant was taken as the crude enzyme extract, whereas the solid remaining residues continued the SSF process until 42 days for final stabilization.

### 2.4. Lyophilisation

The crude enzyme extracts obtained after the extraction at 14th day of SSF (R1, R2 and R3) were frozen to –80 °C prior to lyophilisation using vacuum with a bench top VirTis Sentry 5L freeze dryer. The frozen samples were attached to quickseal valves on stainless steel drum manifolds. The lyophilisation process lasts approximately 24 h. The lyophilised extracts were collected and preserved at 4 °C for further use.

## 2.5. Partial purification and characterization of protease

The crude extracts were concentrated using Amicon® Ultra-15 centrifugal filter devices (Milipore, Ireland) with 10 k molecular weight cut-off (MWCO) Ultracel® low binding regenerated cellulose membrane. The concentrated ultrafiltered liquid was recovered and stored for further experiments of protease characterization. In these processes, recovery yield is defined as the percentage of residual activity with respect to the initial activity of crude extract, whereas purification fold is the quotient between specific enzymatic activity after purification with respect to the specific activity of the initial crude extract.

Molecular weight of proteases was estimated by SDS-PAGE electrophoresis using 12% polyacrylamide (w/v) precast gels (Bio-rad®). The gel was stained with Coomassie Blue G-250 (Bio-rad®). Zymogram was carried out using casein (Sigma-Aldrich) as copolymerized substrate to reveal protease profile from the extracts (Abraham et al., 2014).

The stability of the enzyme was determined by incubating the lyophilised extracts for 1 h at different temperatures within 30–70 °C and different pH values using the following buffers: Acetic acid-sodium acetate 1 M (pH 5), Tris-HCl 1 M (pH 8), Tris-NaOH 1 M (pH 11). The stability was analysed using the Design-Expert software (version 6.0.6) using a full central composite design (CCD) that consisted of 13 experimental points, including five replications at the central point and four star points ( $\alpha = 1$ ). Residual activity was selected as objective function (in %) for each pH and temperature tested assuming that the initial activity of the enzyme is 100%.

The effect of various protease inhibitors such as phenylmethylsulfonyl fluoride (PMSF), trans-epoxysuccinyl-L-leucylamido-(4-guanidino)butane (e64), pepstatin A, and ethylene diamine tetra acetic acid (EDTA) were determined by the addition of the corresponding inhibitors at 1 mM and 10 mM (final concentration) to the aliquot of the protease. The reaction mixtures were pre-incubated at 37 °C for 1 h without the substrate fraction and assay under standard conditions. The recorded residual activities were compared with that of the control (without inhibitors).

## 2.6. Application of alkaline protease in cowhides dehairing

The cowhide was cut in small pieces with the same area (10.68 cm<sup>2</sup>) for the dehairing process. About 0.4 g of lyophilized enzyme extracts was dissolved in 15 mL of Tris-HCl buffer to incubate the hides. The dehairing efficiency of the enzyme was assessed in comparison with the chemical dehairing process, where the initial amount of hair was assumed to be the same for each piece. Additionally a commercial powder provided by for tanning industry was tested. The dehairing process was performed by scrapping the hair using tweezers in a plate fill with water after 24 h incubated with protease or chemicals. The hair was harvested and measured as TSS (total suspended solids). Dehairing was expressed as percentage removal where the hair being removed by the chemical treatment was considered 100%. Briefly, the chemical treatment consists of a sequential treatment of the cow hides with the following reagents: sodium carbonate (15 mL, 0.3%, w/v) with a non-ionic surfactant (0.3%, w/v) (soaking, 22 h), calcium hydroxide (50 mL, 1%, w/v, 1 h) and sodium hydrosulfide (50 mL, 1%, w/v, 30 min in orbital agitation) to simulate the chemical dehairing process used in tannery industries.

## 2.7. Analytical methods

### 2.7.1. Dynamic respiration index (DRI)

On the basis of the methodology to assess the degree of biological stability of the remaining solid material from SSF, the dynamic

respiration index (DRI) was measured using a dynamic respirometer (Ponsá et al., 2010). The determination consists of placing 100 g of sample in a 500-mL Erlenmeyer flask and incubating the sample in a water bath at 37 °C. A constant airflow was supplied through the sample, and the oxygen content in the outgoing gases was measured. From this assay, DRI was determined as the maximum average value of respiration activity measured during 24 h, expressed in g O<sub>2</sub> kg<sup>-1</sup> OM h<sup>-1</sup> (Adani et al., 2006; Ponsá et al., 2010).

DRI was used as a test to determine the stability of organic matter after SSF. In this sense, lower respiration activity can be considered as stable compost (Adani et al., 2004).

### 2.7.2. Protease activity assay

The protease activity was measured using casein (2%) as substrate according to Alef and Nannipieri (1995), with a slight modification as described previously (Abraham et al., 2013). One unit of alkaline protease activity was defined as 1 µg of tyrosine liberated under the assay conditions.

### 2.7.3. Protein determination

Protein concentration was determined by the modified method of Lowry et al. (1951) using bovine serum albumin (BSA) as standard protein. The protein content was estimated by measuring the absorbance at 750 nm using Varian Cary® 50 UV-visible spectrometer.

### 2.7.4. Routine analytical methods

Dry matter (DM) and organic matter contents (OM), total suspended solid (TSS), bulk density and pH in solid samples were determined according to standard methods (TMECC, 2001).

## 3. Results and discussion

### 3.1. Solid-state fermentation

Primarily, the initial DRI of the mixture was considered high,  $4.7 \pm 0.7$  g O<sub>2</sub> kg<sup>-1</sup> OM h<sup>-1</sup> (Table 1) to initiate aerobically degradation during SSF process. The moisture content (>60%) and C/N ratio (11) of the mixture were maintained to favour degradation process to produce protease enzyme during thermophilic and mesophilic condition. The results presented in Fig. 1 showed the protease production and fermentation profiles (temperature and oxygen exhaust content) of SSF. No lag phase was observed because of the previous hydrolysis of hair waste, as pointed in other studies (Du et al., 2008). The fermentation showed a normal operating condition where the thermophilic temperature (60 °C) occurred at the

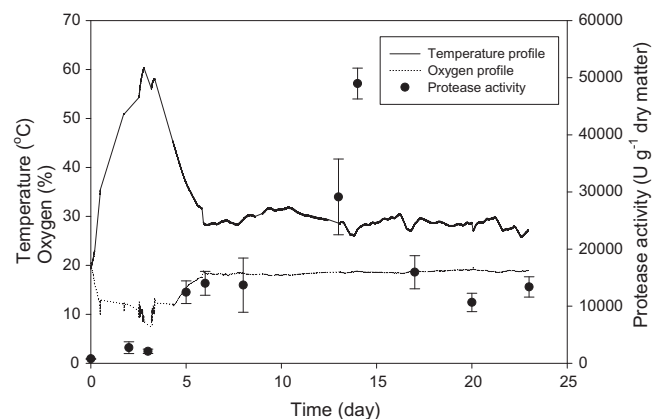


Fig. 1. Solid state fermentation profiles (one replicate is shown) for 23 days of SSF: Temperature (—, solid line), oxygen content in exhausts gas (....., dotted line), protease activity profile (—●—, long dash) from several SSF.

beginning of the SSF (day 2) and decreases towards the end of the fermentation. In Fig. 1, oxygen contents were low during the thermophilic stage as an evidence of high aerobic respiration activity during that period in the profile (Gea et al., 2004). The oxygen profiles showed a similar trend to that of co-composting hair waste and raw activated sludge profiles (Abraham et al., 2014; Barrena et al., 2007b).

To validate the processes performances of the replicates, they were assessed through the statistical comparison of temperature and oxygen profiles that have been summarized in Table 2. Thus, to evaluate the performance of mixtures of hair waste and anaerobically digested sludge (ADS) the area below the temperature curve, the area below sOUR (specific oxygen uptake rate), the maximum protease activity, the specific activity and dry mass reduction were calculated until 14 days of SSF. Apparently, there was no considerable difference between replicates for the temperature curve, where the average was  $499 \pm 15$  °C day<sup>-1</sup>. The coefficients of variation (CV) for all the fermentations were lower than 5%, thus validating statistically the process and confirming non-statistically differences between replicates (de Guardia et al., 2010). Additionally, the maximum specific oxygen uptake rate (sOUR max) and accumulated oxygen content throughout the SSF process was correlated well with a correlation coefficient of 0.951. Overall, the correlation between the area below the temperature curve and the maximum protease activity reached, the sOUR max and the maximum protease activity were significant at  $p < 0.001$ . As sOUR max value also correlated to the increasing value of the area below sOUR (Table 2) ( $p = 0.017$ ), it can be stated that the SSF for the production of proteases from hair and ADS under this pilot conditions is highly reproducible and the results are consistent.

### 3.2. Enzymatic activity profile and extraction

Protease profile is shown in Fig. 1 at day 14th, the highest protease activity production was observed, which resulted in a  $e$  value of  $48,971 \pm 872$  U g<sup>-1</sup> DM with a CV equal to 1.8%. These results are in agreement with previous studies using 4.5 L reactors where the highest activity of protease was observed at 14 days of SSF with hair waste and different co-substrate (Abraham et al., 2014, 2013). Therefore, this time was selected to carry out the extraction of the enzyme in further experiments.

The SSF process was continued until 42 days with the mixture after extraction to complete the entire process that implies the stabilization of the remaining material. The activity of protease at the end of SSF process (42 days) was  $3273 \pm 1342$  U g<sup>-1</sup> DM, showing a significant decrease of activity at end of the fermentation. The average of dynamic respiration index (DRI) of the mixtures at the end of the process (42 days) was lower than  $1$  g O<sub>2</sub> kg<sup>-1</sup> OM h<sup>-1</sup>, which indicates the degradation of biodegradable matter and show that a further stabilization is useful to obtain a very stable compost-like material. Thus, it can be concluded that, after extraction, DRI showed a high biological stability, as reported in previous studies (Gupta et al., 2002; Ponsá et al., 2010).

### 3.3. Partial purification and characterization

Table 3 shows the summary of the partial purification steps tested for alkaline protease in the three replicates (R1, R2 and R3). In all cases, the partial purification of protease resulted in a 2 fold purification factor with 74% of recovery by ultrafiltration using Amicon Ultra-15 centrifugal filter device with 10 kDa MWCO. Additionally, protease activity was not detected in

**Table 2**

Summary of the replicates of solid state fermentation (SSF) using 10-L air tight reactors with hair waste and anaerobically digested sludge as substrates.

	Initial water content of mixture (%)	Bulk density (kg L <sup>-1</sup> )	Process parameters during SSF				Max PA <sup>a</sup> (U g <sup>-1</sup> DM)	sPA <sup>a</sup> (U mg <sup>-1</sup> protein)	Dry mass reduction <sup>a</sup> (%)	Stability after SSF DRI (g O <sub>2</sub> kg <sup>-1</sup> OM h <sup>-1</sup> )
			Area T <sup>a</sup> (°C day <sup>-1</sup> )	sOUR max (g O <sub>2</sub> kg <sup>-1</sup> DM h <sup>-1</sup> )	Area sOUR <sup>a</sup> (g O <sub>2</sub> kg <sup>-1</sup> DM)	Time sOUR max (h)				
<i>Experiment performed with in-situ enzyme extraction</i>										
R1	76.1	0.5	513.4	3.9	387	11.7	52,230 ± 1601	12,615 ± 111	10	0.39 ± 0.04
R2			475.8	3.1	337	11.3	37,732 ± 1608	15,403 ± 909	7	
R3			500.3	5.3	538	10.9	37,782 ± 1514	13,547 ± 626	10	
<i>Control experiment</i>										
C1	73.3	0.67	497.0	2.8	220	48.4	48,354 ± 78	3454 ± 21	11	0.87 ± 0.01
C2			507.9	2.3	165	71.8	49,587 ± 324	4157 ± 86	17	

R1, R2 and R3: replicates SSF experiments; C1 and C2: control SSF experiments.

PA: protease activity; sPA: specific protease activity; OUR: oxygen uptake rate; DRI: dynamic respiration index; DM: dry matter; OM: organic matter.

Values are the average of three replicates of experiments ± standard deviation of triplicates.

<sup>a</sup> The parameters were calculated after 14 days of SSF (maximum protease production).

**Table 3**

Partial purification of protease enzyme from extraction.

Sample	Purification step	Total activity (U)	Total protein (mg)	Specific activity (U mg <sup>-1</sup> )	Recovery (%)	Purification fold
R1	Crude extract	124,410	9.91 ± 0.04	12,560 ± 111	100	1
	Lyophilization	94,408	9.86 ± 0.03	9571 ± 240	76	0.76
	Ultrafiltration	85,180	4.10 ± 0.72	20,796 ± 631	68	1.66
R2	Crude extract	85,830	5.83 ± 0.01	14,715 ± 909	100	1
	Lyophilization	62,180	5.34 ± 0.20	11,646 ± 244	72	0.79
	Ultrafiltration	60,230	3.39 ± 0.16	17,788 ± 163	70	1.21
R3	Crude extract	102,600	6.43 ± 0.01	15,059 ± 625	100	1
	Lyophilization	90,180	6.37 ± 0.28	14,148 ± 375	88	0.89
	Ultrafiltration	86,340	3.34 ± 0.38	25,843 ± 288	84	1.62

R1, R2 and R3: triplicates SSF experiments. Samples were taken after 14 days of SSF (maximum protease production).

Values are the average of three replicates in the experiments ± standard deviation.

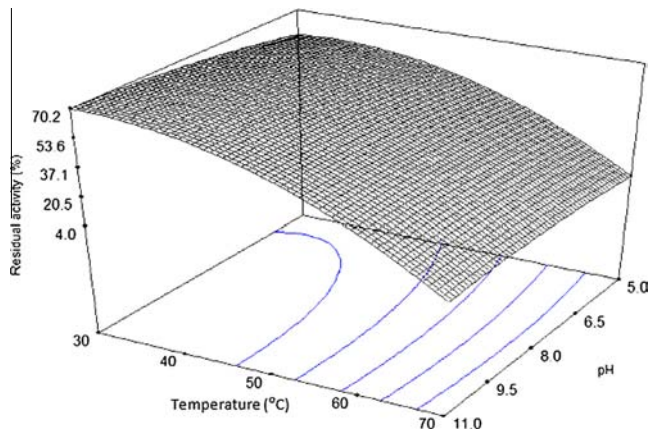


Fig. 2. Response surface of residual protease activity (%) on stability of enzymes with respect to pH and temperature.

Table 4  
Analysis of variance (ANOVA) for the response surface quadratic model.

Source of variations	Sums of squares	Degrees of freedom	Mean square	F-value	P value
Regression	6184.36	5	1236.87	242.97	<0.0001
Residual	35.64	7	5.09		
Pure error	24.8	4	6.2		
Lack of fit	10.84	3	3.61	0.58	
Total	6220	12			

$R^2$  0.9943; adjusted  $R^2$  0.9902; predicted  $R^2$  0.9797.

permeate as the size of alkaline proteases produced were in range between 26 and 100 kDa. Some studies reported that there was no protease activity detectable in all permeates due to the lost as a deposit in the membrane of the tube (Bezawada et al., 2011). However, during lyophilisation the loss of activity resulted in 21%, being this step the most critical for the recovery of protease.

The response surface of protease in front of several conditions of pH and temperature was determined to assess the stability of the protease. For this, it was analysed using the regression equation obtained from the analysis of variances (ANOVA) by the Design Expert software to determine the suitability of the model (Eq. (1)). In the model,  $pHT$  indicates the interaction term between temperature and pH. The negative coefficient of  $T$  (Eq. (1)) suggested that high temperature has a pronounced effect on activity and, as shown in Fig. 2, pH effect becomes insignificant at higher temperatures.

$$\text{Residual activity (\%)} = 52.79 + 4.17pH - 29T - 2.78pH^2 - 3.25pHT \quad (1)$$

Table 4 shows that the regression for residual activity yield model was significant (242.97) and the lack of fit was not significant (0.58) at  $p < 0.0001$  relative to pure error. The lack of fit of the  $F$ -value for the residual yield was less than the  $F_{\text{critical}}$  value ( $\alpha = 0.05$  at degree of freedom 4, 3) of 9.12, which indicates that the treatment differences were highly significant. The fit of the models were checked by the determination of correlation coefficient,  $R^2$ . In this case, the value of the coefficient for residual activity was  $R^2 = 0.9943$ . The values showed that only 0.57% of the variables behaviour is not explained by the model (Amini et al., 2008). The predicted  $R^2$  (0.9797) for the model was in reasonable agreement with the adjusted  $R^2$  of 0.9902, therefore it can be concluded that the proposed model adequately approximated the response surface and it could be used to predict the values of the variables within the experimental domain (Gilmour, 2006; Myers et al., 2004).

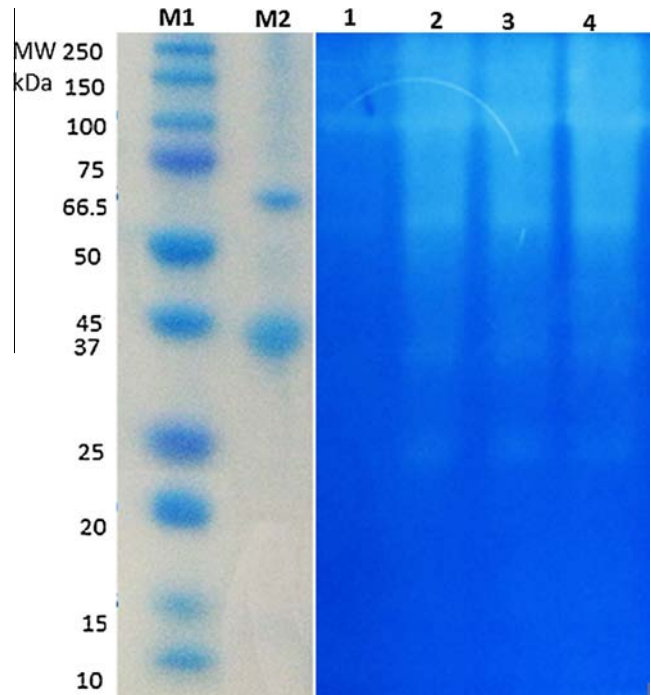


Fig. 3. Zymogram of partially purified enzyme on 12% polyacrylamide gel after SDS-PAGE under non-reducing condition (Lane M1: standard molecular mass marker proteins in kDa; Lane M2: egg albumin (45 kDa); bovine serum albumin (66 kDa); Lane 1: crude extracts; Lane 2, 3, 4: partially purified enzymes from R1, R2 and R3).

The partially purified protease was found to be an alkaline protease displaying the residual activity more than 70% when approaching alkaline pH up to 11 (Fig. 2). As it was stable in alkaline pH up to 11, it can be used for industrial purposes where commercially proteases have highest activity in alkaline pH ranges of 8–12 (Gupta et al., 2002; Kumar et al., 1999). For thermal stability, the enzymes exhibited good activities over a temperature range 30–50 °C in a wide range of alkaline pH from pH 7 to 11. The optimum enzyme activity ( $49,347 \pm 5487 \text{ U g}^{-1} \text{ DM}$ ) was obtained at 30 °C and pH 11. However, the enzymes were rapidly inactivated and retained approximately 4–8% of residual activity after incubation at 70 °C at any tested pH (Fig. 2). These results were in accordance with previous studies (Abraham et al., 2014, 2013) reported that the protease produced from hair waste was highly stable in alkaline and mesophilic temperatures, which coincides with the conditions of the SSF when it is mainly produced (Fig. 1).

The proteolytic activity of concentrated alkaline protease (R1, R2, and R3) subjected to a zymogram revealed four clear hydrolytic zones around the blue background with molecular weight from 26 kDa to 100 kDa (Fig. 3). The molecular weights of the proteases coincided with previous study (Abraham et al., 2014) that were obtained after 14 days of SSF in 4.5 L reactors, when the best results in dehairing were observed. Probably, these proteases were produced by the same type of microorganisms that may coexist in the mixture of hair waste and ADS for protease production.

In the present study, pepstatin A (acid protease inhibitor), e64 (cysteine protease inhibitor), and EDTA (metalloprotease inhibitor) had a minimal effect on the protease activity (Table 5). On the contrary, PMSF (serine protease inhibitors) inhibited the enzyme activity at very low concentration (1 mM). Therefore, the protease produced in this study can be considered as serine protease type. Since serine proteases generally are active at pH 7–11 and have broad substrate specificities it may be used in the dehairing process as reported in other studies (Huang et al., 2003; Ito et al., 2010; Wang et al., 2007).



**Table 5**  
Effect of protease inhibitors on protease activity from different replicates.

Inhibitor	Concentration (mM)	Residual activity (%)		
		R1	R2	R3
Control	–	100	100	100
Pepstatin A	1	98	94	99
	10	97	91	96
PMSF	1	36	47	49
	10	3.8	5.1	6
e64	1	99	98	98
	10	93	87	89
EDTA	1	98.7	94	99.4
	10	81	78	86

The residual activity was assayed under the standard assay conditions in the presence of various inhibitors. 1 mM is the initial concentration of the inhibitors and 10 mM is the final concentration of the inhibitors. Enzyme activities measured in the absence of any inhibitor were taken as 100%.

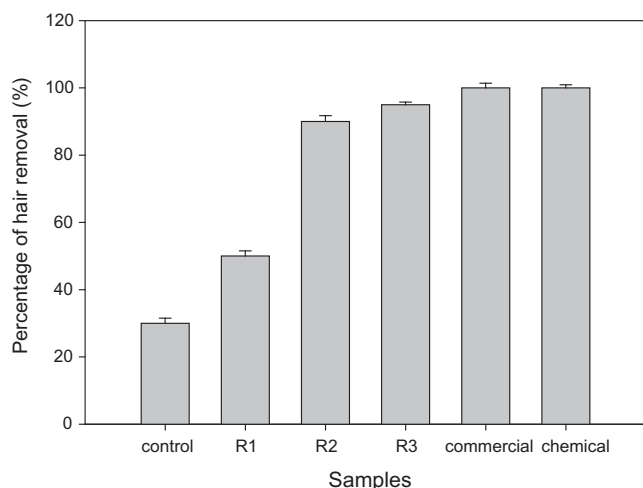


**Fig. 4.** Percentage of enzymatic dehairing with respect to chemical treatment; hair removal of cowhide using the chemical treatment was considered 100% of dehairing. Percentage of hair removal for each treatment was calculated as the hair removed using enzymatic dehairing with respect to chemical dehairing on a dry matter basis.

#### 3.4. Dehairing of cowhides

In order to evaluate the feasibility of the proposed process at industrial scale, the protease produced was tested on dehairing of high pigmentation cowhides. Normally, in tanning industries the solubilisation of black and brown hair is slower compared to the white and calfskin due to melanin and colour pigmentation (Onyuka, 2009).

To validate the possibility of using proteases from SSF in the dehairing process, the lyophilized enzyme (R1, R2, and R3) with similar initial enzymatic activities of  $7556 \pm 129.8 \text{ U cm}^{-2}$ ,  $8561 \pm 12.0 \text{ U cm}^{-2}$  and  $9373 \pm 48.6 \text{ U cm}^{-2}$  respectively, were used for dehairing of black cowhides. Fig. 4 indicates the percentage of hair removal of the raw hide that was processed for dehairing using Tris-HCl buffer as control, enzymatic and chemical treatments for comparison. Additionally, the dehairing activity of the obtained enzyme was compared with a commercial powder used for dehairing that was being used in the tanning industry with a similar activity ( $74,885 \pm 3137 \text{ U mL}^{-1}$  and  $87,588 \pm 1110 \text{ U mL}^{-1}$  for lyophilized extract and commercial powder respectively).

Approximately, between 90% and 95% of hair removal with respect to chemical treatment was observed in treatment with pro-

teolytic enzymes from R2 and R3 after 24 h of incubation. The commercial powder was very close to the chemical treatment (Han et al., 2015b). These results suggest that using an appropriate enzymatic conditions results in good dehairing performance as pointed out in other studies (Asker et al., 2013; Dayanandan et al., 2003; Sundararajan et al., 2011). In the case of R1, protease showed a weaker activity with only 50% of hair removal probably due to the lower specific protease activity already detected in SSF (Table 3). Sivasubramanian et al. (2008) suggested that dehairing of hides is substantially difficult as the structural features and thickness of skin and hide vary greatly; therefore the dehairing efficiency of enzyme may vary accordingly.

Furthermore, it can be stated that the protease produce in this work presents the possibility to be an alternative to chemical dehairing as reported in other studies carried out at lower scales (Dayanandan et al., 2003; Saravanan et al., 2014; Sivasubramanian et al., 2008; Sundararajan et al., 2011).

#### 4. Conclusions

The use of hair waste in SSF was found to be a practical approach to produce alkaline proteases that can be used in the dehairing process. Moreover, in-situ protease extraction could make SSF process easier to scale up. Additionally, after extraction, SSF can be continued with the same mixture to reach final stabilization, similar to that of compost. With regard to the enzyme properties, protease activity was only inhibited by PMSF, suggesting that it belongs to the serine protease group. The enzyme produced has highly and stable alkaline properties with moderate heat stability ( $30\text{--}50 \text{ }^\circ\text{C}$ ), which is of relevance during industrial dehairing application. In conclusion, the process presented can be considered a complete alternative to chemical dehairing. In future works, to improve the efficiency of wastes utilization, the use of hair waste should be investigated with a special focus on biorefinery concepts (possibility of obtaining other valuable products). At the same time, next studies should be focused on a deep economic and environmental study of the entire process.

#### Acknowledgements

The authors thank the Spanish Ministerio de Economía y Competitividad (Project CTM2012-33663-TECNO) for their financial support. N.A. Yazid thanks the Government of Malaysia and University Malaysia Pahang for their financial support.

#### References

- Abidi, F., Limam, F., Nejib, M.M., 2008. Production of alkaline proteases by *Botrytis cinerea* using economic raw materials: assay as biodetergent. *Process Biochem.* 43, 1202–1208.
- Abraham, J., Gea, T., Sánchez, A., 2014. Substitution of chemical dehairing by proteases from solid-state fermentation of hair wastes. *J. Clean. Prod.* 74, 191–198.
- Abraham, J., Gea, T., Sánchez, A., 2013. Potential of the solid-state fermentation of soy fibre residues by native microbial populations for bench-scale alkaline protease production. *Biochem. Eng. J.* 74, 15–19.
- Adani, F., Confalonieri, R., Tambone, F., 2004. Dynamic respiration index as a descriptor of the biological stability of organic wastes. *J. Environ. Qual.* 33, 1866–1876.
- Adani, F., Ubbiali, C., Generini, P., 2006. The determination of biological stability of composts using the dynamic respiration index: the results of experience after two years. *Waste Manag.* 26, 41–48.
- Ahmad, J., Ansari, T.A., 2013. Alkaline protease production using proteinaceous tannery solid waste. *J. Pet. Environ. Biotechnol.* 04, 1–4.
- Alef, K., Nannipieri, P., 1995. *Enzyme Activities, Methods in Applied Soil Microbiology and Biochemistry*. Academic Press Limited, San Diego.
- Amini, M., Younesi, H., Bahramifar, N., Lorestani, A.A.Z., Ghorbani, F., Daneshi, A., Sharifzadeh, M., 2008. Application of response surface methodology for optimization of lead biosorption in an aqueous solution by *Aspergillus niger*. *J. Hazard. Mater.* 154, 694–702.

- Asker, M.M.S., Mahmoud, M.G., El Shebwy, K., Abd el Aziz, M.S., 2013. Purification and characterization of two thermostable protease fractions from *Bacillus megaterium*. J. Genet. Eng. Biotechnol. 11, 103–109.
- Barrena, R., Pagans, E., Vazquez, F., Artola, A., Sanchez, A., 2007a. Full-scale cocomposting of hair wastes from the leather manufacturing industry and sewage sludge. Compost Sci. Util. 15, 16–21.
- Barrena, R., Pagans, E., Artola, A., Vázquez, F., Sánchez, A., 2007b. Co-composting of hair waste from the tanning industry with de-inking and municipal wastewater sludges. Biodegradation 18, 257–268.
- Bezawada, J., Yan, S., John, R.P., Tyagi, R.D., Surampalli, R.Y., 2011. Recovery of *Bacillus licheniformis* alkaline protease from supernatant of fermented wastewater sludge using ultrafiltration and its characterization. Biotechnol. Res. Int., 1–11.
- Dawber, R., 1996. Hair: its structure and response to cosmetic preparations. Clin. Dermatol. 14, 105–112.
- Dayanandan, A., Kanagaraj, J., Sounderraj, L., Govindaraju, R., Rajkumar, G. Suseela, 2003. Application of an alkaline protease in leather processing: an ecofriendly approach. J. Clean. Prod. 11, 533–536.
- De Guardia, A., Mallard, P., Teglia, C., Marin, A., Le Pape, C., Launay, M., Benoist, J.C., Petiot, C., 2010. Comparison of five organic wastes regarding their behaviour during composting: Part 1, biodegradability, stabilization kinetics and temperature rise. Waste Manag. 30, 402–414.
- Du, C., Lin, S.K.C., Koutinas, A., Wang, R., Dorado, P., Webb, C., 2008. A wheat biorefining strategy based on solid state fermentation for fermentative production of succinic acid. Bioresour. Technol. 99, 8310–8315.
- Gea, T., Barrena, R., Artola, A., Sánchez, A., 2004. Monitoring the biological activity of the composting process: oxygen uptake rate (OUR), respirometric index (RI), and respiratory quotient (RQ). Biotechnol. Bioeng. 88, 520–527.
- Gilmour, S.G., 2006. Response surface designs for experiments in bioprocessing. Biometrics 62, 323–331.
- Gupta, R., Beg, Q., Lorenz, P., 2002. Bacterial alkaline proteases: molecular approaches and industrial applications. Appl. Microbiol. Biotechnol. 59, 15–32.
- Gupta, R., Ramnani, P., 2006. Microbial keratinases and their prospective applications: an overview. Appl. Microbiol. Biotechnol. 70, 21–23.
- Haddar, A., Fakhfakh-Zouari, N., Hmidet, N., Frikha, F., Nasri, M., Kamoun, A.S., 2010. Low-cost fermentation medium for alkaline protease production by *Bacillus mojavensis* A21 using hulled grain of wheat and sardinella peptone. J. Biosci. Bioeng. 110, 288–294.
- Han, W., Liu da, N., Shi, Y.W., Tang, J.H., Li, Y.F., Ren, N.Q., 2015a. Biohydrogen production from food waste hydrolysate using continuous mixed immobilized sludge reactors. Bioresour. Technol. 180, 54–58.
- Han, W., Lam, W.C., Melikoglu, M., Wong, M.T., Leung, H.T., Ng, C.L., Yan, P., Yeung, S. Y., Lin, C.S.K., 2015b. Kinetic analysis of a crude enzyme extract produced via solid state fermentation of bakery waste. ACS Sustain. Chem. Eng. 3, 2043–2048.
- Huang, Q., Peng, Y., Li, X., Wang, H., Zhang, Y., 2003. Purification and characterization of an extracellular alkaline serine protease with dehairing function from *Bacillus pumilus*. Curr. Microbiol. 46, 169–173.
- Intergovernmental Panel on Climate Change (IPCC), 2003. Good Practice Guidance for Land Use, Land-Use Change and Forestry. National Greenhouse Gas Inventories Programme, Japan.
- Ito, M., Yamada, T., Makimura, K., Ishihara, Y., Satoh, K., 2010. Intracellular serine protease from *Candida glabrata* species detected and analyzed by zymography. Med. Mycol. 1, 29–35.
- Kanagaraj, J., Velappan, K.C., Chandra Babu, N.K., Sadulla, S., 2006. Solid wastes generation in the leather industry and its utilization for cleaner environment – a review. J. Sci. Ind. Res. (India) 65, 541–548.
- Khan, F., 2013. New microbial proteases in leather and detergent industries. Innov. Res. Chem. 1, 1–6.
- Kumar, C.G., Tiwari, M.P., Jany, K.D., 1999. Novel alkaline serine proteases from alkalophilic *Bacillus* spp.: purification and some properties. Process Biochem. 34, 441–449.
- Lowry, O.H., Rosebrough, N.J., Farr, a.L., Randall, R.J., 1951. Protein measurement with the Folin phenol reagent. J. Biol. Chem. 193, 265–275.
- Mukherjee, A.K., Adhikari, H., Rai, S.K., 2008. Production of alkaline protease by a thermophilic *Bacillus subtilis* under solid-state fermentation (SSF) condition using *Imperata cylindrica* grass and potato peel as low-cost medium: characterization and application of enzyme in detergent formulation. Biochem. Eng. J. 39, 353–361.
- Myers, R.H., Montgomery, D.C., Vining, G.G., Borror, C.M., Kowalski, S.M., 2004. Response surface methodology: a retrospective and literature survey. J. Qual. Technol. 36, 53–78.
- Onyuka, A., Bates, M., Attenburrow, G., Covington, A., Antunes, A., 2012. Parameters for composting tannery hair waste. JALCA 7, 123–130.
- Onyuka, A., 2009. Sustainable management of tannery hair waste through composting. Doctoral Thesis. The University of Northampton.
- Ponsá, S., Gea, T., Sánchez, A., 2010. Different indices to express biodegradability in organic solid wastes. J. Environ. Qual. 39, 706–712.
- Puyuelo, B., Gea, T., Sánchez, A., 2010. A new control strategy for the composting process based on the oxygen uptake rate. Chem. Eng. J. 165, 161–169.
- Raj, A., Khess, N., Pujari, N., Bhattacharya, S., Das, A., Rajan, S.S., 2012. Enhancement of protease production by *Pseudomonas aeruginosa* isolated from dairy effluent sludge and determination of its fibrinolytic potential. Asian Pac. J. Trop. Biomed. 2, 1845–1851.
- Ravindran, B., Kumar, a.G., Bhavani, P.S.A., Sekaran, G., 2011. Solid-state fermentation for the production of alkaline protease by *Bacillus cereus* 1173900 using proteinaceous tannery solid waste. Curr. Sci. 100 (5), 726–730.
- Saravanan, P., Renitha, T.S., Gowthaman, M.K., Kamini, N.R., 2014. Understanding the chemical free enzyme based cleaner unhairing process in leather manufacturing. J. Clean. Prod. 79, 258–264.
- Sivasubramanian, S., Murali Manohar, B., Rajaram, A., Puvanakrishnan, R., 2008. Ecofriendly lime and sulfide free enzymatic dehairing of skins and hides using a bacterial alkaline protease. Chemosphere 70, 1015–1024.
- Sundararajan, S., Kannan, C.N., Chittibabu, S., 2011. Alkaline protease from *Bacillus cereus* VITSN04: potential application as a dehairing agent. J. Biosci. Bioeng. 111, 128–133.
- The US Department of Agriculture and the US Composting Council, 2001. Test Methods for the Examination of Composting and Compost. Edaphos International, Houston.
- Uyar, F., Baysal, Z., 2004. Production and optimization of process parameters for alkaline protease production by a newly isolated *Bacillus* sp. under solid state fermentation. Process Biochem. 39, 1893–1898.
- Wang, H.Y., Liu, D.M., Liu, Y., Cheng, C.F., Ma, Q.Y., Huang, Q., Zhang, Y.Z., 2007. Screening and mutagenesis of a novel *Bacillus pumilus* strain producing alkaline protease for dehairing. Lett. Appl. Microbiol. 44, 1–6.



Contents lists available at ScienceDirect

## Journal of Molecular Catalysis B: Enzymatic

journal homepage: [www.elsevier.com/locate/molcatb](http://www.elsevier.com/locate/molcatb)



# The immobilisation of proteases produced by SSF onto functionalized magnetic nanoparticles: Application in the hydrolysis of different protein sources

Noraziah Abu Yazid, Raquel Barrena, Antoni Sánchez\*

Composting Research Group, Department of Chemical, Biological and Environmental Engineering, Escola d'Enginyeria, Universitat Autònoma de Barcelona, 08193, Bellaterra, Barcelona, Spain

### ARTICLE INFO

#### Article history:

Received 30 September 2016  
Received in revised form  
19 December 2016  
Accepted 10 January 2017  
Available online xxx

#### Keywords:

Protease  
Protein-rich waste  
Solid state fermentation  
Hydrolysis  
Immobilisation

### ABSTRACT

Alkaline proteases produced from protein-rich waste (hair waste and soya residues) by solid state fermentation (SSF) were immobilised onto functionalized magnetic iron oxide nanoparticles (MNPs) using glutaraldehyde as a crosslinking agent. The covalent binding method had a better immobilisation yield compared to simple adsorption, retaining 93%–96% ( $459 \pm 106$  U/mg nanoparticles,  $319 \pm 34$  U/mg nanoparticles) of hair waste and soya residues proteases, respectively after crosslinking with 5% glutaraldehyde for 6 h. However, the adsorption immobilisation yield was 47%–54% after 8 h for both proteases. MNPs and immobilised proteases were characterized using transmission electron microscopy (TEM), scanning electron microscopy (SEM), Fourier transform infrared spectroscopy (FT-IR) and electron diffraction. Our results indicated successful crosslinking between the proteases and amino-functionalized MNPs. The operational stability (pH and temperature) and storage stability of free and immobilised enzyme were also analysed. Despite the fact that the optimum pH of free and immobilised proteases was identical in the alkaline region, the immobilised proteases reached their optimum condition at higher temperatures ( $40^\circ\text{C}$ – $60^\circ\text{C}$ ). After 2 months of storage at  $4^\circ\text{C}$ , the immobilised proteases showed good stability, retaining more than 85% of their initial activity. The high magnetic response of MNPs render an ease of separation and reusability, which contributes to the residual activity of both immobilised proteases on MNPs retaining more than 60% of their initial values after seven hydrolytic cycles. These results showed the enhancement of the stability of the crosslinking interactions between the proteases and nanoparticles. The immobilised proteases were capable of hydrolysing selected proteins (casein, oat bran protein isolate, and egg white albumin). However, differences in the degree of hydrolysis were observed, depending on the combination of the protease and type of substrate used.

© 2017 Elsevier B.V. All rights reserved.

## 1. Introduction

Because of the proteolytic nature of alkaline proteases, they have been commercially utilised for industrial applications, explicitly in the food, pharmaceutical, textile, detergent, and leather industries [1,2]. Their specific role in protein hydrolysis has drawn worldwide attention regarding the versatility of these enzymes for biotechnological applications. Currently, the general cost of protease production is very high, considering the cost of substrates, commercial media and maintenance of cultures used for inoculation. For this reason, the need to develop novel processes with

higher yields is highly recommended from a commercial point of view [3].

Different options have been considered to reduce the cost and increase the utilization of proteases. One of the most promising alternatives is solid state fermentation (SSF), which allows the procurement of value-added products using inexpensive waste as a solid substrate. SSF has been successfully applied in the production of proteases using protein-rich waste without the need to inoculate a specific microorganism [4,5]. In addition to recycling the abundant solid waste produced by industries as cheap substrates, SSF avoids the hassle of maintaining cultures since microorganism can develop mutations over time [6]. Economically, no additional cost is required, as there is no restricted sterilized environment required to produce proteases through SSF since a specific microorganism for inoculation is not involved.

\* Corresponding author.

E-mail address: [antoni.sanchez@uab.cat](mailto:antoni.sanchez@uab.cat) (A. Sánchez).

Apart from that, soluble proteases are susceptible to autolysis, which leads to their rapid inactivation. The instability and lack of flexibility, reusability and recovery make their use a challenge for commercialization. Therefore, the use of immobilisation enzymes offers an attractive method in which immobilised enzymes have enhanced stability that allows for their recyclability and simple recovery without contamination of the final product [7]. There are five basic enzyme immobilisation methods, including simple adsorption, covalent binding, encapsulation, crosslinking, and entrapment [8].

Of all the methods, covalent binding provides firm binding between the enzyme and carrier, thus avoiding enzyme leakage as it can be regulated by using specific functional groups ( $-\text{NH}_2$ ,  $-\text{SH}$ ) [9]. This method of immobilisation provides an efficient way to increase the stability and flexibility of enzyme reusability and recovery [10]. Coupling agents, such as glutaraldehyde, maleic anhydride and genipin, have been widely used as their functional groups can interact with the functional groups of modified carriers and proteins [10,11]. Glutaraldehyde can be used either to alter enzymes after immobilisation or to activate the support for enzyme immobilisation. In addition, the use of glutaraldehyde can increase protein stability, thus avoiding protease autolysis [2,12].

In recent years, the immobilisation of enzymes onto nano-materials, particularly iron oxide magnetic nanoparticles (MNPs), to form nanobiocatalysts has attracted much attention in some fields of research, including biolabeling, bioseparation, biosensors, biofuel cells, and environmental analysis [9,13]. The use of MNPs has been particularly attractive for immobilisation because of their special characteristics, such as their high surface area, simple manipulation and separation by the application of an external magnetic field, biocompatibility, biodegradability, and low toxicity [10,14]. There are several studies reporting the application of purified protease immobilised on magnetic supports [15–18]; however there are only a few studies that have exploited MNPs for crude protease immobilisation and further use in protein hydrolysis and synthesis [19].

In this work, the use of relatively inexpensive enzyme preparative for immobilisation onto functionalized MNPs and crosslinking with glutaraldehyde was assessed. The goal was to test the viability of using low-cost proteases derived from animal (hair waste) and vegetable (soy fibre residues) protein-rich waste that were produced by SSF after being immobilised onto functionalized MNPs in the hydrolysis of different type of proteins. The relative differences in terms of stability and reusability between the free and immobilised enzymes were significant, exhibiting the feasibility of the immobilised enzymes produced in this work. Also, the magnetic properties of the support render a convenient separation between the substrate and the enzymes within the catalytic system.

## 2. Materials and methods

### 2.1. Material and reagents

Ferric chloride ( $\text{FeCl}_3 \cdot 6\text{H}_2\text{O}$ ), ferrous sulphate ( $\text{FeSO}_4 \cdot 7\text{H}_2\text{O}$ ), (3-aminopropyl)-triethoxysilane (3-APTES, 97%), glutaraldehyde solution (50%), cetyl-trimethyl-ammonium bromide (CTAB), trichloroacetic acid (TCA), Folin-Ciocalteu reagent, casein from bovine milk, and egg white albumin were obtained from Sigma-Aldrich (Spain). Oat bran containing 17.6% protein was purchased from a supermarket (Mercadona, Spain). Hair waste with a protein content of 75.6% was obtained from the local tanning industry located in Igualada, Barcelona, and soya fibre residues with a protein content of 25.1% were received from Natursoy, Spain.  $\beta$ -mercaptoethanol, tricine sample buffer, 10%–20% Mini-PROTEAN gels, and Coomassie 250 stain were purchased from Bio-Rad

(Spain). All other chemicals were from commercial sources and were of analytical grade.

### 2.2. Preparation of the protease enzyme concentrates from protein-rich waste using SSF

Two different sources of alkaline proteases were produced from protein-rich waste, hair waste and soya fibre residues using solid state fermentation (SSF) as described elsewhere [4,5]. Briefly, hair waste and soya fibre residues were individually mixed with anaerobically digested sludge at a weight ratio of 1:2, and then, the mixtures were added to a bulking agent (wood chips) at a volumetric ratio of 1:1. SSF was undertaken in triplicate using 10 l air-tight reactors for approximately 1–3 weeks. Later, the proteases, Phw from hair waste and Psr from soya fibre residues, were extracted from the reactors using Tris-HCl buffer (50 mM, pH 8.1). The times for extracting proteases for different substrates were specified for each case based on the maximum activity of the protease produced during SSF. Phw at day 14th yielded  $787 \pm 124 \text{ U/g DW}$ , and Psr at day 4th yielded  $634 \pm 24 \text{ U/g DW}$ . The extracts were ultrafiltered through Amicon Ultra-15 centrifugal filter devices (Millipore, Ireland) with a 10 kDa molecular weight cut-off (MWCO) prior to lyophilisation. The initial activities after lyophilisation for Phw and Psr were 466 U/ml and 330 U/ml, respectively.

### 2.3. Preparation of oat bran protein isolate (OBPI)

The preparation of oat bran protein isolate (OBPI) was performed as described elsewhere [20] with slight modifications. Briefly, oat bran was added to 1.0 M NaCl at a ratio of 1:8 (w/v), and the pH was adjusted to 9.5 using 1.0 M NaOH. The mixture was agitated for 30 min at room temperature. Then, the supernatant was collected after centrifuged at  $5000 \times g$  for 25 min at  $4^\circ\text{C}$ . The pH was adjusted to 4 with 1.0 M HCl prior to centrifugation at  $5000 \times g$  for 40 min at  $4^\circ\text{C}$ . The supernatant was then discarded, and the protein isolate was dissolved in Milli-Q water and adjusted to pH 7 with 0.1 M NaOH. The protein isolate was lyophilised and stored at  $-20^\circ\text{C}$  for future use.

### 2.4. Synthesis of amino-functionalized $\text{Fe}_3\text{O}_4$ magnetic nanoparticles (MNPs)

Magnetic nanoparticles (MNPs) were synthesised by co-precipitation in water phase [21,22] with slight modifications. A mixture of 25 mM ferrous sulphate and 50 mM of ferric chloride were dissolved in 100 ml of Milli-Q water with the addition of 0.1% of CTAB as a stabiliser. The mixture was stirred at  $40^\circ\text{C}$  for 1 h under the nitrogen atmosphere. Then, 125 ml of deoxygenated NaOH (0.5 M) was added dropwise to the mixture, and the mixture was left for 1 h at  $40^\circ\text{C}$  to let the solution chemically precipitate. The resultant MNPs were separated magnetically and washed five times with Milli-Q water. The recovered MNPs were dried overnight at  $60^\circ\text{C}$ .

The surface of the MNPs was modified using a silanization reaction. Approximately 0.61 g of MNPs was dispersed in a solution containing 3.05 ml of APTES, 0.763 ml of Milli-Q water, and 45.75 ml of methanol. The mixture was ultrasonically agitated for 30 min. Then, 10 ml of glycerol was added and heated at  $90^\circ\text{C}$  for 6 h, and the mixture was stirred until separation. The surface-modified MNPs were recovered by applying a magnet, and they were washed three times with Milli-Q water.

### 2.5. Immobilisation of alkaline proteases (Phw, Psr)

To begin with immobilisation of protease onto surface-modified MNPs, 1 ml of alkaline protease from hair waste (Phw) with an ini-

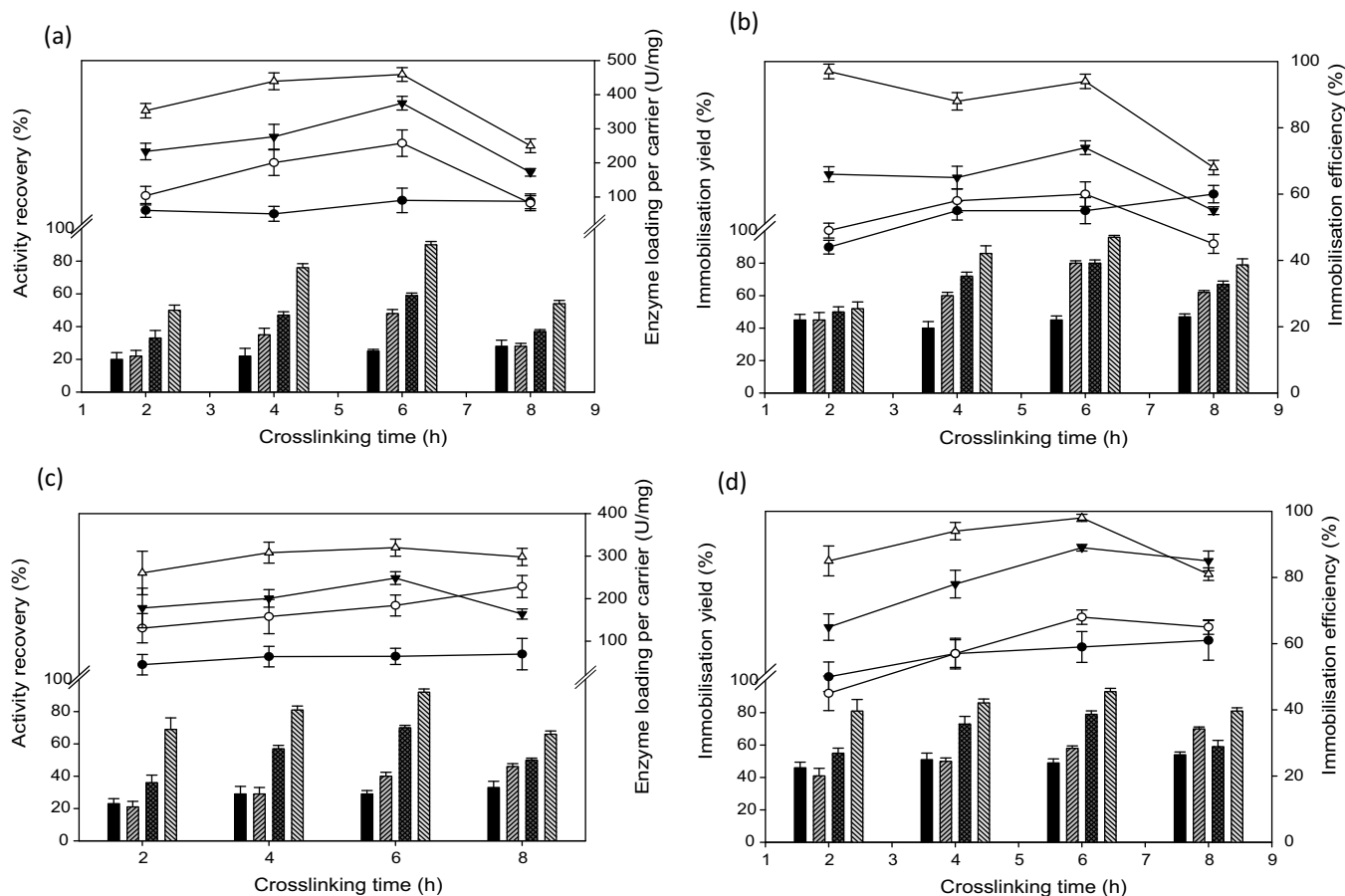


**Fig. 1.** The effect of the glutaraldehyde (GA) concentration and crosslinking time on the activity recovery of (a) Phw and (c) Psr with 0% GA (simple adsorption) (■), 1% GA (▨), 2.5% GA (▩), and 5% GA (▧); enzyme loading per carrier of (a) Phw and (c) Psr with 0% GA (simple adsorption) (●), 1% GA (○), 2.5% GA (▼), and 5% GA (▲); immobilisation yield of (b) Phw and (d) Psr with 0% GA (simple adsorption) (■), 1% GA (▨), 2.5% GA (▩), and 5% GA (▧); immobilisation efficiency of (b) Phw and (d) Psr with 0% GA (simple adsorption) (●), 1% GA (○), 2.5% GA (▼), and 5% GA (▲) onto amino-functionalized MNPs.

tial activity 466 U/ml and alkaline protease from soya residue (Psr) with an initial activity 330 U/ml, respectively, was dissolved in 9 ml of Tris-HCl buffer (pH 8.1). Then, 100 mg of amino-functionalized MNPs was dispersed into the mixture. Afterwards, the activation of the NH<sub>2</sub> groups in the nanoparticles was carried out by adding glutaraldehyde as a crosslinking agent at various concentrations (1%, 2.5%, and 5% (v/v)) in the mixtures, followed by gentle agitation at 4 °C for 8 h. Subsequently, the MNPs with the immobilised proteases (MNPs-protease) were separated by a magnetic field and washed five times with Tris buffer (50 mM, pH 8.1) to remove any unbound glutaraldehyde and enzyme. Finally, the MNPs-protease were resuspended in 1 ml of Tris buffer (50 mM, pH 8.1) and stored at 4 °C for further application.

For immobilisation via adsorption, approximately 100 mg of naked MNPs were dispersed in 9 ml of the Tris buffer solution (50 mM, pH 8.1). Then, 1 ml of free alkaline protease from hair waste (466 U/ml) or soya residue (330 U/ml) was added. The mixture was gently agitated at 4 °C for 8 h. Later, the immobilised proteases were magnetically separated and treated as previously described.

The immobilisation yield (%) and the amount of immobilised protease (Phw<sub>im</sub>, Psr<sub>im</sub>) loading on MNPs (U/mg) were calculated using following equations (Eqs. (1) and (2) [15,23]:

$$\text{Enzyme loading (U/mg)} = (U_i - U_{sp})/W \quad (1)$$

$$\text{Immobilisation yield (\%)} = (U_i - U_{sp})/U_i \times 100 \quad (2)$$

Where U<sub>i</sub> is the initial enzyme activity (U), U<sub>sp</sub> is the enzyme activity in the supernatant after immobilisation (U), and W is the weight

of MNPs used for immobilisation (mg). Furthermore, the immobilisation efficiency (%) and activity recovery (%) were calculated as follows (Eqs. (3) and (4) [23]:

$$\text{Efficiency (\%)} = (U_e/U_{imm}) \times 100 \quad (3)$$

$$\text{Activity recovery (\%)} = (U_e/U_i) \times 100 \quad (4)$$

Where U<sub>e</sub> is the activity of bound enzyme that is measured in the immobilisate (U), U<sub>imm</sub> is the immobilised enzyme activity determined from subtracting the remaining enzyme activity in the supernatant from the initial activity (U).

## 2.6. Characterization of the immobilised enzymes

Functionalized MNPs before and after immobilisation were characterized using high resolution transmission electron microscopy (HRTEM, JEM-2011/JEOL) and scanning electron microscopy (SEM, Zeiss Merlin). The samples were prepared by placing a drop of the sonicated solutions on a copper grid, and then, the samples were allowed to dry. Samples with the immobilised enzyme were stained with uranyl acetate (2%) prior to analysis. Functionalized nanoparticle immobilisation was then confirmed using Fourier Transform Infrared spectroscopy (FT-IR, Bruker Tenser 27) within a range of 500–4000 cm<sup>-1</sup>.

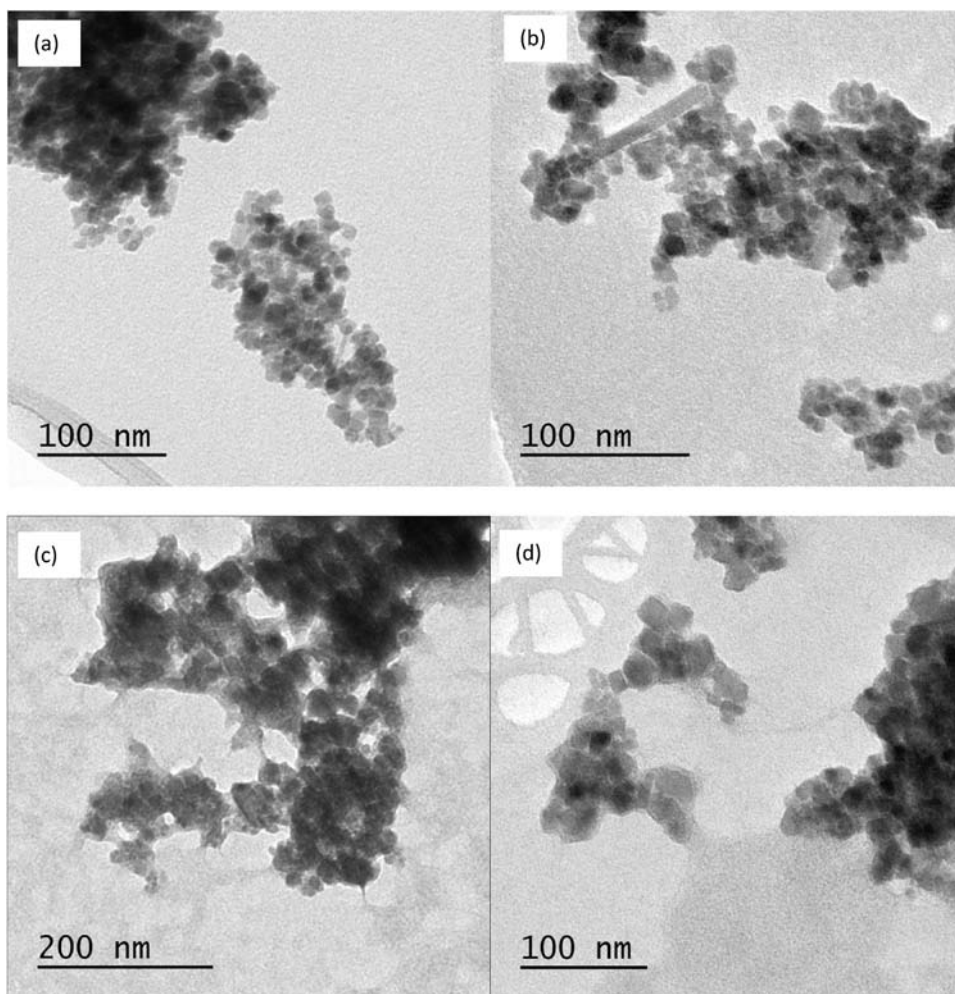


**Fig. 2.** TEM images at a magnification of 30,000 $\times$  of (a) naked MNPs, (b) amino-functionalized MNPs, (c) amino-functionalized MNPs after being immobilised with Phw, and (d) amino-functionalized MNPs after being immobilised with Psr.

### 2.7. Stability of immobilised protease

The storage stability was determined by maintaining the immobilised enzymes via crosslinking and simple adsorption at 4 °C for 60 days. The activity of the enzymes was measured at day 0th as the initial activity, while the activity for the 60th and 7th days were used as the final activity of the immobilised enzymes and free enzymes, respectively.

To study the operational stability, both immobilised and free enzymes were incubated for 1 h at various pH and temperature values according to the response surface of the central composite design (CCD) performed using the Design-Expert software (version 6.0.6). The CCD consisted of 13 experimental points, including five replications at the central point and four star points ( $\alpha=1$ ). The pH was adjusted using the following buffers: acetic acid-sodium acetate 1 M (pH 5), Tris-HCl 1 M (pH 8), and Na<sub>2</sub>HPO<sub>4</sub>-NaOH 0.05 M (pH 11). Analysis of variance (ANOVA) was conducted to determine the significance of the main effects.

The residual activity of each factor was calculated by assuming that the initial activity of the immobilised or free enzyme is 100%.

### 2.8. Reusability of immobilised protease

The reusability of immobilised proteases from hair waste (Phw) and soya fibre residue (Psr) was tested on casein as a model protein. The initial activities of the immobilised enzymes were

measured and compared with seven consecutive repeated uses of immobilised enzymes under the assay conditions. After each cycle, immobilised enzymes were magnetically separated and washed with Tris-HCl buffer (50 mM, pH 8.1). Then, they were resuspended in fresh medium and incubated at 50 °C for 120 min. The activity of immobilised enzymes from the first batch was considered to be 100%.

### 2.9. Application of immobilised proteases in protein hydrolysis

Prior to hydrolysis, 4% (w/v) suspension of selected proteins (casein from bovine milk, egg white albumin, and OBPI) in Tris-HCl buffer (50 mM, pH 8.1) were incubated at 50 °C for 15 min. Then, the reaction was initiated by adding 1 ml of free enzymes (330–460 U/ml) or 1 ml immobilised enzymes suspension (319–459 U/mg NP) into 9 ml of substrate. The mixture was incubated in a water bath at 50 °C with mechanical agitation at 100 rpm. An aliquot of 6 ml was withdrawn at 0.5, 2, 4, 6, and 24 h. The free enzyme activity was deactivated by heating the samples in boiling water for 15 min. Then, the samples were cooled by placing the samples in a cold water bath for 15 min. Afterwards, the samples were centrifuged at 5000  $\times$  g for 15 min to separate any impurities or enzyme from the hydrolysate. The immobilised enzyme was separated from the hydrolysate by a magnetic drive. The hydrolysate was kept frozen at –80 °C prior to lyophilisation.

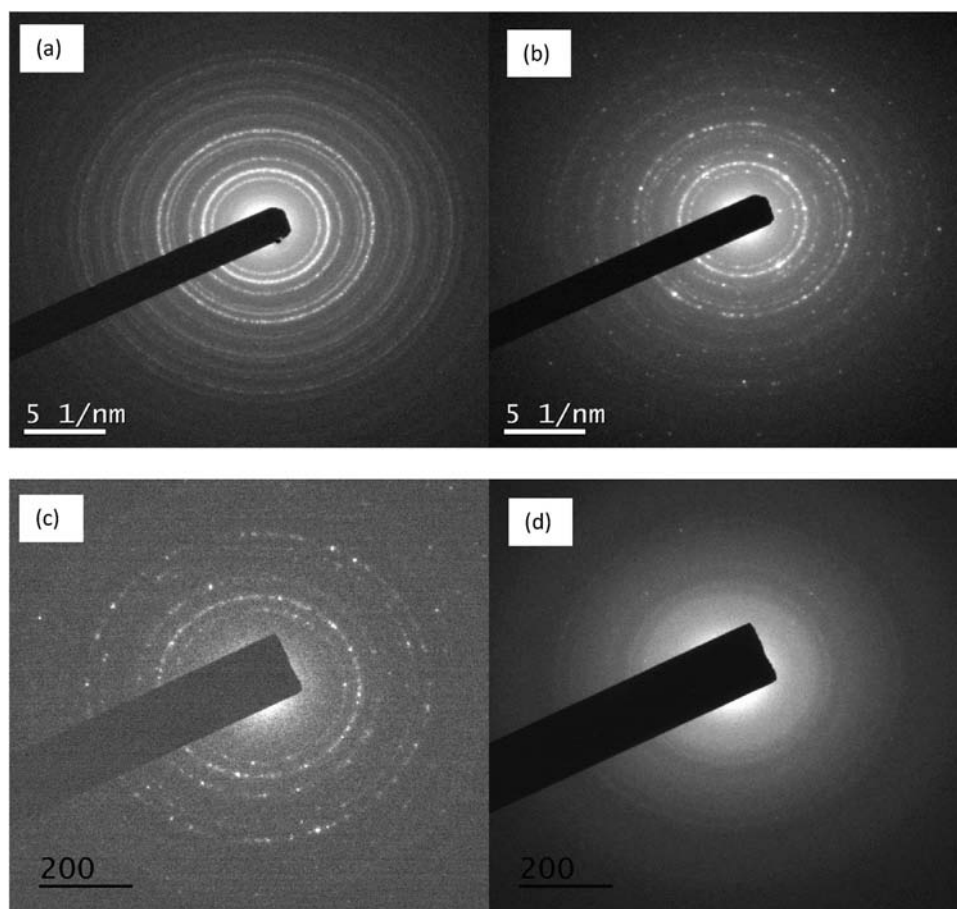


**Fig. 3.** The electron diffraction images of (a) naked MNPs, (b) MNPs after the addition of CTAB, (c) MNPs after surface modification with APTES, and (d) MNPs after the immobilisation of the enzymes Phw and Psr.

## 2.10. Analytical methods

### 2.10.1. Protease assay

The proteolytic activity of the free and immobilised protease was determined using casein as a substrate according to method described by Alef and Nannipieri [24] with slight modifications. Briefly, 1 ml of the enzyme extract (free enzyme) or 0.1 g of immobilised protease in 0.9 ml of Tris buffer (pH 8.1) was added to 5 ml of a 2% (w/v) casein solution and incubated at 50 °C and 100 rpm for 1 h. The reaction was terminated by adding 5 ml of 15% (w/v) TCA. The samples were centrifuged at 10,000 rpm for 10 min at 4 °C. An aliquot of 0.5 ml of the supernatant was added to the alkaline reagent prior to the addition of 0.5 ml of 25% (v/v) Folin-Ciocalteu phenol reagent. The resulting solution was incubated at room temperature in the dark for 1 h. The absorbance was measured at 700 nm using a tyrosine standard. One unit of alkaline protease activity was defined as the liberation of 1  $\mu$ g of tyrosine per minute under the assay conditions. All activity tests were performed in triplicate.

### 2.10.2. Total protein content determination

The total protein content was determined by the Lowry method [25] using bovine serum albumin (BSA) as a standard. The absorbance was analysed at 750 nm using an UV-vis spectrophotometer (Varian Cary 50).

### 2.10.3. Degree of hydrolysis

The degree of hydrolysis was determined by quantifying the soluble protein content after precipitation with TCA [19,26]. 1 ml of

protein hydrolysate was mixed with 1 ml of 10% (w/v) TCA and incubated at 37 °C for 30 min to allow for precipitation. This was followed by centrifugation (10,000  $\times$  g, 10 min). Then, the soluble protein content in the supernatant was determined by the Lowry method [25], and it was expressed in milligrams. The degree of hydrolysis (DH) was determined using the following equation (Eq. (5)):

$$\text{DH}(\%) = \frac{\text{soluble protein content in 10\% TCA}}{\text{total protein content}} \times 100 \quad (5)$$

### 2.10.4. Electrophoresis

Tricine-SDS PAGE was used to observe the pattern of smaller proteins generated after the hydrolysis reaction. Electrophoresis was performed using 10–20% Mini-PROTEAN Tris-Tricine gels under denaturing and reducing conditions. The reduction was achieved by heating the sample at 90 °C for 5 min in the presence of  $\beta$ -mercaptoethanol (2% v/v). The gel was fixed with methanol (40% v/v) and acetic acid (10% v/v) and subsequently stained with Coomassie Brilliant Blue R-250. Then, the gel was destained with a solution containing methanol, acetic acid, and water (20:4:26 v/v).

## 3. Results and discussion

### 3.1. Immobilisation of Phw and Psr onto magnetic nanoparticles

The Phw and Psr enzymes from SSF were immobilised onto magnetic nanoparticles via simple adsorption and crosslinking with glutaraldehyde (GA). Both methods were carried out for 8 h with the aim of investigating the effect of time and crosslinker

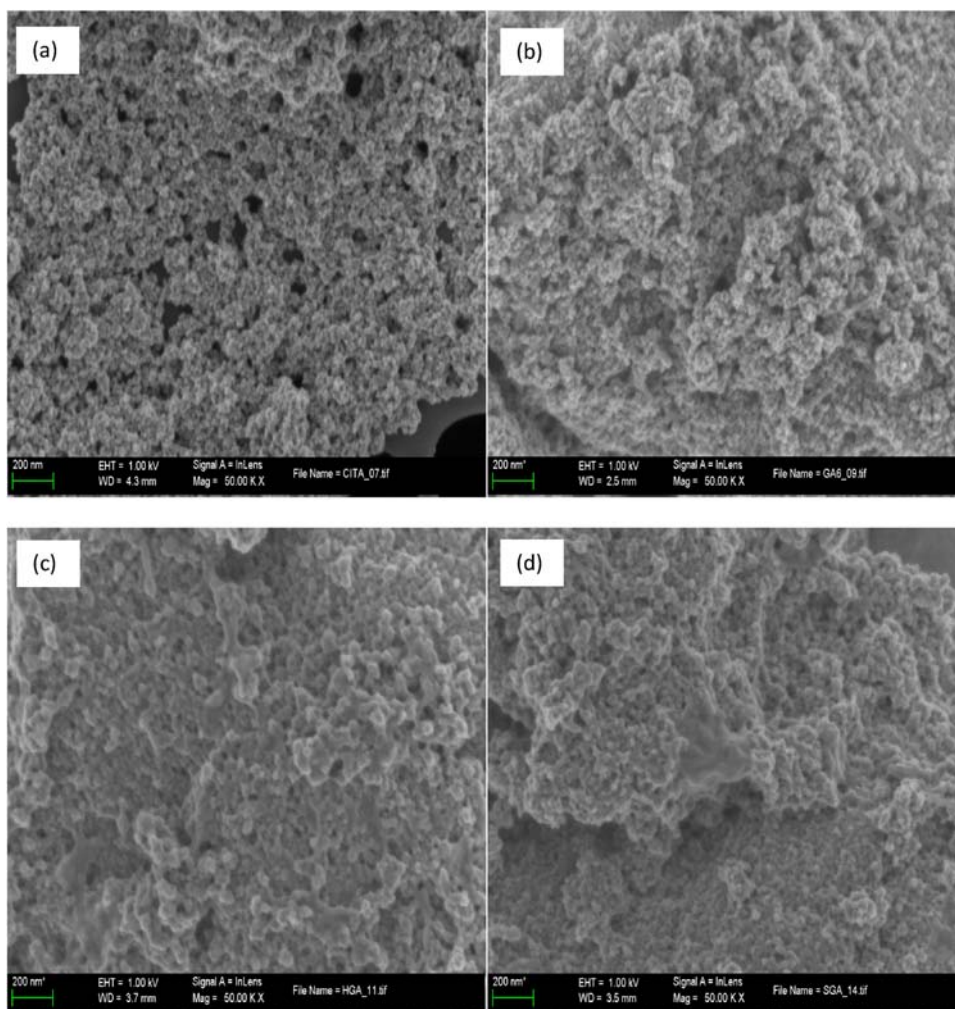


**Fig. 4.** The SEM images at 50.00 KX magnification of (a) naked MNPs, (b) amino-functionalized MNPs, (c) amino-functionalized MNPs after being immobilised with Phw, and (d) amino-functionalized MNPs after being immobilised with Psr.

concentration on immobilisation (Fig. 1). The simple adsorption yielded a maximum activity recovery of 28% with an activity loading of  $87 \pm 22$  U/mg NP for Phw and of 33% Psr (activity loading of  $70 \pm 17$  U/mg NP) after 8 h of immobilisation (Fig. 1a and c). The immobilisation efficiency for both Phw and Psr in simple adsorption increased during 8 h with a maximum of 60–61% efficiency yield, while the maximum immobilisation yield in simple adsorption for both Phw and Psr were 47% and 54%, respectively (Fig. 1b and d). The surfaces of naked MNPs likely possess high reactivity, which makes them susceptible to degradation under particular environmental conditions. This fact could involve weaker binding forces that contribute to the poor stability of the protein attachment's to the surface [9,27].

Immobilisation via the crosslinker showed good results for both enzymes studied (Phw and Psr). The immobilisation yield increased according to the increase in the GA concentration from 1%–5% up to 6 h; then, it decreased abruptly for Phw (Fig. 1b). Only when using Psr with 1% GA, the immobilisation yield continues increasing (Fig. 1d). Maximum activity recovery and immobilisation yields were obtained after 6 h of crosslinking time, 90% and 96% respectively, which is (equivalent to an activity load of  $459 \pm 106$  U/mg NP) for Phw with 5% GA (Fig. 1a and b). Similarly in Psr with 5% GA the maximum activity recovery and immobilisation yield were 92% and 93%, respectively (equivalent to activity loading of  $319 \pm 34$  U/mg NP) (Fig. 1c and d). In addition, the immobilisation via crosslinker was superior to simple adsorption as both of the

enzymes (Phw, Psr) showed good immobilisation efficiency in the range of 45%–98% during 6 h of immobilisation time (Fig. 1b and d). This indicated that the crosslinking time and GA concentration play an important role during the immobilisation of enzymes in this study. As GA plays a role as a spacer arm for the carriers by providing aldehyde groups to couple to free amine groups from the enzymes, forming imines, it can also act as a denaturing agent [12]. Additionally, some studies obtained different crosslinking times (between 1 h–4 h) and GA concentrations (from 1% to 6%), implying good biocompatibility for these specific enzymes [12,21,28,29].

### 3.2. Characterization of the functionalized nanoparticles used for immobilisation

Transmission electronic microscopy (TEM) images of MNPs before and after modification with APTES and after the enzymes immobilisation onto the activated surface were compared (Fig. 2). The average particle size of naked MNPs slightly increased from 10.2 nm (Fig. 2a) to 16.1 nm (Fig. 2b) after surface modification with APTES. This effect has been observed previously in other studies [30,31]. After surface modification with APTES, fewer nanoparticle aggregates formed. As suggested previously [10], surface modifications of magnetic nanoparticles can improve their solubility and help avoid aggregation of particles. In Fig. 2c and d, a layer covering surface of MNPs upon immobilisation of the proteases (Phw and Psr) can be seen. The thickness of this layer covering the surface of



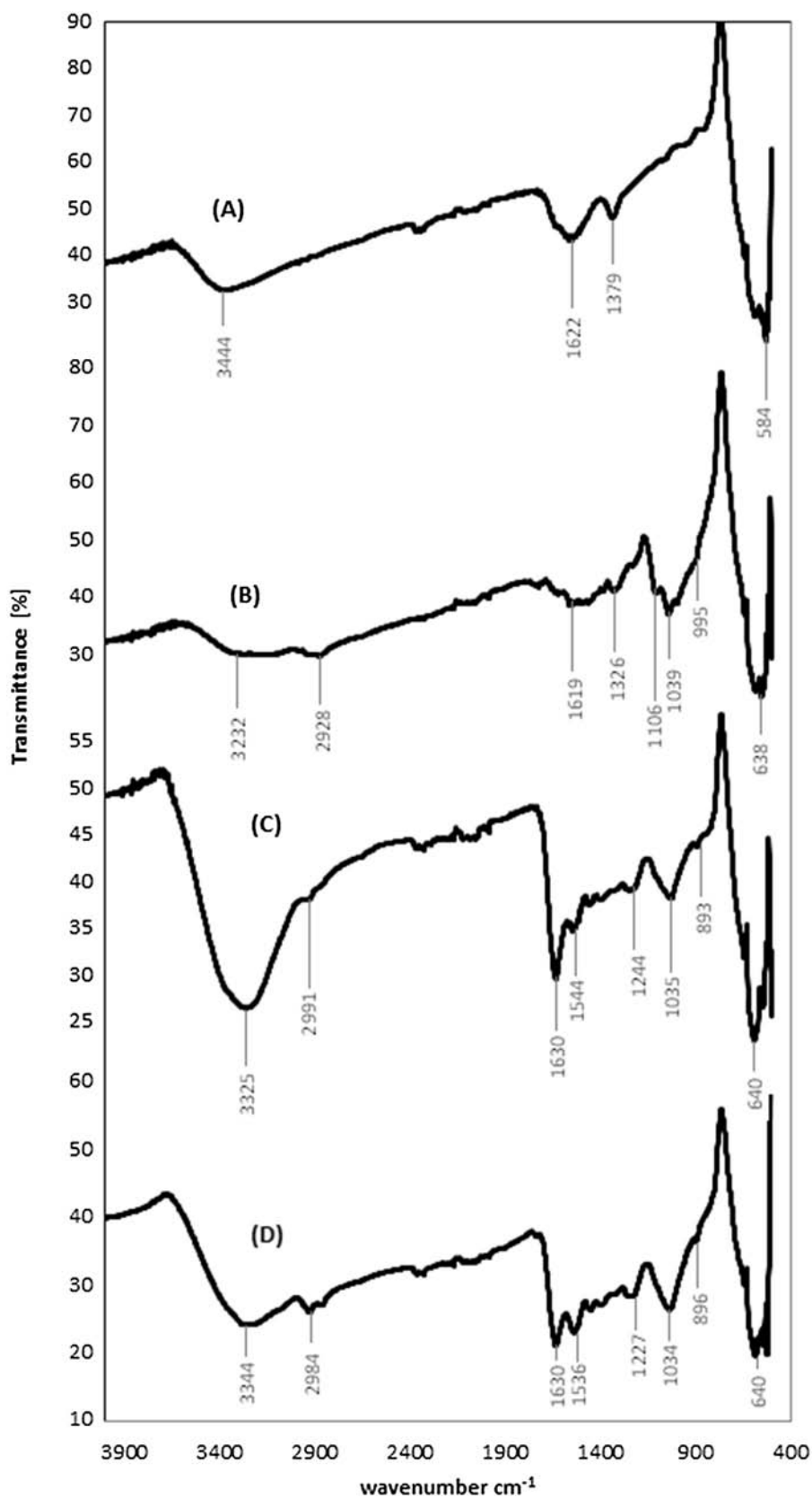


**Fig. 5.** The FT-IR spectra of (A) naked MNPs, (B) amino-functionalized MNPs, (C) amino-functionalized MNPs after immobilisation of Phw, and (D) amino-functionalized MNPs after immobilisation of Psr.

**Table 1**  
Analysis of variance (ANOVA) for the response surface quadratic model for immobilised (Phw.im and Psr.im) and free (Phw.free and Psr.free) enzymes.

Protease	Source of variation	Sums of square	Degree of freedom	Mean square	F-value	Prob > F
Phw.im	Regression	12107.4	5	2421.5	50.47	<0.0001
	Residual	335.9	7	47.98		
	Pure error	150	4	37.5		
	Lack of fit	185.9	3	61.95		
	Total	12443.2	12			
Psr.im	Regression	5108.7	5	1021.7	50.99	<0.0001
	Residual	140.3	7	20		
	Pure error	58.8	4	14.7		
	Lack of fit	81.5	3	27.2		
	Total	5248.9	12			
Phw.free	Regression	3382.4	3	1127.5	105.4	<0.0001
	Residual	96.3	9	10.7		
	Pure error	20.8	4	5.2		
	Lack of fit	75.5	5	15.1		
	Total	3478.7	12			
Psr.free	Regression	6452.3	3	2150.8	101.1	<0.0001
	Residual	191.5	9	21.3		
	Pure error	32.3	4	8.1		
	Lack of fit	159.2	5	31.8		
	Total	6643.8	12			

Phw.im: R<sup>2</sup> 0.9730, adj R<sup>2</sup> 0.9537, pred R<sup>2</sup> 0.8519.Psr.im: R<sup>2</sup> 0.9733, adj R<sup>2</sup> 0.9542, pred R<sup>2</sup> 0.8260.Phw.free: R<sup>2</sup> 0.9723, adj R<sup>2</sup> 0.9631, pred R<sup>2</sup> 0.9315.Psr.free: R<sup>2</sup> 0.9712, adj R<sup>2</sup> 0.9616, pred R<sup>2</sup> 0.9224.**Table 2**  
The storage stability of free and immobilised enzymes created via crosslinking with glutaraldehyde (GA) and via adsorption (adsorp) during 60 days of storage.

Enzymes	Initial activity (U/ml)	Final activity (U/ml)	Residual activity (%)
Phw.GA	501 ± 72	458 ± 51	91
Psr.GA	346 ± 69	297 ± 84	86
Phw.adsorp	190 ± 15	77 ± 9	41
Psr.adsorp	152 ± 9	46 ± 5	30
Phw.free	537 ± 26	91 ± 21 <sup>a</sup>	17
Psr.free	358 ± 29	42 ± 3 <sup>a</sup>	12

The standard deviation was calculated from 3 replicates.

<sup>a</sup> The final activity was determined after 7 days of storage.

MNPs was estimated to be approximately 5.1 nm for Psr and 8.4 nm for Phw, indicating an increase in the size of the particles.

Based on electron diffraction analysis (Fig. 3) of the TEM images, the crystalline structure of the particles was not affected by surface modifications. Fig. 3a shows a clear loop, confirming the crystalline structure of MNPs. After surface modification by APTES or CTAB as a stabilizer, the crystalline structure was not modified; however, the size of some nanoparticles was enlarged, as observed in Fig. 3b and c. Once protease immobilisation was performed, the structure of the nanoparticles became an amorphous structure, confirming that the enzyme covered the surface of the nanoparticles (Fig. 3d). The surface of the naked MNPs and functionalized MNPs can be observed in SEM images (Fig. 4a and b). The small and spherical particles with well-defined edges are observed as in other studies [32]. In contrast, in Fig. 4c and d, the edge surface of nanoparticles is smooth because they are covered by the enzymes, indicating that the immobilisation of proteases onto functionalized MNPs was successful.

The surface modification and immobilisation of proteases (Phw and Psr) onto nanoparticles was confirmed by a comparison of the FT-IR spectra of naked MNPs, functionalized MNPs, and Phw and Psr immobilised onto functionalized MNPs. The FT-IR spectrum in Fig. 5A shows a strong absorption peak at 584 cm<sup>-1</sup>, which could correspond to Fe–O, as indicated in other studies [33,34]. It has been suggested that this strong peak could be due to the stretching vibration mode associated with metal–oxygen absorption. In

this region, the stretching vibration peaks related to metal (ferrites in particular) in the octahedral and tetrahedral sites of the oxide structure were found [31]. In Fig. 5A, the peaks at 1662 cm<sup>-1</sup> and 3444 cm<sup>-1</sup> were due to the bending and stretching vibration of –OH, respectively [35]. After grafting with APTES, the characteristic peak of the Fe–O bond shifted from 584 cm<sup>-1</sup> to 638 cm<sup>-1</sup> and 640 cm<sup>-1</sup> because of the formation of the Fe–O–Si bond (Fig. 5B–D). The shifting of the absorption peaks to high wavenumbers is due to the greater electronegativity of –Si(O–) compared to H, which contributes to the bond forces for Fe–O bonds [36]. Additional strong peaks at 1039 cm<sup>-1</sup>, 1035 cm<sup>-1</sup>, and 1034 cm<sup>-1</sup> correspond to the Fe–O–Si bending vibrations, indicating that alkyl silanes are successfully attached to functionalized MNPs (Fig. 5B–D). Additionally, the presence of silane groups was observed at 995 cm<sup>-1</sup>, 893 cm<sup>-1</sup>, and 896 cm<sup>-1</sup> and were from the stretching vibrations of the Si–OH and Si–O–Si groups from APTES [35,36]. Characteristic peaks of the immobilised enzymes attached via the crosslinker (Fig. 5C and D) were observed at 1536 cm<sup>-1</sup>, 1544 cm<sup>-1</sup> and 1630 cm<sup>-1</sup> because of the C=N and C=O absorption from the glutaraldehyde and NH<sub>2</sub> from the enzyme [29]. Small shifts in intensity from 2928 cm<sup>-1</sup> (Fig. 5B) to 2991 cm<sup>-1</sup> (Fig. 5C) and 2984 cm<sup>-1</sup> (Fig. 5D) correspond to the C–H stretching vibration from the methyl group [37], which illustrated the effect before and after the immobilisation of the enzymes. Additionally, in Fig. 5C and D, there were broad and strong peaks at 3325 cm<sup>-1</sup> and 3344 cm<sup>-1</sup>, which indicated the vibration modes of the O–H and –NH groups from enzymes that interact with nanoparticles, which has been suggested previously [19].

### 3.3. Operational stability of immobilised Phw and Psr

The operational stability in terms of temperature and pH is an important criterion in the application of immobilised enzymes [2,38]. To study this factor (Phw.im, Psr.im), various pH values (5–11) and temperatures (30 °C–70 °C) were tested, and the results were compared with those of free enzymes (Phw.free, Psr.free). The results were analysed using analysis of variance (ANOVA) to indicate the significant factor influencing the stability of both enzymes. The ANOVA results in Table 1 show that the regression coefficients had a high statistical significance ( $p < 0.05$ ) and show

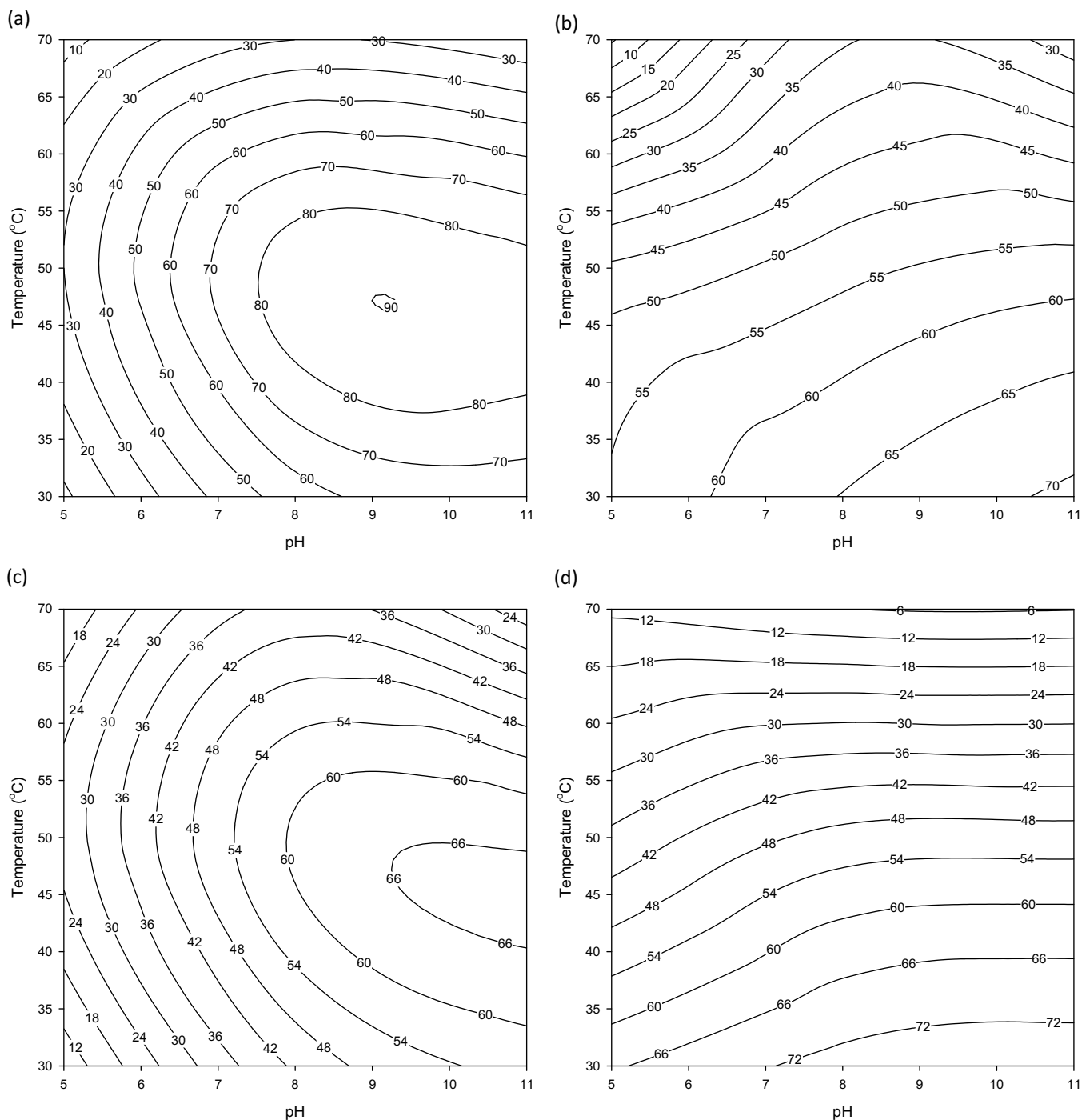


**Fig. 6.** Contour plots of the residual activity (%) of the enzymes in terms of their operation stability as a function of pH and temperature of (a) immobilised Phw, (b) free Phw, (c) immobilised Psr, and (d) free Psr.

the values obtained for the coefficient of determination for both Phw.im and Psr.im ( $R^2$  0.9730 and  $R^2$  0.9733) and Phw.free and Psr.free ( $R^2$  0.9723 and  $R^2$  0.9712, respectively). The values indicated that the model of the immobilised enzymes could not explain only 2.7% of the variables behaviour, while with the free enzymes the value was 2.8–2.9%. For immobilised enzymes, the calculated F-value ( $\alpha = 0.05$ ,  $DOF = 4,3$ ) was 9.12 for the regression. This value was higher than the tabulated F-values (1.65, 1.85), indicating that the treatment differences were highly significant. Similarly, in free enzymes, the obtained F-values (2.90, 3.94) were less than the criti-

cal F-value ( $F_{0.05(4,5)} = 5.19$ ), reflecting the significance of the model. The following Eqs. (6) – (9) represent the second order polynomial model of the residual activity for the experimental data:

$$\begin{aligned} \text{Residual Phw.im (\%)} = & -407.2 + 56.5\text{pH} + 10.1\text{T} \\ & -2.6\text{pH}^2 - 0.1\text{T}^2 - 0.16\text{pHT} \end{aligned} \quad (6)$$

$$\begin{aligned} \text{Residual Psr.im (\%)} = & -275.9 + 41.8\text{pH} + 6.3\text{T} \\ & -1.8\text{pH}^2 - 0.05\text{T}^2 - 0.17\text{pHT} \end{aligned} \quad (7)$$

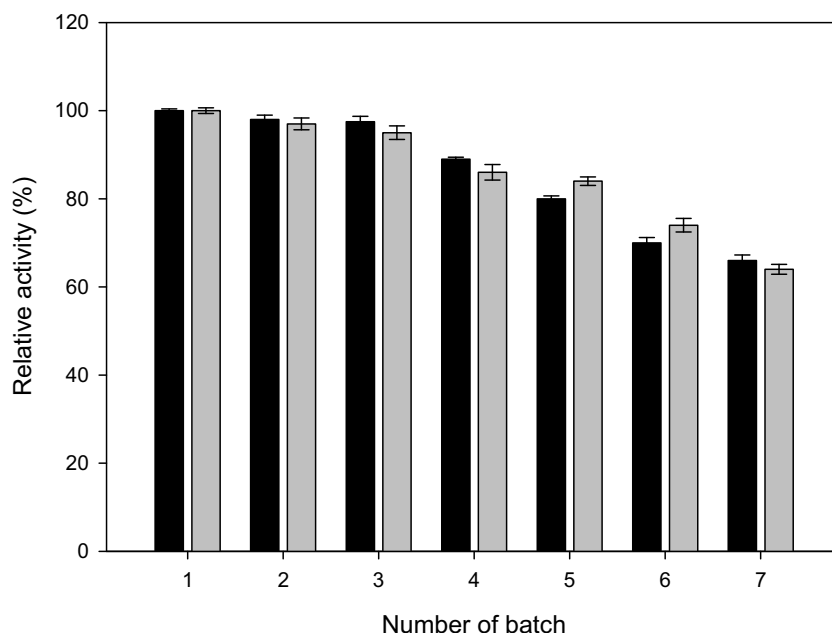


Fig. 7. The reusability of immobilised Phw (■) and immobilised Psr (□) onto amino-functionalized MNPs using casein as a model substrate for the hydrolysis reaction.

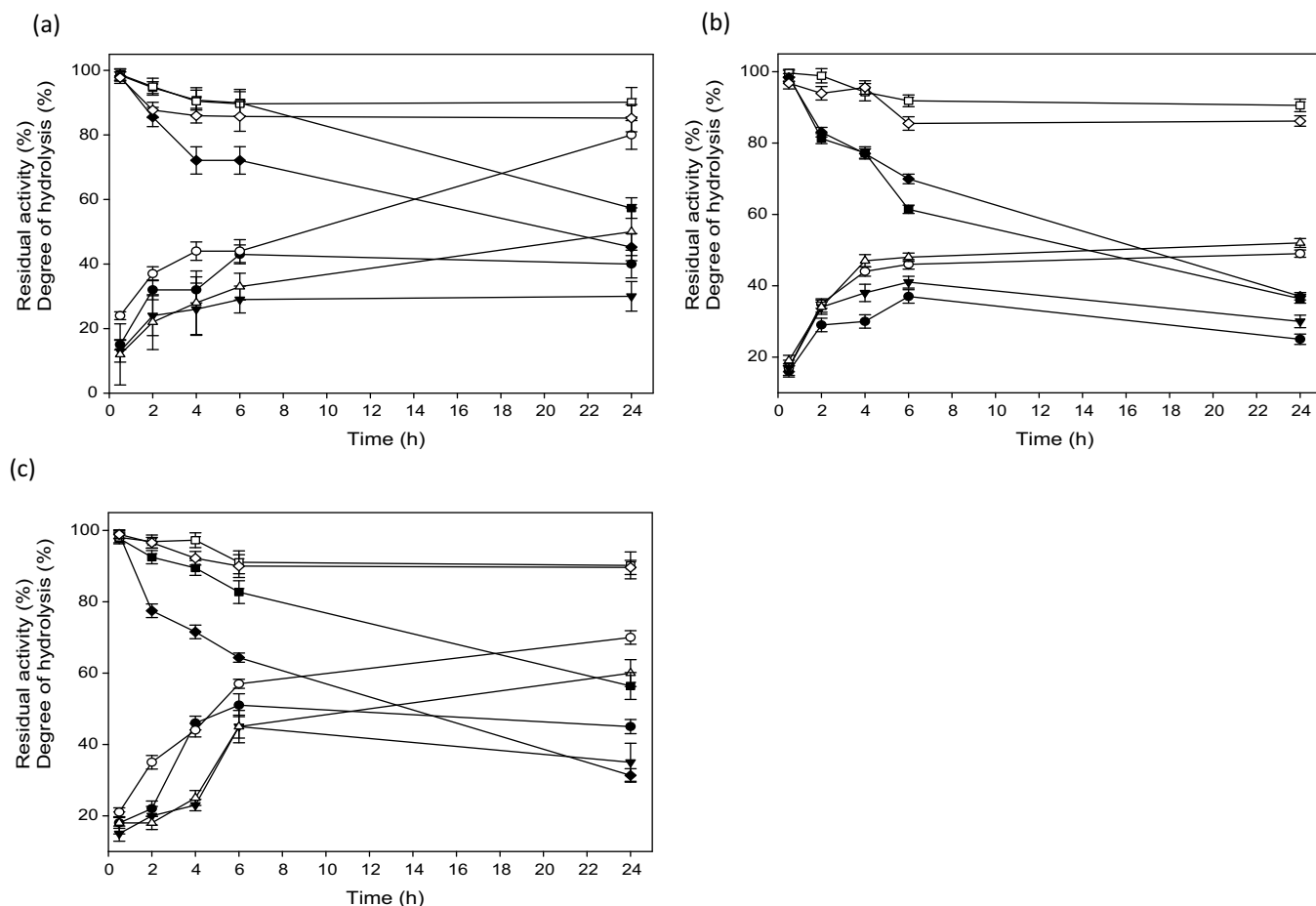
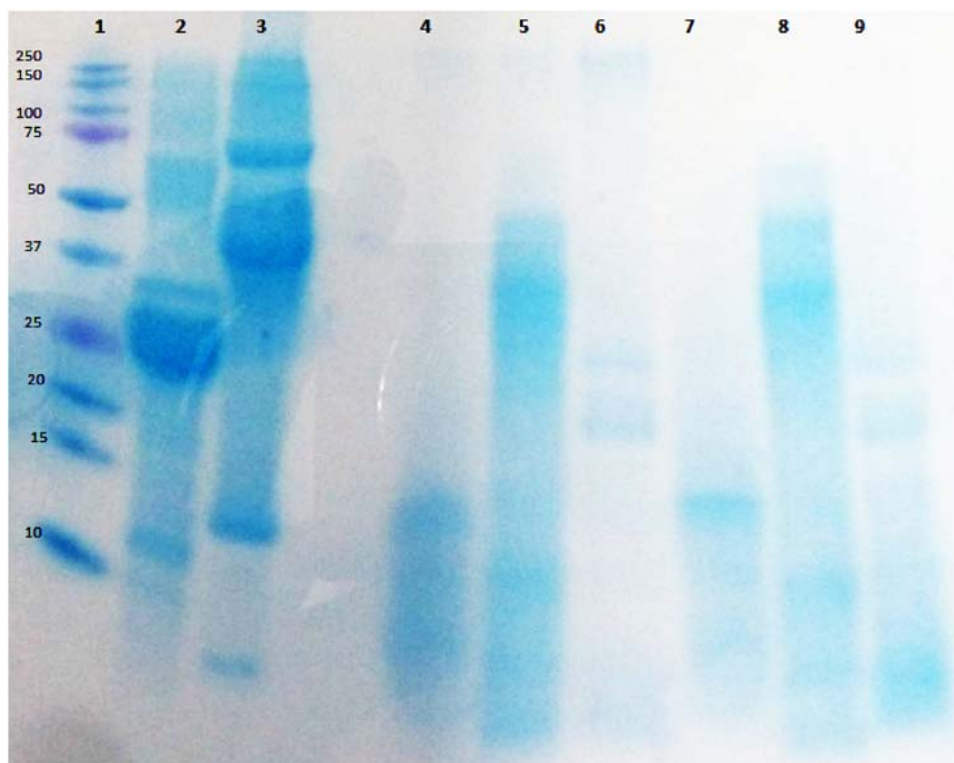


Fig. 8. The degree of hydrolysis of the selected protein hydrolysates obtained from the hydrolysis of immobilised Phw (○), free Phw (●), immobilised Psr (□), and free Psr (▼) with (a) casein; (b) oat bran protein isolate (OBPI); and (c) egg white albumin. The residual activity of immobilised Phw (□), free Phw (■), immobilised Psr (◇) and free Psr (◆) in 50 °C during 24 h.



**Fig. 9.** SDS-PAGE of the hydrolysates after reduction using 2-mercaptoethanol for selected proteins before and after treatment with the immobilised proteases; (1) Molecular mass marker; (2) casein; (3) egg white albumin; (4) hydrolysate from casein after treated with immobilised Phw; (5) hydrolysate from egg white albumin after treatment with immobilised Phw; (6) hydrolysate from OBPI after treatment with immobilised Phw; (7) hydrolysate from casein after treatment with immobilised Psr; (8) hydrolysate from egg white albumin after treatment with immobilised Psr; (9) hydrolysate from OBPI after treatment with Psr.

$$\text{Residual Phw.free (\%)} = 22.2 + 2.5\text{pH} + 1.5T - 0.026T^2 \quad (8)$$

$$\text{Residual Psr.free (\%)} = 66.4 + 1.04\text{pH} + 0.54T - 0.021T^2 \quad (9)$$

For free enzymes, the models were reduced by removing the interaction between pH and temperature, as it was not significant to the stability of the free enzymes.

Contour plots of the second order polynomial model were generated as a function of the independent variables of pH and temperature for immobilised and free enzymes. The contour plots of free Phw and Psr exhibited their stability under mesophilic conditions (30 °C–40 °C). Free enzymes were stable over a broad range of pH values (Fig. 6b and d), with no optimum condition obtained in the range tested (pH 5–11). However, both of the immobilised enzymes had improved the stability by achieving their optimum condition in the alkaline region (pH 8–11) with thermophilic temperature stability ranging from 40 °C to 60 °C for immobilised Phw (Fig. 6a) and 40 °C to 55 °C for immobilised Psr (Fig. 6c).

### 3.4. Storage stability of immobilised Phw and Psr

Storage stability plays a crucial role in the use immobilised proteases, as the shelf life determines the viability of an immobilised enzyme over time [39]. The storage stabilities of enzymes immobilised via a crosslinker (Phw.GA and Psr.GA) and adsorption (Phw.adsorp and Psr.adsorp) were tested by dispersing the immobilised enzymes in Tris buffer and maintaining them at 4 °C for 60 days. Free enzymes (Phw.free and Psr.free) were used as controls to monitor the durability of enzyme activity. Phw.free and Psr.free were not stable in solution, as their activity decreased over time. This fact could be related to the behaviour of the proteases, as they tend to autolyse themselves by nucleophilic attack

on the intermediate in a presence of water [1,40]. After 7 days of storage at 4 °C, the residual activity of Phw.free and Psr.free was less than 17% (Table 2). There was a significant decrease in the activity of the immobilised enzyme via adsorption over 60 days of storage, with a residual activity of less than 45%. The weak bonding between the enzyme and nanoparticles could induce partial desorption during the period of storage. Generally, immobilisation via adsorption involves relatively weak interactions, such as electrostatic interactions, hydrogen bonds, van der Waals forces and hydrophobic interactions, which tend to strip off enzymes from the carrier easily, thus leading to a loss of activity and contamination of the reaction media [9]. However, the enzymes immobilised via crosslinking (Phw.GA and Psr.GA) retained 91% and 86% of their residual activity, respectively, after 60 days of storage at 4 °C (Table 2). These results show that enzymes immobilised created by crosslinking provide a distinctive advantage in stability over immobilised enzymes created by adsorption at a longer duration of storage.

### 3.5. Reusability of immobilised Phw and Psr

For the sake of the cost-effective use of enzymes, reusability is a critical factor to consider [41]. The reusability of immobilised Phw and Psr created using crosslinking was evaluated in a repeated batch process using fresh casein as a model protein in each batch cycle (Fig. 7). Both immobilised Phw and Psr retained 66% and 64% of their activity, respectively, after 7 cycles, indicating a significant enhancement of the stability of the crosslinking interaction between the proteases and nanoparticles. In this work, testing the reusability was feasible, as the immobilised enzymes were easily separated by a magnetic force.

### 3.6. Application of immobilised Phw and Psr in the hydrolysis of proteins

Casein has been used as a model protein to evaluate the degree of hydrolysis (DH) of immobilised enzymes created via crosslinking and free Phw or Psr. The results of the hydrolysis are shown in Fig. 8a. The DH of immobilised Phw (24%) was higher than that of free Phw (15%) during the first 30 min of reaction time (Fig. 8a). The maximum DH was achieved after 24 h and was 80% for immobilised Phw and 40% for free Phw. Besides, the residual activity of both immobilised Phw and Psr were stable for 24 h whereas the residual activity of free Phw and Psr had decreased pronouncedly after 24 h at 50 °C indicating an improvement of process efficiency and thermal stability of the immobilised enzymes [19]. The higher stability may be possibly due to the multipoint covalent binding of protease to the solid support that limit the flexibility and conformational mobility of the enzyme, hence inhibits unfolding or denaturation of the enzyme [42]. Likewise, the DH of immobilised Psr (12%) showed the same rate as that of free Psr (13%) and continued to increase over time with a similar profile, reaching the maximum DH 30% in free Psr and 50% in immobilised Psr after 24 h of reaction time. Thus, the immobilised enzymes in the present study could enhance the ability of free enzymes to hydrolyse protein, as shown by the model protein, reflecting that the active enzymes were successfully immobilised.

The effect of both proteases (Phw and Psr) was also evaluated in hydrolysis of the protein source from animals (egg white albumin) and vegetables (oat bran protein isolate). The hydrolysis of oat bran protein isolate (OBPI) corroborated the efficiency of immobilised Phw and Psr, as they had a higher DH compared to free Phw and Psr over a longer duration (Fig. 8b). These results agree with those obtained using functionalized magnetite nanoparticles to hydrolyse soya protein isolates and whey protein isolates [29,43]. It seems that Psr exhibited a higher DH than (free and immobilised) Phw when using a vegetable protein source. In the hydrolysis of egg white albumin, immobilised Psr reached a maximum DH 60% after 24 h and free Psr achieved maximum DH 45% after 6 h, while Phw reached a maximum DH of 70% and 51% for immobilised and free Phw, respectively (Fig. 8c). Hence, the different source of the proteases seems to be a distinct behaviour that depends on the substrate source; in fact, it could determine the choice of enzymes according to the application, as suggested by others [2].

SDS-PAGE of the hydrolysates from selected proteins (casein, OBPI, egg white albumin) is shown in Fig. 9. The presence of several smaller peptides with low molecular weights support the idea that proteins were hydrolysed by immobilised protease derived from an animal source (Phw) and vegetable source (Psr). Similar profiles were obtained for both immobilised enzymes (Phw and Psr), showing their ability to perform the reaction after being grafted on nanoparticle surfaces created by crosslinking with glutaraldehyde.

## 4. Conclusion

Low-cost proteases obtained through the SSF of protein-rich wastes (hair waste and soya fibre residues) were successfully immobilised onto functionalized MNPs over a relatively short time. The ease of the separation and reusability of these enzymes in comparison with free enzymes could be considered an advantage of their use in industrial processes. Additionally, stability was enhanced from mesophilic to thermophilic conditions under alkaline conditions, preventing autolysis of the enzymes and maintaining their initial activities for 2 months with only 9%–14% activity loss. Immobilised Phw and Psr were able to hydrolyse some proteins derived from plant and animal sources with a high degree

of hydrolysis, indicating that they are promising for immobilised enzyme applications in a wide range of industrial processes.

## Acknowledgments

The authors thank the Spanish Ministerio de Economía y Competitividad (Project CTM2015-69513-R) for their financial support. N.A. Yazid thanks the Government of Malaysia and University Malaysia Pahang for their financial support. Raquel Barrena is grateful to TECNIOspring fellowship programme (no. TECSPR15-1-0051) co-financed by the European Union through the Marie Curie Actions and ACCIÓ (Generalitat de Catalunya).

## References

- [1] M.B. Rao, A.M. Tanksale, M.S. Ghatge, V.V. Deshpande, Molecular and biotechnological aspects of microbial proteases, *Microbiol. Mol. Biol. Rev.* 62 (1998) 597–635.
- [2] O.L. Tavano, Protein hydrolysis using proteases: an important tool for food biotechnology, *J. Mol. Catal. B: Enzym.* 90 (2013) 1–11.
- [3] A.K. Mukherjee, H. Adhikari, S.K. Rai, Production of alkaline protease by a thermophilic *Bacillus subtilis* under solid-state fermentation (SSF) condition using *Imperata cylindrica* grass and potato peel as low-cost medium: characterization and application of enzyme in detergent formulation, *Biochem. Eng. J.* 39 (2008) 353–361.
- [4] J. Abraham, T. Gea, A. Sánchez, Potential of the solid-state fermentation of soy fibre residues by native microbial populations for bench-scale alkaline protease production, *Biochem. Eng. J.* 74 (2013) 15–19.
- [5] N.A. Yazid, R. Barrena, A. Sánchez, Assessment of protease activity in hydrolysed extracts from SSF of hair waste by and indigenous consortium of microorganisms, *Waste Manag.* 49 (2016) 420–426.
- [6] S.S. Kim, H.S. Lee, Y.S. Cho, Y.S. Lee, C.S. Bhang, H.S. Chae, S.W. Han, I.S. Chung, D.H. Park, The effect of the repeated subcultures of *Helicobacter pylori* on adhesion motility, cytotoxicity, and gastric inflammation, *J. Korean Med. Sci.* 17 (2002) 302–306.
- [7] C. Mateo, J.M. Palomo, G. Fernandez-Lorente, J.M. Guisan, R. Fernandez-Lafuente, Improvement of enzyme activity, stability and selectivity via immobilization techniques, *Enzyme Microb. Technol.* 40 (2007) 1451–1463.
- [8] M. Asgher, M. Shahid, S. Kamal, H.M.N. Iqbal, Recent trends and valorization of immobilization strategies and lignolytic enzymes by industrial biotechnology, *J. Mol. Catal. B: Enzym.* 101 (2014) 56–66.
- [9] J. Xu, J. Sun, Y. Wang, J. Sheng, F. Wang, M. Sun, Application of iron magnetic nanoparticles in protein immobilization, *Molecules* 19 (2014) 11465–11486.
- [10] X. Jin, J.F. Li, P.Y. Huang, X.Y. Dong, L.L. Guo, L. Yang, Y.C. Cao, F. Wei, Y. Di Zhao, H. Chen, Immobilized protease on the magnetic nanoparticles used for the hydrolysis of rapeseed meals, *J. Magn. Magn. Mater.* 322 (2010) 2031–2037.
- [11] I.A. Cavello, J.C. Contreras-Esquivel, S.F. Cavalitto, Immobilization of a keratinolytic protease from *Purpureocillium lilacinum* on genipin activated-chitosan beads, *Process Biochem.* 49 (2014) 1332–1336.
- [12] H.J. Chae, M.J. In, E.Y. Kim, Optimization of protease immobilization by covalent binding using glutaraldehyde, *Appl. Biochem. Biotechnol.* 73 (1998) 195–204.
- [13] S.A. Ansari, Q. Husain, Potential applications of enzymes immobilized on/in nano materials: a review, *Biotechnol. Adv.* 30 (2012) 512–523.
- [14] P. Xu, G.M. Zeng, D.L. Huang, C.L. Feng, S. Hu, M.H. Zhao, C. Lai, Z. Wei, C. Huang, G.X. Xie, Z.F. Liu, Use of iron oxide nanomaterials in wastewater treatment: a review, *Sci. Total Environ.* 424 (2012) 1–10.
- [15] A. Sahu, P.S. Badhe, R. Adivarekar, M.R. Ladole, A.B. Pandit, Synthesis of glycinamides using protease immobilized magnetic nanoparticles, *Biotechnol. Rep.* 12 (2016) 13–25.
- [16] S.-L. Cao, X.-H. Li, W.-Y. Lou, M.-H. Zong, Preparation of a novel magnetic cellulose nanocrystal and its efficient use for enzyme immobilization, *J. Mater. Chem. B* 2 (2014) 5522–5530.
- [17] S. Cao, H. Xu, X. Li, W. Lou, M. Zong, Papain@magnetic nanocrystalline cellulose nanobiocatalyst: a highly efficient biocatalyst for dipeptide biosynthesis in deep eutectic solvents, *ACS Sustain. Chem. Eng.* 3 (2015) 1589–1599.
- [18] S. Cao, Y. Huang, X. Li, P. Xu, H. Wu, N. Li, W. Lou, Preparation and characterization of immobilized lipase from *Pseudomonas cepacia* onto magnetic cellulose nanocrystals, *Sci. Rep.* 6 (2016) 1–12.
- [19] R. Sinha, S.K. Khare, Immobilization of halophilic *Bacillus* sp. EMB9 protease on functionalized silica nanoparticles and application in whey protein hydrolysis, *Bioprocess Biosyst. Eng.* 38 (2015) 739–748.
- [20] S. Jodayree, Antioxidant Activity of Oat Bran Hydrolyzed Proteins in Vitro and in Vivo, Doctoral Thesis, Carleton University Ottawa, Ontario, 2014.
- [21] T.G. Hu, J.H. Cheng, B.B. Zhang, W.Y. Lou, M.H. Zong, Immobilization of alkaline protease on amino-functionalized magnetic nanoparticles and its efficient use for preparation of oat polypeptides, *Ind. Eng. Chem. Res.* 54 (2015) 4689–4698.

- [22] A. Abo Markeb, A. Alonso, A.D.A.D. Dorado, A. Sánchez, X. Font, Phosphate removal and recovery from water using nanocomposite of immobilized magnetite nanoparticles on cationic polymer, *Environ. Technol.* 3330 (2016) 1–14.
- [23] R.A. Sheldon, S. Van Pelt, Enzyme immobilisation in biocatalysis: why, what and how, *Chem. Soc. Rev.* 42 (2013) 6223–6235.
- [24] K. Alef, P. Nannipieri, *Methods in Applied Soil Microbiology and Biochemistry—Enzyme Activities*, Academic Press, San Diego, 1995.
- [25] O.H. Lowry, N.J. Rosebrough, A.L. Farr, R.J. Randall, Protein measurement with the Folin phenol reagent, *J. Biol. Chem.* 193 (1951) 265–275.
- [26] M.P.C. Silvestre, H.A. Morais, V.D.M. Silva, M.R. Silva, Degree of hydrolysis and peptide profile of whey proteins using pancreatin, *Braz. Soc. Food Nutr.* 38 (2013) 278–290.
- [27] D.A. Cowan, R. Fernandez-Lafuente, Enhancing the functional properties of thermophilic enzymes by chemical modification and immobilization, *Enzyme Microb. Technol.* 49 (2011) 326–346.
- [28] S. Prasertkittikul, Y. Chisti, N. Hansupalak, Deproteinization of natural rubber using protease immobilized on epichlorohydrin cross-linked chitosan beads, *Ind. Eng. Chem. Res.* 52 (2013) 11723–11731.
- [29] S.N. Wang, C.R. Zhang, B.K. Qi, X.N. Sui, L.Z. Jiang, Y. Li, Z.J. Wang, H.X. Feng, R. Wang, Q.Z. Zhang, Immobilized alcalase alkaline protease on the magnetic chitosan nanoparticles used for soy protein isolate hydrolysis, *Eur. Food Res. Technol.* 239 (2014) 1051–1059.
- [30] H. Quanguo, Z. Lei, W. Wei, H. Rong, H. Jingke, Preparation and magnetic comparison of silane-functionalized magnetite nanoparticles, *Sens. Mater.* 22 (2010) 285–295.
- [31] J.A. Lopez, F. González, F.A. Bonilla, G. Zambrano, M.E. Gómez, Synthesis and characterization of Fe<sub>3</sub>O<sub>4</sub> magnetic nanofluid, *Rev. Latinoam. Metal. Mater.* 30 (2010) 60–66.
- [32] M.R. Ladole, A.B. Muley, I.D. Patil, M.I. Talib, R. Parate, Immobilization of tropizyme-P on amino-functionalized magnetic nanoparticles for fruit juice clarification, *J. Biochem. Technol.* 5 (2014) 838–845.
- [33] I.J. Bruce, T. Sen, Surface modification of magnetic nanoparticles with alkoxy silanes and their application in magnetic bioseparations, *Langmuir* 21 (2005) 7029–7035.
- [34] M. Yamaura, R.L. Camilo, L.C. Sampaio, M.A. Macedo, M. Nakamura, H.E. Toma, Preparation and characterization of (3-aminopropyl)triethoxysilane-coated magnetite nanoparticles, *J. Magn. Magn. Mater.* 279 (2004) 210–217.
- [35] D.L. Pavia, G.M. Lampman, G.S. Kriz, J.A. Vyvyan (Eds.), *Introduction to Spectroscopy*, 5th ed., Cengage Learning, United State of America, 2015.
- [36] R.A. Bini, R.F.C. Marques, F.J. Santos, J.A. Chaker, M. Jafelicci, Synthesis and functionalization of magnetite nanoparticles with different amino-functional alkoxy silanes, *J. Magn. Magn. Mater.* 324 (2012) 534–539.
- [37] P.E.G. Casillas, C.A.R. Gonzalez, C.A.M. Pérez, Infrared spectroscopy of functionalized magnetic nanoparticles, in: T. Theophile (Ed.), *Infrared Spectrosc.—Mater. Sci. Eng. Technol.*, InTech, 2012, pp. 405–420.
- [38] R.J.S. De Castro, H.H. Sato, Production and biochemical characterization of protease from *Aspergillus oryzae*: an evaluation of the physical-chemical parameters using agroindustrial wastes as supports, *Biocatal. Agric. Biotechnol.* 3 (2014) 20–25.
- [39] A.G. Kumar, S. Swarnalatha, P. Kamatchi, G. Sekaran, Immobilization of high catalytic acid protease on functionalized mesoporous activated carbon particles, *Biochem. Eng. J.* 43 (2009) 185–190.
- [40] R. Beynon, J.S. Bond (Eds.), *Proteolytic Enzymes: A Practical Approach*, 3rd ed., University Press, Oxford, 2001.
- [41] T. Chen, W. Yang, Y. Guo, R. Yuan, L. Xu, Y. Yan, Enhancing catalytic performance of β-glucosidase via immobilization on metal ions chelated magnetic nanoparticles, *Enzyme Microb. Technol.* 63 (2014) 50–57.
- [42] R.K. Singh, Y.W. Zhang, N.P.T. Nguyen, M. Jeya, J.K. Lee, Covalent immobilization of beta-1,4-glucosidase from *Agaricus arvensis* onto functionalized silicon oxide nanoparticles, *Appl. Microbiol. Biotechnol.* 89 (2011) 337–344.
- [43] E.M. Lamas, R.M. Barros, V.M. Balcao, F.X. Malcata, Hydrolysis of whey proteins by proteases extracted from *Cynara cardunculus* and immobilized onto highly activated supports, *Enzyme Microb. Technol.* 28 (2001) 642–652.